COMMONWEALTH OF AUSTRALIA

DEPARTMENT OF NATIONAL DEVELOPMENT

BUREAU OF MINERAL RESOURCES, GEOLOGY AND GEOPHYSICS

BULLETIN No. 83

Morphology and Sediments of the Timor Sea

BY

TJEERD H. VAN ANDEL
Scripps Institution of Oceanography
La Jolla, California

and

J. J. VEEVERS
Bureau of Mineral Resources, Geology & Geophysics
Canberra, Australia

Issued under the Authority of the Hon. David Fairbairn,
Minister for National Development
1967

1290/7/66—1300 Bks.

COMMONWEALTH OF AUSTRALIA

DEPARTMENT OF NATIONAL DEVELOPMENT
MINISTER: THE HON. DAVID FAIRBAIRN, D.F.C., M.P.
SECRETARY: R. W. BOSWELL

BUREAU OF MINERAL RESOURCES, GEOLOGY AND GEOPHYSICS
DIRECTOR: J. M. RAYNER

THIS BULLETIN WAS PREPARED FOR PUBLICATION IN THE GEOLOGICAL BRANCH
ASSISTANT DIRECTOR: N. H. FISHER

Published by the Bureau of Mineral Resources, Geology and Geophysics
Canberra A.C.T.

FOREWORD

This Bulletin is the fruit of a joint venture between Scripps Institution of Oceanography and the Bureau of Mineral Resources, Geology and Geophysics, which started in 1960 with Veevers accompanying van Andel on the cruises of *Malita* and *Stranger*, which formed part of Scripps Institution's contribution to the International Indian Ocean Expeditions. Subsequently, Veevers spent a year at Scripps Institution and worked with van Andel on the analysis of material collected in the field. The Bureau acknowledges its debt to Scripps Institution and, in particular, to van Andel for initiating this joint project, and for the unstinted help given to one of its officers.

This is the first publication of the Bureau to deal with marine geology, and it serves as evidence of the Bureau's expanding interest in the offshore area surrounding Australia. It is gratifying that our first publication in this field has as senior author such a distinguished marine geologist as van Andel.

J. M. RAYNER,
Director.

CONTENTS

ILLUSTRATIONS

TABLES

PLATES (back pocket)

SUMMARY

The Timor Sea region discussed in this Bulletin covers the Sahul Shelf and Timor Trough between 123° and 130° East longitude. The area includes a wide, stable continental platform bordered on one side by an ancient, low-lying, deeply weathered continent, and on the other by a moderately deep, tectonically unstable geosynclinal trough. The purpose of this Bulletin is to describe and interpret the morphology of this area, to define and characterize the sedimentary facies and their distribution patterns, and to discuss the topographic, oceanographic, geological, and biological factors that control them. The study forms part of a series of investigations of modern sedimentary facies in a variety of geological settings along the continental margins.

The Timor Trough has a maximum depth of 1750 fathoms; it is closed at both ends by sills at approximately 1000 fathoms. The southern slope is gentle and depositional, the northern slope rocky, irregular, and steep. The axial portion consists of several longitudinal depressions separated by low sills and partially filled with sediment. The north-eastern slope is interrupted by two deep subsidiary basins. The trough is separated from the Sahul Shelf by a series of small, steep-sided banks rising from the upper continental slope to within 12 fathoms of the surface. These banks probably originated in shallow water as a broken fringing reef and continued to grow during subsidence of the shelf margin.

The Sahul Shelf consists of a central basin (the Bonaparte Depression) with a depth of approximately 60 to 70 fathoms, surrounded on three sides by shallow rises. Superimposed on this regional relief is a system of channels, terraces, and flat-topped banks. The topography is strikingly similar to that of the adjacent land. Many channels cut entirely across the rises, suggesting an antecedent drainage system. The tops of banks and terraces can be shown by correlation and tracing on detailed bathymetric charts to be parts of several regional subhorizontal surfaces. These surfaces show elevations and depressions corresponding to the basin and rises of the area. The upper surfaces converge toward the edge of the shelf, the lower surfaces toward the crests of the rises. The upper surfaces are considered the seaward extensions of Tertiary erosional plains of the adjacent land, so the shelf must have been uplifted, weathered, and denuded during that period. Subsequent deformation of the shelf resulted in the formation of the basin and rises, while the drainage system became antecedent. The shelf subsided to its present position in the Pleistocene, probably concomitant with the uplift of Timor and the depression of the Timor Trough. The lower shelf surfaces were formed by erosion and aggradation during glacial low stands of sea level. This history of uplift, erosion, subsidence, and marine invasion repeats similar pre-Cainozoic cycles. On the basis of the submarine topography, the main structural trends of north-western Australia can be extrapolated on to the shelf with some confidence.

The sediments of the Timor Sea are generally thin, except perhaps on the southern slope and bottom of the Timor Trough. The coarser fractions are predominantly calcareous, but the fine silt and clay are of terrigenous origin and have been derived from the Australian rivers and from the islands along the northern margin of the Timor Trough.

The bottom and slopes of the Timor Trough are covered with silty clays containing planktonic Foraminifera. Below 1000 fathoms, the sediments are rich in Radiolaria. Both carbonate content and grainsize decrease outward from the edge of the Sahul Shelf, which must therefore be the principal source of coarse sediment and of calcareous material. Deepwater calcarenites, which sometimes show graded bedding, and are composed of planktonic Foraminifera, are fairly common. They have the character of turbidites, but originated below the upper continental slope.

The sediments of the Sahul Shelf have been strongly influenced by the postglacial transgression. During the last glacial maximum, the shoreline was at a depth of 60 to 70 fathoms near the edge of the shelf. Except for a restricted, but marine, lagoon in the Bonaparte Depression, the entire shelf was subaerially exposed and subjected to weathering in a climate with substantially less precipitation than today. Calcareous concretions (kunkar) were produced in abundance by soil-forming processes. The postglacial transgression rapidly flooded the outer and central shelf and covered the region with transgressive skeletal calcarenites containing numerous reworked kunkar pellets. Around the shallow banks on the rises, these transgressive deposits consist largely of reworked coral debris. Landward of the 40-fathom contour, the transgressive sediments are partly terrigenous in origin. Zones of high quartz concentration indicate extensive development of littoral sediments supplied by the rivers during temporary still stands in the transgression.

At the present time, sedimentation on the shelf is restricted to certain areas. Foraminiferal calcarenites are forming on the outer shelf; they become finer grained and more planktonic in composition toward the edge of the shelf. Silty clays with molluscan debris are being deposited fairly rapidly in deeper, more sheltered areas. A thick blanket of such clays that occurs in the Bonaparte Depression is the product of currents carrying suspended sediment from the Ord and Victoria Rivers. Thin calcirudites consisting mainly of large Foraminifera and coralline algae are accumulating slowly on the shallow banks of the rises. A similar assemblage, dominated by *Halimeda*, covers the very shallow shelf edge banks. No evidence of major recent growth of coral reefs has been found outside the immediate coastal area and a few places on the outer western rise.

On the central and inner shelf, with the exception of the Bonaparte Depression, relict transgressive calcarenites occur at the surface. Sedimentation in this zone is very slow, and the deposits are continuously reworked by burrowing organisms and waves. Much of the skeletal material is strongly glauconitized. Modern sediments are forming in the littoral zone shoreward of the 10-fathom contour.

The depositional facies of the Timor Sea are similar to those of other calcareous shelves, although precipitated carbonate in the form of oolites or aragonite needles is conspicuously absent. This absence may be due to the great distance between the cool water of the open ocean, rich in carbon dioxide, and the shallow turbulent zone where precipitation normally occurs. The facies also bear a striking resemblance in origin and distribution patterns to those of modern terrigenous shelves.

INTRODUCTION

1. Purpose and Scope of Investigation

Recent sediments have been studied for many different reasons. Some investigators are interested in modern sediments for their own sake: the dynamics of sedimentation, the processes of diagenesis, and the responses of a sediment to its environment form their primary goal. Other studies have been specifically designed to facilitate the application of modern sediment data to problems in palaeogeography and stratigraphy. In recent years the interests and needs of the petroleum industry have stimulated considerable research in modern sedimentation along these lines, and several large regional studies have appeared in print.

Many of these studies deal with essentially the same geological setting, situated in stable areas of low relief of depositional origin. In these areas the supply of terrigenous sediments from distant sources is high, and the water of the basins communicates freely with the open ocean. The sedimentary facies of such areas are quite similar (van Andel & Postma, 1954; Shepard, Phleger & van Andel, 1960), and their arrangement in space can now be predicted in general terms. Other studies, such as those of the California Borderland (Emery, 1960) or the Gulf of California (van Andel & Shor, 1964), deal with regions of greater instability, high relief, a more variable sediment supply, and varying degrees of geographic and oceanographic isolation. Their sedimentary facies have, to a certain extent, a character of their own, and the facies patterns are distinct from those of the basins mentioned before.

The present study deals with still another geological setting. The Sahul Shelf is a very wide continental platform, one of the widest in the world. It is in open connexion with the Indian Ocean and the seas of Indonesia (Fig. 1.1). On one side the Sahul Shelf is bordered by a vast, old, low-lying, deeply weathered and eroded hinterland, on the other by the moderately deep and tectonically unstable Timor Trough. At the present time, the Sahul Shelf receives little terrigenous sediment from the Australian continent, and sedimentation is slow and mainly biogenous in origin. In many ways, the setting is probably quite similar to that of many Palaeozoic and Mesozoic epicontinental seas. The purpose of this Bulletin is to define and characterize the broad sedimentary facies units occurring in the area; to establish their regional distribution patterns; and to discuss the oceanographic, geological, morphological, and biological factors that control them. We hope that as such studies are carried out along similar lines and with similar methods in areas of different settings, a pattern of facies and facies control will emerge that will allow a better understanding and more reliable predictions of ancient sedimentary facies and palaeogeography.

Previous work on the sediments and morphology of the Timor Sea is quite scarce, although early speculations have appeared (Molengraaff, 1922; van Bemmelen, 1949). The Snellius Expedition visited parts of the region, and some data on bathymetry and sediments have appeared in expedition reports (Kuenen, 1935; Kuenen & Neeb, 1943). A more detailed discussion, based mainly on data from hydrographic charts, is contained in a more recent series of papers by Fairbridge (1950, 1953; Teichert & Fairbridge, 1948; Carrigy & Fairbridge, 1954).

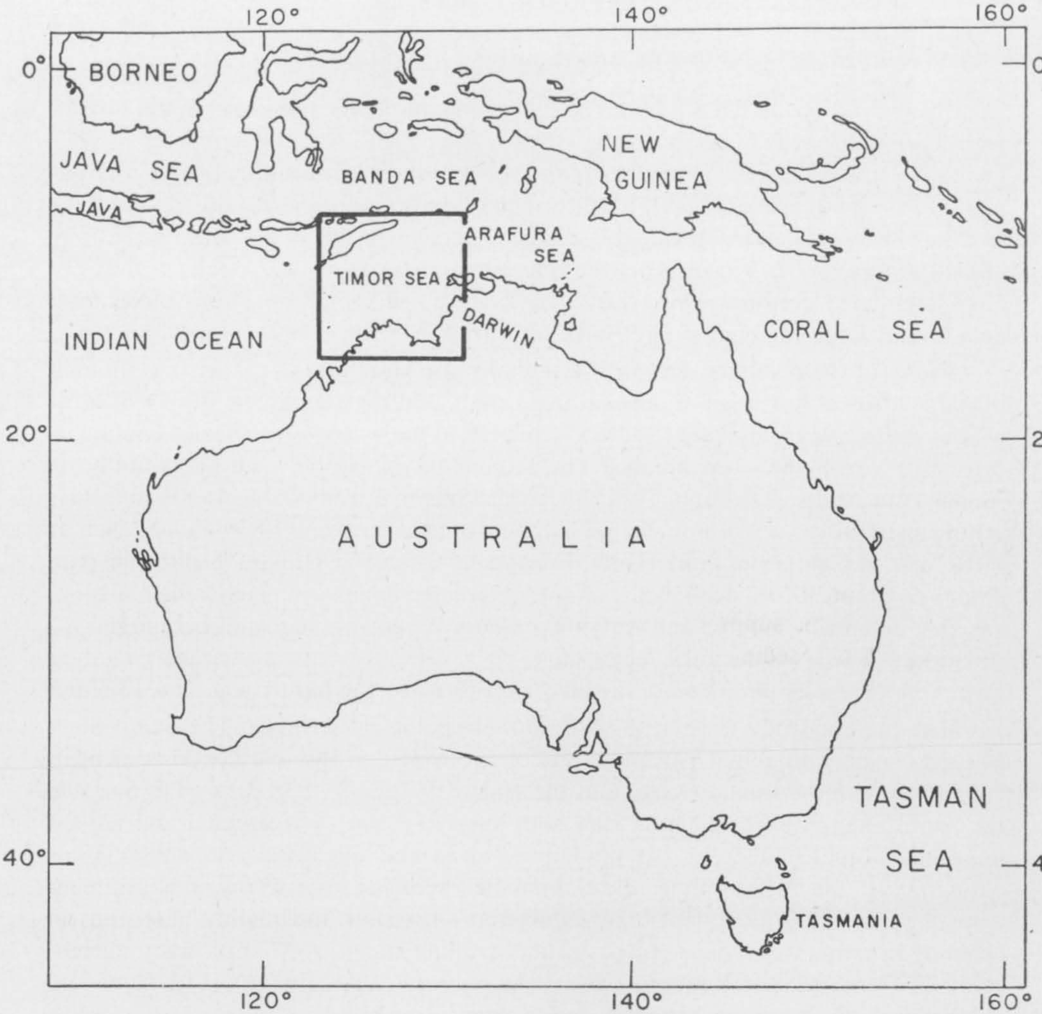

Fig. 1.1—Location of area of study.

The present study has some important limitations. Only surface samples and short cores have been obtained, and little geophysical work has been carried out. Hence, only a two-dimensional picture of sediment patterns could be obtained. The small-scale topographical complexity of the area is great, and the sample spacing, although as good as or better than that for many of other shelves, cannot do justice to local variations. Consequently, the patterns are greatly generalized. Moreover, because of an almost total absence of reliable navigation aids, the nearshore zone and areas near reefs have been avoided in the work at sea, and only sediments in water deeper than 10 fathoms have been sampled. These limitations are important when evaluating the conclusions presented and their applicability to ancient carbonates.

Samples and observations have been collected mainly on two cruises of the Scripps Institution of Oceanography: on M.V. *Malita* in November-December 1960, and on R.V. *Stranger* in April 1961. Both cruises formed part of Scripps' participation in the International Indian Ocean Expeditions (van Andel, Curray, & Veevers, 1961). A total of 377 sampling stations was occupied, two hydrocasts and 212 bathythermograph records were taken, and continuous echo-sounding records were obtained. Moreover, on Scripps' *Monsoon* (1960) and *Lusiad* (1962–1963) Expeditions, six piston cores were collected from the Timor Trough and the central depression of the Sahul Shelf.

Bottom samples were obtained with a short gravity corer with a 2·5-inch plastic liner, with an orange-peel grab, and with a light basket and a heavy chain-bag dredge. A small pipe dredge with sample bag was used with the large dredges to obtain a representative sample of the finer sediment. Treatment and laboratory analysis of the samples will be discussed in Chapter 6.

2. Geology and Coastal Morphology of Bordering Lands

General geology of Timor and north-western Australia

Timor, the westernmost island of the Lesser Sunda Island Chain, is a highly complex orogene of alpine structure that forms part of the Timor/East Celebes Geosyncline (Fig. 2.1). Neighbouring islands represent fragmentary portions of the same history. The stratigraphy and structural history of the island, after Lemoine (1959), may be summarized as follows. A tectonic complex, probably autochthonous (Permian and Triassic flysch with intercalated pelagic limestone) and parautochthonous (Jurassic and Cretaceous limestone), is overlain by an overthrust complex of metamorphic rocks, sediments, and volcanics (Permian schist, Jurassic radiolarian jasper, Jurassic and Cretaceous slates, Eocene limestone, conglomerate and tuffs, and lower Miocene reef limestone and tuff); eruptive rocks of Mesozoic and Miocene age; and a thick, tectonically chaotic marl and shale with lenses of massive limestone. Intense deformation accompanied by overthrusting took place during the Miocene. In the Pliocene, a postorogenic series of coarse clastics (molasse) was formed, and at the end of the Tertiary the island was eroded to sea level and invaded by the sea, while reefs grew up along its margins. Rapid uplift that brought the island to its present height started in the Pleistocene, while the Timor Trough subsided. This uplift is probably still continuing. According to van Bemmelen (1949, pp. 510–545), the island and its neighbours form part of the outer Sunda orogenic arc, while the Timor Trough represents the foredeep separating it from the Australian continental block. In general, the structural trends of Timor are parallel to the axis of the island.

Vening Meinesz, Umbgrove, & Kuenen (1934), on the basis of gravity measurements at sea, described a broad belt of negative isostatic anomalies bordering the outer Banda Arc and extending into the Timor Trough. Gravity measurements on Timor itself in 1949 and 1954 (Lemoine, 1959, p. 205) show the existence of strong positive Bouguer anomalies along the north coast (up to +160 milligals) and weak negative Bouguer anomalies along the south coast (—20 milligals). Gravity observations on R.V. *Argo* in 1960 (Helfer, Caputo & Harrison, 1962) indicate positive

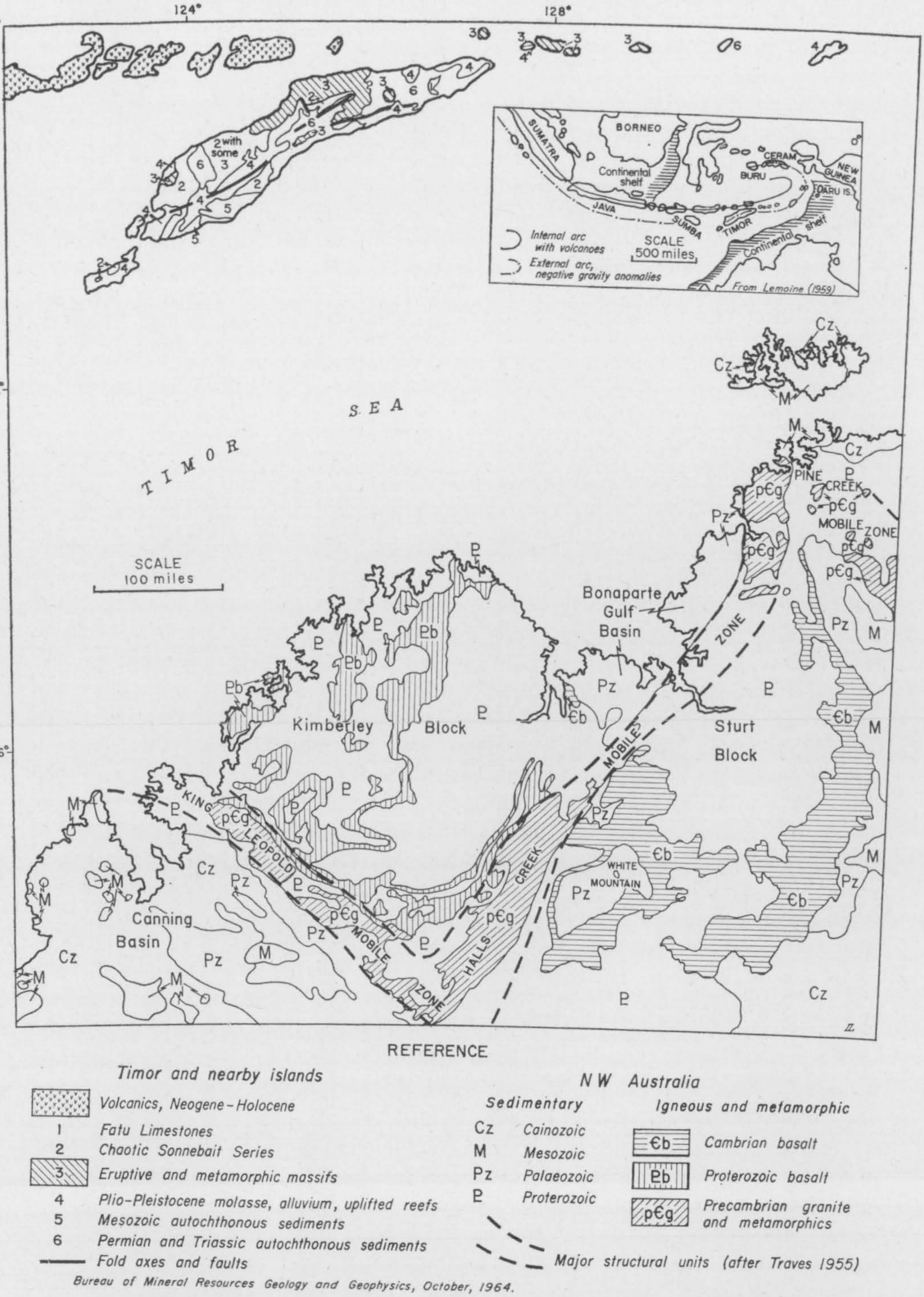

Fig. 2.1—Geological map of the land areas bordering the Timor Sea. Simplified after the *Geological Map of Australia and Oceania*, **and Lemoine (1959).**

Bouguer anomalies over the Trough (+65 milligals at 9° 47′ S., 126° 48′ E.; 50 nautical miles from the south-east coast) and negative anomalies nearer the island (—42 milligals at 9° 25′ S., 126° 10′ E.; 20 miles from the coast).

No greater geological contrast can be found than that which exists between Timor and the parts of Australia bordering on the Timor Sea. Against the changeful geological history of Timor, spanning a brief 250 million years, may be set the long, monotonous history of north-western Australia, with its basement of Archaean and older Proterozoic crystalline rocks that are at least 2000 million years old. This basement is overlain by barely disturbed younger Proterozoic and Palaeozoic sediments (mainly quartzose sandstones) and basic volcanics. Mesozoic rocks, which exceed a thickness of 1000 feet on Melville and Bathurst Islands and in the Canning Basin to the south but are much thinner elsewhere, are the final major deposits of this long history. The main structural units of the area (Fig. 2.1), as described by Traves (1955), are (1) the King Leopold and Halls Creek Mobile Zones of older Precambrian crystalline rocks and younger Precambrian folded and faulted sediments, (2) the Precambrian Pine Creek Mobile Zone of older Precambrian sediments and granite, (3) the Sturt Block of low-dipping younger Precambrian sediments, (4) the Kimberley Block of low-dipping Precambrian sediments and volcanics, and (5) the Bonaparte Gulf Basin of low-dipping to horizontal Palaeozoic sediments and Mesozoic residuals. Major faults and joint systems in the blocks and basins parallel the trends of the adjoining mobile zones.

Many areas of north-western Australia are covered by a thick weathered crust, lateritic and siliceous in nature (duricrust), which contributes a large amount of material to the rivers. The crust is most completely preserved on the divides, but it has been generally stripped away on lower terraces in the valleys. It is probably of upper Cretaceous to middle Tertiary age. Only incipient lateritization has taken place during the Quaternary.

Besides alluvial valley fill, the only other Cainozoic deposits are the Tertiary freshwater sandy clays and sandstones, which are up to 100 feet thick, of Bathurst and Melville Islands, and the White Mountain Formation (Traves, 1955). The latter is represented by 300 feet of siltstone and sandstone capped by chert containing Gastropods (*Planorbis*) and Foraminifera of probable young Tertiary age (Fig. 2.1). The work of A. R. Lloyd (1966), who has found the same Foraminifera in numerous other deposits in northern Australia, indicates that these sediments are the product of a widespread middle Tertiary transgression. Such a transgression must have extended more than 150 miles inland and would require subsequent uplift of the entire land area to its present position at 1000 feet above sea level. It is worth noting that in New Guinea the middle or late Miocene was a period of widespread basin subsidence and transgression, during which even the stable shelf of South New Guinea was invaded by the sea (Visser & Hermes, 1962, p. 198). The White Mountain Formation possibly belongs to this transgressive phase.

The stratigraphy of the Bonaparte Gulf Basin (Traves, 1955) is a record of repeated marine invasion followed by uplift and denudation. Fairbridge (1953) has discussed the structural similarities of the three western Australian sedimentary basins and has traced their seaward extensions on to the continental shelf and slope. He has suggested that the western and north-western Australian region has been part of the continental block since Precambrian times and has undergone a series of limited transgressions and regressions, each following essentially the same structural lines.

The Cainozoic geomorphology of north-western Australia, discussed by Christian & Stewart (1953), Stewart, Twidale, & Bradley (1960), Wright (1963), Paterson (in press), and Hays (1966), encompasses a series of erosional surfaces. The oldest surface recognized by Hays is the pre-Cretaceous Ashburton-Murchison Surface (= Gondwana Surface of King, 1949). The next younger surface, the Tennant Creek Surface (= Australian Surface of King; Bradshaw Surface of Wright), is a composite one. The southern part was carved by southward scarp retreat out of the Ashburton-Murchison Surface, and the erosional products were deposited as the freshwater and marine Lower Cretaceous sequence. Lateritization of the southern part of the surface had started by the Upper Cretaceous. Concomitant with the retreat of the sea during continued uplift in the early Tertiary, lateritization spread northward over the newly exposed folded and eroded Lower Cretaceous sediments; it even spread over the post-Cretaceous freshwater sands and clays of Bathurst and Melville Islands. Therefore, the Tennant Creek Surface is diachronous.

The Wave Hill Surface (= Maranboy Surface of Wright) was carved out of the Tennant Creek Surface, probably in the Miocene, and some of the erosional products perhaps were deposited in a southerly advancing sea as the White Mountain Formation. During and after the retreat of this sea, the area was warped and faulted to produce prominent features such as the Joseph Bonaparte Gulf, Daly River drainage basin, Pine Creek Upwarp, Van Diemen Gulf, and Melville and Bathurst Islands. Antecedent streams deepened their valleys and later were drowned by the sea to form features such as Apsley and Dundas Straits. The White Mountain Formation was uplifted to almost 1000 feet above sea level, and erosion has since developed a local relief of 500 feet.

A complex erosional and depositional Coastal Plain Surface (Koolpinyah Surface; Hays, 1966), in which several stages can be recognized, developed during the Pleistocene. This surface has been only incipiently lateritized.

No specialized geomorphological work has been done in the north Kimberley area; present knowledge, summarized by Stewart, Twidale, & Bradley (1960), essentially agrees with Hays' description. King (1949) considers that the Kimberleys constitute a relic of the Gondwana surface, and Hays (personal communication) regards the oldest surface represented in the eastern part of the Kimberleys to be older than the Tennant Creek Surface.

To illustrate the land surfaces of the northern part of the Northern Territory, topographic cross-sections (Fig. 2.2) have been prepared from recently published contour maps. In order to provide ready comparison with cross-sections of the Sahul Shelf, to be presented later, the vertical exaggerations of the sections are the same as those in Plate 4. Where recognized, the various surfaces described by Hays have been indicated. Section AA′ shows these surfaces converging near the coast and separating inland at the Pine Creek Upwarp. East-west Section CC′, situated some 10 miles south of Darwin, is typical of the greater part of the region. This section shows lower relief than Section AA′ and elevations of accordant summits between 150 and 200 feet.

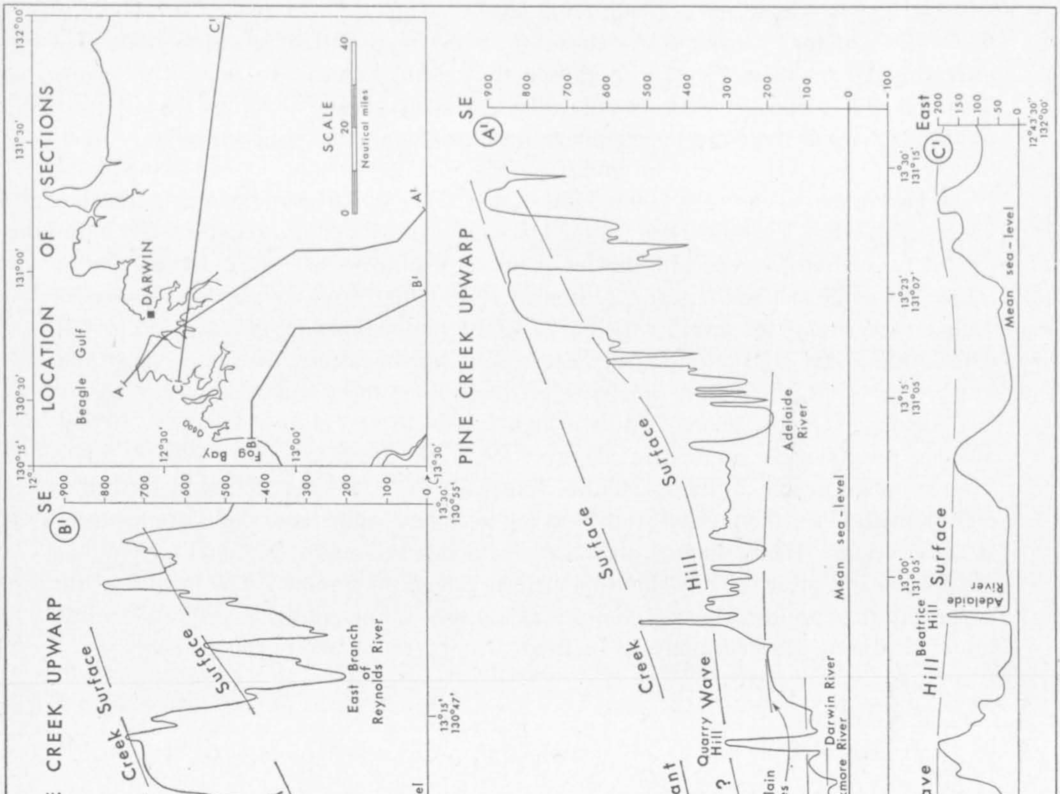

Fig. 2.2—Topographic cross-sections of the north-western part of Northern Territory, Australia. Vertical exaggeration corresponds to that of Plate 4. The sections were drawn from contour maps to the scale 1 : 50,000 (contour interval 50 feet), published by Royal Australian Survey Corps. Section AA' from maps 5073-II, 5072-I, 5072-II, 5172-II, 5171-IV, 5171-III; section BB' from maps 4972-II, 5072-III, 5071-I, 5071-II; section CC' from maps 5272-I, 5272-IV, 5172-I, 5172-II, 5072-I, 5072-IV.

During the Quaternary, eustatic sea level changes led to repeated drowning of the mouths of major rivers and deposition of extensive estuarine sediments. The intermittent rises in sea level also caused the mature streams to deposit extensive flood plain alluvium in their broad valleys. Hays (1966) identifies four depositional episodes in the Mary River plains north of Pine Creek and considers it likely that several sea level changes of enough importance to produce distinct depositional cycles have taken place. Christian & Stewart (1953) and Paterson (in press) postulate a recent fall of sea level of 20 feet for the Darwin and Ord-Victoria regions, accounting for the exposure of extensive estuarine plains now above sea level, but they give no evidence for the age of the plains. Stewart et al. (1960) have found no evidence for such a lowering of sea level in the north Kimberley region, nor has Russell (1963), who studied sea cliffs along the western and north-western coasts of Australia. Fairbridge (1954, 1958), on the basis of raised shorelines and radiocarbon dates, has postulated the presence of a recent high sea level stand at approximately 10 feet, but his results have been seriously questioned by Shepard (1961, 1964). Shells from a ' raised beach ' in the Joseph Bonaparte Gulf (V–386) were dated by the radiocarbon method for the present study and found to be recent; these shells are regarded as adventitious. Thus there is no reliable evidence for sea level stands higher than the present one after the low stand of the last glacial maximum. The history of the streams in the regions, which is complex as a result of low gradients and low divides, cannot, without detailed analysis, be used to unravel the geomorphic history.

Coastal morphology

The coastal morphology of north-western Australia is complex. The north-eastern side of the Kimberley Block is a moderately high cliff coast, oriented approximately parallel to the trend of a major joint set which itself parallels the King Leopold Mobile Zone. Along the southern Joseph Bonaparte Gulf, the coast is a broad plain of mud flats up to 15 miles wide that includes the estuaries of the Ord and Victoria Rivers. A considerable amount of suspended mud is carried through these estuaries into the open sea. The eastern side of the Gulf coast line consists of low lateritized outcrops of Permian and Mesozoic rocks, and of modern coastal sediments.

Melville and Bathurst Islands have a superstructure of 1000 feet of low-dipping Cretaceous sediment, overlain in the northern part by about 100 feet of Tertiary freshwater deposits. The islands are a low-dipping cuesta, 400 feet high, with a short scarp face along the south edge and a long dip-slope face toward the north. Morphologically, the islands form a unit; Apsley Strait, which divides them, probably originated as a result of Pleistocene drowning of a north-flowing river.

The south coast of Timor is bordered by a narrow coastal plain 1 to 7 miles wide and is fed by numerous small streams. Most of the plain is an uplifted depositional shoreline terrace; the estuaries and deltas of the Australian coast are lacking. This condition is a reflection of continuing uplift of the island that began in the Pleistocene and exceeds the postglacial rise in sea level which drowned the rivers of north-western Australia.

According to Joubin (1912) and Fairbridge (1950), fringing reefs occur on the north and east coasts of Melville Island and on the north coast of Bathurst Island, intermittently along the mainland coast south of Melville Island to the Victoria River estuary, and on the Kimberley coast east of Cape Londonderry. The south coast of Timor, with two exceptions, is free of living coral reefs (Joubin, 1912), but they skirt almost the entire island of Roti. Platform reefs, such as the Holothuria Banks and others (Fairbridge, 1950), are widespread on the inner part of the Sahul Shelf, just off the north Kimberley coast. They form a broad zone from Cape Londonderry westward. Seaward from this area, platform reefs, several of them having islands, are developed along the Londonderry Rise. To the west of the area studied, several atolls also occur on the deeper outer shelf (Scott Reef, Seringapatam Atoll), all of which have been described in some detail by Teichert & Fairbridge (1948). These authors assume that the banks have been formed entirely by reef growth; however, reef capping on rock prominences is a possible alternative, at least for the larger shoal reefs.

3. Climate and Oceanography

Climate

Both Timor and north-western Australia have a monsoon climate, with a wet season during the north-west monsoon (summer) and a dry season during the south-east monsoon (winter). In north-western Australia, the south-east monsoon is augmented by the south-east trade winds. The dry season lasts from July to October on the south coast of Timor (Silva, 1956) and from May to October in north-western Australia. The mean annual rainfall on the south coast of Timor ranges from 60 inches at Fohorem to 120 inches at Iliomar. In north-western Australia, the rainfall varies from 60 inches (range 30 to 80 inches) on the coast at Darwin to 15 inches at Gordon Downs, 200 miles inland. The coastal strip of north-western Australia is warm and humid; Darwin has a mean annual temperature of 82° F. with a small diurnal range and a mean relative humidity of 68 percent. Wyndham, with only 26 inches of rainfall and an annual mean relative humidity of 52 percent, has Australia's highest recorded mean temperature of 84° F. Thunderstorms occur up to 100 days per year on the north Kimberley Coast, and up to 85 days per year at Darwin. This subequatorial coastal climate extends inland for a distance ranging from 90 miles south-east of Darwin to 10 miles south of Wyndham. Farther inland, to a distance of 150 miles, the rainfall drops off progressively to 15 inches, humidity decreases, and the diurnal temperature range increases. At sea the mean annual precipitation of 37·5 inches is exceeded considerably by a mean annual evaporation of 71·5 inches (Wyrtki, 1961, Table 2).

The Timor Sea lies athwart the shifting boundary between the south-east trade winds and the monsoon. The monsoon blows from the south-east from April to November, and from the north-west from December to March. The trade and monsoon winds augment one another from April to November (the dry season), when the dominant wind is from the south-east quadrant (Fig. 3.1). The sum of hourly winds recorded on R.V. *Stranger* from 6 to 20 April 1961 (Fig. 3.1, inset)

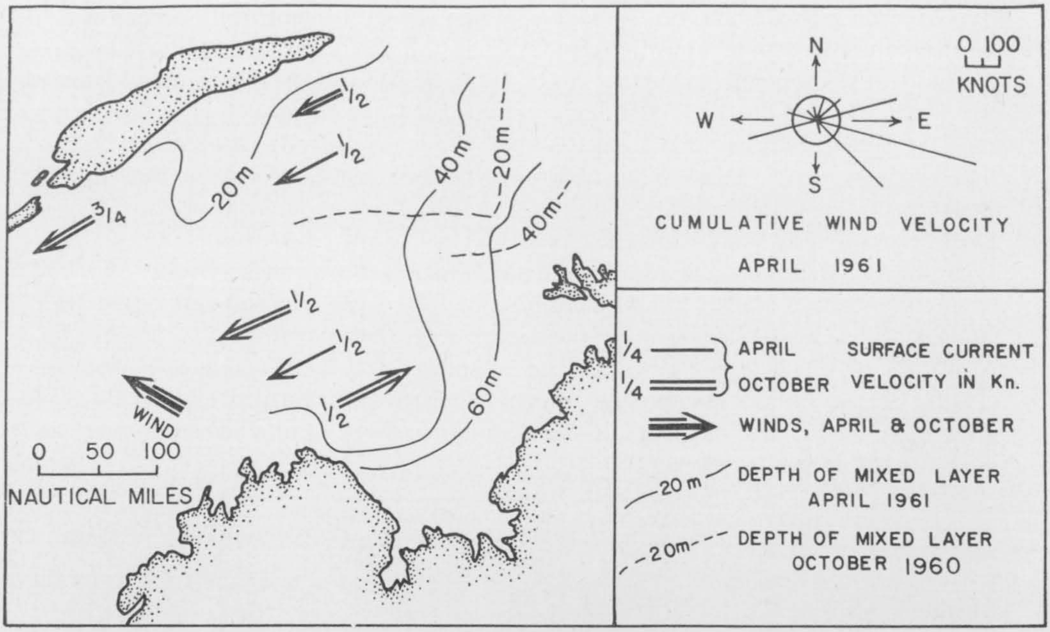

Fig. 3.1—Wind and current distribution in the Timor Sea. Data from Wyrtki (1961) and Royal Dutch Meteorological Institute (1949).

shows that the dominant wind in this period blew from the sector 60° to 150°; the only other wind of any significant magnitude blew from 240° to 270°. The strongest wind recorded was 24 knots, and it came from the dominant direction of 90° to 120°.

From December to March (the wet season) the wind at sea is variable due to interaction between the south-east trades and the north-west monsoon. In January the south-east trades are deflected and blow with little force almost parallel to the north-western Australian coast toward the north-east. North-westerlies prevail in March, giving way in April to the south-east trades.

Tropical cyclones, lasting from 12 to 24 hours, occur in the period December to April. Commonly the winds reach velocities of 50 to 90 knots, exceptionally as great as 140 knots. Squalls that occur from October to April, rarely lasting longer than 3 hours, develop winds of 30 to 100 knots.

Drainage

Main drainage and maximum altitudes of the lands bordering the Timor Sea are shown in Figure 3.2. The River Benain, which is 70 miles long, is the longest of the rivers that drain the southern half of Timor. The total area of Timor draining into the Timor Sea is 5500 square miles. By contrast, about 250,000 square miles of north-western Australia drain into the Timor Sea.

No records of discharges and sediment loads are available for the streams of Timor, and only incomplete records are available for those of north-western Australia (Table 3.1). Measurements of suspended sediment exist for only the Ord River, at a gauging station 50 miles upstream from the river mouth. The average annual suspended sediment load is 7,000,000 tons; the average sediment content of flood waters, which account for 80 percent of the total discharge, is 0·3 percent. No records of bed load exist.

TABLE 3.1
DISCHARGE OF RIVERS IN NORTH-WESTERN AUSTRALIA*

River	Mean annual discharge in millions m^3	Maximum recorded monthly discharge in millions m^3	Drainage area in square miles
Ord	3500 (1944–59)	14,439 (Jan., 1959)	17,000
Daly	2600 (1960–63)	....	18,000

* Based on information received from the West Australian Department of Public Works and from the Northern Territory Administration, Division of Water Resources.

The rivers of north-western Australia flow only intermittently, because of the sharply defined dry and wet seasons: after heavy showers in the wet season, they overflow their banks, but in the dry season they shrink to a series of waterholes. These great fluctuations in flow lead to constant changes in the local importance of erosion, transport, and deposition. Most rivers have long gorges cut through resistant strata and have broad, alluviated tracts. The gradient is low everywhere; the Ord River is only 600 feet above sea level 280 miles above its mouth, and the Victoria River is 500 feet above sea level 300 miles above its mouth.

Oceanography

Present knowledge of the oceanography of the Timor Sea is based on scattered observations made from numerous British, French, and Dutch ships, starting in the early 1800's. However, unlike the Banda Sea to the north, which has been the subject of several oceanographic expeditions, the Timor Sea still awaits detailed study. The most complete treatment to date has been given by Wyrtki (1961; see also Rochford, 1962, 1963); some additional information obtained on Scripps cruises in 1960 and 1961 has been added here.

Sea and swell. Strong, gusty winds during the dry season (south-east trades) are responsible for moderate to rough seas; the main swell is from the south-east. During the north-west monsoon, the sea is usually smooth to moderate, except when disturbed by squalls; the swell comes from the north-west, west, and south-west. In April 1961, wave height did not exceed 3 feet and the sea was calm most of the time. In October 1960, the highest recorded waves were 3 to 5 feet; later, during the R.V. *Malita* survey in November-December 1960, the sea usually was mirror smooth, occasionally ruffled by a squall.

Surface circulation. According to Wyrtki (1961, pp. 26–27), a south-westward current prevails throughout the year in the Timor Sea, its axis running close to the coast of Timor (Fig. 3.1). From April to September this current reaches the Australian coast, although its velocity decreases in that direction. From October to

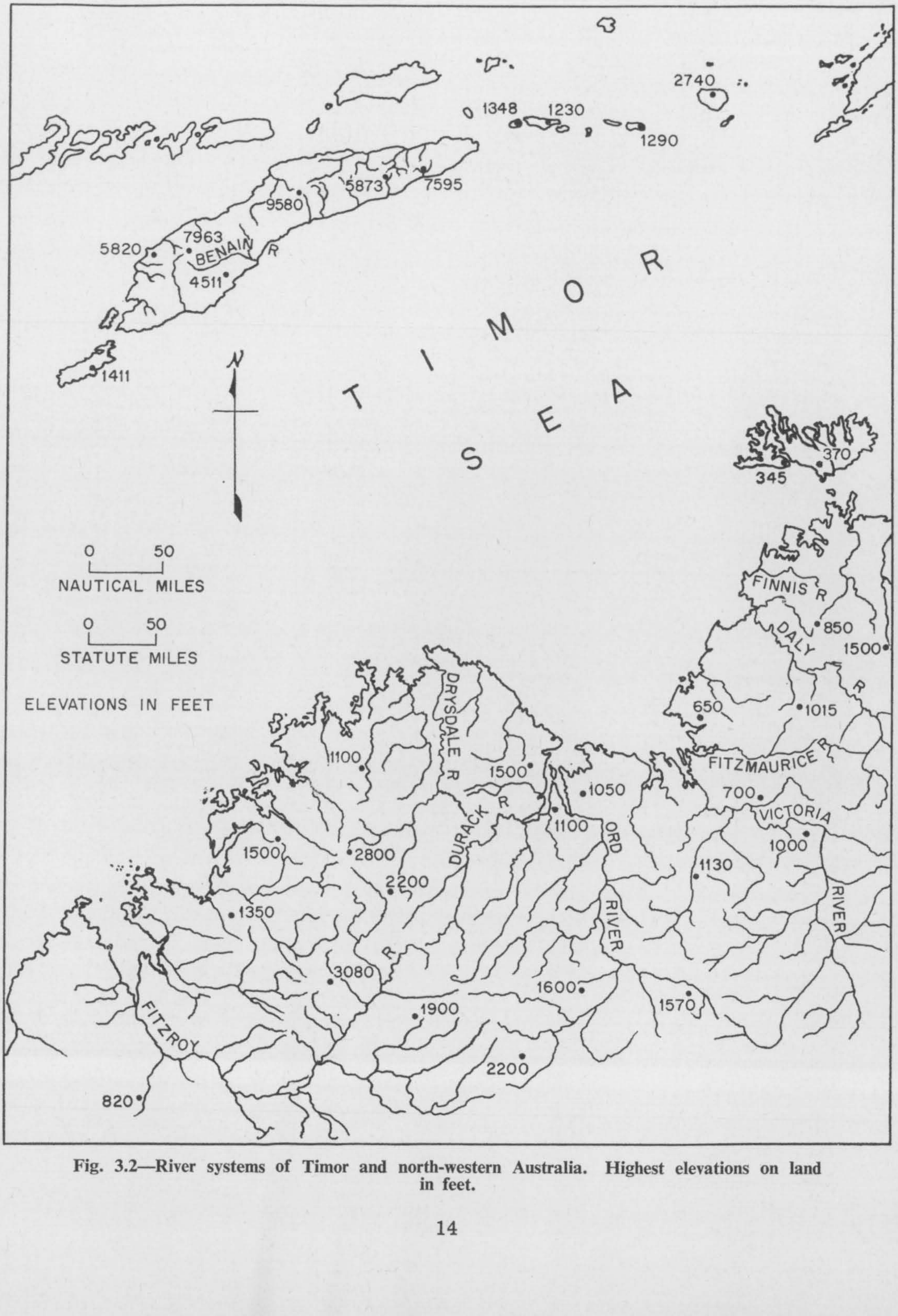

Fig. 3.2—River systems of Timor and north-western Australia. Highest elevations on land in feet.

March the south-easterly winds create a weak local current toward the north-east off the Australian coast. During October to April, the Timor Current derives its water from a current that flows eastward along the north coast of the Lesser Sunda Islands, turning around the eastern end of Timor. Only at the time of the full development of the south-east monsoon, from June to September, is the Timor Current supplied by water from the upwelling region in the Arafura and Banda Seas. Wyrtki (1961, p. 136, Table 12) has calculated that the Timor Current transports between $1 \cdot 0$ and $1 \cdot 5 \times 10^6$ cubic metres/second westward. For comparison, the Gulf Stream transports 25×10^6 cubic metres/second through the passage between Cuba and Florida.

Temperature. During August the minimum mean monthly temperature of the surface waters in the Bonaparte Gulf is 23° C. (73·4° F.: Royal Dutch Meteorological Institute, 1949). The maximum exceeds 29° C. (84° F.) from November to February. Throughout the year the air and surface water temperatures are approximately the same; the water is slightly warmer (about 0·2 C.) than the air except from June to August, when the reverse is true.

During the R.V. *Stranger* cruise in April 1961, maximum recorded temperatures were 31·3° C. (88·3° F.) in the Bonaparte Gulf (station V–186) and 28·7° C. (83·7° F.) near the south-east coast of Timor (V–257). During the cruise of R.V. *Argo* in October 1960, surface water temperatures ranged from 27·0° C. (80·6° F.) to 31·0° C. (87·8° F.).

Structure. Bathythermograph records taken in April 1961 indicate that waters within about 60 nautical miles of the Australian coast and Bathurst Island (out to the 35-fathom contour) are mixed down to the bottom. Farther seaward the base of the mixed layer rises closer to the surface in depths ranging from 20 to 50 metres. A few observations made from R.V. *Argo* in October 1960 in the area north-west of Bathurst Island show that the top of the thermocline lies between 20 and 50 metres, about 30 metres shallower than it was in the same area in April 1961 (Fig. 3.1). These observations agree with Wyrtki's (1961, p. 31) summary: 'Over the Sahul Shelf the homogeneous layer reaches down to the bottom in the shallower parts, but over the deeper parts water of higher density is found below the homogeneous layer which is about 40m deep.' A hydrocast in the Bonaparte Depression at station V–277 (65 fathoms), taken in April 1961, showed a temperature decrease from 30·94° C. at the surface to 27·32° C. at the bottom, and a decrease of the oxygen content from 4·37 ml/L at the surface to 2·77 ml/L near the bottom. These values are normal for water of this depth.

According to Wyrtki (1961, p. 99), deep Indian Ocean water enters the Timor Trough from the south-west over the sill between the Sahul Shelf and the island of Roti. The deeper entering water is probably Antarctic Intermediate Water (Rochford, 1963), while between 200 and 500 metres water from the Northern Indian Ocean is introduced in the Trough (Rochford, 1964a). The temperature minimum in the trough lies only a little below the sill depth of 1940 metres, and the oxygen content is relatively high. A hydrocast taken on R.V. *Stranger* at station V–319, at the deepest point of the basin (3220 metres), showed very close agreement with Wyrtki's values for temperature minima and oxygen concentration (Fig. 3.3).

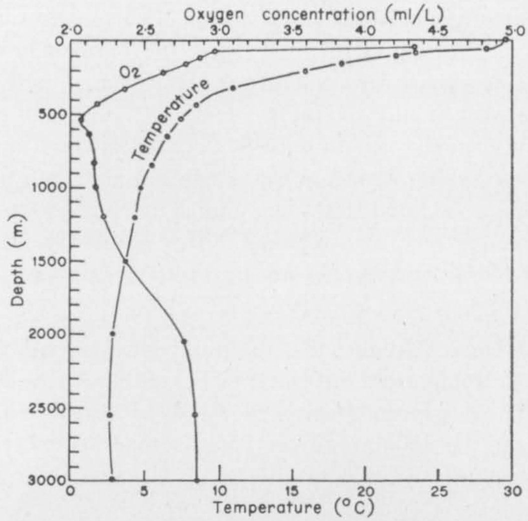

Fig. 3.3—Vertical distribution of temperature and oxygen content in the Timor Trough at station V-319 (location on Plate 5).

The possible occurrence of upwelling along the edge of the Sahul Shelf is controversial (Rochford, 1962; Wyrtki, 1962). This problem will be discussed in Chapter 10 in connexion with the distribution of organic matter.

Tides. The semidiurnal tides of the Indian Ocean prevail in the Timor Sea, and, according to Wyrtki (1961), the tidal amplitude reaches more than 200 cm (6·6 feet) over large parts of the Sahul Shelf and increases to a maximum of 900 cm (29 feet) in Queen's Channel. The range at Darwin is 600 cm (20 feet). Strong currents are generated by these tides, particularly in the numerous estuaries, and may be major agents in scouring the shallower parts of the sea floor and in transporting sediment. The *Australia Pilot* (British Admiralty, Vol. 5, 1948) reports tidal currents up to 7 knots in the Victoria River estuary and up to 6 knots in the Cambridge Gulf. The tidal wave coming from the Indian Ocean advances faster over the deep Timor Trough than over the Sahul Shelf, causing considerable refraction and generally alternating north-westerly and south-easterly currents.

SUBMARINE MORPHOLOGY AND STRUCTURE

4. Morphological Description

Surveys and data

Bathymetric data for the Sahul Shelf and Timor Trough are available from a variety of sources. The coverage and origin of the principal sets of observations used are shown in Figure 4.1.

During the 1960 and 1961 Scripps cruises, echo-sounding records were obtained on the shelf with an EDO-UQN echo-sounder, and in the trough with a Precision Depth Recorder (PDR, Westrex Corporation) and an EDO transceiver. Continuous records are available for nearly the entire track of both cruises. Positioning was by astronomical fixes and dead reckoning, radar fixes on Timor, and shore sights near the Timor coast and the entrances to Darwin. In areas covered by the Royal Australian Navy (R.A.N.) surveys, the cruise track was adjusted to the more accurate R.A.N. charts. No adjustments have been made in the Scripps surveys for differences in tidal level; consequently, the shelf depths are accurate only to approximately 2 fathoms. The deep-water soundings have not been corrected for changes in sound velocity with temperature, depth, and salinity.

Between 1944 and 1958, several detailed surveys of the approaches to Darwin were carried out by the R.A.N. (Chart AUS 309; locations on Fig. 4.1). These surveys are based on anchored buoys positioned by astronomical fixes, and the data have been reduced to Indian Low Water Springs. For the present study, copies of the original smooth sheets were individually contoured on a 5-fathom interval, reduced photographically to a uniform scale of approximately 7·5 nautical miles to the inch, and compiled into a contour map with 10-fathom contours. Occasionally, sounding discrepancies at the margins of some adjoining and overlapping sheets required adjustment. Agreement between our own soundings and those of the R.A.N. is generally good except for minor position adjustments, due to less accurate positioning of the Scripps vessels.

Soundings obtained by the 1960 and 1961 Scripps cruises, by R.V. *Argo* of Scripps during the 1960 Monsoon Expedition, and by the Snellius Expedition in 1929–1930, were used for the Timor Trough. Irreconcilable discrepancies between the Snellius data, obtained with a visual readout echo-sounder (Kuenen, 1935), and our own data are fairly common, so that only a small portion of the Snellius data could be used.

The resulting bathymetric chart (Pl. 1) is uneven in quality. Considerable detail is shown in the region covered by the R.A.N. surveys; south-east and north-west of this area, only broad generalized contours based on Scripps data and published hydrographic charts are given. In the southern region, these contours are probably quite realistic; all records show smooth bottom and gentle slopes, and little or no irregular relief. The north-western part of the shelf area, on the other hand, has complex relief and rapid depth changes and cannot be contoured properly on the basis of the available data. The relief in this area probably is quite similar to that shown in the northernmost R.A.N. sheets. To indicate the topography of the shelf edge and shelf edge banks, use has been made of chart AUS 309; the bank pattern certainly is not accurate, and some of the shoals shown have not been confirmed.

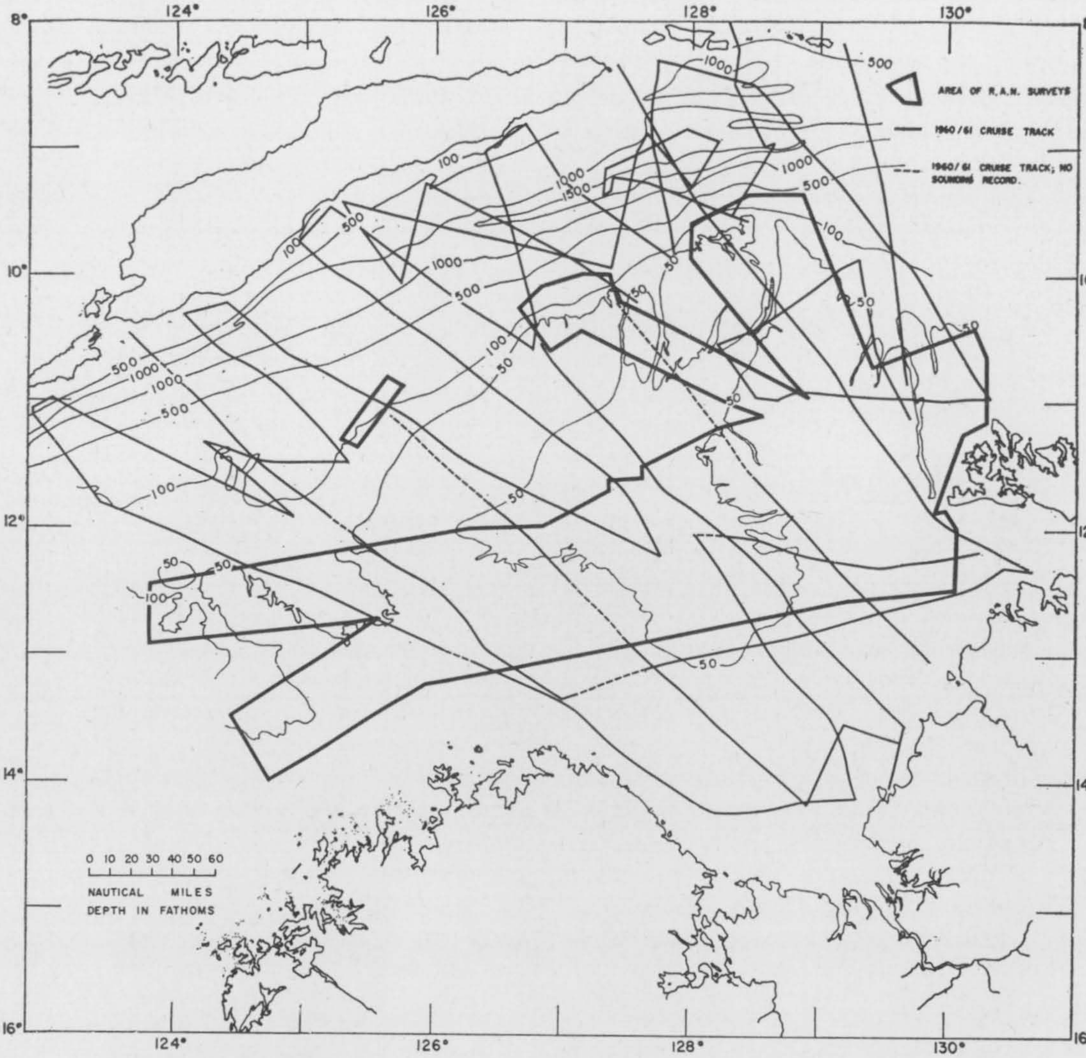

Fig. 4.1—Bathymetric coverage of the Timor Sea by Royal Australian Navy surveys (heavily outlined areas) and expedition tracks of R.V. *Malita* (1960) and R.V. *Stranger* (1961).

The topography of the Timor Trough is broadly generalized, and where details of the relief are shown, they must be considered a representation of the type of relief rather than of the precise shape and location of its features. This is particularly true of the complex area in the north-eastern part of the trough.

General description of the area; the Timor Trough

Two morphological provinces can be distinguished within the area of study: the *Sahul Shelf* and the *Timor Trough*, separated by the shelf edge and a complex system of banks on the upper continental slope (Figs 4.2, 4.3). The Sahul Shelf is a broad, shallow platform that forms the seaward extension of the Australian continent. It is some 350 to 400 nautical miles wide at its widest point and has a maximum depth of 134 fathoms in a shelf valley. The shelf has a flat bowl shape (Figs 4.2, 4.3) with a broad central depression, the Bonaparte Depression. This depression is generally smooth, having gentle slopes, a maximum depth of approximately 80 fathoms, and few hills and banks. Its south-eastern extension forms a large embayment in the Australian coastline, the Bonaparte Gulf. The depression is surrounded in the south-west, north-west, and north-east by shallow elevations, the Londonderry, Sahul, and Van Diemen Rises; it is connected with the Timor Trough by a narrow, winding, deep valley, the Malita Shelf Valley. The rises generally deepen toward the north-west from minimum depths of 15 to 20 fathoms and are studded with banks and traversed by channels.

The Timor Trough is an elongate, moderately deep basin that forms part of van Bemmelen's (1949, p. 53, Pl. 41) Sunda Foredeep, separating the outer Sunda Arch from the stable Australian Platform. The portion of the Timor Trough discussed in this paper is about 100 nautical miles wide and attains a maximum uncorrected depth of 1752 fathoms. At its south-western end the Timor Trough is separated from the Indian Ocean by a sill with a depth of approximately 1000 fathoms. In the east, a sill of less than 1200 fathoms separates the Timor Trough from the more easterly Sermata and Aru Basins, which also reach depths in excess of 1700 fathoms.

The north-western slope of the Timor Trough is highly irregular, with numerous steep hills, pinnacles, steps, and scarps (Fig. 4.4). Although the regional gradient averages approximately 3°, local slopes are often 10° or steeper. West of 125° 30′E., the steps and terraces are generally narrow, and a single slope exists; east of this longitude the region north of the basin axis is complex and contains several subsidiary, sometimes flat-floored troughs. These troughs widen eastward and are separated by ranges of hills (Fig. 4.4, Sections a-c; Fig. 4.5). Sounding coverage is inadequate to delineate the complex topography of this area, but its structural trend, parallel to the trend of the Timor-Leti-Sermata island chain (van Bemmelen, 1949, pp. 472–479), is clear.

The floor of the deepest part of the Timor Trough is variable in width and shape (Figs 4.5, 4.6). Sections with a flat floor alternate with uneven bottom, sometimes suggestive of slumping (Fig. 4.6, Sections G, I, J), and at both ends the trough narrows to a V-shape. The width varies from 1 to 7 nautical miles. The flat floors have one or more subsurface reflecting horizons at depths varying from 2 to 8 fathoms below the surface (Fig. 4.6), indicating recent rapid filling. Longitudinally (Fig. 4.5), the trough slopes gently eastward at approximately 10 feet per mile from the western sill to a deep point at 125° 20′ E. Eastward are a small rise (Fig. 4.5), and then another east-north-east slope of 18 feet per mile to the deepest point near station V–319. At this point a detailed survey (Fig. 4.7) shows walls of 6° to 12° bordering the flat floor. The floor here has a local north-easterly slope of about 18 feet per mile at a very slight angle to the basin axis, indicating a sediment source on the southern side due south of V–319. The variability in slope, depth, and morphology along the axis of the Timor Trough suggests that the trough is composed of several sub-basins, which are now largely filled.

The south-eastern slopes of the Timor Trough are generally smooth with only occasional small hills and valleys (Fig. 4.4). In the upper part, the slope varies from 0·3 to 1·0°; the lower part is generally somewhat steeper (2–3°). Major irregularities are rare. North of Hibernia Reef (Fig. 4.4, profile f), a steep scarp occurs from 230 to 340 fathoms, above a small flat-floored subsidiary basin. North-east of Echo Shoal (Fig. 4.4, profile c), a broad basin with an undulating floor interrupts the slope; east of here the slope is irregular and several steeper slopes and scarps occur. Beyond 128° 30′ E. the slope again is smooth and gentle.

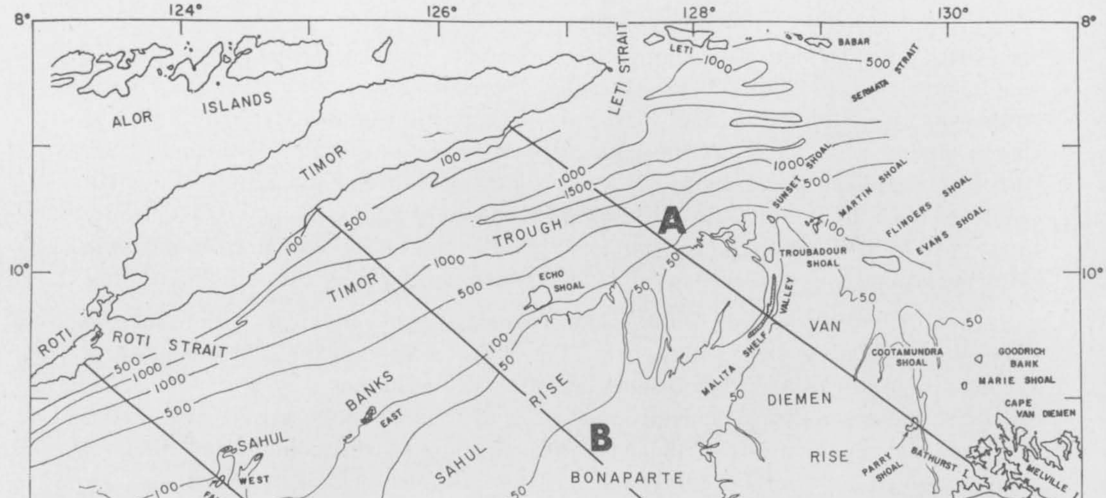

Fig. 4.2—Generalized morphology of the Timor Sea, and geographical names of the Timor Sea region; location of the cross-sections shown on Fig. 4.3.

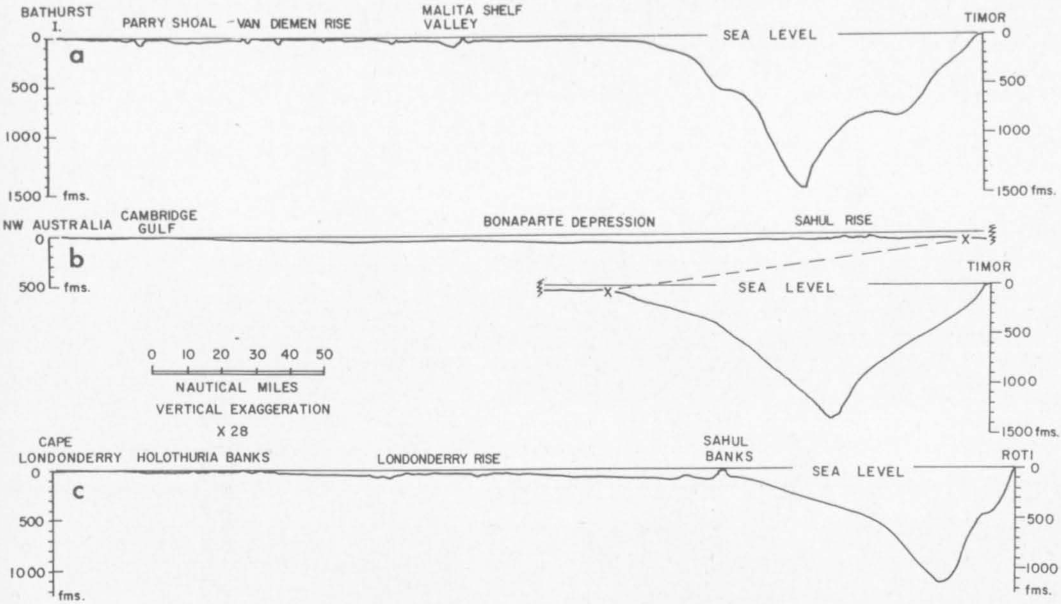

Fig. 4.3—Generalized southeast-northwest cross-sections of the Sahul Shelf and Timor Trough. Locations on Fig. 4.2.

South-east of the eastern tip of Timor, the Australian slope is steeper than the Timor slope (Fig. 4.4, Section b); in Sections c and d, the slopes are equal, and in Sections e and f the Timor slope is steeper. This migration of the position of the steepest slope is an expression of the fact that the axis of the Timor Trough is slightly oblique to the parallel trends of Timor and the Sahul Shelf edge (Fig. 4.5). This pattern would arise if a crust of uniform thickness and composition were subjected to stress along a north-south direction. The main components of the stress would then be normal and parallel to the lineaments of Timor and the Sahul Shelf edge and would produce a trough with its axis oblique to these lineaments.

The sounding lines are approximately perpendicular to the basin strike. Hence, the presence or absence of submarine canyons and slope valleys cannot be established with certainty. Several small V-shaped valleys occur in the sounding profiles (shown schematically in Fig. 4.6).

The morphology indicates that principal deposition in the history of the Timor Trough has taken place on the south-eastern slopes and on the bottom of the trough. The long, smooth depositional slopes of this side of the trough suggest a long history of uninterrupted deposition. Only locally, between 123° and 124° E. and between 127° and 128° E., are these slopes affected by possibly structurally controlled irregularities. On the north-western side, on the other hand, structural effects appear to control the morphology entirely, even though Timor and other sediment sources are near.

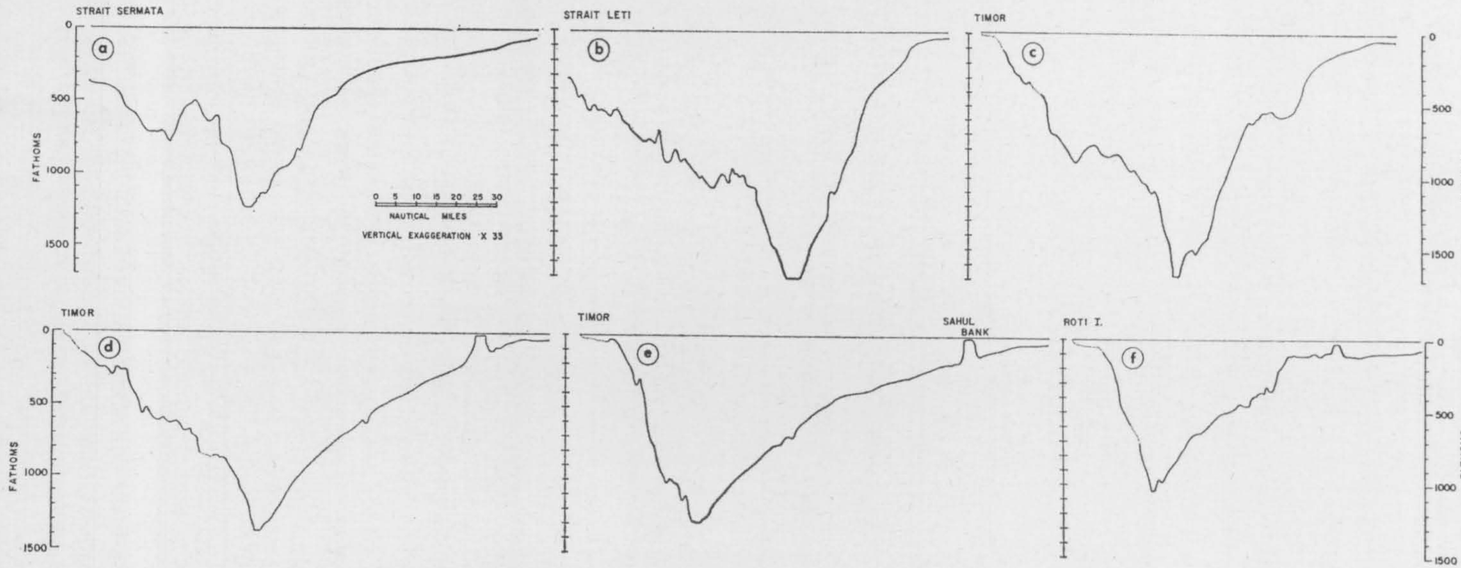

Fig. 4.4—Cross-sections of the Timor Trough, compiled from echo-sounding records of R.V. *Stranger* expedition, 1961. North and west on the left; locations on Fig. 4.5.

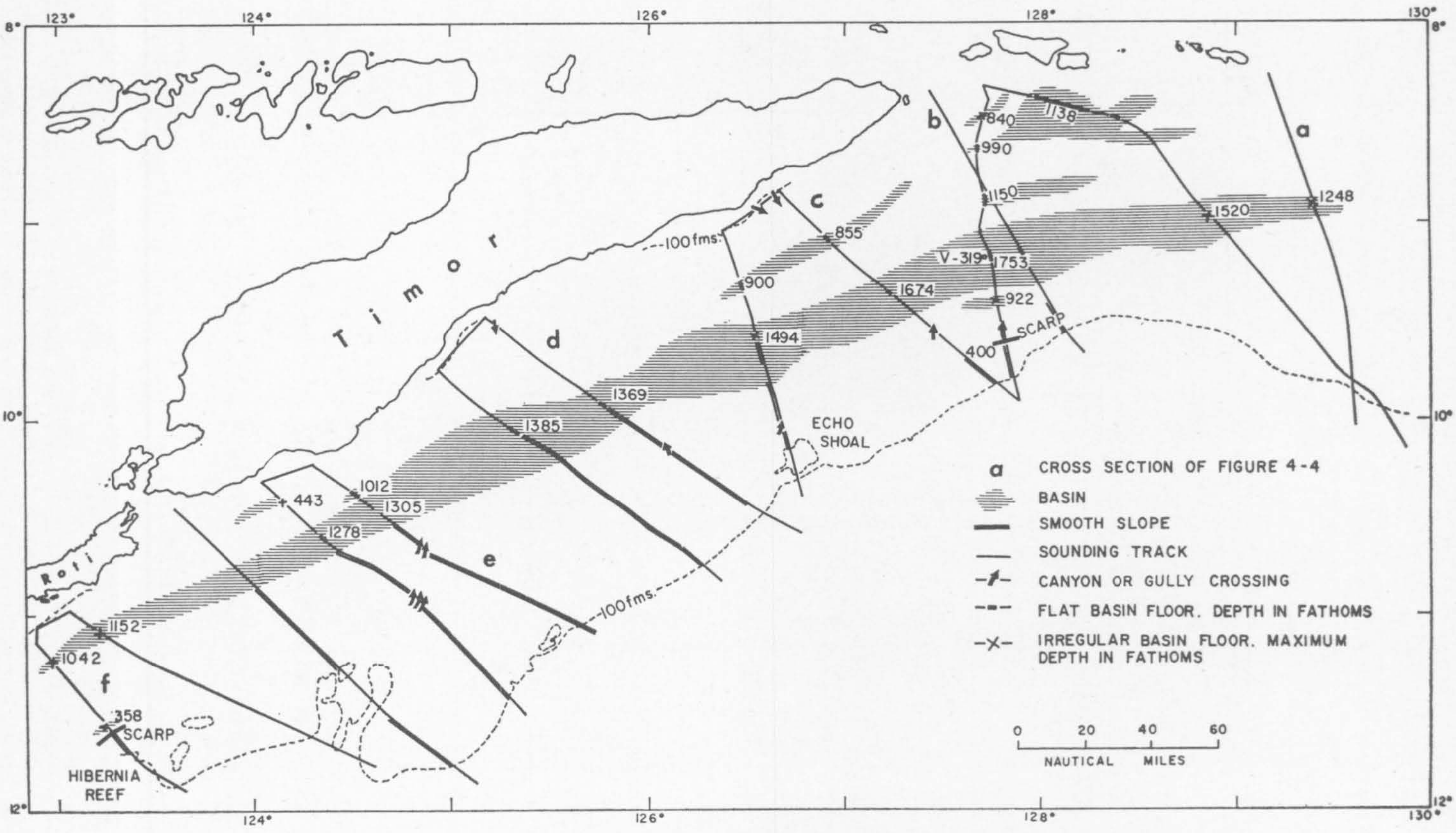

Fig. 4.5—Morphological features of the Timor Trough. Shelf edge simplified. Cross-sections of Fig. 4.4 are indicated by thin lines and letters.

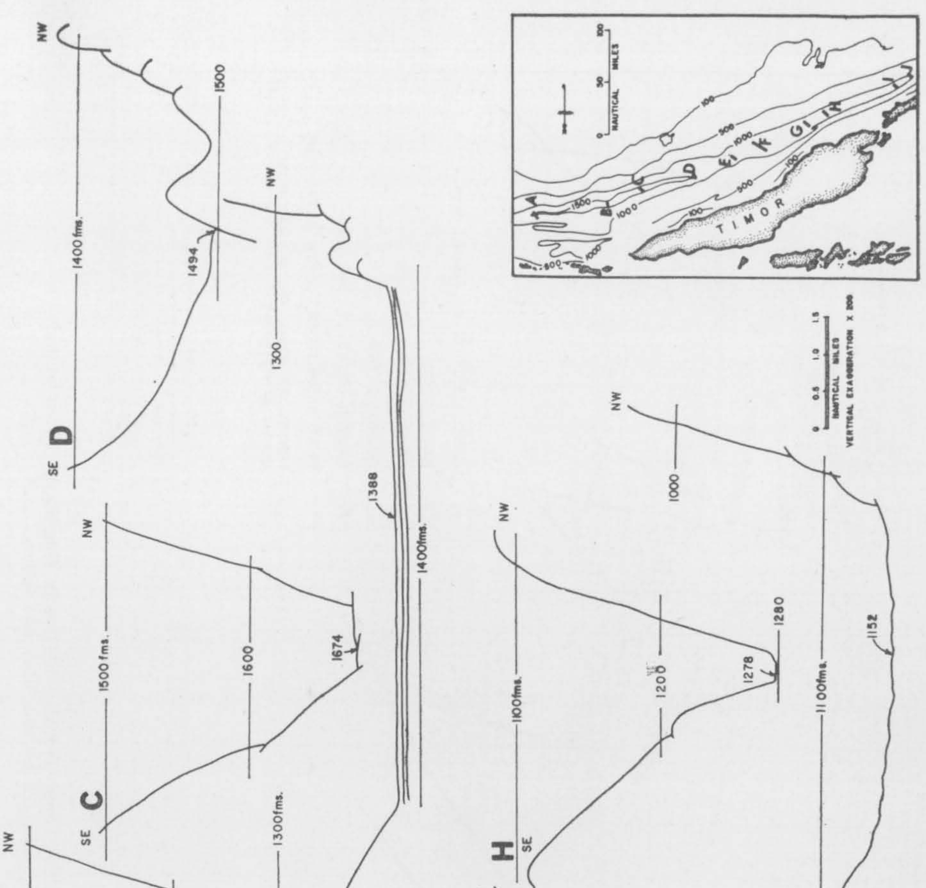

Fig. 4.6—Cross-sections of the floor of the Timor Trough and adjacent slopes. Traced directly from echo-sounding records of the 1961 R.V. *Stranger* expedition. Locations on insert. Subsurface reflectors are shown in sections B, E, and F. Note parabolic side echoes on steep slopes and hilly floors.

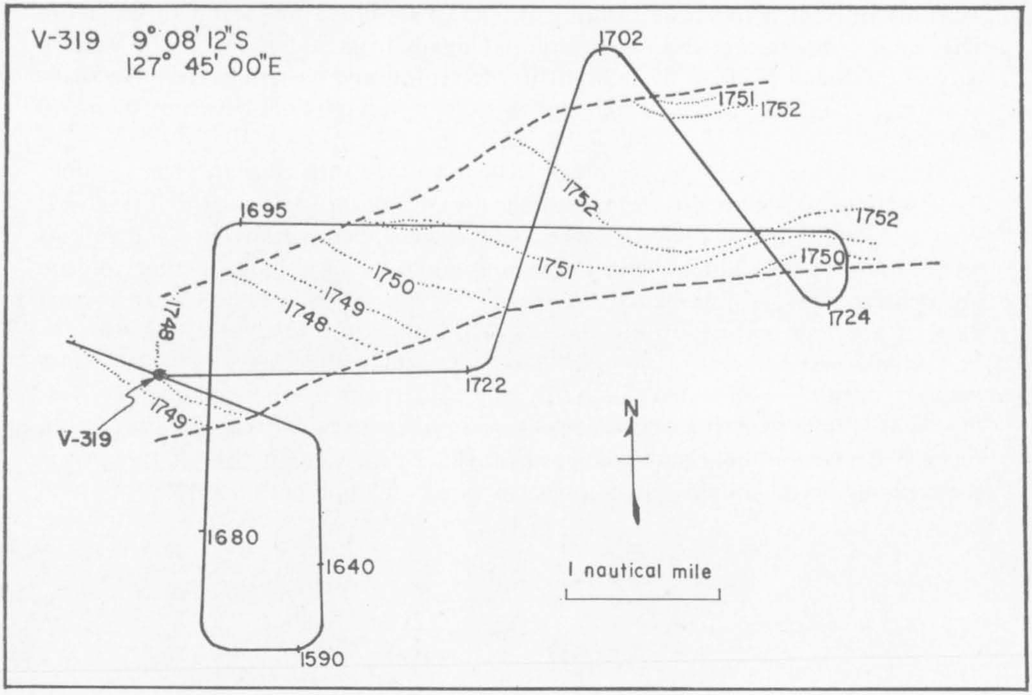

Fig. 4.7—Detailed contours (dotted lines) of a small portion of the floor of the Timor Trough at its deepest point near station V-319 (location on Fig. 4.5). Slope topography not shown. Depths are in fathoms and are uncorrected. Heavy solid line is survey track, heavy broken line is edge of flat floor. Navigation by dead reckoning from astronomic fix on station V-319.

Shelf edge and shelf edge banks

A narrow zone of rather complex topography, comprising the uppermost portion of the continental slope, its banks, and the shelf edge, forms the boundary between the Timor Trough and the Sahul Shelf. The uppermost continental slope is generally smooth, has a low gradient (0·3–0·5°), and is cut only locally by gullies and minor canyons. This large area of gentle, even slopes suggests a major depositional apron bordering the edge of the Sahul Shelf.

Kuenen (1935) and Fairbridge (1953; Teichert & Fairbridge, 1948) mention a major break in slope and abrupt downward steepening at approximately 300 fathoms along the margin of the Sahul Shelf, which they considered the structural edge of the Australian Platform. From its great depth, as compared to the usual depth of shelf edges (approximately 72 fathoms, Shepard, 1963, p. 257), these authors inferred major downwarping of the platform edge, related to the deformation of the Timor Trough. The information now available shows clearly that in the area of this investigation such a major, persistent break at considerable depth does not exist (Fig. 4.4). From the bottom of the trough the slope gradually decreases upward, and the only regional break in slope is located at approximately 60 to 75 fathoms. It is usually marked by a small scarp, 5 to 10 fathoms in height (Fig. 4.8, profiles 2, 5, 6, 8). This scarp, a common feature on continental shelves of the world, is generally attributed to erosion during the late Pleistocene low stand of sea level. The depth of the foot of this scarp varies regionally from 78 fathoms in the western part of the Sahul Shelf to 56 fathoms in the central and eastern parts. No scarp exists east of 129° E., where the change in slope is very gradual between 50 and 70 fathoms.

From 125° E. to 129° E., the break in slope and the shelf edge are close together and the 60- to 100-fathom contours describe the edge of the shelf quite well (Fig. 4.9) West of 125° E., the shelf edge is more complicated. Gentle transverse undulations between 60 and 200 fathoms give the various contours an irregular outline, and no well-defined break in slope exists. A sharp shelf edge exists only north of Hibernia Reef, at approximately 100 fathoms (Fig. 4.8, profile 9). Elsewhere, the scarp at 76 fathoms lies well within the shelf, and a broad, undulating outer shelf exists beyond. The complexity may be partly due to deposition around numerous shelf edge banks rather than to the existence of a structural pattern. Except for the portion between Barracuta Shoal and Vulcan Shoal (Pl. 2), the western part of the area is not well surveyed. In this portion a clear break in slope occurs between 50 and

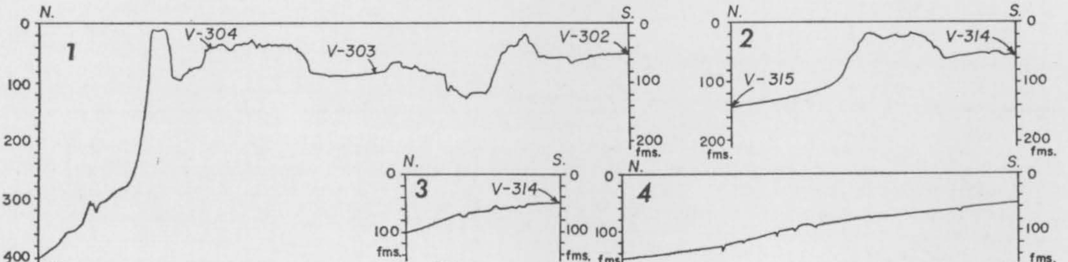

Fig. 4.8—Cross-sections of the edge of the Sahul Shelf and of the shelf edge banks. Traced directly from echo-sounding records of the 1961 *Stranger* expedition. Locations on Fig. 4.9.

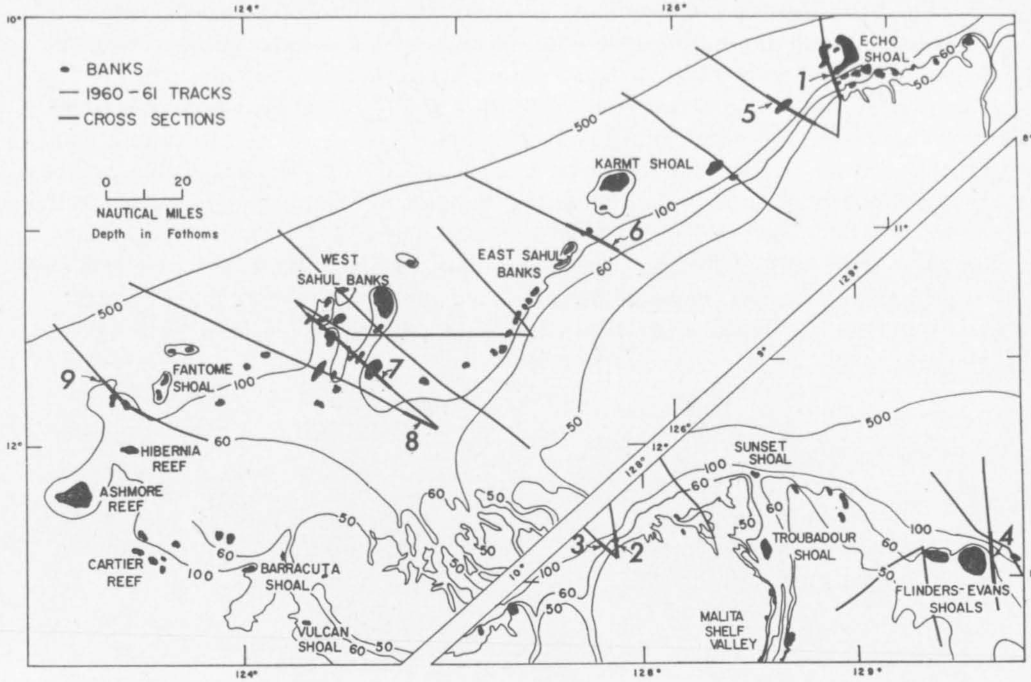

Fig. 4.9—Bathymetry of the edge of the Sahul Shelf, and distribution of shelf edge banks (shown in black). Upper left: western part; lower right: eastern part. Thin lines are sounding tracks of 1961 *Stranger* expedition; heavy numbered lines indicate cross-sections of Fig. 4.8. Bathymetry between 126° and 129° East longitude contoured from surveys by the Royal Australian Navy.

60 fathoms, but at 90 fathoms the bottom levels out to form a wide outer shelf. According to Fairbridge (1953), this outer shelf terminates in a break in slope at 300 fathoms.

The edge of the shelf nearly everywhere is bordered by banks, to which Fairbridge (1950) has referred as a 'broken barrier'. The existing hydrographic charts (e.g., AUS 209) show numerous shoals in this region, although many of them are unconfirmed. Figure 4.9 shows all these shoals, together with those confirmed by the R.A.N. detailed surveys and the Scripps soundings. Most banks are small and no more than a few miles in diameter (Pl. 2). Larger banks seem to be complexes of small banks grouped close together and surrounded by depositional aprons (Echo Shoal, Pl. 2, West Sahul Banks). The banks normally have steep slopes varying from 12 to 33°, with an average of 20° (Table 4.1); an irregular talus slope usually is found at the bottom (Fig. 4.8). The bank tops are remarkably flat; ridges and pinnacles are rare.

On the upper continental slope, most banks rise from depths varying from 180 to 110 fathoms. No banks have been found at 300 fathoms, as reported by Teichert & Fairbridge (1948) and Fairbridge (1953); the hydrographic charts show some banks at this depth, but our survey has not confirmed their existence. East of Echo Shoal many banks rise from the shelf edge and outer shelf in depths from 90 to 50 fathoms.

The banks form a nearly continuous string along most of the shelf margin; of 15 crossings made during the 1960–1961 surveys, all but three crossed at least one bank. Eastward from 125° E., the banks are spaced in a narrow, linear belt. The individual knolls are separated from each other and from the shelf edge by narrow, deep depressions, the East Sahul and Echo Shoal groups (Pl. 2) presenting good examples; it is possible that the entire area has essentially the same pattern. The West Sahul group, on the other hand, is a complex non-linear cluster located both on the flat outer shelf in 100 to 110 fathoms and on the upper slope. Individually, however, the banks are very similar to those farther east. Westward, available information is inadequate; banks on the outer shelf and upper slope seem to be common between Fantome Banks and Hibernia Reef, and from Ashmore Reef to Vulcan Shoals.

TABLE 4.1
CHARACTERISTICS OF SHELF EDGE BANKS

	Slope in degrees	Outer base in fathoms	Flat tops in fathoms	High pinnacles in fathoms	Terraces and knickpoints
Fantome Bank Region			10–15(6)	4(2)	
North of Hibernia Reef	12–14	110, rising from outer shelf (2)	18(4)		
Ashmore Reef-Cartier Island-Vulcan Shoal			16–18(7) 8–0(4)		
West Sahul Banks	19–33	110–115 (outer shelf) 130–160 (upper slope)	12–13(8)		35(2), 41(3) 51–52(5)
East Sahul Banks	15–21	110–150(8)	11–12(7)	7(1)	38(1), 51–52(2), 62(1)
Echo Shoal	15–27	160–180(3)	36–38 (main level) 14–17 (banks, 4)	12(3)	
Echo Shoal, inner banks	13–15	110–120(9)	24–28 (main level) 17–19(9)		38(1)
Troubadour Shoal—Evans Shoal			20(2) 12(3) 7–8(3)		

Numbers in parentheses are number of observations.
Slopes, terraces and knickpoints, and base depths taken from 1960–1961 Scripps surveys; tops from these and R.A.N. surveys and AUS 209.

An interesting group in the central part of the region is formed by Echo Shoal and banks farther east to Sunset Shoal. Echo Shoal itself (Pl. 2) is a large platform with a principal surface at 36 to 38 fathoms, cut by channels. From this surface smaller knolls rise to 20 to 18 fathoms, with occasional pinnacles at 12 fathoms. Near the shelf edge is a linear group of smaller banks, which is very similar in size and distribution to the East Sahul group, except for a shallower base and a deeper top (Table 4.1). The inner members of this group are incorporated within the shelf edge. This inner group of banks has a main platform of 24 to 28 fathoms, with minor flat-topped ridges at 17 to 18 fathoms, generally located on the northeastern side. The shape of the contours, especially in the eastern part of the area, suggests strongly that this group of banks, originally similar to the Sahul Banks, has become included in the shelf through depositional outbuilding.

In addition to the major bank top levels, the terraces, knickpoints, and subsidiary surfaces are quite commonly developed at 50 to 55, 36 to 38, 24 to 25, and 17 to 19 fathoms (Table 4.1). All of these may be related to erosion at former lower sea level stands.

Over most of the area, the tops of the banks are remarkably close to 12 fathoms (Table 4.1; Fig. 4.8). Such a 12-fathom level has been observed in other parts of the world (Fairbridge, 1961; Shepard, 1963, p. 367). Curray (1960) has assumed a temporary still stand of the rising postglacial sea at that level; it is also possible that the sea rose to a maximum at that level prior to the last glaciation (Curray, 1961). Reef growth on the banks may have continued to the 12-fathom level but failed to keep pace with the rapid changes that occurred later. Alternatively, erosion may have planed the banks at that point during sea level stands lower than those to which the reefs had been adjusted by growth.

The positions relative to the shelf edge and the depths of the bank tops show an interesting symmetry along the margin of the Sahul Shelf. The highest tops occur both in the extreme east and west; the lowest occur in the central portion, where the majority of the banks also are incorporated in the shelf edge. Teichert & Fairbridge (1948) have explained the banks as being coral reefs, which started in shallow water and continuously grew upward, while the edge of the shelf subsided since the late Tertiary. If this theory is correct, and other evidence discussed in the next section supports it, the central banks may have ceased to grow sooner than those to the east and west, perhaps as a result of rapid deposition on the outer shelf that made them part of the shelf edge.

Teichert & Fairbridge (1948) considered that the Sahul Banks and banks farther east are analogous to the shelf edge banks west of our area (Scott Reef, Seringapatam Atoll, Ashmore Reef). The detailed data presented here show that there is a major difference between the small but numerous submerged banks in the area of study, and the large circular reefs and atolls, often 20 miles in diameter, that break the surface farther west. The Sahul Banks show no evidence of having originated as atolls or large shoal reefs. On the whole, they rather closely resemble a poorly developed barrier of the Great Barrier Reef type (Fairbridge, 1950).

Geomorphology of the Sahul Shelf

The topography of the Sahul Shelf (Pl. 1), which, compared with that of most other continental shelves, is highly complex, consists of two principal morphological elements: (1) a regional system of rises and depressions, and (2) a superimposed topography of banks, terraces, and channels. The major rises and depressions have been named by Fairbridge (1953), but the data now available indicate that the pattern is rather more complicated than that shown in his paper (compare Figs 4.2 and 4.10 with Pl. I, Fairbridge, 1953). In addition to the two transverse rises distinguished by Fairbridge, a third one exists which parallels the shelf edge and is separated from the Van Diemen Rise by the Malita Shelf Valley. The Van Diemen Rise itself contains a central depression oriented east-west. South of the Van Diemen Rise, several isolated banks form an east-west trend passing through Flattop Bank. The Londonderry Rise also is complex and consists of an eastern and a western branch, separated by a depression with numerous channels. The western branch seems to extend as far as Ashmore and Hibernia Reefs, although topographic control for its north-western portion is quite inadequate. It is this west branch that seems to be the seaward continuation of the Kimberley Block referred to by Fairbridge. The arcuate eastern branch extends from Cape Londonderry to the western end of the Sahul Rise. East of the east branch is a series of large banks. Its relation to the Sahul and East Londonderry Rises is obscured by considerable dissection and by a lack of topographic control at its northern end.

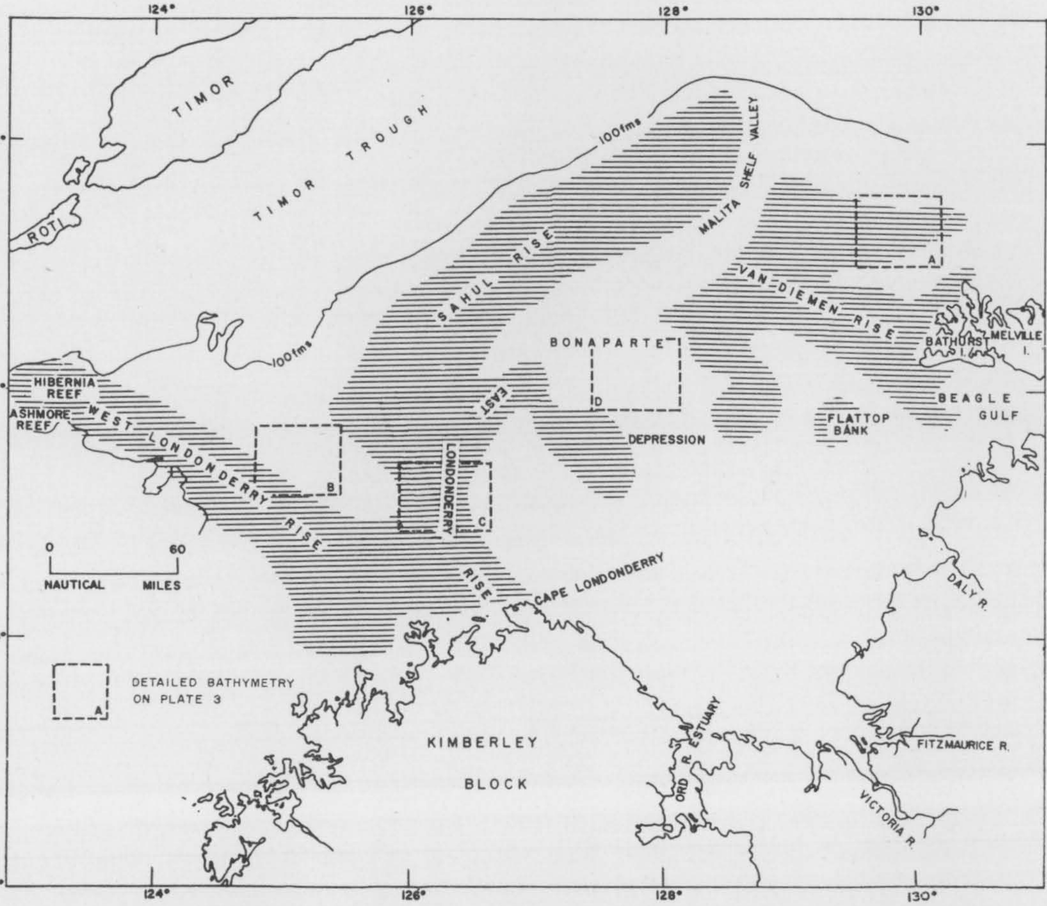

Fig. 4.10—Regional topography of the Sahul Shelf. Rises are shown by shading. Areas outlined by broken lines and indicated with letters are shown in detail on Plate 3.

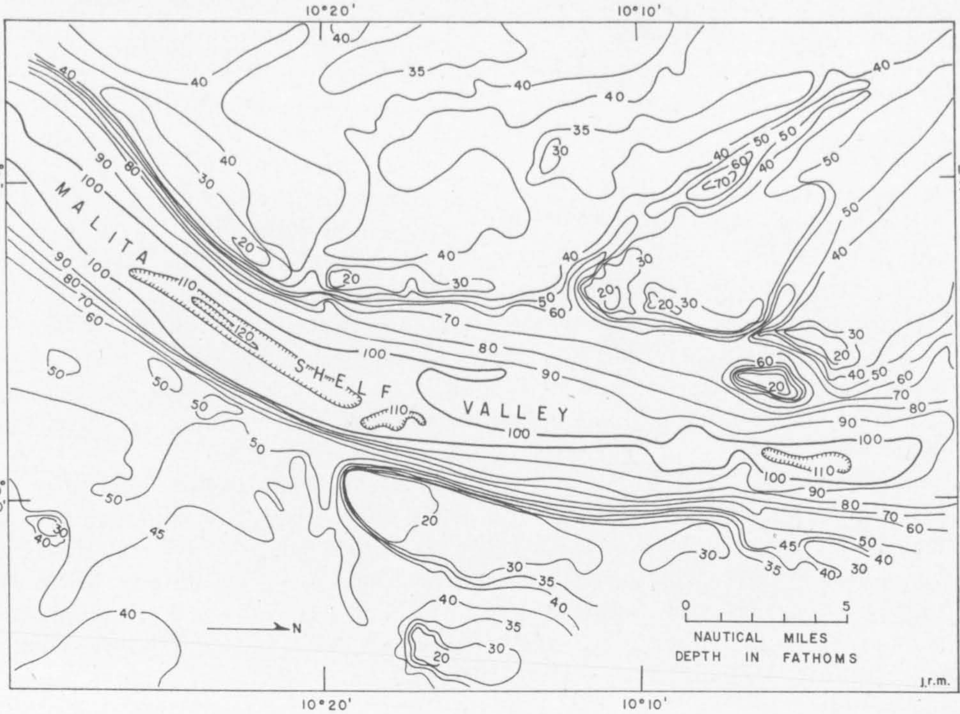

Fig. 4.11—Detailed bathymetry of the Malita Shelf Valley and bordering banks. Contoured from surveys by the Royal Australian Navy.

The Van Diemen, Sahul, and East Londonderry Rises surround the Bonaparte Depression, which funnels into the Malita Shelf Valley toward the north-east. The east flank of this depression is quite steep, the west flank very gentle. Southward, the depression merges into a broad, featureless plain, which apparently is a depositional apron originating from the streams between the Beagle Gulf and the Ord River Estuary.

The Malita Shelf Valley (Fig. 4.11) is a long, narrow, curved channel connecting the Bonaparte Depression with the Timor Trough. It has a maximum depth of 134 fathoms in the central part between the Sahul and Van Diemen Rises. Near the shelf edge the depth of the channel is approximately 60 fathoms, and where the valley joins the Bonaparte Depression the maximum depth is 76 fathoms. At the narrowest point the width is about 3 nautical miles, and the sides are quite steep (Fig. 4.11; Fig. 4.12; profiles g, h). The valley is fringed on both sides by small, steep, oblong or round banks rising from fairly deep water (Fig. 4.11). These banks are similar to the shelf edge banks described earlier and may have the same origin.

The intricate relief of banks, terraces, and channels that is superimposed on the broad regional topography (Figs 4.12, 4.13) is illustrated by four detailed bathymetric maps on Plate 3. Closely spaced banks separated by narrow and somewhat sinuous channels characterize the Van Diemen Rise (Pl. 3-A; Fig. 4.12, profiles a, b, d, e, f, i). The tops of the banks are quite flat; the slopes are steep (7–19°) and occasionally are interrupted by terraces. On the north and south flanks of the rise, the level of the bank tops gradually slopes down from 15 to 30 fathoms; farther down, the banks are replaced by broad terraces. Westward, the slope is more abrupt. The channels have a northerly trend and traverse the entire rise, including its central depression. The deepest parts of the channels occur where they cut through the highest parts of the rise (Fig. 4.14); here channel depths vary from 60 to 110 fathoms below sea level, and from 40 to 90 fathoms below the rims. All channels shoal toward the outer shelf, where they end at a fairly uniform depth of 50 to 55 fathoms (Fig. 4.13). In the central depression, the channels are broad, shallow, and poorly defined (Fig. 4.12, profile a). The topography of the banks, the parallel orientation, and the shape of the channels render the Van Diemen Rise very similar to Bathurst and Melville Islands, and it may actually represent a submerged continuation of the same landscape. The Van Diemen Rise also strikingly resembles the Aru Islands, which are farther north on the shelf between Australia and New Guinea (Fairbridge, 1951; Verstappen, 1959).

The crest of the Sahul Rise is close to its south-eastern margin; here there is a zone of banks that are similar to those of the Van Diemen Rise, although not so high. The central and north-western parts of the rise do not have many banks, but instead they are characterized by broad terraces with flat surfaces. Several transverse channels with northerly trends are found where the Sahul Rise is well mapped (Fig. 4.13); farther west, other channels have been crossed by single sounding lines (Fig. 4.12, profile k). The channels of the Sahul Rise also are deeper in their central parts than at both ends, and they shoal to 50 to 55 fathoms on the outer shelf (Fig. 4.13). This may be attributed either to recent deformation of the rises, or, more probably, to closing of both ends of the channels by bars during the post-glacial sea level rise.

On the Londonderry Rise, banks are numerous but generally widely spaced and separated by broad terraces and relatively wide, shallow channels (Pl. 3-B, C). The principal channel system crosses the east branch with a westerly trend and is deflected northward in the depression between the east and west branches (Fig. 4.13). Again, the channels are deepest where they traverse areas of high banks, shoal toward the inner and outer ends, and are less well developed in the central part of the rise.

The Bonaparte Depression (Pl. 3-D) is an area of gentle slopes and subdued relief. A few widely scattered banks rise from 10 to 40 fathoms above the basin floor (Fig. 4.12, profile 1). The deepest part, which has a maximum depth of 80 to 85 fathoms, is located close to the eastern margin of the basin. Channel systems occur on the east and west flanks, but not in the deep area that connects the Depression with Malita Shelf Valley. The east and west flanks have broad, stepped, level terraces that are bounded by small scarps (Fig. 4.12, profiles m, o, p) and descend toward the basin center. Subsurface reflections in many sounding records (Fig. 4.12, profiles 1, m, n, p) indicate the presence of buried hard surfaces or beds of different lithology at shallow depths ranging from 2 to 12 fathoms below the surface. Some of these surfaces appear to be buried channels or depositional onlap on to highs. The subsurface reflections and the smooth topography so sharply contrasting with that of the rises suggest relatively rapid, recent deposition in the depression.

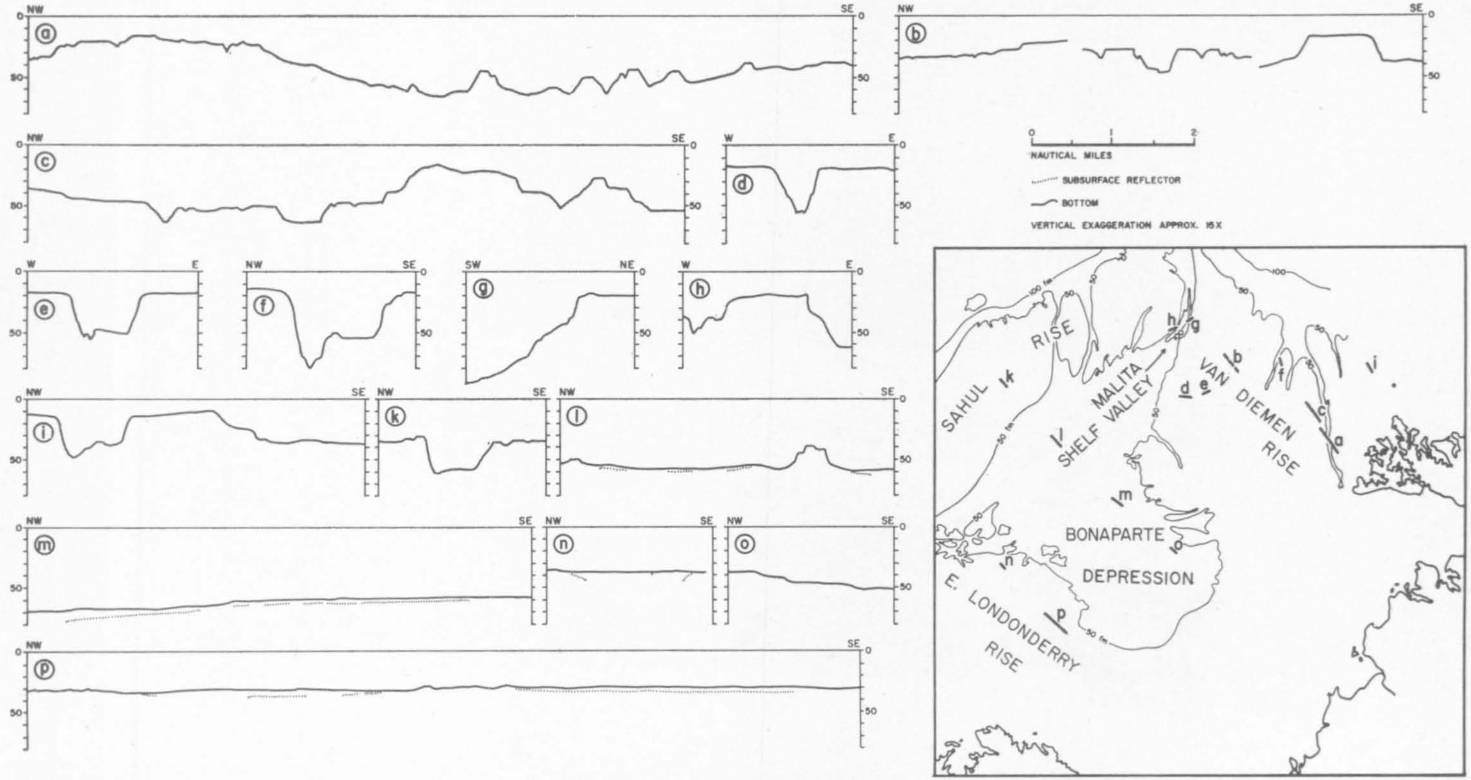

Fig. 4.12—Cross-sections of characteristic features of Sahul Shelf relief. Subsurface reflectors shown as dotted lines. Traced from echo-sounding records of the 1960 *Malita* and the 1961 *Stranger* expeditions.

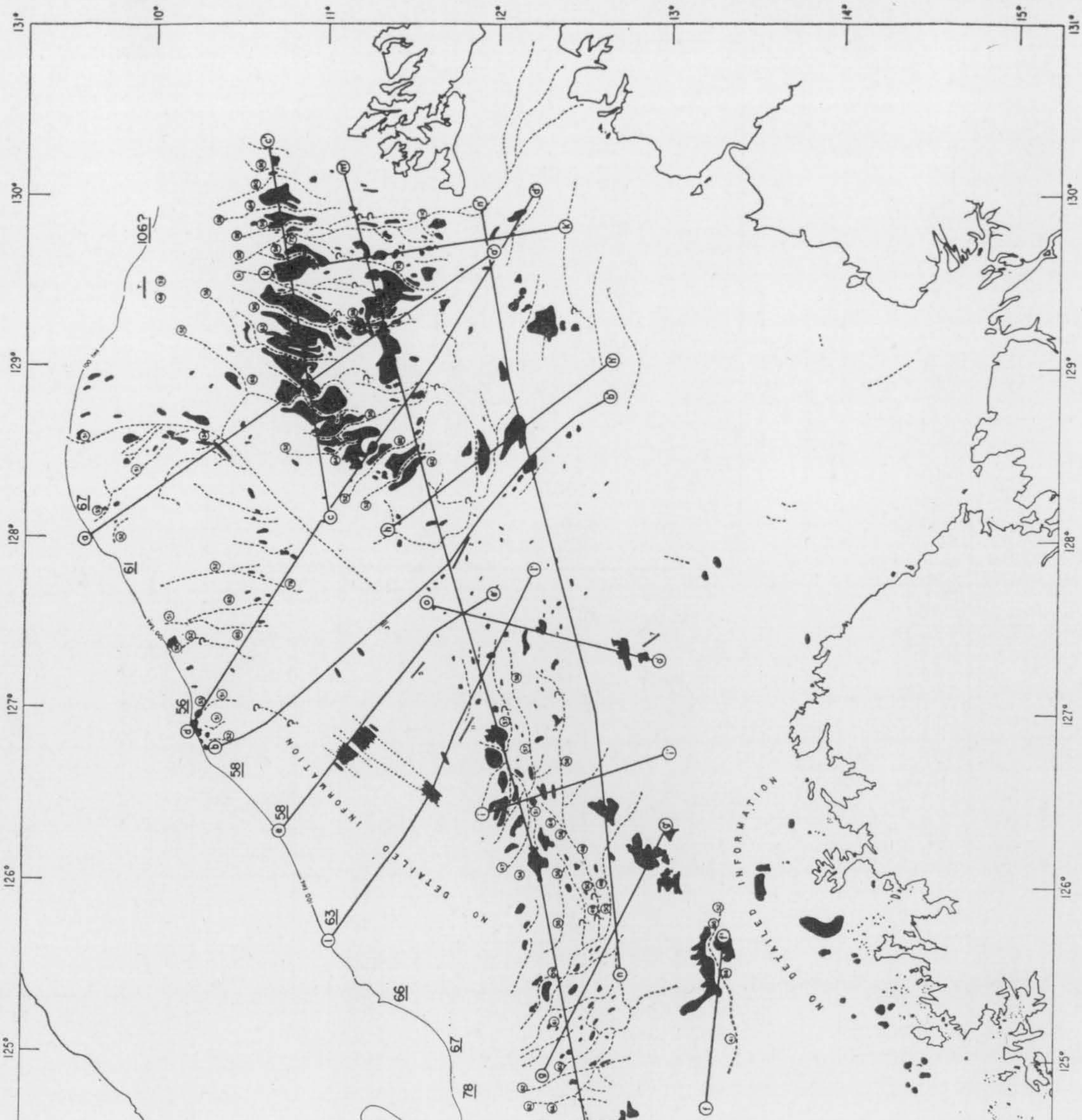

Fig. 4.13—Distribution of banks and channels on the Sahul Shelf. Depth of base of shelf edge scarp indicated by underlined numbers. Maximum depths of channels shown in circles. Lines with letters are locations of cross-sections of Plate 4.

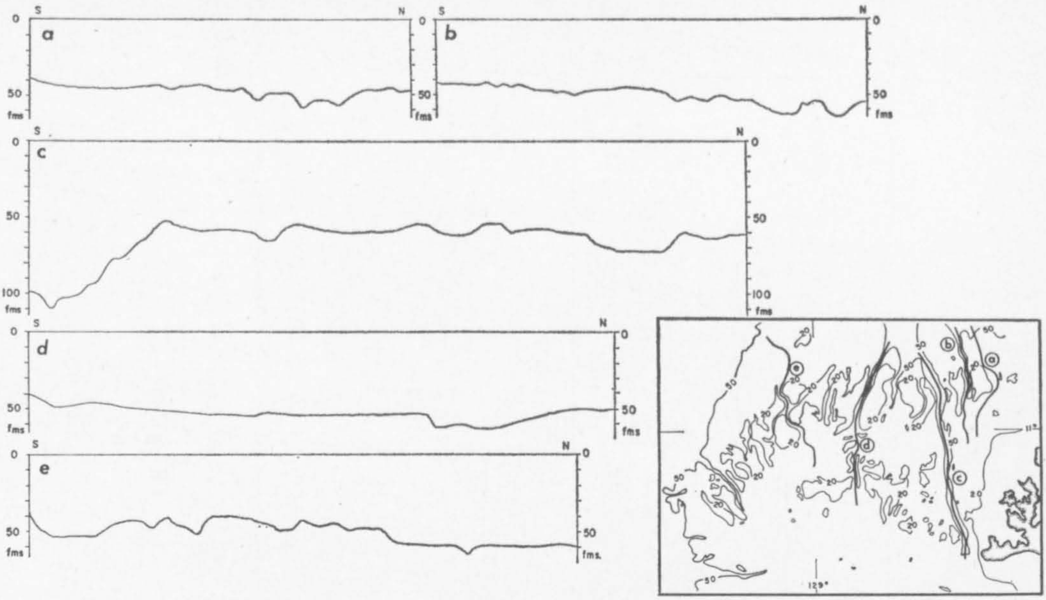

Fig. 4.14—Longitudinal profiles of channels through the Van Diemen Rise. Plotted from Royal Australian Navy soundings, using deepest soundings along talweg.

The entire south-eastern part of the shelf between the 10-fathom contour and the Bonaparte Depression has very smooth bottom and low relief. Banks and hills are rare and channels have been found only near the major estuaries. Featureless topography with low gradients also occurs everywhere along the outer shelf between the 45-fathom contour and the shelf-edge scarp. Rapid late Quaternary deposition may have produced the smooth bottom.

The most striking feature of the shelf topography is the widespread occurrence of flat, subhorizontal surfaces separated by short, steeper slopes. The profiles of Plate 4 clearly show this ubiquitous step topography and the subordinate occurrence of undulating, irregular, and slope topography. The profiles have been drawn with great vertical exaggeration, but careful analysis of detailed sounding charts shows that the flat steps and banks and the short, steep boundary slopes are real. Usually, the flat surfaces are very nearly horizontal with gradients of less than 0.3 feet per nautical mile and show only minor surface irregularities rarely exceeding 10 to 20 feet in height. The boundary slopes are quite variable, ranging from 16 to 75 feet per nautical mile, with a most common value of approximately 40 feet per nautical mile. The flat surfaces that occur on a large number of levels are developed both as bank tops and as terraces and benches. Samples collected from these surfaces show that they are covered with unconsolidated sediment to an unknown depth.

It is possible to correlate many of the stepped surfaces over large parts of the Sahul Shelf on the basis of depth, sequence, regional dip, intersections of profiles, and areal continuity when traced from profile to profile on detailed maps. On Plate 4, such correlations have been indicated with broken lines ; those that could be

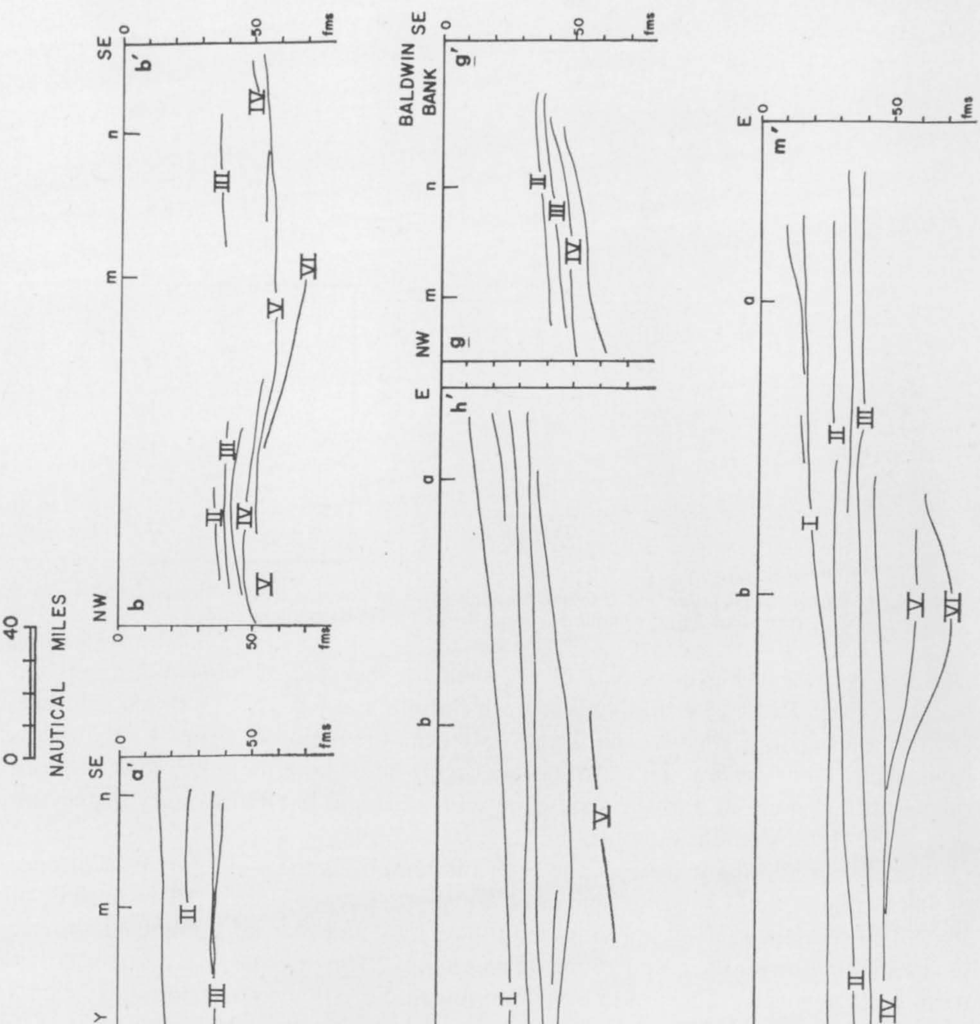

Fig. 4.15—Attitudes of regional surfaces on the Sahul Shelf, based on correlations of Plate 4. Locations of cross-sections on Fig. 4.13.

traced over most of the shelf have been labelled with Roman numerals. Naturally, these correlations are quite uncertain, and others that are different from those shown are possible. However, it is reasonably certain that many of the stepped banks and terraces can be considered parts of surfaces of large regional extent.

The higher surfaces (I and II on Pl. 4) are developed only on the rises and occur mainly as bank tops. Nearly all higher bank tops can be assigned to one of these levels. Only the shelf edge reefs, the small banks fringing the Malita Shelf Valley, and the banks close to the Kimberley coast cannot be correlated well with any of the regional surfaces. Between the rises and across the Bonaparte Depression, the correlation of the upper surfaces is quite uncertain and depends largely on the relation to Surface IV. In these areas, the correlation lines of Plate 4 and Figure 4.15 merely indicate correlation, not attitude. Regionally, Surfaces I and II seem to dip north-westward and converge in the same direction (Fig.4.15).

Surfaces III and IV can be traced with some confidence over a much larger portion of the shelf. On the rises, these surfaces are mainly developed as terraces between banks and occasionally as valley floors. Beyond the rises the surfaces form the broad terraces that fringe the flanks of the Bonaparte Depression and of the outer shelf. Within the Bonaparte Depression, and in the depression between the east and west branches of the Londonderry Rise, these surfaces are developed as bank tops.

Below Surface IV, several more levels can be distinguished that form terraces and valley floors on the slopes of the rises, and bank tops in the Bonaparte Depression. The correlation of these surfaces across the rises is very uncertain. The surfaces appear to be closely spaced near the crests of the rises and to diverge toward the center of the Bonaparte Depression and, less markedly, toward the shelf edge.

The regional topography of rises and depressions, which can be recognized in all surfaces (Fig. 4.15), is most pronounced in Surface IV and lower, but even for this group the difference in level between the lowest and highest points on each surface is quite small. The pronounced rise and depression topography apparent on the bathymetric charts is largely due to the preservation of higher surfaces on the rises and to their absence in the depressions, but only in small part is it due to relief in the various regional surfaces themselves.

Several planes of more local extent and numerous small terraces, benches, and notches exist at various depths. Although some of these may be related to Pleistocene sea level changes, as Fairbridge (1953) suggests, the complexity of the area prevents a firm correlation with known sea level positions.

Van Andel et al. (1961) have suggested late Quaternary downwarping of the central shelf. The present more detailed study has failed to substantiate this view.

5. Tentative Interpretation of the Structure and History of the Timor Sea Region

Geomorphological history

The structural history of the shelf and the origin of its relief may be tentatively inferred from the bathymetry discussed above. Although the almost total absence of geophysical and stratigraphical data renders any such interpretation very speculative, some hypotheses are considered here.

The origin of the broad regional relief appears fairly well established. In the existing literature, the regional relief of basins and rises and the associated shelf edge banks have been considered evidence of regional epeirogenic deformation and of slow downwarping of the outer shelf and upper slope. Geomorphic studies of the adjacent land areas (Hays, 1966; Paterson, in press; also see Chapter 2) have demonstrated the existence of widespread gentle deformations of the Cretaceous and Cainozoic land surfaces, and Fairbridge (1953) has correlated positive and negative areas of land with the rises and basins on the shelf. The cross-sections of Figure 4.15 seem to confirm the existence of regional uplift and subsidence on the order of several tens of feet. The information obtained in the present study, although not decisive, supports a structural interpretation of these broad relief features.

Two principal hypothesis can be advanced to explain the banks, channels, and terraces superimposed on the regional relief.

1. The Sahul Shelf is a region of prolific past or present development of platform reefs. The topography is comparable to that of portions of the Great Barrier Reef, as described by Fairbridge (1950). Molengraaff (1922), Fairbridge (1950), and Rodgers (1957) all refer to the abundance of reefs in the Sahul Shelf region. The present study has provided no evidence of active reef growth on most banks; many bank levels are below a reasonable depth for reef development, but the reef topography might have been inherited from former lower sea level stands.

2. The bank, terrace, and channel topography is of subaerial origin and represents a series of weathering and erosion surfaces formed during a period of uplift of the shelf, and subsequently drowned. Thus, the submarine topography is simply the submerged equivalent of the adjacent land, which it closely resembles. An earlier account of this hypothesis appears in van Andel & Veevers (1965).

The morphology of those areas where the banks are not very closely spaced (Pl. 3-C) shows a superficial resemblance to those parts of the Great Barrier Reef where platform reefs dominate. The morphology may also resemble that of the area just north of the Kimberley coast, where the many shoals and islands are said to be reefs (Fairbridge, 1950). The comparison is hampered by the lack of detailed maps of platform reef areas, but the similarities appear to be superficial and the cross sections of Plate 4 do not indicate a reef origin. Moreover, for the higher parts of the Sahul and Van Diemen Rises, where the banks are closely spaced and separated by narrow channels, a reef origin is improbable.

The reef hypothesis relates the formation of a large number of bank top levels to growth or erosional adjustment to several different sea level stands. The Pleistocene provided such a series of lower sea level stands, but there is no accurate knowledge of the sea level positions. Studies of the effects of late Quaternary sea level changes indicate that only still stands of long duration can produce widespread bank and terrace levels. A complex sequence of phases of reef growth and sedimentation, followed by periods of valley and terrace cutting and correlated with well-timed periods of deformation and sea level change, would be required to explain the observed facts. Although the hypothesis of reef origin cannot be eliminated at this time, we do not consider it a probable one mainly because of the dissimilarity between the Sahul Shelf topography and that of known areas of platform reefs, and also because of the complexity of the genetic system required.

The second hypothesis was originally suggested by Fairbridge (1953). Much of the relief of the Sahul Shelf, especially that of the higher parts of the Sahul and Van Diemen Rises, is strikingly similar to the topography of Melville and Bathurst Islands and to that of the Aru Islands. These islands, which consist of a sedimentary sequence of flat-lying or low-dipping beds, are dissected by subaerial erosion (Fairbridge, 1951; Verstappen, 1959; Hays, 1966) along ancient river courses or joint systems now drowned by the sea. Moreover, the relief of the adjacent parts of north-western Australia (Fig. 2.2) also markedly resembles the shelf topography as shown on Plate 4. Although this second hypothesis is not at this time amenable to proof, we consider these topographic similarities sufficiently convincing to discuss at some length the interesting consequences for the late structural history of the north-western margin of the Australian continent.

A comparison of the cross sections of Plate 4 and Figure 2.2 suggests that the upper surfaces of the Sahul Shelf (I–III) represent the northward and north-westward extensions of the Tennant Creek and Wave Hill Surfaces of the adjacent land. The lower surfaces of the shelf (IV and below) can be tentatively correlated with Hays' Coastal Plain Surfaces. Since the land surfaces are often complex because of local geological control (Paterson, in press) and are separated from those of the Sahul Shelf by a broad zone in which no information is available, precise correlations between the surfaces on land and those of the shelf remain uncertain.

All surfaces on the shelf follow the regional pattern of relief. It is probable that this is due to regional deformation during and after their formation rather than to an original system of valleys and divides faithfully followed by each subsequent surface. Deformation of the Wave Hill Surface on land (Hays, 1966) can be readily aligned with the deformations on the shelf. Consequently depth contours on each surface mainly reflect the later deformation (Fig. 5.1, A, B) and give an idea of its magnitude, although precise determinations are complicated by concomitant changes in base level to which the subsequent surfaces were adjusted, particularly those formed during the Pleistocene. However, if the surfaces are due to subaerial weathering and erosion, regional variations in the vertical distance between them and regional convergences and divergences should provide a key to the topography during the formation of each pair. Surfaces I and II, II and III (Fig. 5.1, C) show no convergences over the rises nor divergences over the depressions, as would be expected if these features had existed during formation of the surfaces. These surfaces converge rather uniformly toward the north and west, indicating a regional dip in those directions and a shoreline somewhere near the present edge of the shelf. This regional dip fits well with the pattern of south-to-north channels that now cross the Van Diemen and Sahul Rises. These channels may be explained as antecedent drainage, similar to the antecedent system of the Melville and Bathurst Islands. Consequently, the Malita Shelf Valley, which now drains Bonaparte Depression toward the north-east, must be a later development. At this time, its origin remains a mystery.

Surfaces III and IV, and even more markedly those below IV, show pronounced divergences toward the shelf edge and toward Bonaparte Depression, and show convergences toward the crest of the rises (Fig. 5.1, D). Contours on these lower surfaces show that the difference in depth between rises and depressions increases from

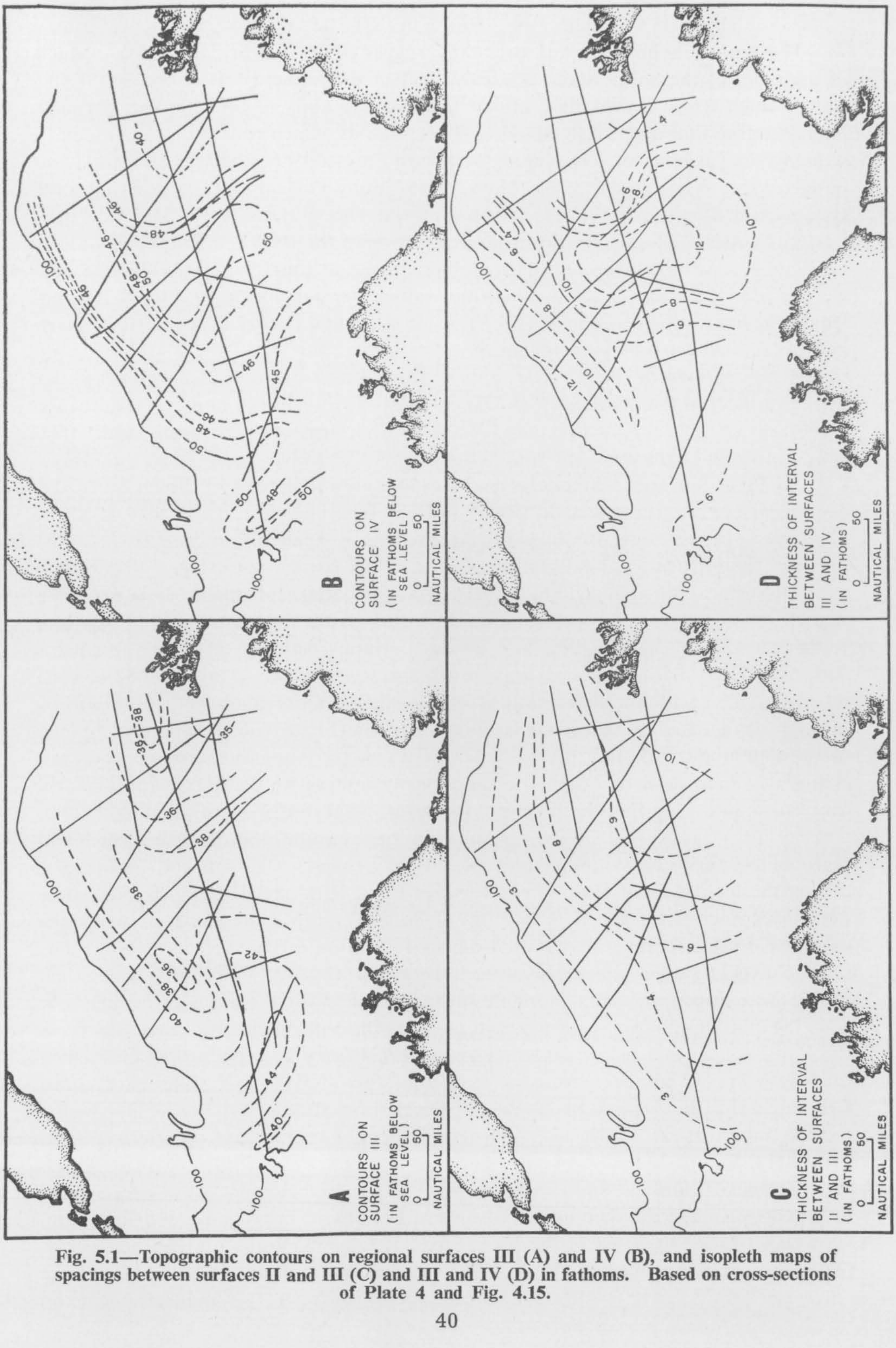

Fig. 5.1—Topographic contours on regional surfaces III (A) and IV (B), and isopleth maps of spacings between surfaces II and III (C) and III and IV (D) in fathoms. Based on cross-sections of Plate 4 and Fig. 4.15.

the older higher to the younger lower levels. From this we may conclude that the deformation began after the formation of Surface III and continued during the construction of all younger surfaces. Detailed analysis of contour maps and of spacings between surfaces indicates that the Van Diemen and Sahul Rises formed fairly early and may partially predate Surface III, and that the west branch of the Londonderry Rise may be even older. Formation of the Sahul and Van Diemen Rises appears to have partially deflected drainage to the west, producing a channel system that, as a result of uplift of the east branch of the Londonderry Rise, subsequently became antecedent. Subsidence of the Bonaparte Depression eventually robbed this sytem of its reasons for existence, and the channels are now generally wide and vaguely defined. On the other hand, the system cutting through the Sahul and Van Diemen Rises must have been active during each Pleistocene low stand of sea level, and accordingly is still sharply defined and deeply cut.

The older surfaces are mainly developed as bank tops, the younger ones as depositional terraces and valley floors. Thus, Surfaces I, II, and III may be predominantly erosional, as are the corresponding upper surfaces on land, whereas Surface IV and lower sets are depositional in the depressions and partially erosional on the rises. The changes in climate and base level provided by the Pleistocene appear to form the best explanation for this lower set of surfaces, as they do for the Coastal Plain surfaces on land.

If this interpretation is in general correct, the shelf morphology is essentially the product of subaerial erosion, modified by epeirogenic deformation. The excellent preservation of the subaerial land forms implies that little marine sedimentation has taken place since the entire region was temporarily or permanently submerged below sea level. The shelf must be an area mainly of sediment bypassing. On the other hand, the long, smooth slope toward the Timor Trough and the prograding of the shelf edge near Echo Shoal demonstrate long and continuous sedimentation in this area. It seems quite probable that the Timor Trough slope has received sediment continuously since the uplift and denudation of the shelf and adjacent continent began, and that the Trough is a major receptacle for the erosion products of north-western Australia since the late Cretaceous. On the shelf itself, a thin blanket of marine carbonates is apparently present on all bank tops and terraces. Softer and probably more rapidly deposited sediments occur in the Bonaparte Depression, as shown by the presence of subsurface sound reflectors, and in the south-western portions of the shelf. The slopes of the various regional surfaces suggest, however, that little more than a thin late Tertiary and Pleistocene blanket could be present even on the deepest portions of the shelf.

From these considerations the later history of the Sahul Shelf may be reconstructed tentatively as follows. At some undetermined time during the middle or late Tertiary, the entire Sahul Shelf was above sea level and in the process of slow uplift, with the resulting formation of a series of stepped erosional surfaces. A long period of emergence preceded the first uplift, as indicated by the thick laterites of the Tennant Creek Surface. A possibly short but widespread Miocene transgression (White Mountain Formation) may have intervened, but its deposits were later largely removed. During this period of uplift, drainage was to the north and west to a shoreline located near the present shelf edge. In shallow water, just beyond the coastline, a string of small patch reefs (almost a thin barrier reef) formed, possibly while the outer shelf and upper slope subsided slowly enough for reef growth to keep up with it. A thick upper Tertiary sediment sequence may have accumulated in the Timor Trough during this time.

Van Bemmelen (1949, pp. 521–541, Pl. 30) states that in the very late Pliocene or early Pleistocene, the Timor Trough was a fairly shallow basin, and that Timor and Roti were low and partly invaded by the sea. Lower Pleistocene reefs, which were subsequently uplifted to considerable altitudes during the later Pleistocene, existed on both the islands. This phase of uplift, which was accompanied by marked subsidence of the Timor Trough, probably is still continuing. Apparently the subsidence was slow enough that reef growth along the hinge line could keep up with it, but it was much faster than regional deposition. The present position of the reef tops indicates a subsidence of more than 600 to 800 feet for the upper slope.

A gentle epeirogenic deformation of the shelf, which formed first the Van Diemen and Sahul Rises, then the Londonderry Rise, appears to have started about the time that Surface III was being formed. The pre-existing northward and westward drainage cut into the rises, creating the present antecedent channel systems. The deformation culminated in the development of the Bonaparte Depression and its outlet through the Malita Shelf Valley, and may still continue.

If we assume that all surfaces were formed while the entire region was above present sea level, a total subsidence of 400 feet must have followed to bring the lowermost surface to its present position. Since the youngest surfaces were probably formed near the end of the Pleistocene, this would leave only a short time interval for this major amount of subsidence. It is more likely that subsidence of the shelf began considerably earlier, perhaps after Surface III was formed and about the same time as Timor rose and the Timor Trough deepened. The lower surfaces, which were probably excavated during glacial low-stands from sediments deposited during sea level rises and high-stands, cannot be well correlated, and the corresponding sea level stands are not well known. Hence, the beginning of the subsidence of the shelf cannot be established with any certainty.

Thus we come to the same conclusion as did van Bemmelen (1949, p. 721), that the Sahul Shelf and adjacent land, as the stable foreland of the Indonesian orogenes, are subject to slow epeirogenic responses to the orogenic disturbances of the bordering geosynclines. The late Cainozoic history of the Sahul Shelf is one of gentle regional uplift, erosion, and deformation, followed by subsidence, shallow marine invasion, and limited marine deposition. This sequence, probably twice repeated in the Cainozoic, is part of a long series of similar events that started in the early Precambrian and appears to have followed the same structural trends throughout its history (Fairbridge, 1953).

The configuration of land and sea on the Sahul Shelf during the last maximum lowering of sea level in late Pleistocene time is of great interest in the interpretation of the sediment distribution and, incidentally, for the history of migrations of faunas and early man on to the continent. This subject will be discussed at some length in Chapter 11.

Structural trends

The obvious correlations between the rises and depressions on the shelf of north-western and western Australia and the blocks and basins of the adjacent land have induced Fairbridge (1953) and Teichert (1958) into considerable speculation concerning the seaward extrapolation of land geology. Such extrapolations into the region where the contrasting terrains of Timor and Australia must meet are indeed tempting, but pertinent information is scarce and geological speculations based on bathymetry are generally unwarranted. This is well illustrated by Boutakoff's (1963) essay on the geology of the offshore areas of north-western Australia, based on new contouring of Admiralty Chart 475. Overlooking the Admiralty's caution that ' the whole of the coasts of north-western Australia, as well as the area lying between them and Timor are as yet imperfectly charted and examined ', Boutakoff postulated several ridges along the outer edge of the shelf and suggested that they are almost completely submerged folded ranges. Examination of the chart shows that, whatever the merit of the idea itself, the bathymetric data do not permit this conclusion, and that Boutakoff's contouring is wholly controlled by his hypothesis and not by reasonable analysis of the data. For example, two shoals reported in the 1860's from the deep Indian Ocean, one known only from a single sounding, and the other seen but not sounded and not since rediscovered, are the basis of the ' Corona Tectogene ' and the ' d'Artagnan Swell ', which are features 100 miles long and 30 miles wide. In Boutakoff's view, Stevenson Shoal and other shoals 120 miles north-east of the Montebello Islands are important links between the coastal anticlines of North-west Cape and Rough Range and his postulated ' Rowley-Scott Ranges '. These shoals no longer exist, having been deleted in 1954 from Chart 475 and replaced by depths of 150 fathoms. Whatever their origin, the Rowley Shoals, Scott Reef, and Seringapatam Atoll have the morphology of atolls and they rise from the outer shelf. By disregarding contradictory soundings, Boutakoff has extended what the chart shows to be pinnacles into the crests of ' mountain ranges '. With the increasing interest in offshore geology, the likelihood of such unwarranted speculations is becoming greater, to the peril of a reasonable understanding of the structure of the continental margins.

The chief structural and morphological features of the Timor Sea and the adjacent land are remarkably regular (Fig. 5.2) and may be grouped into five units:

1. *A north-east trend* is followed on land by the Halls Creek Mobile Zone, parallel to the west coast of the Kimberley Block and to the eastern and western margins of the Bonaparte Gulf Basin, and followed in the sea by the south-western and central parts of the Sahul Rise.

2. The *north-west trend* includes on land the King Leopold Mobile Zone, parallel to a major system of joints in the Kimberley Block, as evidenced by the Prince Regent River. This system is also parallel to the north-east coast of the Kimberley Block, to parts of the south-western margin of the Bonaparte Gulf Basin, and to the north-eastern margin of the Pine Creek Mobile Zone. In the sea, this trend is evident in the Leveque and West Londonderry Rises and in part of the East Londonderry Rise.

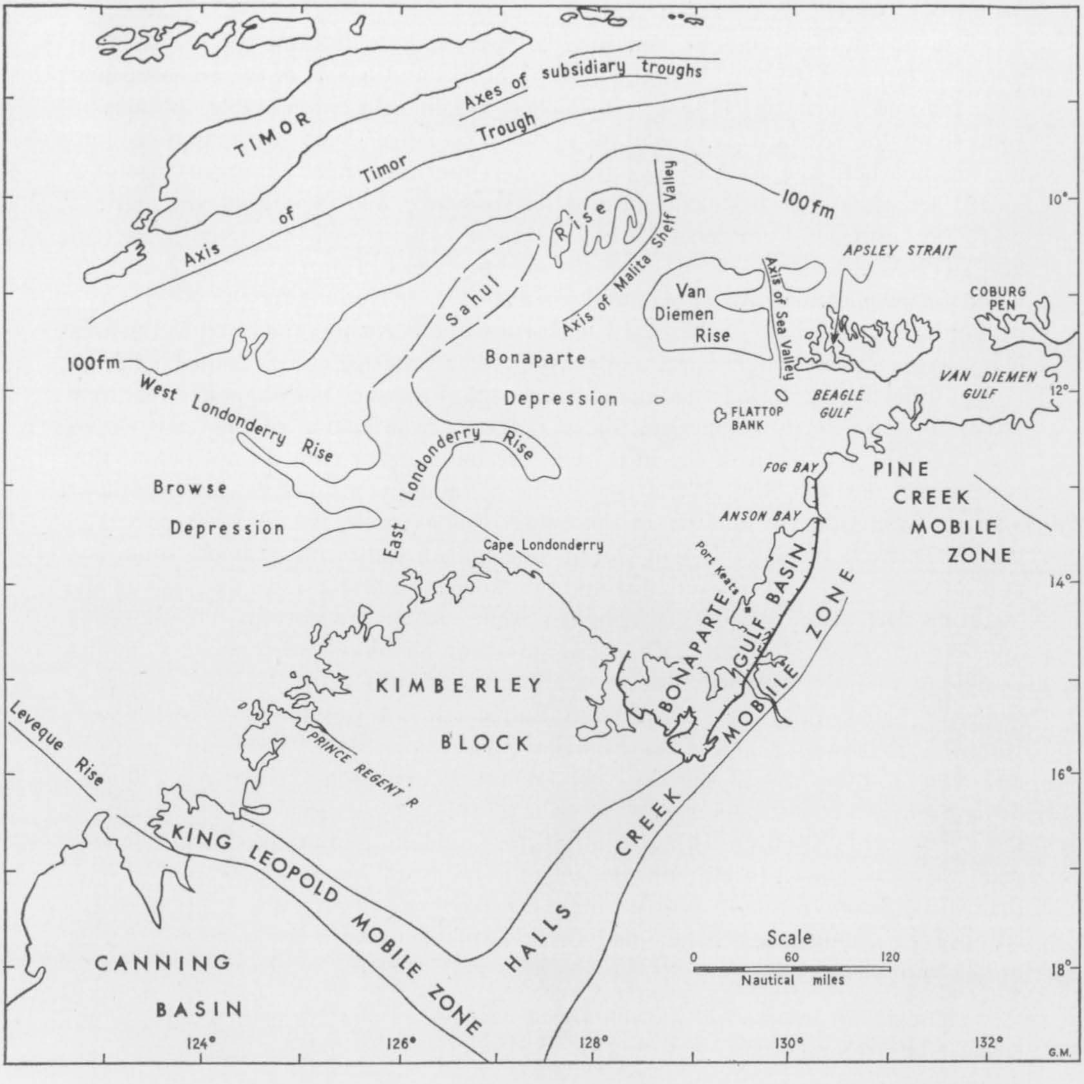

Fig. 5.2—Structural trends of north-western Australia and their extrapolation into the Timor Sea.

3. A *westerly trend* is exhibited on land by the north coast of the Northern Territory, with a westward extension through Coburg Peninsula, and by Bathurst and Melville Islands on to the Van Diemen Rise, with its east-west central depression. South of this feature and parallel to it are the Van Diemen and Beagle Gulfs, and southward again is a line of shoals, including Flattop Bank.

4. A *north trend* occurs in the northern parts of Halls Creek and Pine Creek Mobile Zones and continues in the marine valley that separates the Van Diemen Rise and Bathurst Island.

5. An *east-north-east trend* is shown by Timor, and the edge of the Sahul Shelf as roughly indicated by the 100-fathom contour; the axis of the Timor Trough is slightly oblique to this trend, as noted earlier.

In north-western Australia, the pattern of north-east and north-west trends is an expression of primary lineaments initiated in the Precambrian and reactivated later. This pattern is repeated on the Sahul Shelf and may be regarded as evidence that the basement of parts of the shelf is Precambrian. A positive Bouguer gravity anomaly of +65 milligals occurs over part of the Sahul Rise (Helfer et al., 1962), but part or all of this anomaly may be attributable to structures related to the Timor Trough.

The only westerly trends in the northern part of Northern Territory are in Archaean rocks; the Proterozoic rocks do not significantly follow this trend (Dunn, 1962). Consequently, Van Diemen Gulf and Bathurst and Melville Islands and associated lineations on the Sahul Shelf are probably the result of Cainozoic movements not obviously related to the older trends.

The north trend is shown well by a positive Bouguer anomaly that passes through Anson and Fog Bays (see Langron, Fig. 3, *in* Dunn, 1962), where it corresponds with the edge of the Bonaparte Gulf Basin. This gravity anomaly continues through Beagle Gulf (Helfer, pers. comm.) to Bathurst Island. It is a fundamental lineament in Precambrian rocks, but it does not affect to any appreciable degree the overlying Cretaceous rocks of the island. The same trend is seen again in the long, north-trending sea valley west of Bathurst Island and in the northern part of the Malita Shelf Valley. Both the Malita Shelf Valley and, on land, the Halls Creek Mobile Zone show a change in trend from north-east to north, east of a line joining Port Keats with the middle of the Malita Shelf Valley.

Hartman's unpublished report (1964) of a Commonwealth-subsidized offshore aeromagnetic survey shows that the eastern margin of the Bonaparte Gulf Basin lies near the southern end of the sea valley west of Bathurst Island. At latitude 11° 30′ S., this margin turns sharply toward Apsley Strait and then north again.

Hartman's survey also shows that from Cape Londonderry the nonmagnetic section rapidly thickens toward the north-northeast, but is relatively thin over the area of Ashmore Reef and Cartier Island. A very thick nonmagnetic section occurs beneath the Bonaparte Depression. If the rises and depressions discussed in the previous section of this paper are indeed stucturally controlled, then these observations suggest that they are probably a rejuvenation of very ancient structural patterns. Further geophysical work will be required to examine these structural problems in more detail.*

---

* A comprehensive aeromagnetic survey of the Sahul Shelf has now shown that the regional morphology corresponds with depth of magnetic basement (Veevers & van Andel, *Mar. Geol.*, in press).

SEDIMENTS AND DEPOSITIONAL FACIES

6. Introduction and Methods

In the following chapters, the petrography of the surface sediments of the Timor Sea and its relation to past and present environments will be discussed. Most cores are short, and the grabs and dredges recover surface samples only. Hence, the investigation is concerned almost entirely with the surface sediment layer between 0 and 10 cm. Emphasis is placed on regional lithological characteristics because of the reconnaissance nature of the sampling pattern and because of the lack of detailed environmental information. The principal problems to be discussed are: (1) the dispersal of land-derived sediment as a function of the location of sediment sources, of the topography, and of the current patterns; (2) the composition of the sediments in relation to texture, topography, biological control, and history of sedimentation; and (3) regional aspects of sedimentation in the Timor Trough. A fruitful analysis of these problems and a comparison of Timor Sea sediments with modern marine calcareous deposits elsewhere demand an understanding of the effects of post-Pleistocene sea level changes, and of the nature and distribution of the relict deposits associated with them.

The locations of samples are shown on Plate 5, and their positions, depths, and descriptions have been tabulated in Appendix A. The results of the laboratory analyses are contained in Appendices B–E. Little palaeontological information is included in this report; taxonomic and ecologic studies of the Foraminifera by A. R. Loeblich, Jr, of the Ostracoda by F. M. Swain, and of the Mollusca by J. W. Valentine are in progress and will be reported elsewhere.

The samples taken in the Timor Sea are of several different kinds, including 311 gravity cores varying in length from 10 to 70 cm, 6 piston cores from 50 to 334 cm long, 55 surface samples obtained with orange peel grab samples and pipe dredges, and 53 basket dredge hauls. The core samples were sealed on board in their plastic liners, the others stored in sample bags. The samples obtained on the Malita cruise in 1960 had to be shipped to California commercially, and due to poor storage conditions they lost a considerable amount of water and became discoloured before they could be analysed. Cores collected in 1961 have been stored permanently at 34° F. and still are essentially fresh.

All cores were sliced longitudinally in the laboratory, and half of each core was resealed in a polystyrene tube for future reference. The other half was described, noting colour by means of a Rock Color Chart, published by the Geological Society of America, and photographed if it showed minor structures or bedding. X-radiographs were made of many samples to detect structure not visible on the surface (Calvert & Veevers, 1962). From this half of the core, samples were taken at 0 to 1 cm for foraminiferal studies, and from 1 to 11 cm for petrography and chemical analysis. Equivalent quantities of the surface samples, presumed to represent a thin surface layer, were used. All samples were homogenized before analysis.

Laboratory procedures for sediment-petrographical analysis are shown on the analysis flow chart of Table 6.1. The procedures are conventional and a few comments are sufficient. The following numbers refer to the stages shown on the chart.

TABLE 6.1

ANALYSIS FLOW CHART

Subsample 1–11 cm

1. Disperse by soaking in distilled water
2. Sieve in distilled water on 2·0 and 0·062 mm sieves

Fraction >2·0 mm

3. Dry and sieve on 4, 8, 16, and 32 mm sieves
4. Weigh
5. Determine composition under binocular microscope

Fraction 2·0–0·062 mm

6. Dry and weigh
7. Split into three subsamples

Fraction <0·062 mm

8. Split into four subsamples

Subsample a

9. Release into water-filled settling tube
10. Collect graded sample in plastic vial and dry
11. Impregnate with plastic
12. Prepare longitudinal thin section
13. Point-count under petrographic microscope

Subsample b

14. Wet approximately 3 gms
15. Obtain size distribution in sedimentation balance

Subsample c

16. Use for coarse fraction analysis with binocular microscope
17. Use for heavy and light mineral analysis

Subsample d

18. Determine total carbon with LECO Carbon Analyzer

Subsample e

19. Weigh and acidize
20. Wash with distilled water to remove chlorides
21. Determine organic carbon with LECO Carbon Analyzer

Subsample f

22. Grainsize analysis by pipette

Subsample g

23. Retain for clay mineral study

24. Determine carbonate carbon in fine fraction by difference

25. Use data from steps 4, 15, and 22 to compute size distribution

(1). Since excellent and stable dispersion was obtained in distilled water, no chemical peptizers were used.

(9). The method is a modification of the one used by Houbolt (1957). Approximately 16 grams of sample was allowed to settle in a glass tube 75 cm long and 18 mm in diameter, which had a plastic vial attached to the lower end. The graded sample was lithified in the vial with *Glas-skin Plastic Resin*, and sample and vial were cut lengthwise. A large thin section was prepared from one half, while the other half was retained for preparation of polished or etched surfaces. The graded thin section facilitates identification of particles and allows a quantitative analysis of the relation between grainsize and composition.

(13). A discussion of the petrographic analysis of the thin sections will be presented in Chapter 9.

(15). A recording sedimentation balance (van Andel, 1964, p. 268) was used for the determination of the size distribution of the fraction 2·0 to 0·062 mm.

(17). Heavy mineral separations were made in tetrabromoethane, after treatment with 9 percent hydrochloric acid to remove carbonates.

(18). Total carbon was determined by oxidation in an induction furnace at 1600° C. with tin and copper accelerators. The carbon dioxide was filtered to remove sulphur gases and measured gasometrically in a LECO Carbon Analyzer. The reproducibility of the method is approximately 0·02 percent, and very small samples can be analysed rapidly.

(19). Organic carbon was determined in the same manner after repeated leaching of the sample with 7·5 percent hydrochloric acid to remove carbonates and after washing the samples repeatedly with distilled water to remove chlorides. This last step is crucial in the presence of much calcium carbonate. The results have been expressed in Appendix C as percent by weight on the basis of the fraction finer than 0·062 mm.

(22). Size analysis of the fine fraction was carried out by conventional pipette method, using withdrawals for the fractions finer than 0·062, 0·031, 0·016, 0·008, 0·004, and 0·002 mm.

(24). The amount of carbonate in the fine fraction was obtained by subtracting the amount of organic carbon measured in (19) from total carbon measured in (18), and multiplying it with the appropriate factor to express it as percent calcium carbonate on the basis of the fraction finer than 0·062 mm (' fine carbonate '). The carbonate content of the entire sample was then computed by subtracting the amount of noncalcareous material in the sand fraction (2·0–0·062 mm), as determined by point counting of thin sections, from the total weight of this fraction, and by adding this to the amount of fine carbonate and the amount of sample in the fraction coarser than 2·0 mm. This coarsest fraction contains only negligible amounts of noncalcareous material. The ' total carbonate ' is expressed in percent by weight on the basis of the total sample.

(25). Calculations of grainsize distributions were carried our on a Control Data Corporation 1604 electronic high-speed computer. The program used (van Andel, 1964, p. 238) yields standard sample statistics and tabulations and graphs of the cumulative and differentiated frequency distributions in 0·25-phi steps. The phi scale (Krumbein & Pettijohn, 1938, p. 85) will be used throughout this paper for grainsizes; the conversion is $\phi = -\log_2 \xi$ where ξ is the diameter in millimetres.

7. Lithology and Lithofacies Distribution

Texture of surface sediments

In many regional studies of modern terrigenous sediments (for example, Curray, 1960; Shepard, 1956; Shepard & Moore, 1955; van Andel, 1964), textural variations are discussed in terms of the proportions of sand, silt, and clay (Shepard, 1954). This approach has proved fruitful for regional facies studies, although more sophisticated analysis is required to evaluate environmental control and the dynamics of sedimentation. In the study of modern carbonates, on the other hand, the texture of the sediments has not received much attention. A simple textural classification, which is still in use in a variety of modifications, was proposed by Grabau (1904). Various authors have presented textural variations by means of the percentage distribution of the matrix fraction (e.g., Purdy, 1963; Ginsburg, 1956; Daetwyler & Kidwell, 1959; Folk, 1959). The boundary between the fine matrix and coarse-grain fractions usually is taken at 0·062 mm. Simplified textural terms are included in most classifications of carbonate rocks (see Ham, 1962).

For the description of the regional textural distribution of the Timor Sea sediments, Shepard's (1954) classification has the advantage of taking into account three size classes instead of two, and of permitting a comparison with noncalcareous shelf sediments. The names of the end members in this system (Fig. 7.1) can be readily replaced by calcarenite, calcisiltite, and calcilutite (Grabau, 1904; Pettijohn, 1957, p. 401). If also changed, the qualifiers are clumsy; it is preferable to retain Shepard's terms in their purely textural sense, as they were intended. This is justified by the fact that the silt and clay fractions in large part are not calcareous, and are of terrigenous origin.

Shepard's classification refers only to the fraction finer than 2 mm. For the coarser portion, a system of qualifiers is used:

Trace to 5% coarser than 2 mm	*slightly calciruditic* (shelly, gravelly)
6 to 30% coarser than 2 mm	*sandy* (silty, clayey, calcarenitic) *calcirudite* (shell, gravel)
81 to 100% coarser than 2 mm	*calcirudite* (shell, gravel)

The sediments of the Sahul Shelf are predominantly coarse grained (Fig. 7.2; Appendix B). Calcarenites and clayey and silty calcarenites cover all rises and most of the shallow nearshore areas. The coarsest calcarenites are found in water less than 20 fathoms deep, between Clarence Strait and Queen's Channel, north of Cape Londonderry, on bank tops of the Van Diemen Rise, and in two zones bordering the middle part of the Malita Shelf Valley. Coarse calcarenites also are associated with the shelf edge banks.

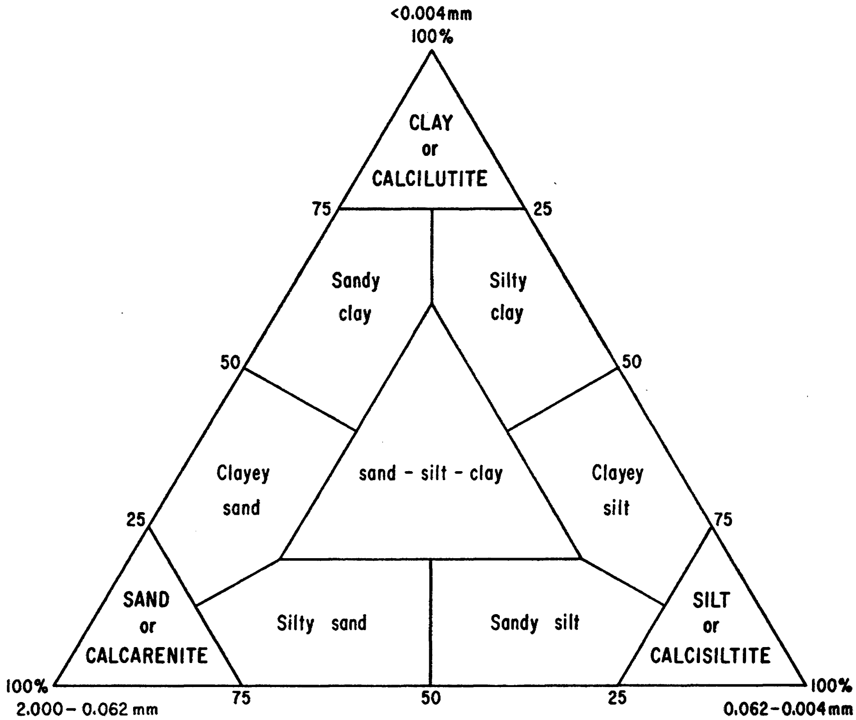

Fig. 7.1—Textural classification of Timor Sea sediments, based on modifications of system proposed by Shepard (1954).

The Bonaparte Depression below 50 fathoms is filled with silty and sandy calcilutites. Coarser sediments occur on and around two bank areas at 12° S. latitude on both sides of the Depression. The sediments are finest in the deepest northern part of the Depression, but the Malita Shelf Valley and its south-western entrance are covered with coarser material.

Compared with other continental shelves, the sediments of the Sahul Shelf are very coarse grained. Eighty-five percent of the shelf area surveyed is covered with calcarenites, whereas sands occupy 50 percent of the Gulf of Mexico Shelf between the Mississippi River and the Rio Grande, 45 percent of the Guayana-Orinoco Shelf, and 70 percent of the shelves of the Gulf of California.

The deposits of the Timor Trough are silty clays like those of equivalent depth and distance from the shelf in other parts of the world (e.g., Peru-Chile Trench, Trask, 1961; California offshore basins, Emery, 1960; Gulf of California, van Andel, 1964). The deposits are separated from the Sahul Shelf by a narrow band of sand-silt-clay at the top of the continental slope. On the Timor side, silty clays extend almost to the shore; only two cores from the continental shelf have coarser sediments. A few scattered deepwater cores contain enough planktonic Foraminifera to be classified as calcarenitic clays.

The distribution of the calcirudite fraction (Fig. 7.3) is only partly related to that of the fraction finer than 2 mm. The sediments of the shallowest bank tops of the Van Diemen and Londonderry Rises and those along the western part of the shelf edge are calcarenitic calcirudites. Other rise deposits are quite universally calciruditic, except for those on the western Sahul Rise. The fine sediments of the northern Bonaparte Depression are essentially free of very coarse material, but in the central and southern parts, enough shell debris is present to produce markedly bimodal size distributions. No very coarse material occurs in the Timor Trough.

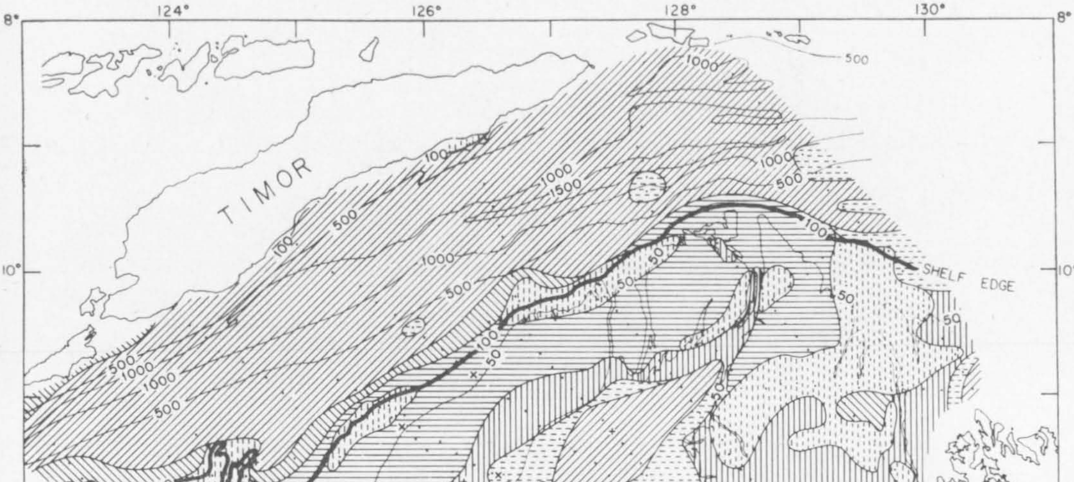

Fig. 7.2—Distribution of textural types in surface sediments of the Timor Sea. Anomalous samples indicated by + (too coarse) and × (too fine). Of 348 samples, only 11 (3.2 percent.) do not fit the pattern. Five of these, all too coarse, are from tops or flanks of small banks.

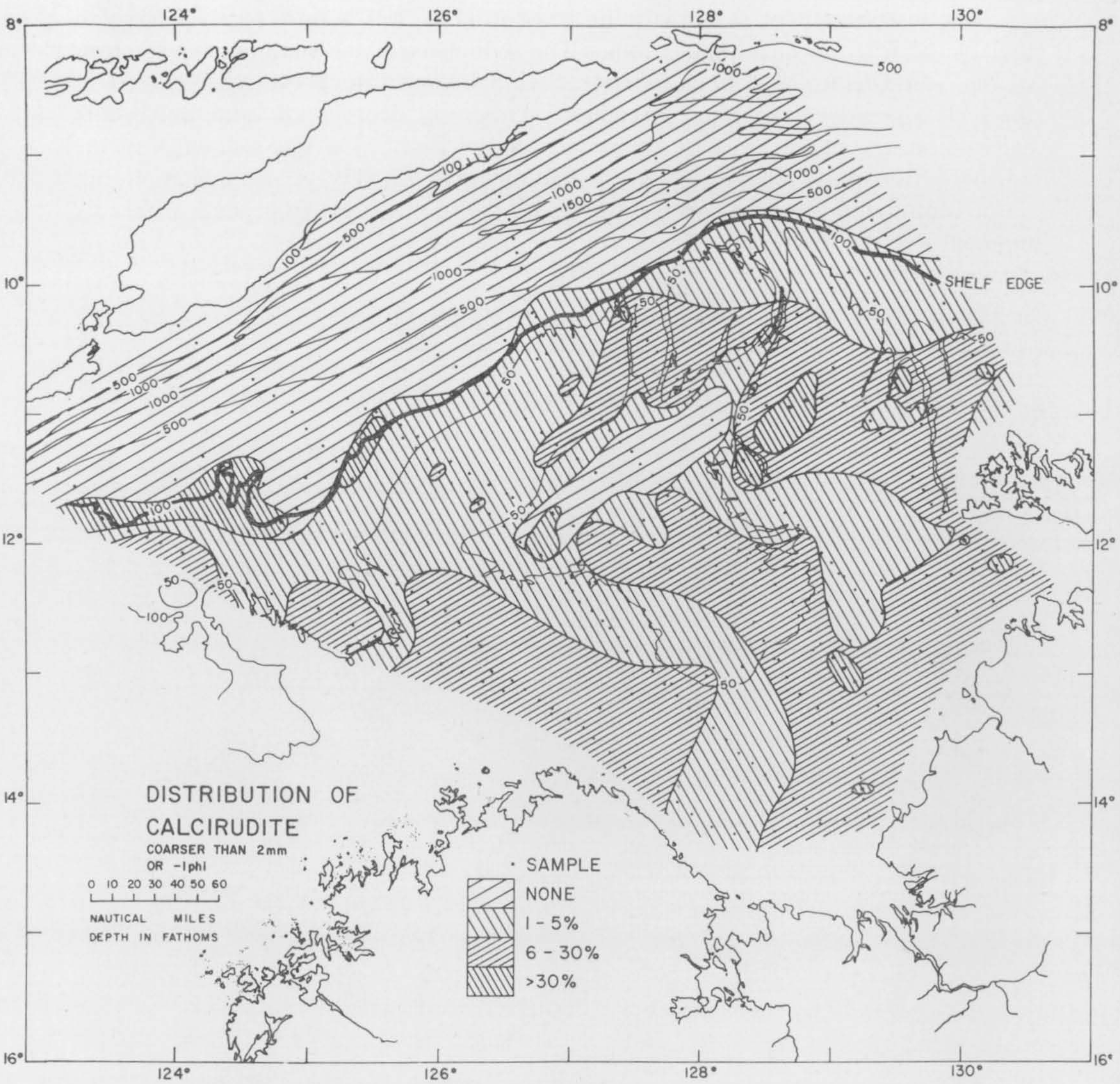

Fig. 7.3—Distribution of calcirudite (coarser than 2 mm) fraction in percent by weight in surface sediments of the Timor Sea.

The sediments of the Timor Sea can be considered as a series of mixtures between a calcarenite and a silty calcilutite containing 25 to 35 percent silt (Fig. 7.4). The position of the sediments within this series is related to depth (Fig. 7.5). At depths shallower than 25 fathoms, all deposits are calcarenites, which contain very little fine material. On the other hand, samples below 100 fathoms are fine grained; with increasing depth they show a clear progression toward finer textures, mainly through loss of sand-sized material. In contrast, the samples between 25 and 100 fathoms are extremely variable in texture and represent almost the entire available range. The 25 to 50 fathoms and 50 to 100 fathoms groups have the same coarse limit, but the latter group extends somewhat farther to the fine side. The textural variability is partly due to topography in these depth zones, where the most varied topography and the most abrupt relief of the area occur. Moreover, the zones have been strongly affected by the postglacial transgression, so that some of the textures reflect earlier and shallower environmental conditions.

The distribution of samples in the sand-silt-clay diagram is very similar to that of the sediments of the north-western Gulf of Mexico from the Mississippi Delta to the Mexican border (Fig. 7.4). On the basis of texture alone, the calcareous sediments of the Sahul Shelf cannot be distinguished from the terrigenous deposits of the Gulf of Mexico, suggesting that conditions of transportation, either past or present, rather than the ecology and biology of carbonate environments control the texture of the Sahul Shelf sediments. On the other hand, shelf sediments near

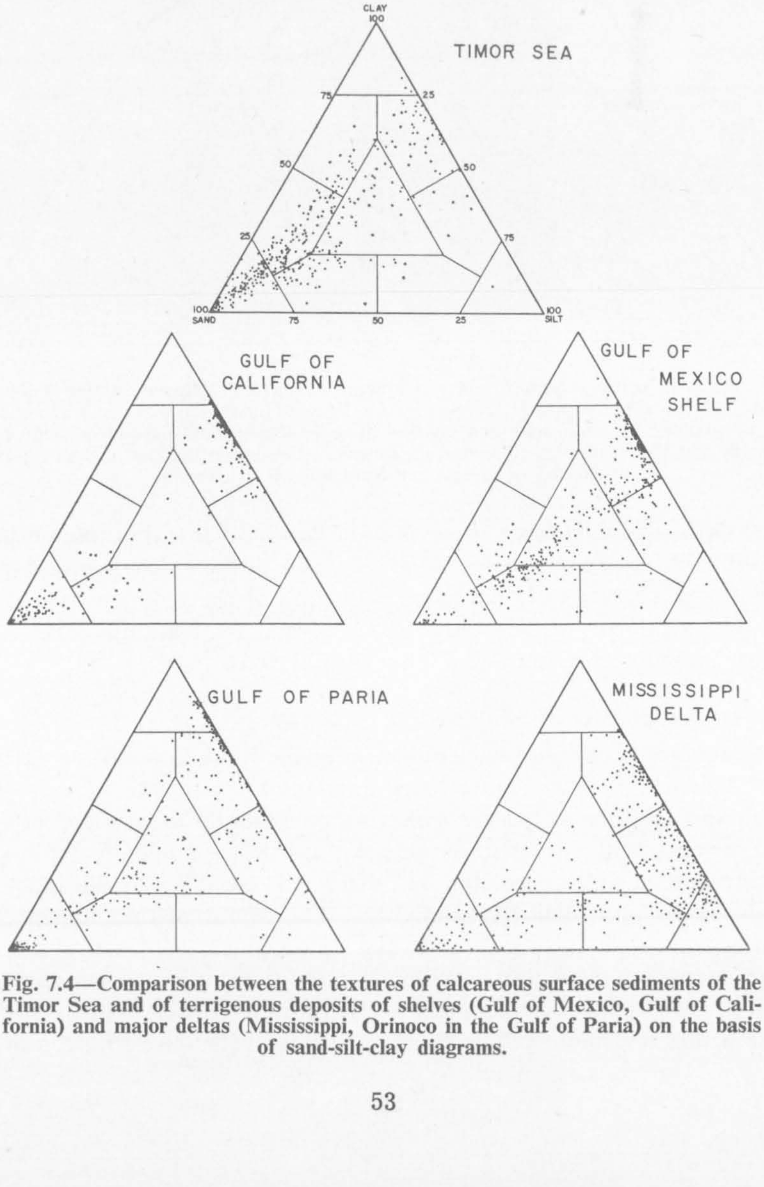

Fig. 7.4—Comparison between the textures of calcareous surface sediments of the Timor Sea and of terrigenous deposits of shelves (Gulf of Mexico, Gulf of California) and major deltas (Mississippi, Orinoco in the Gulf of Paria) on the basis of sand-silt-clay diagrams.

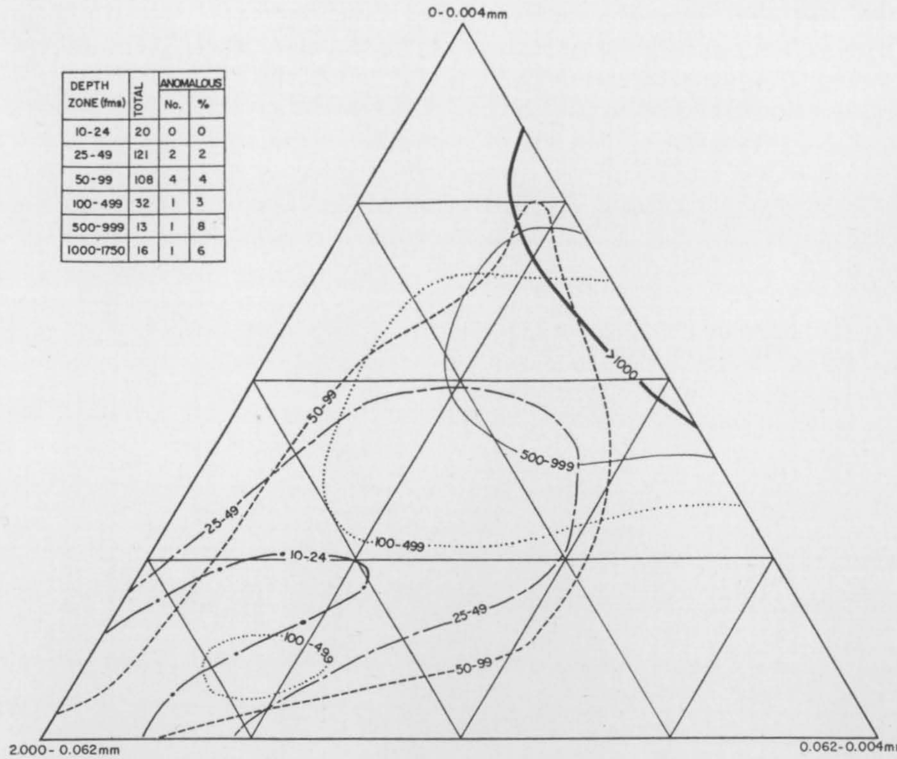

DEPTH ZONE (fms)	TOTAL	ANOMALOUS No.	ANOMALOUS %
10-24	20	0	0
25-49	121	2	2
50-99	108	4	4
100-499	32	1	3
500-999	13	1	8
1000-1750	16	1	6

Fig. 7.5—Relation between texture and water depth of surface sediments of the Timor Sea. Lines labelled with water depths in fathoms enclose textural points for that depth zone. Insert: number of samples for each zone and number of anomalous points outside delineated area. Between 100 and 1750 fathoms, all anomalous samples either are at the foot of shelf edge banks or consist of deepwater foraminiferal calcarenite.

large deltas (Mississippi, Orinoco in the Gulf of Paria) differ from those of the northwestern Gulf of Mexico and the Sahul Shelf because of the much greater importance of the silt fraction, apparently a diagnostic feature of the sediments of large river systems. The sediments of the Gulf of California are texturally discontinuous; intermediate mixtures between sand and silty clay are rare.

Colour of surface sediments

Sediment colours have been determined with the Rock Color Chart (Geological Society of America, 1959). Colour determinations for samples V-2 to V-163 were made approximately one year after collection on partially dried material; samples that were obviously discoloured were excluded. For samples V-165 to V-377, colours were determined immediately on board. There is no significant difference between the two sets of data (Appendix A). The colour of the fine-grained sediments varies from light olive grey to dusky yellow-green, with many intermediate values and degrees of saturation. Within this range there is no systematic pattern of variation. With increasing content of sand-sized particles, the colour tends to become lighter and more yellowish, ranging from light olive to greenish yellow.

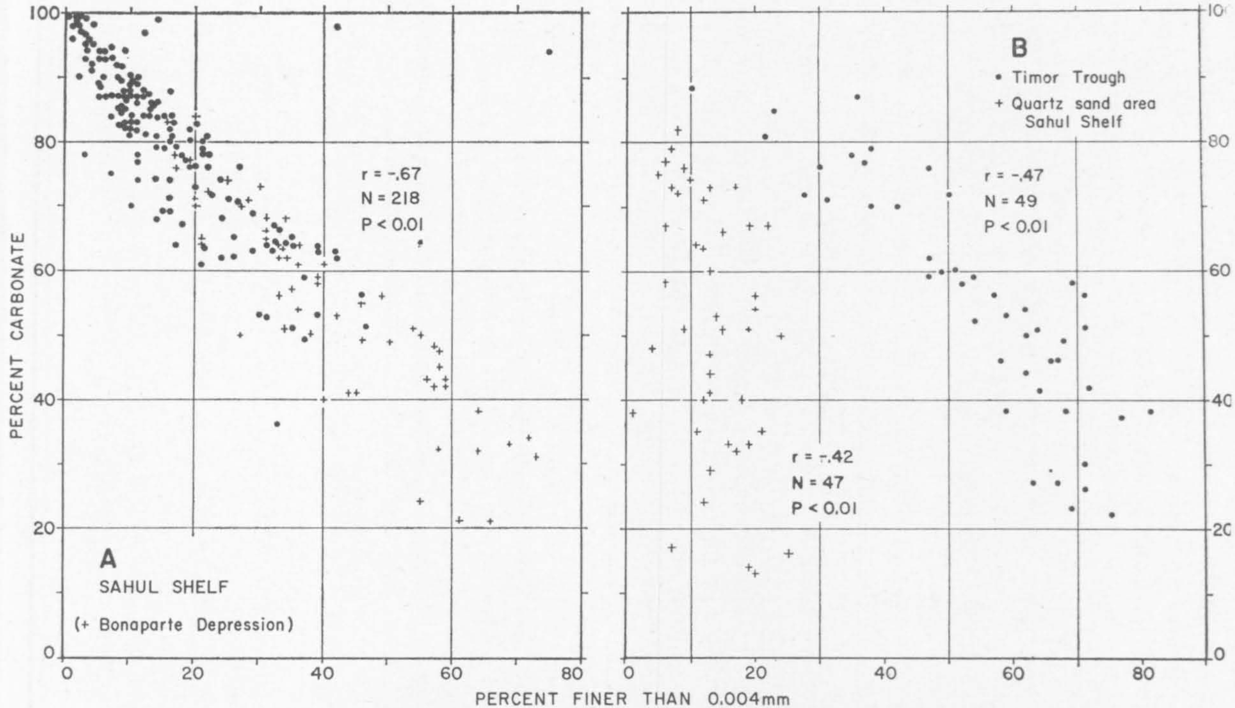

Fig. 7.6—Relation between calcium carbonate content and grainsize (expressed as clay content; percent by weight finer than 0.004 mm) of surface sediments of the Timor Sea. ***P*** **is the probability that the correlation is due to chance,** ***N*** **is the number of samples,** ***r*** **is product moment correlation coefficient.**

In many nearshore samples, the colours are distinctly brown and yellowish brown or reddish brown, as a result of a high content of brown calcareous nodules. Very dark grey and black colours have not been observed. The yellowish and olive tones of the sediments clearly distinguish them from those of terrigenous areas of deposition, such as the Gulf of Paria and the Gulf of California, where sediment colours range from greenish grey to olive green and olive grey. This difference is due to the abundance of white and yellowish skeletal carbonate.

Calcium carbonate content

The Timor Sea sediments range from clayey marls and calcareous sands to marls and pure calcarenites, according to Pettijohn's classification (1957, Fig. 99). The carbonate content varies from 15 to 100 percent (Appendix C) and is dependent on grainsize. In The Sahul Shelf samples (Fig. 7.6A), clay content, as a measure of grainsize, and carbonate content have a strong negative correlation; most of the variance can be explained as being the result of mixing, in varying proportions, an essentially carbonate-free sediment containing more than 95 percent clay, and a pure calcarenite. As a result, the carbonate distribution on the shelf (Fig. 7.7) very closely reflects the textural pattern, with pure calcarenites and calcirudites on the rises and clayey marls in the depressions.

Samples from the shallow nearshore region from Bathurst Island to Cape Londonderry do not follow the clay-carbonate relationship of the rest of the shelf. The sand fraction of many samples in this region contains appreciable amounts of terrigenous material, mainly quartz; the deposits are quartzose calcarenites and calcareous quartz sands. The negative correlation between clay content and carbonate in these samples (Fig. 7.6B), although significant, is not good, and carbonate-free samples contain only about 20 percent clay. More than half of the variability is not due to texture, but to a varying supply of terrigenous sand.

The carbonate content of the Timor Trough sediments also is negatively correlated with clay content (Fig. 7.6B), but again less than half of the variance can be attributed to textural variations. This group of samples occupies a field located to the upper right above the Sahul Shelf set, indicating that the clay fraction itself is much richer in carbonate here than on the shelf. In part, the variation can be considered to be a product of mixing a pure calcarenite with a calcareous clay containing approximately 15 percent carbonate. The regional distribution in the trough shows a marked gradient from a high carbonate content on the upper slope along the Sahul Shelf to slightly calcareous clays along the coast of Timor, similar to the gradient described by Emery (1956) for the Persian Gulf. This gradient is partly due to textural control ; the upper slope deposits along the Sahul Shelf are significantly coarser than the other trough deposits. Over most of the trough, however, the carbonate gradient in large part must be attributed to provenance factors (see Chapter 8).

Glauconite

Glauconite is a minor but widespread component of the Sahul Shelf sediments. The mineral is absent in the Timor Trough. Ginsburg (1957) has stated that glauconite had not been reported from modern shallow carbonates; studies of the Bahamas (Illing, 1954; Purdy, 1963), the Florida shelf (Ginsburg, 1956; Gould & Stewart,

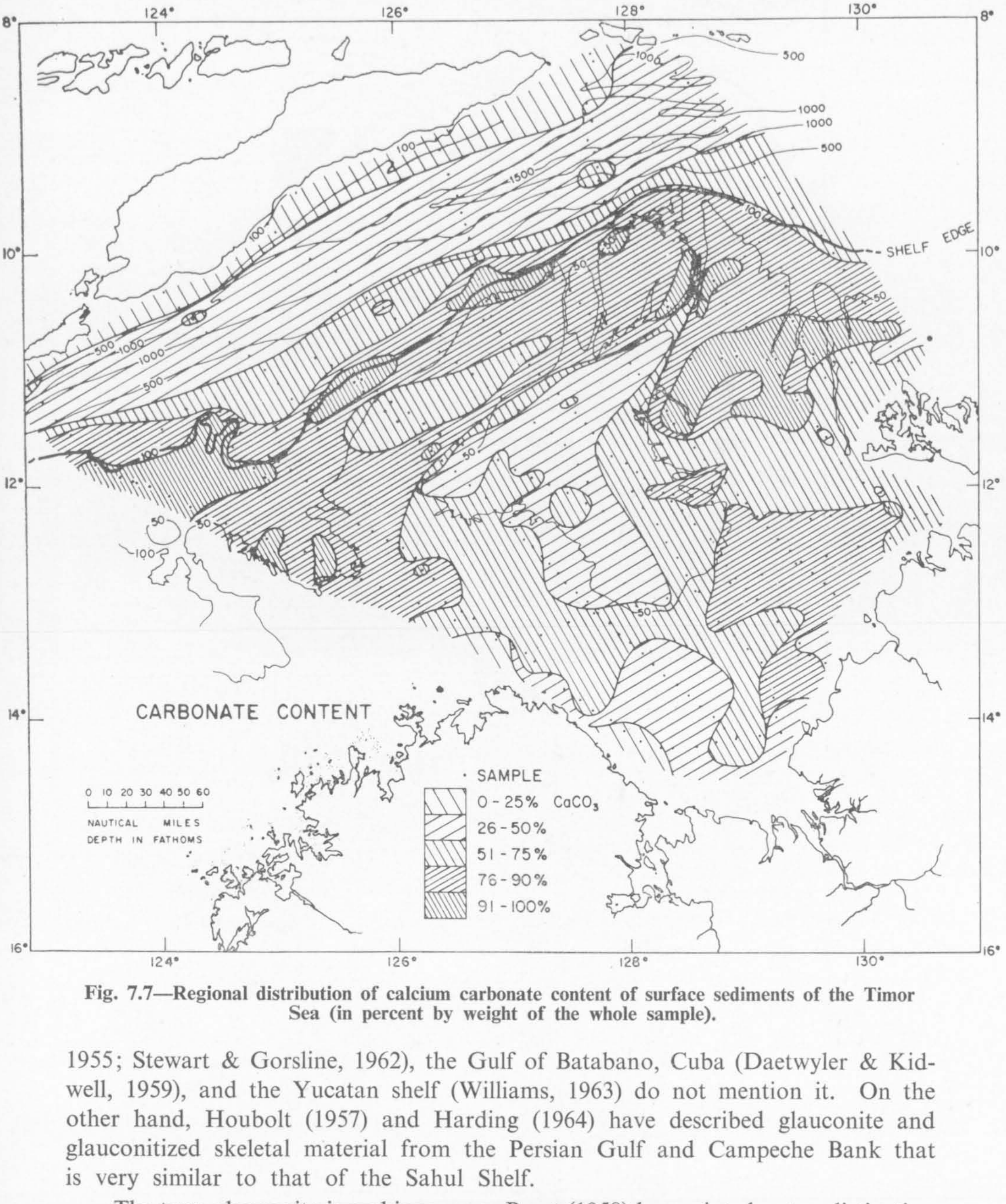

Fig. 7.7—Regional distribution of calcium carbonate content of surface sediments of the Timor Sea (in percent by weight of the whole sample).

1955; Stewart & Gorsline, 1962), the Gulf of Batabano, Cuba (Daetwyler & Kidwell, 1959), and the Yucatan shelf (Williams, 1963) do not mention it. On the other hand, Houbolt (1957) and Harding (1964) have described glauconite and glauconitized skeletal material from the Persian Gulf and Campeche Bank that is very similar to that of the Sahul Shelf.

The term glauconite is ambiguous; as Burst (1958) has pointed out, a distinction has to be made between *mineral glauconite* (see Hower, 1961) and glauconite as a broad field name for green fine-grained sedimentary pellets. The term is used here in the latter sense. Recently, more rigorous descriptions are replacing the older, loose usage (Pratt, 1963; Ehlman, Hulings & Glover, 1963).

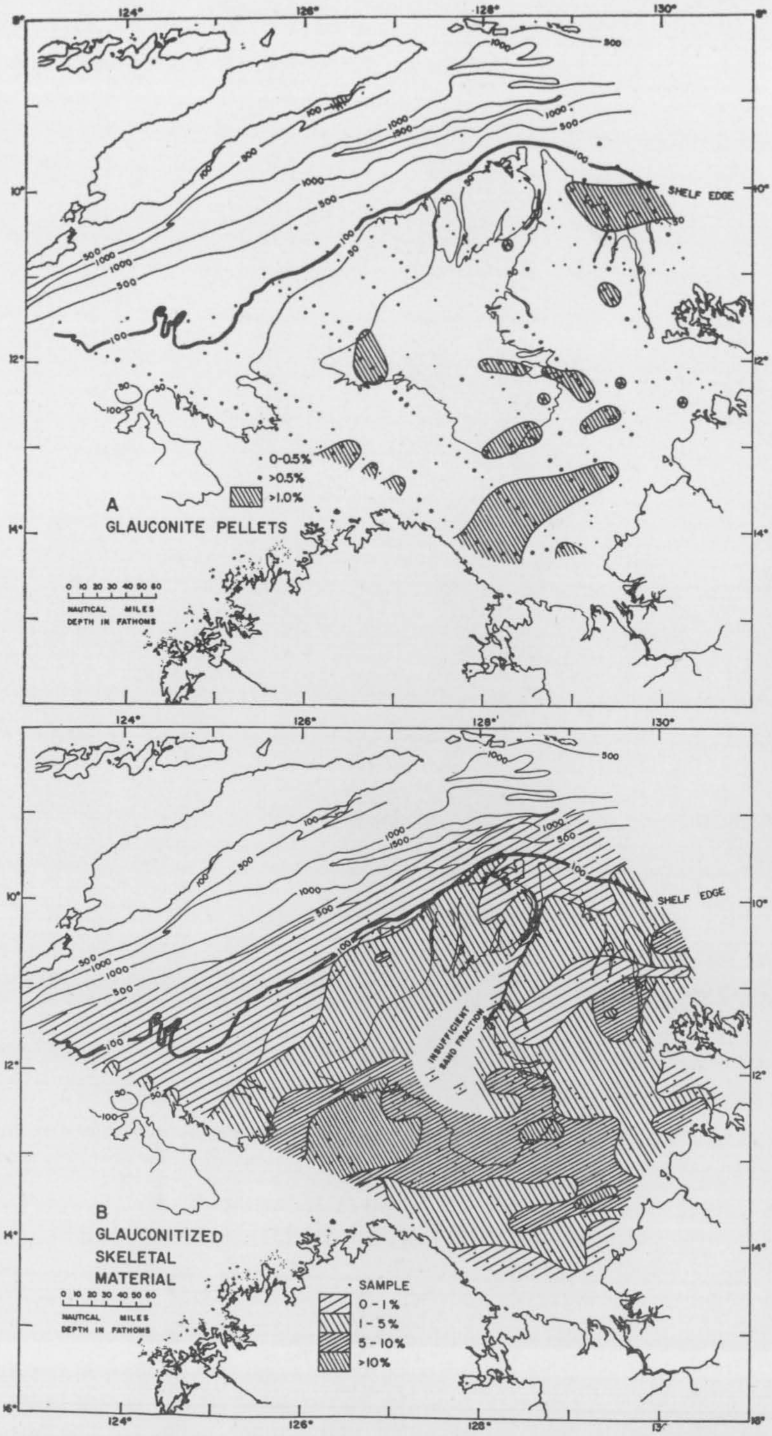

Fig. 7.8—Regional distribution of pelletal glauconite (A) and glauconitized skeletal material (B) in surface sediments of the Timor Sea. Glauconite concentrations expressed in volume percent of the fraction 2.0-0.062 mm on the basis of point counts of thin sections.

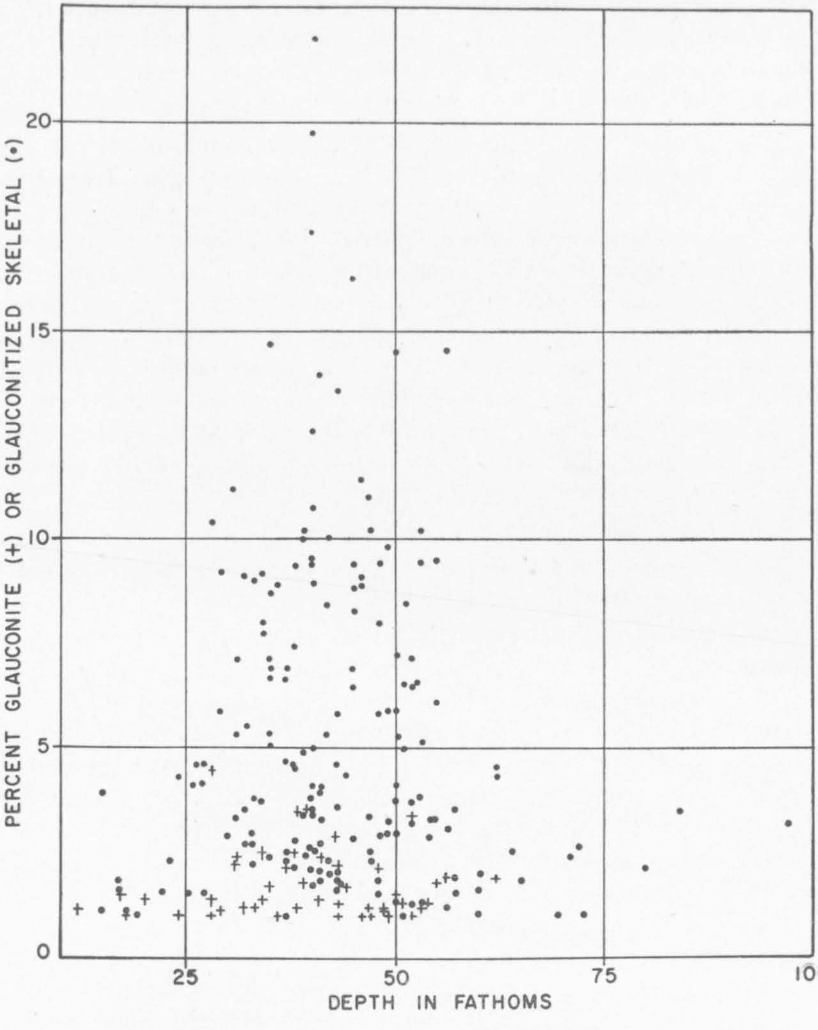

Fig. 7.9—Relation between glauconite percent (volume percent in the fraction 2.0-0.062 mm) and depth of occurrence below sea level.

The Timor Sea glauconites can be broadly divided into two groups: (1) free glauconite pellets and (2) glauconite internal moulds and replacements. The size of pellet glauconite, which forms only a small part of the total glauconite (Appendix D), ranges from 0·1 to 0·25 mm. The pellets usually have an irregularly ellipsoidal shape and a smooth waxy surface. Only a few samples from the upper slope of the Timor Trough contain Foraminifera chamber fillings. Most of the pellet glauconite consists of gastropod chamber fillings, in contrast to the pelletal glauconite on other continental shelves, which generally consists largely of foraminiferal moulds (Curray, 1960, p. 244; van Andel, 1964, p. 250; Pratt, 1963). The regional distribution of pelletal glauconite on the Sahul Shelf is very patchy and appears to be almost random (Fig. 7.8). The highest concentrations occur locally in water shallower than 45 fathoms (Fig. 7.9). Small amounts of pelletal glauconite are characteristic for relict postglacial transgressive sediments on continental shelves. The pelletal glauconite of the Sahul Shelf may belong in the same facies.

The second group of glauconites consists of internal moulds of small gastropods and benthonic Foraminifera (such as *Elphidium*, *Quinqueloculina*, *Textularia*, and *Amphistegina*), which are still enclosed in the tests. More rarely, the glauconite has invaded bryozoan and molluscan skeletal material. No glauconite was seen in coral fragments. The glauconite varies in colour from yellowish green to clear emerald green. There is abundant evidence of replacement of skeletal material with veins and blebs of glauconite, of glauconite impregnation, and of simultaneous corrosion of chamber walls and glauconite deposition. The mineral often invades even very small and remote chambers and canals in complexly structured Foraminifera. These observations suggest that the mineral did not simply form by alteration of clay washed into the shells, but at least in part was precipitated from solution, either directly or through precursor layer-lattice silicates.

From a detailed petrographical-mineralogical study of the Sahul Shelf glauconites by Heath (in press), the following description of the mineralogical composition of the glauconites is quoted:

> ' Glauconites of the Sahul Shelf sediments are invariably disordered and all belong to Burst's (1958) third and fourth classes (interlayered glauconites and glauconites containing two or more argillaceous minerals). The replacement glauconites, which partly impregnate biogenous carbonate, and partly fill chambers of Foraminifera, and pore spaces in echinoderm and bryozoan fragments, vary in composition from interlayered " mineral glauconite " to iron-rich montmorillonite, with variable amounts of admixed iron-rich chlorite (up to 80 percent), to pure iron-rich montmorillonite. The pellets consist of pure iron-rich chlorite, or a mixture of chlorite and interlayered " mineral glauconite " to iron-rich montmorillonite. The expandable layers usually constitute less than 60 percent of the interlayered fraction. The pellets appear to have formed inside the chambers of small gastropods and, in terms of chemistry and crystallinity, are more highly evolved than the replacement glauconites. Both morphotypes are rich in authigenic components and contain only small cores of fine quartz and altered phyllosilicate detritus. Detrital clay minerals seem to have been necessary for the development of the glauconite masses, and probably acted as nuclei or templates upon which elements present in solution in the pore water could crystallize out. The early stage of invasion of the carbonate is invariably a clear yellow pure montmorillonite, which subsequently transforms to a green glauconite.'

Glauconitized skeletal material is very widespread on the Sahul Shelf (Fig. 7.8) and is much more abundant than pelletal glauconite. It is more common on the rises than in low-lying areas, although the flat-topped banks of the Van Diemen Rise are free from it, and it occurs most abundantly in a wide east-west belt between 12° and 14° S. latitude. Here, from 6 to 20 percent of the entire sand fraction is partially glauconitized. There is no correlation between the distributions of pelletal and replacement glauconite. Replacement glauconite is commonest in water depths between 20 and 60 fathoms, and pelletal glauconite between 20 and 45 fathoms (Fig. 7.9), both in the depth zone where relict postglacial transgressive deposits are most widespread (see Chapter 11). The broad zone of replacement glauconite cannot be related to any environmental controls known at this time.

Regional lithofacies distribution

The distribution patterns of the petrographic properties described in previous sections can be summarized in the form of a regional lithofacies map, serving as a basis for the consideration of specific problems in following chapters. The construction of this map requires a petrographical classification. Although at this stage the classification cannot be a genetic one, texture and carbonate content must be emphasized, since the principal problems of this paper are the relation between topography and sediment properties, and the dispersal of the noncalcareous terrigenous fraction.

In recent years, an increase of interest in carbonate rocks has led to numerous proposals (see papers in Ham, 1962) for revision, enlargement, or replacement of such traditional classifications as those of Grabau (1913) or Pettijohn (1957, p. 382). These new classifications are all at least partly genetic and derive from a wide variety of objectives (Ham & Pray, 1962), but have in common the fact that they are oriented toward pure carbonates. The Timor Sea sediments are in large part not pure carbonates, and the proposed systems do not permit their meaningful classification. Moreover, one of our objects is to compare the sediments of this calcareous shelf with those of terrigenous shelves. Consequently, a classification has been devised which suits the special nature of this problem and at the same time is closely related to elements of other carbonate classifications.

It is becoming increasingly clear that for detrital carbonates, simple size terms do not offer a meaningful grouping and are of less importance than measures of sorting that provide some clue to the energy of the environments of deposition and reworking (Dunham's 'currents of delivery and removal', 1962). Most investigators have used the proportion of fine-grained material (matrix, micrite), variously defined, as such a measure (Ham & Pray, 1962). Inspection of Figure 7.4 shows that the sediments of the Sahul Shelf can be understood as a series of mixtures of calcarenite and silty calcilutite. Thus, a grouping into textural classes, 'calcarenite' (sand); 'muddy calcarenite' (muddy sand), including silty sand, clayey sand, and sand-silt-clay; and 'mud' (silty clay and sandy clay), is closely related to the matrix content and at the same time to sediment classifications widely used for terrigenous sediments.

An accepted lower limit for limestone is 50 percent carbonate by weight (Folk, 1959). Sediments containing more than 90 percent carbonate are pure calcarenites or calcilutites; those containing less than 10 percent carbonate are pure sands and clays. The resulting classification, based on texture and carbonate content, is shown in the legend of Figure 7.10. Three principal areas can be distinguished in this map: a predominantly clayey region in the Timor Trough, a zone of pure calcarenites on the outer shelf, and a complex region of mixed sediments on the central and inner shelf. The calcareous clays of the Timor Trough, which are largely of terrigenous

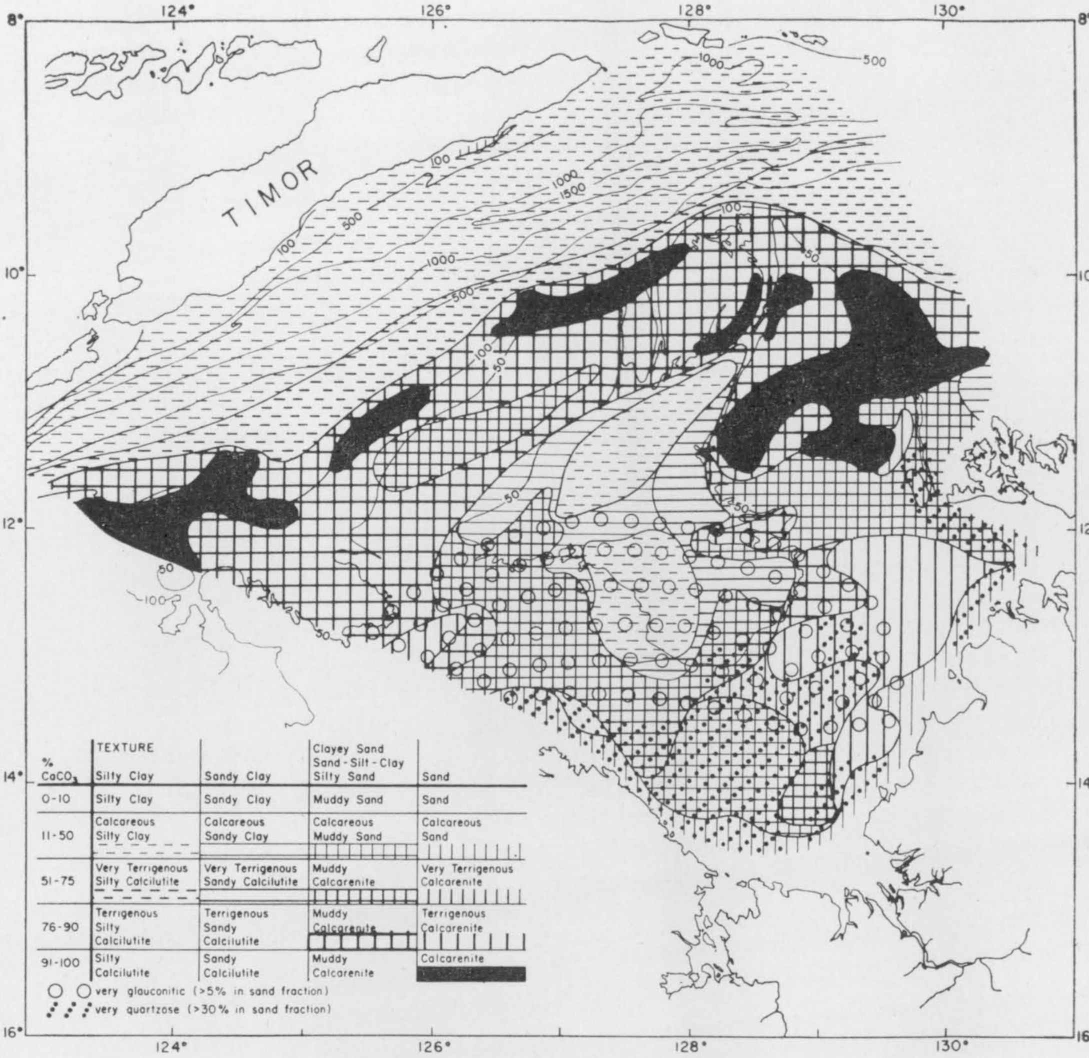

Fig. 7.10—Lithofacies distribution of surface sediments of the Timor Sea. One degree latitude equals 60 nautical miles.

origin, are separated from the shelf by a narrow zone of calcilutite, apparently resulting from the dispersal of fine calcareous debris from the shelf edge and shelf edge banks. In sharp contrast to these fine sediments of mixed composition, the deposits of the outer shelf are dominantly coarse pure calcarenites representing the principal zone of pure limestone of the region. In this zone, the purity of the carbonates is a direct function of grainsize.

Landward of the pure carbonate belt, the complexity of the pattern is largely due to topographic effects. The deep settling basin of the Bonaparte Depression accumulates mainly fine-grained, and therefore terrigenous, material, whereas on the shallower, more turbulent rises and banks, the sediments are coarser and consequently more calcareous. A calcilutite zone along the eastern edge of the Bonaparte Depression is produced by the shedding of calcareous detritus from the bordering rows of banks. On the other hand, the lithofacies pattern of the inner shelf and the Joseph Bonaparte Gulf is not primarily the result of topographic control. In this area of very subdued relief, regional variations of sand supply from the various rivers combine with relict dispersal patterns from the postglacial transgression (see Chapter 11) to form alternating zones of high and low carbonate content in predominantly coarse-grained sediments.

8. Sources and Dispersal of Terrigenous Components

The good negative correlation between carbonate content and grainsize discussed in the previous chapter shows that most of the noncalcareous phase resides in the fine fraction. With the possible exception of small amounts of authigenic material, this component is derived from land. Consequently, the regional distribution of fine terrigenous material is inversely reflected in a map of the carbonate content of the silt-clay fraction. The use of the silt-clay fraction as a reference base instead of the total sample eliminates strong textural control of the map pattern. The gradients of this map (Fig. 8.1) are clear and simple. Along the Australian coast the fine fraction is dominantly terrigenous, but the rapid seaward increase in carbonate content indicates that seaward dispersal of the terrigenous suspended matter is limited. This coastal clay zone is approximately 30 nautical miles wide, similar to the width of the zone of active clay deposition on other continental shelves (Curray, 1964).

In two places, a tongue of low carbonate content extends out onto the Sahul Shelf for a considerable distance. The contours of Figure 8.1 suggest that a plume of suspended material from the Ord and Victoria Rivers is carried northward close to the Kimberley coast and then spreads for more than 200 nautical miles in a north-easterly direction across the Bonaparte Depression. Another clay tongue extends westward on to the central shelf from the nearshore zone north of Bathurst and Melville Islands. Current patterns for December to March, the period of maximum runoff for this part of Australia, and thus of maximum supply of suspended matter, are shown on Figure 8.1. There is good agreement between these currents and the tongues of fine terrigenous material extending beyond the nearshore zone. Similar close interdependence of current patterns and clay dispersal for the north-western Gulf of Mexico has been described by Curray (1960).

Clay supply from the Roti-Timor island chain is indicated by a decrease of carbonate content from the Sahul Shelf across the Timor Trough. The gradient is less steep than along the Australian coast, possibly because of greater depth of water and consequent probability of long settling times, slumping, or turbidity currents. Carbonate content also decreases toward the eastern end of the Timor Trough, suggesting a supply of suspended clay by the Timor Current from the east. In both cases, an alternative explanation of the carbonate gradients may be found by assuming that the fine carbonate is supplied from the Sahul Shelf, while clay is deposited at a uniform rate over the entire trough area.

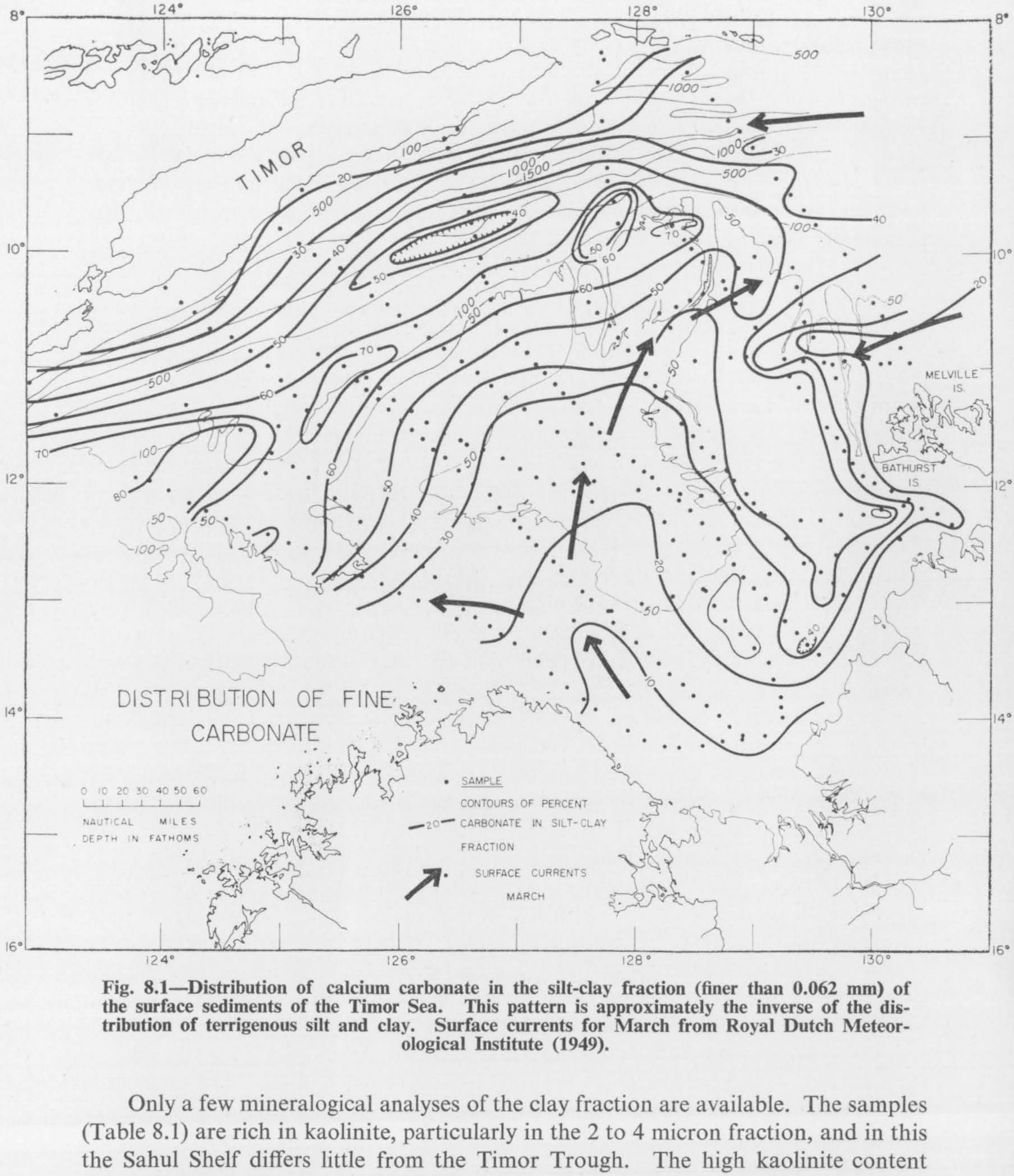

Fig. 8.1—Distribution of calcium carbonate in the silt-clay fraction (finer than 0.062 mm) of the surface sediments of the Timor Sea. This pattern is approximately the inverse of the distribution of terrigenous silt and clay. Surface currents for March from Royal Dutch Meteorological Institute (1949).

Only a few mineralogical analyses of the clay fraction are available. The samples (Table 8.1) are rich in kaolinite, particularly in the 2 to 4 micron fraction, and in this the Sahul Shelf differs little from the Timor Trough. The high kaolinite content distinguishes the Timor Sea sediments from those of the Gulf of California (Calvert, 1964), Gulf of Mexico (Pinsak, 1958), and the Orinoco region (van Andel & Postma, 1954). The abundance of kaolinite in the Timor Sea sediments may be due to the presence of a large deeply weathered lateritic hinterland. Goldberg & Griffin

(1964) and Yeroshchev-Shak (1961) have observed a similar concentration of kaolinite in the equatorial Atlantic, as a result of supply by large rivers draining lateritic hinterlands.

TABLE 8.1

CLAY MINERAL COMPOSITION OF TIMOR SEA SEDIMENTS IN PERCENT

(analyses by Ronald J. Gibbs)

Sample No.	Fraction	Illite	Kaolinite	Montmorillonite	Poorly Crystallized
V–275	<2 microns	29	29	32	10
	2–4 microns	36	46	8	10
V–294	<2 microns	33	25	32	10
	2–4 microns	22	52	16	10
V–308	<2 microns	25	33	32	10
	2–4 microns	22	48	20	10

The distribution of coarse terrigenous material in the Timor Sea is very limited. One sample near the coast of Timor (V–312) is a greywacke containing 15 percent quartz, 10 percent feldspar, 43 percent rock fragments, 20 percent skeletal carbonate, and 12 percent matrix. All other shelf samples collected along the island coasts are fine grained. Along the Australian coast a broad belt of calcareous sands and sandy calcarenites extends on to the inner shelf from Bathurst Island to Cape Londonderry (Fig. 8.2), with highest concentrations of terrigenous material in the western part of the Bonaparte Gulf. Elsewhere on the shelf, the sand fraction is essentially free of terrigenous material, although scattered samples, even near the edge of the shelf, contain rare quartz grains. On the Londonderry Rise, a spotty pattern of low quartz percentages extends to the edge of the shelf.

On the inner shelf, the distribution pattern of quartz consists of alternating zones of high and low concentrations (Fig. 8.2). This pattern does not fit a simple model of seaward dispersal and progressive dilution with skeletal material. The variability is not a function of grainsize; the correlation between the median size of the sand fraction and the quartz content is not significant at the one percent level, although there is a weak preference for the 0·35–0·50 mm size grade. The quartz distribution appears to be somewhat related to water depth (Fig. 8.3); highest concentrations are found in the 10–15, 22–28, 35–38, and 45–48 fathom zones, while at intermediate depths the values are generally low. This zonal pattern and the limiting depth of 50 fathoms suggest a correlation with littoral dispersal during stillstands in the postglacial rise of sea level (Chapter 11; see also Curray, 1960).

The mineralogical composition of these sands has been determined by von der Borch (1965). The sands are quartzose, and the terrigenous fraction contains more than 95 percent quartz. In the western part of the Bonaparte Gulf, 1 to 5 percent feldspar appears regularly (Fig. 8.4, insert). In view of the analytical error, the patchiness of this pattern is not significant. On the basis of the heavy mineral suites

(Table 8.2), two provinces that are separated by a narrow mixed zone can be distinguished. The Ord-Victoria province is characterized by an amphibole-epidote suite, probably derived from the Ord (Carroll, 1947) and Victoria Rivers. The Darwin province has a tourmaline-zircon suite and, in its western part, contains some hypersthene probably supplied by the Finniss, Reynolds, and Daly Rivers. The province is probably derived from the extensive older sediments, especially from the thick laterites, occurring in the adjacent hinterland. The juxtaposition of the mineral provinces with no more than a narrow mixing zone suggests that mineral transport has taken place mainly normal to the edge of the basin with little longshore drift, even during postglacial lower sea level stands.

TABLE 8.2

HEAVY MINERAL ASSOCIATIONS FROM THE SAHUL SHELF

(Based on analyses by C. C. von der Borch)

Percent by point-counts of 100 transparent grains per sample

	Zircon	Tourmaline	Garnet	Staurolite	Kyanite	Epidote	Amphibole	Augite	Hypersthene	Titanite	Others
Darwin Association (N = 11)											
Mean	33·6	49·0	0·7	3·7	0·7	1·2	2·0	1·8	1·2	1·9	4·2
Standard deviation	6·0	6·9	0·4	4·7	1·9	1·9	2·2	2·7	1·5	2·6	3·4
Darwin Hypersthene Association (N = 7)											
Mean	20·9	55·5		2·8	0·6	0·6	2·3	1·6	9·0	1·1	5·6
Standard deviation	5·4	12·2		1·7	1·6	0·6	3·3	2·9	2·7	1·4	4·4
Ord-Victoria Association (N = 22)											
Mean	2·0	6·7	1·3	0·7		14·5	61·4	3·2	5·9	0·8	3·5
Standard deviation	1·9	3·2	1·4	1·1		16·7	24·2	2·6	4·1	1·3	2·8

Various authors have stressed the relationship between sediment composition and the tectonics of the source area and depositional basin (for a review, see Krumbein & Sloss, 1963, p. 503). For some modern sedimentation areas, these concepts have been questioned (Curray, 1960; van Andel, 1960, 1964), but the Timor Sea fits the postulated relationship well. Although a modest amount of movement has been assumed for the Sahul Shelf in previous sections of this paper, the area can reasonably be considered a stable platform (Krumbein & Sloss, 1963, p. 419). The thin deposits on a major unconformity, and the prevalence of skeletal calcarenites, of quartzose sands, and of quartz-glauconite calcarenites are generally considered typical for this tectonic environment (Krumbein & Sloss, 1963, p. 503). It is probable that the high quartz content and the virtual absence of feldspar and other less stable components are due to single-cycle maturation by lateritic weathering rather than to the multicycle history generally postulated for this type of sediment (see Potter & Pryor, 1961).

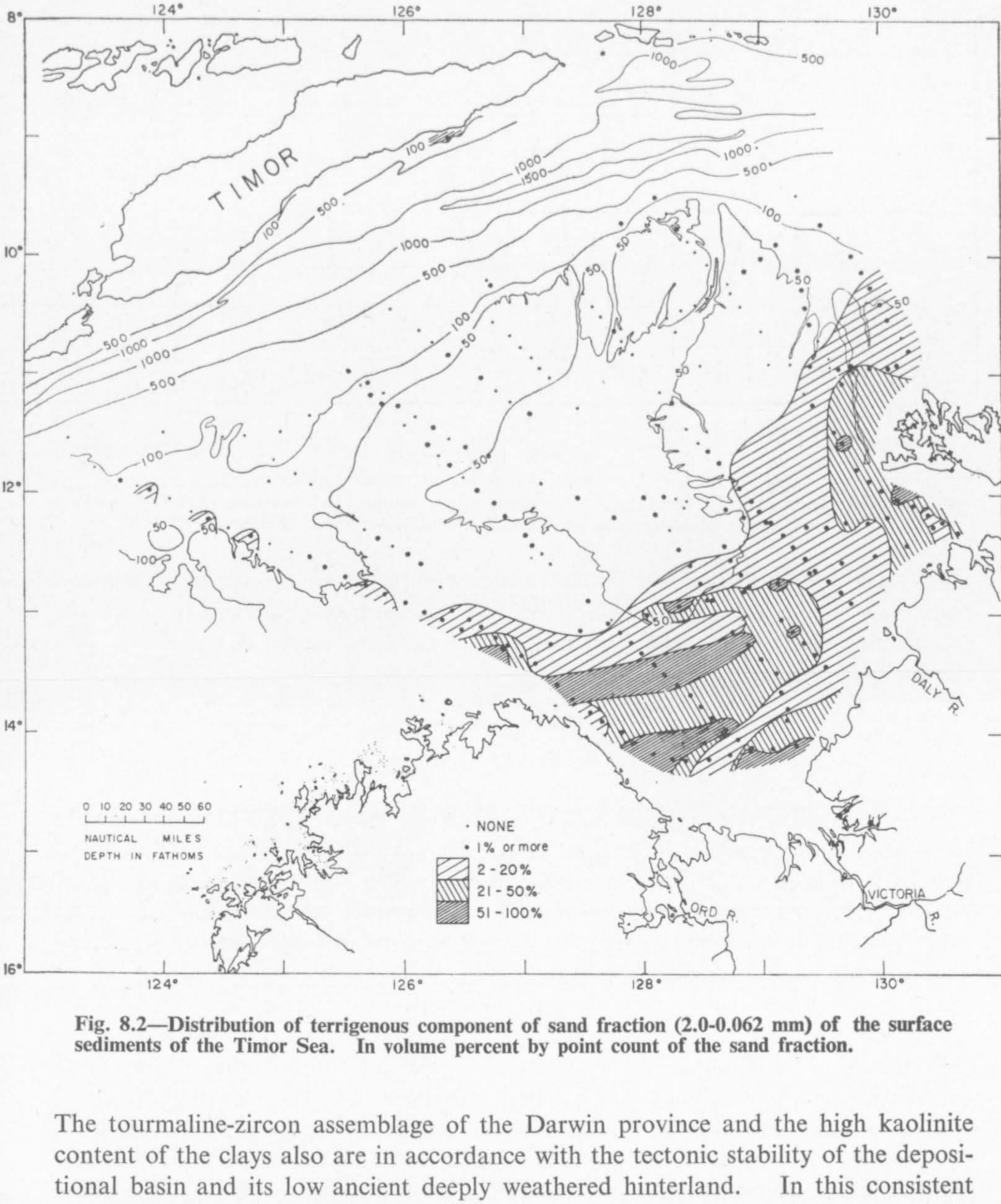

Fig. 8.2—Distribution of terrigenous component of sand fraction (2.0-0.062 mm) of the surface sediments of the Timor Sea. In volume percent by point count of the sand fraction.

The tourmaline-zircon assemblage of the Darwin province and the high kaolinite content of the clays also are in accordance with the tectonic stability of the depositional basin and its low ancient deeply weathered hinterland. In this consistent picture, the amphibole-epidote association forms an apparent contradiction, especially since it occurs in a highly mature quartz sand. The Ord and Victoria Rivers almost certainly obtain the bulk of their bedload from deeply weathered terrain which yields little but quartz and small amounts of stable heavy minerals. Apparently, however, there is enough additional erosion of fresh bedrock (probably Antrim Plateau Volcanics) to dilute this material with small amounts of fresh debris, containing such high percentages of feldspar and unstable heavy minerals that they

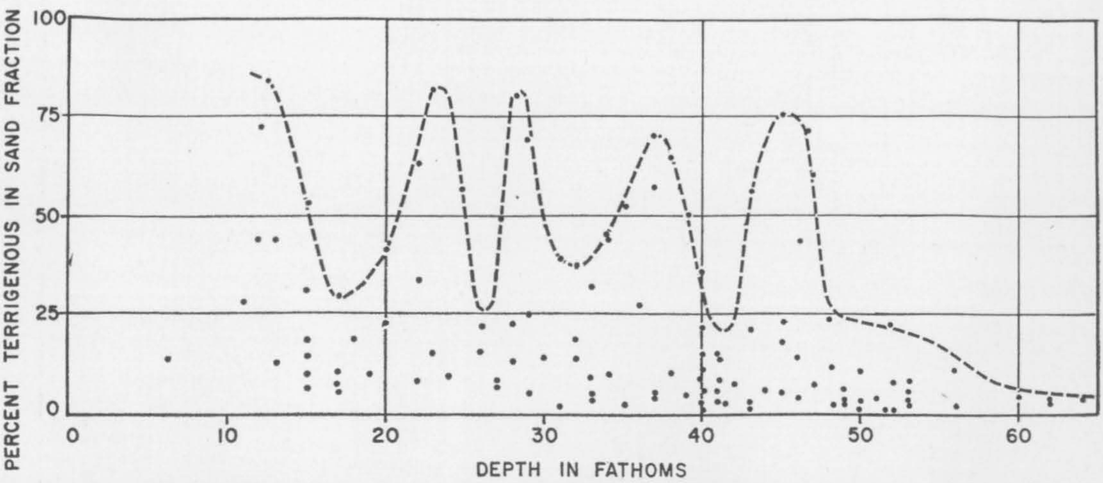

Fig. 8.3—Relation between percentage terrigenous grains in the sand fraction (2.0-0.062 mm) and depth of samples below sea level. Envelope curve sketched.

slightly affect the bulk composition and almost completely change the heavy mineral assemblage. This lack of correlation between heavy mineral assemblages and the general composition and degree of maturity of the source area is not uncommon elsewhere (van Andel, 1960).

9. Coarse Fraction Composition and Biofacies of the Sahul Shelf

Methods and constituents

The coarse fraction (coarser than 0·062 mm) of the Sahul Shelf sediments to a large extent is composed of skeletal material. Hence, with the exception of a limited area of terrigenous deposits, a composition study is a study of biogenous facies. These facies may be ecologically controlled and derived from organisms living *in situ*, either now or in the past, or they may have been redistributed and modified by physical and chemical agents. In that case, the compositional facies reflect not ecology, but other environmental factors, mainly transporting agents.

Procedures for the analysis of particle composition in carbonate sediments have been developed by Houbolt (1957), Ginsburg (1956), and Purdy (1963). Ginsburg's and Purdy's thin section technique has been used here, modified by using artificially graded samples following Houbolt. Particle identifications have been based on comparison with thin sections of selected Sahul Shelf skeletal material and on descriptions in the literature (mainly Cole, 1954; Cushman, Todd, & Post, 1954; Ginsburg, 1956; Illing, 1954; Johnson, 1951, 1952, 1954, 1961; Purdy, 1963, Wells, 1954a, b). The data were obtained by point count (Chayes, 1956) of 300 points at 0·3 mm spacing. Data are given in Appendix D to the first decimal; obviously the estimates do not have that degree of reliability. As shown by van der Plas & Tobi (1965), the population estimate, based on a count of 300 grains and with 95 percent confidence, will lie between +3 and —3 percent of a sample estimate of 10 percent, and between + 6 and — 6 percent of a sample estimate of 50 percent. The following conventions

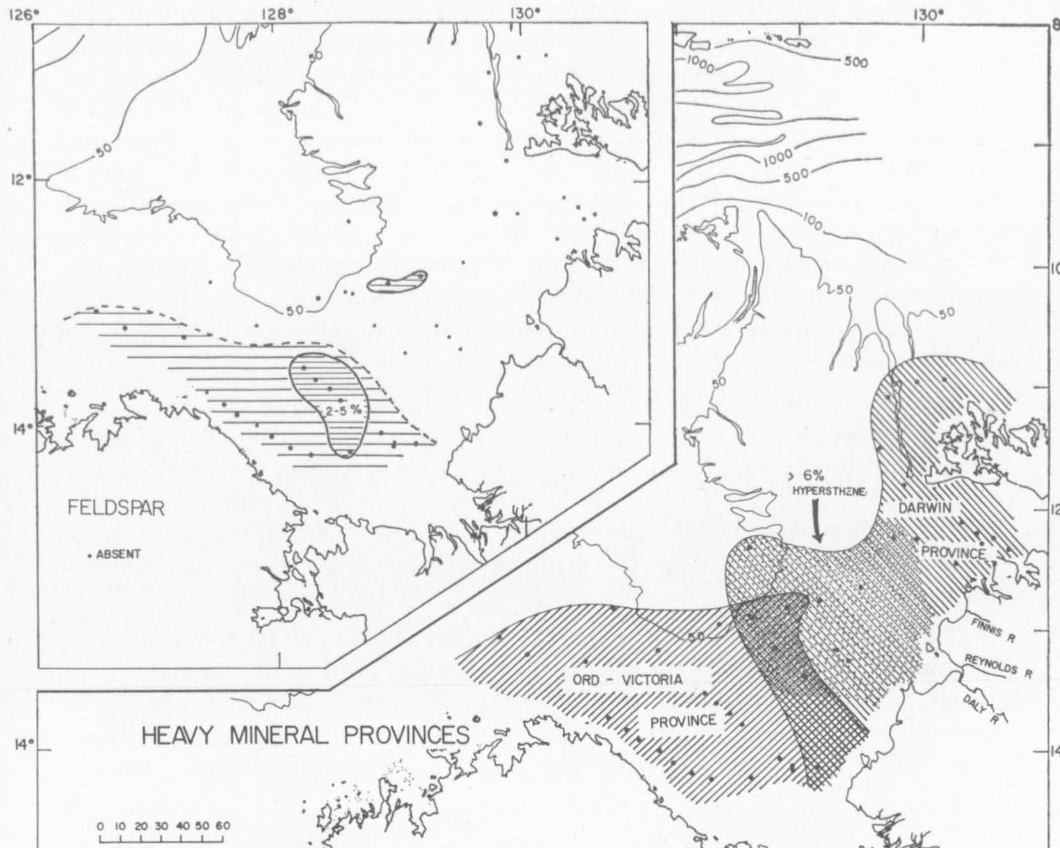

Fig. 8.4—Heavy mineral provinces and distribution of feldspar (in percent of the terrigenous fraction of the 2.0-0.062 mm size grade) in the surface sediments of the Sahul Shelf. The area with more than six percent hypersthene in the heavy fraction is shown with dotted pattern. Map based on data from von der Borch (1965). Insert: Small dots are samples without feldspar.

have been used in the point counts. Composite grains containing a major component, or grains filled or encrusted with other material, were counted according to principal components; voids within grains were tabulated as grains; other voids were omitted; partially glauconitized grains were counted as the original material and also tabulated as glauconitized material (this second tabulation was not included as part of the 300 counts), then later expressed as a percentage of glauconitized material with reference to the sum of all others. Count lines were run parallel to the size gradient (perpendicular to planes of equal grainsize) and terminated when the results of a series of full counting lines exceeded 300 points.

Halimeda was tabulated separately; all other calcareous algae, predominantly *Lithothamnium* and *Amphiroa*, were combined. The Foraminifera were divided into two groups: (1) Large Foraminifera, including *Marginopora*, *Heterostegina*, *Amphistegina*, *Cycloclypeus*, *Alveolinella*, *Calcarina*, *Sorites*, *Operculina*, Peneroplids, and large Miliolids; and (2) Small Foraminifera, comprising all others. Encrusting Foraminifera were combined with Bryozoa. A Miscellaneous group contains *Millepora*, worm tubes, Ostracoda, Pteropods, and Crustacea; this group usually is insignificant. Skeletal fragments of unknown origin, including those that were too strongly altered or too small for identification, were tabulated as Unidentified. This group rapidly increases in importance with decreasing size; although the lower limit varies with particle type, fractions finer than 0·06 mm are largely unidentifiable in thin section.

Non-skeletal material, except for detrital terrigenous grains, lithoclasts, and some glauconite pellets, is very rare. Elements of the large variety of non-skeletal carbonate grains distinguished by Illing (1954), Ginsburg (1956), Purdy (1963), and Williams (1963), ranging from ooids to aggregates, are found only occasionally. Only faecal pellets and ooids, although both rare, were common enough to merit separate listing; the others were grouped with pyrite, plant fragments, etc., in a Miscellaneous category.

The ooids of the Sahul Shelf consist of a coating of generally randomly oriented, more rarely radial or concentric microcrystalline calcium carbonate around a large nucleus, which is usually quartz or sometimes a fine-grained sandy mud pellet. The outer surface is generally smooth and shiny. The carbonate coating is yellow-brown. True ooids or oolitic coatings on skeletal material have not been observed.

A variety of consolidated calcareous rock fragments, including calcite-cemented skeletal debris, cemented quartzose calcarenite and calcareous quartz sand, and consolidated calcareous mud, were grouped together as *lithoclasts*. The group is petrographically and probably genetically heterogeneous.

This composition study deals exclusively with the fraction coarser than 0·06 mm. The composition of the clay fraction, discussed earlier, is dominantly terrigenous. Thus, the composition and origin of the silt fraction remain unknown. This implies that for the Sahul Shelf, on the average, the composition of more than 80 percent of the sediment has been examined (Appendix B).

Correlations between components

Eleven of the 17 components distinguished in Sahul Shelf thin sections are quantitatively or diagnostically important. Inspection of the data reveals positive or negative covariance of several components. Since the data matrix is too large to establish rigorously such relationships, a product moment correlation matrix for all 17 variables tabulated in Appendix D was computed on the basis of 251 samples. From this matrix of correlations between all possible pairs of variables, a hierarchy diagram was constructed (Fig. 9.1) according to the method of Sokal & Michener (1958). This diagram shows quantitatively and rigorously the level of association of all components and higher order groups.

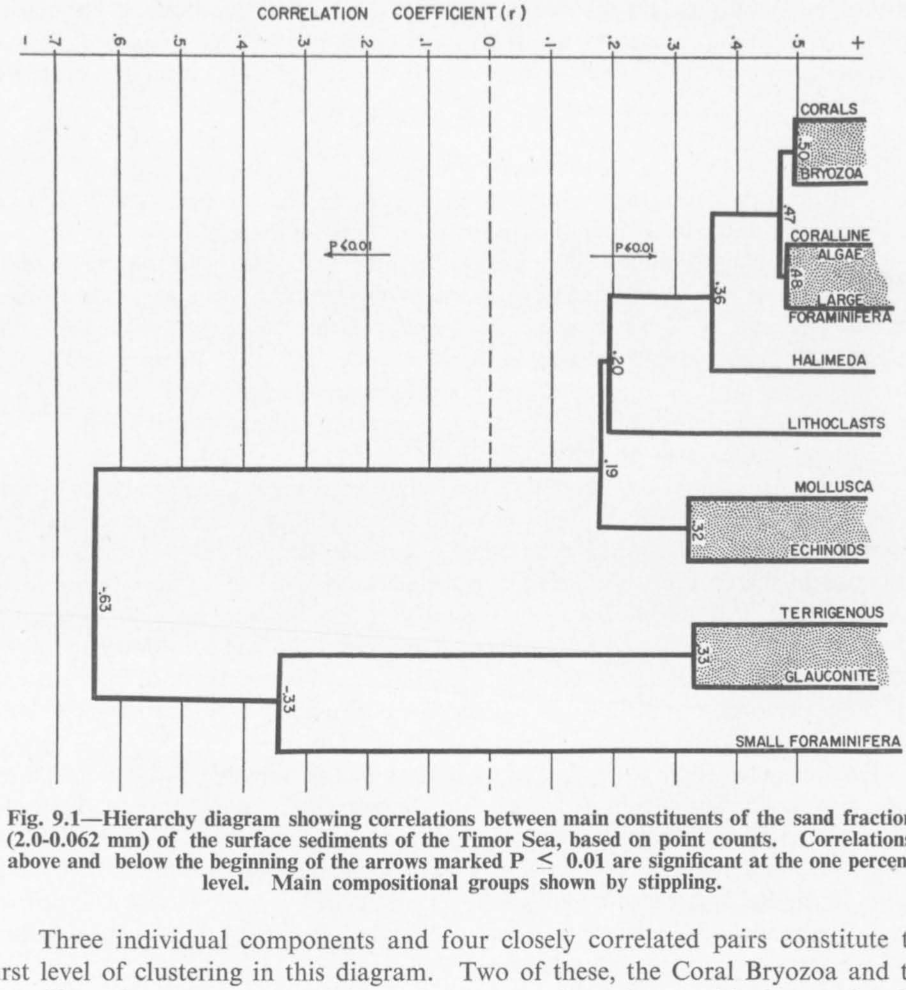

Fig. 9.1—Hierarchy diagram showing correlations between main constituents of the sand fraction (2.0-0.062 mm) of the surface sediments of the Timor Sea, based on point counts. Correlations above and below the beginning of the arrows marked P $\leq$ 0.01 are significant at the one percent level. Main compositional groups shown by stippling.

Three individual components and four closely correlated pairs constitute the first level of clustering in this diagram. Two of these, the Coral Bryozoa and the Coralline Algae Large Foraminifera clusters, are themselves positively correlated at a high level. These secondary clusters correlate positively with *Halimeda*. The Lithoclasts and the Mollusca/Echinoid clusters join the previous group at a barely significant level. This entire hierarchical tree itself shows a high degree of mutual exclusivity with the Terrigenous/Glauconite cluster and with the Small Foraminifera.

Thus, seven compositional assemblages probably make up in first approximation the data set of Appendix D. Each of these is characterized by a first-order pair or single variable. The Coral/Bryozoan, Algae/Large Foraminifera, and *Halimeda* first-order suites combine to a larger, still closely related group, which is one of four weakly or negatively correlated super-assemblages. The other first-order groups are the Small Foraminifera, Mollusca/Echinoid, and Terrigenous/Glauconite assemblages.

It must be noted that this hierarchy diagram is based on compositions expressed as percentages. Such a closed data system contains built-in interlocking relationships (Chayes, 1960, 1962; Krumbein, 1962), and the strongly negative correlations between major groups are at least in part caused by strongly positive correlation within the groups. Since no adequate theory of interlocking in closed systems exists at this time, the correlation matrices of percentage data must be interpreted conservatively.

Compositional assemblages and their distribution

It is apparent from the correlations of Figure 9.1 that several associations can be expected in the compositional data matrix. Some of these associations are characterized by a single component and are sufficiently independent of the others that a percentage map would adequately record their distribution patterns. Others either are characterized by more than one component or are so closely related to other groups that such a simple technique would not be sufficient. Consequently, it is desirable to identify, within the data matrix, existing compositional assemblages on the basis of the entire set of variables, and to map the regional distribution of entire associations, rather than of individual components.

The environmental parameters of the Sahul Shelf region, including small-scale topography, are very poorly known. The existing knowledge is inadequate to govern or even to assist in the erection of a causal system underlying the variation contained in the data matrix. Hence, a deductive analysis of compositional facies is impossible. The assemblages composing the data set will have to be defined inductively and depositional environments inferred from them. Mapping of the regional distribution of such inductive assemblages and comparison of map patterns with broad environmental information can then be used to evaluate environmental control.

For this case, where a large set of numerical data is available and *a priori* knowledge of casual relationships is inadequate, Imbrie (1963, 1964; Imbrie & Purdy, 1962; Imbrie & van Andel, 1964) has developed a mathematical model based on factor analysis (Harman, 1960). Purdy (1963) has applied this model in facies studies in the Bahamas; a more advanced version, called vector analysis, will be used here. The model and its computational procedures have been described by Imbrie (1963; Imbrie & van Andel, 1964).

The vector analysis is used here to select from a set of determinations of sample compositions those samples that represent the most extreme composition (Q-mode of vector analysis). The samples are the end members of the system in the same sense that orthoclase, albite, and anorthite are the end members of a set of feldspar compositions expressed as oxides. After the end members of the system have been identified, all other samples are expressed in terms of the *proportions* (not percentages) of the end members contributing to their composition. The number of end members needed to account for a large portion of the variance of the data set is usually much smaller than the number of variables; and the structure of the set can thus be considerably simplified. It must be noted, however, that the minimum number of end members required to account for a specific part of the variance is not necessarily the same as the number of causes operating to produce the variance.

Thus, vector analysis provides a continuous-variable type of classification of the samples based on composition (Rodgers, 1950; Hempel, 1952). The model does not make any assumptions concerning the frequency distribution of the data, nor does it provide any hypotheses relating the end members and the distribution of their proportional contributions to causal effects. Interpretations of the results can be based on the assumption that each end member represents a causal factor or a set of environmental conditions in its most extreme form. Evaluation of the end member samples, map patterns of their proportional distributions, and environmental data can be used to aid in the erection of explanatory hypotheses.

Computations for the present study have been carried out on a Control Data Corporation 3600 electronic computer, using a programme designed by John M. Wild, Jr (Factor Analysis System (FAST), University of California, San Diego; Computer Center Report UCSD–64–03, July, 1964). The analysis was carried out on untransformed percentage data, using a cosine-theta correlation matrix (Imbrie & Purdy, 1962), a principal axis factor solution, a normalized varimax rotation (Harman, 1960), and an oblique vector projection (Imbrie & van Andel, 1964).

Of the 377 stations of the Timor Sea survey, 251 contained enough coarse material for a thin section analysis. Since the computer programme allows only a 200 $\times$ 200 data matrix for the Q-mode, 51 samples were eliminated from the data set by use of a random-number table. A second data set of 200 was prepared by substituting these 51 samples for randomly selected samples in the first set. The end members identified are identical or very similar for both sets of data, and oblique vector projections generally are closely comparable, showing that the sets are equivalent.

The hierarchy diagram of Figure 9.1 suggests that at least six end members may be present. Consequently, in different passes, 5, 6, 7, and 8 factors were extracted (Table 9.1). In all four cases, the first three end members are identical in composition, representing suites dominated by Small Foraminifera, Mollusca, and Terrigenous material, respectively. A Lithoclast suite, although of somewhat lower rank, also is present in all four cases. These four end members correspond to those four groups in Figure 9.1 that are not significantly correlated or strongly negatively correlated with each other and the other groups. The fifth end member of the 5-factor set has a composition indicative of the cluster of large Foraminifera, coralline Algae, Bryozoa, coral, and *Halimeda* of Figure 9.1. Extraction of additional factors resolves this end member into three separate ones, characterized by large Foraminifera, coralline Algae with corals and Bryozoa, and *Halimeda*, respectively. The *Halimeda* end member, although compositionally well defined, has extremely limited regional distribution; it is dominant in a few samples and essentially absent in all others. Further extraction yields an additional eighth end member, but it occurs in significant proportion in only a few samples, and the correspondence between the two data sets for this factor is very poor. The regional distribution of this end member is essentially random.

Hence, six end members appear to account for essentially all usable information contained in the data matrix. The regional distribution of the proportional contributions of these six end members to the composition of all samples is shown on the maps of Figures 9.2 and 9.3. The distribution of the *Halimeda* end member, obtained from a 7-factor extraction, has been superimposed on the Large Foramini-

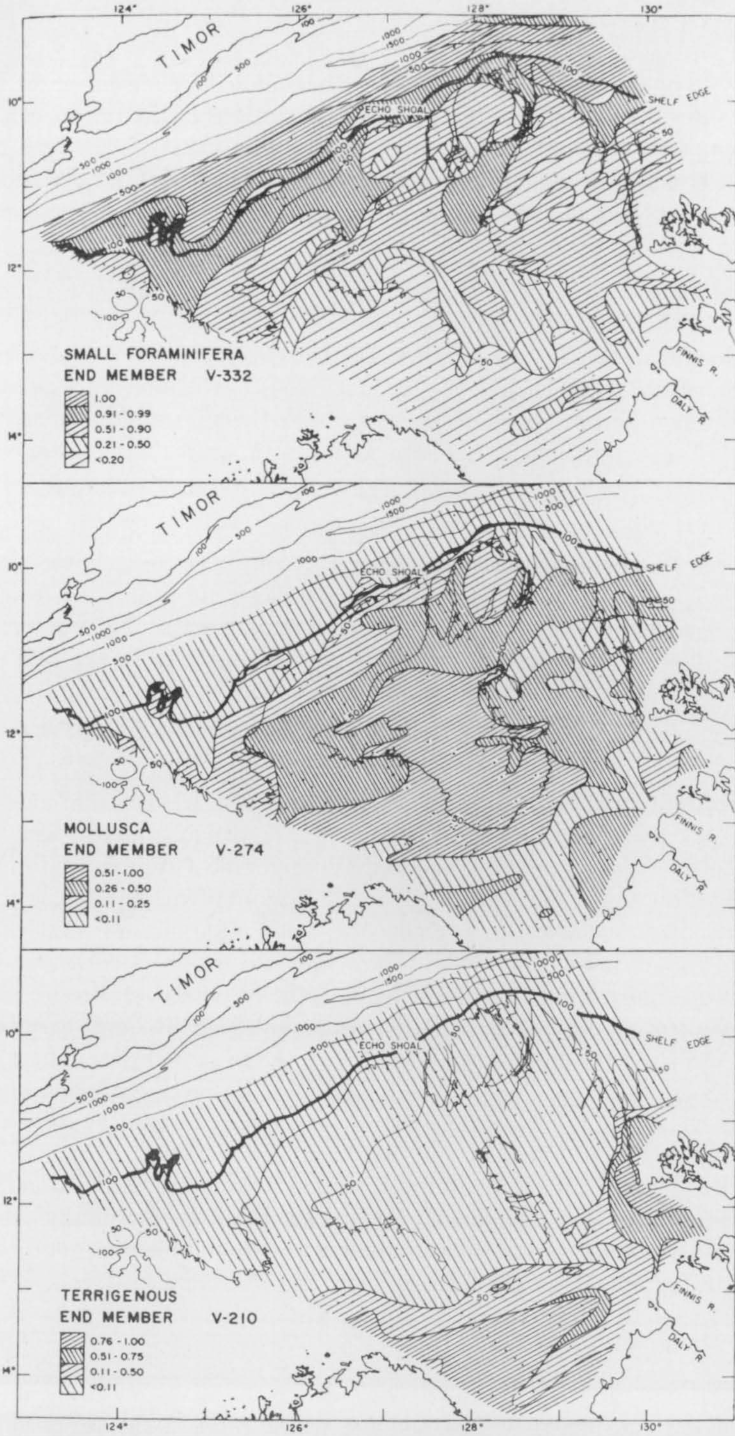

Fig. 9.2—Vector projection maps for the Small Foraminifera, Mollusca, and Terrigenous end members of the composition of the surface sediments of the Timor Sea. Contours are based on proportional contributions of end members to each sample, not on percentages. Dots are sample locations. Fraction 2.0-0.062 mm.

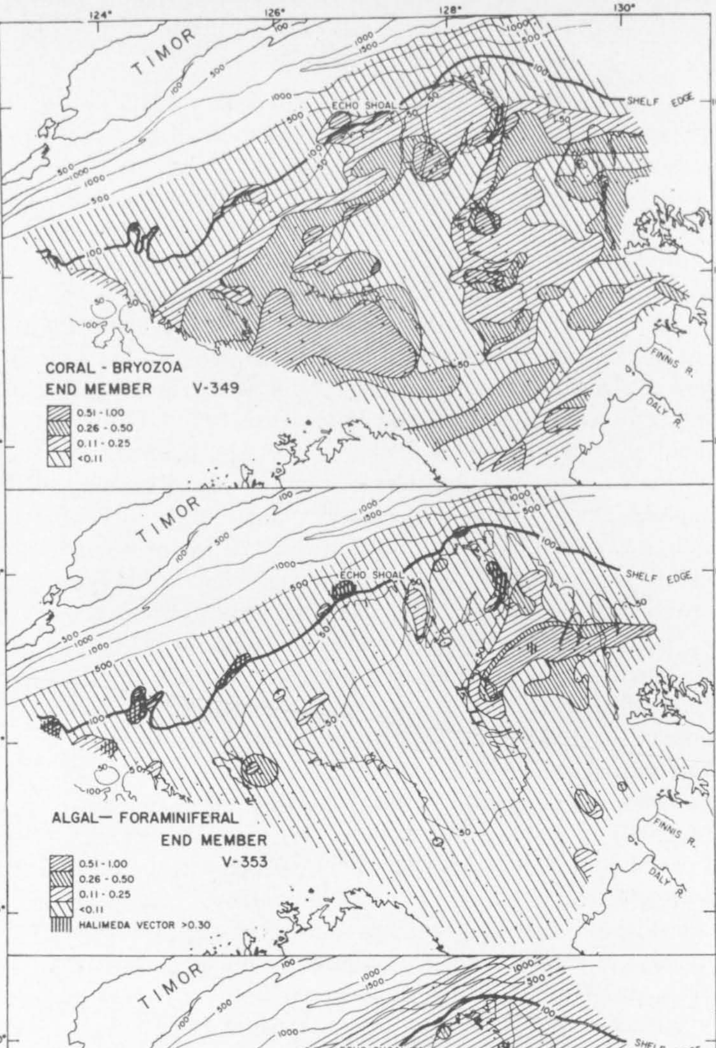

Fig. 9.3—Vector projection maps for the Coral-Bryozoa, Algae-Foraminifera, and Lithoclast end members of the composition of the surface sediments of the Timor Sea. Distribution of *Halimeda* end member shown by heavy shading in centre map. Contours are based on proportional contributions of end members to each sample, not on percentages. Dots are sample locations. Fraction 2.0-0.062 mm.

fera/Coralline Algae map. The contours are based on all data points but take into account topographic information and the composition of the very coarse fraction where data is sparse.

The *Small Foraminifera end member* is the dominant one and constitutes the regional background on which the distribution patterns of the others are superimposed. The end member sample (V–332) essentially consists of small Foraminifera only. Small percentages of alcyonarian spicules are widespread in the outer shelf samples. Many samples contain a high proportion of the Small Foraminifera end member; 42 samples have proportionalities of 0·90 or more for it. The dominant regional trend is a regular seaward increase, so that this end member is almost exclusively present on the outer shelf and in the trough. Only the shelf edge banks and some bank areas of the outer Londonderry Rise interrupt the pattern. The primary seaward gradient is modified by marked landward bending of the contours in the Bonaparte Depression and the Malita Shelf Valley. Proportional values normal for the outer shelf thus are found in this area more than 100 miles inward from the shelf edge. A narrow zone of fairly high concentration also occurs in the south-western Joseph Bonaparte Gulf. Anomalously low values are found in the bank areas at 12° S. latitude on either side of the Bonaparte Depression and on the banks of the Van Diemen, Londonderry, and Sahul Rises.

The regional distribution pattern appears to be primarily a function of increasing distance from land and increasing water depth, and it shows a close correspondence to the broad regional relief of the Sahul Shelf.

The same simple distribution pattern, showing a regular seaward increase and minor interruptions by bank areas, is shown by the ratio between planktonic and benthonic Foraminifera (Fig. 9.4; Appendix E; expressed as the percent planktonic specimens with reference to the sum of all Foraminifera). The values show a regular increase in an offshore direction, with contours approximately parallel to the shore line. The banks on the rises are represented by lower percentages of planktonic Foraminifera; a westward-extending tongue near Bathurst Island may be related to the current distribution in this area (cf. Fig. 8.1), which brings in coastal water. The irregularities are superimposed on this regional pattern. The end member occurs in intermediate proportions on the banks bordering the Bonaparte Depression at 12° S. latitude and, without topographic control, in nearshore areas of the Clarence Strait and the Daly River, and eastward from the Kimberley Coast.

Although the distribution of the *Mollusca end member* is in part clearly related to the Bonaparte Depression, its pattern apparently is not so simple a function of distance from shore or regional relief as is that of the Small Foraminifera end member.

The *Terrigenous end member* is restricted entirely to the inner shelf in the Bonaparte Gulf. The end member sample (V–210) is dominated by a single component; of 38 samples in which the end member dominates, 18 have proportionalities above 0·90. Its distribution shows a peculiar zonal pattern that is not related to topographic features. As has been discussed elsewhere (Chapter 11), it is probably related to the postglacial transgression.

The *Coral/Bryozoa end member* is a composite suite, characterized by fairly high percentages of corals and Bryozoa, characteristically accompanied by several other components, such as large Foraminifera and coralline Algae. The end member sample itself (V–349) contains 18 percent terrigenous grains, but this is incidental; 8 other samples in which this end member occurs with proportionalities above 0·75 all contain less than 5 percent terrigenous material.

This end member is concentrated on the banks of the middle Londonderry Rise, on the narrow, highest part of the Sahul Rise, on the bank areas bordering the Bonaparte Depression, and around the large group of shallow banks of the Van Diemen Rise. These shoals of less than 20 fathoms are themselves free of this assemblage, which is also unimportant on the shelf-edge banks of similar depth. The end member is patchily distributed in nearshore areas of the Bonaparte Gulf, and there is no apparent relation to local topography.

Another bank facies is the *Algae/large Foraminifera end member*, which is so closely related to the Coral/Bryozoa end member that extraction of only 5 factors combines the two. A 7-factor resolution separates a *Halimeda* end member in addition to the two others. The Algae/large Foraminifera end member sample (V–353) is characterized by an abundance of Large Foraminifera with lesser amounts of Coralline Algae. No other constituents, not even corals or Bryozoa, are significantly and constantly associated with these components. The end member and its

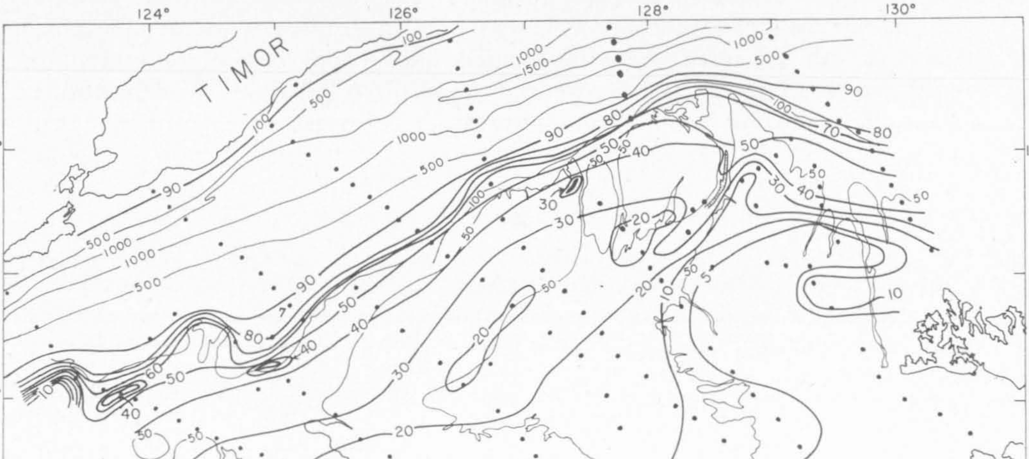

Fig. 9.4—Contours of the regional distribution of planktonic Foraminifera in proportion to the total number of Foraminifera in the sand fraction (2.0-0.062 mm) of the surface sediments of the Timor Sea. Dots are data points. Planktonic percentage =

$$\frac{\textbf{100 x number of planktonic specimens}}{\textbf{number of all Foraminifera}}$$

Halimeda relative have a very restricted areal distribution; high proportions occur only on the shallowest banks in depths of less than 20 fathoms. The main areas of occurrence are the shelf-edge banks and the shoals of the Van Diemen Rise.

The composition of the *Lithoclast end member* (sample V–14) is not very characteristic, and its areal distribution is complex and difficult to interpret. The main areas of concentration are the inner shelf in the Bonaparte Gulf and parts of bank areas on the rises. Only occasionally does the end member constitute a large part of the sample. To a large extent its complex nature may be due to failure to distinguish between different types of lithoclasts. A calcite-cemented quartzose calcarenite appears to be most common on the inner shelf, cemented skeletal debris most common on the rises.

Composition of the calcirudite fraction

Many samples contain substantial amounts of material coarser than 2 mm (Appendix B; Fig. 7.3). The calcirudite fraction covers a very wide size range and varies from a few grains to very large quantities, rendering a quantitative analysis difficult. Therefore, only a qualitative description was prepared, based on macroscopic and binocular microscope description. The samples can be grouped in a small number of descriptive categories, and although there is considerable variation within each, most samples could be assigned to the proper category without difficulty. In samples with very small calcirudite fractions, the sampling error of this procedure is probably very large. A qualitative estimate of the reliability of the data can be obtained by comparing Figure 7.3 and the calcirudite composition map of Figure 9.5.

TABLE 9.1

END MEMBERS OF SAHUL SHELF COMPOSITION SYSTEM, BASED ON VECTOR ANALYSIS OF 251 THIN SECTIONS OF THE FRACTION BETWEEN 2·00 AND 0·06 MM

A. Reference Vectors and Communalities (percent of Variance Accounted for) obtained by Vector Analysis of Two Sets of Randomly Chosen Data (see text)

5 Factors	6 Factors	7 Factors	8 Factors	Communality in Percent
V–336	V–332	V–332	V–334	65·5
V–274	V–274	V–274	V–274	15·6
V–210	V–210	V–202/210	V–202/210	10·2
V–353	V–353	V–350	V–350	3·4
V–14	V–349	V–349	V–349	1·7
	V–14	V–14	V–14/169	1·2
		V–231	V–231	0·7
			V–272/148	0·6
			residual	1·1

TABLE 9.1 (*continued*)

B. COMPOSITION OF REFERENCE VECTORS IN PERCENT BASED ON POINT COUNTS OF 300 POINTS PER SAMPLE

[(Diagnostic Components Italicized)

Sample Number	Coralline Algae	*Halimeda*	Coral	Large Foraminifera	Small Foraminifera	Mollusca	Echinoids	Bryozoa	Lithoclasts	Terrigenous	Glauconite	Miscellaneous
Smqll Foraminifera End Member												
V–332					*98·3*		·7					1·0
V–334					*93·8*						·8	5·4
V–336				·7	*87·2*		·7			1·1	·7	9·6
Mollusca End Member												
V–274		1·3	3·8	3·4	7·7	*68·9*	3·8	4·3	1·3	2·1		3·4
Terrigenous End Member												
V–202			·4		5·8	2·5	·8	·4	·8	*79·9*	4·3	5·1
V–210	·3		1·0	·7	1·0	4·9	1·7	·3	1·4	*86·1*	·3	2·3
Large Foraminifera/Algae End Member												
V–350	*3·9*	*2·1*	4·9	*44·4*	4·2	12·0	3·9	4·9	9·1			10·6
V–353	*4·5*	*9·0*	8·9	*39·1*	3·1	9·3	9·3	2·2	6·3	·3		8·0
Coral/Bryozoa End Member												
V–349	1·6	1·6	*16·3*	7·2	6·8	6·0	6·4	*20·3*	7·6	18·0	·8	7·4
Lithoclast End Member												
V–14		·9	·6	9·3	12·5	15·6	12·5	2·9	*37·4*	1·9	2·2	4·2
V–169		·6	2·1	7·5	8·3	23·1	3·8	5·8	*36·6*	6·8	1·5	3·9
Halimeda End Member												
V–231	4·8	*49·6*	9·9	17·7	·7	4·4	1·0	6·4	3·4	·4		1·7
Miscellaneous												
V–148	·3		1·4	6·8	28·4	15·8	17·5	9·1	3·9	6·3	·7	9·8
V–272	5·0	4·0	24·9	4·7	6·1	22·2	2·0	5·7	13·5			11·9

The *Brown Pellet Suite* is characterized by an abundance of brown, generally smooth, rounded or irregularly shaped pellets or nodules, ranging in size from 2 to 8 mm. The surface usually is lustrous, and the colour varies from moderate brown to pale yellowish brown or pale reddish brown. Rare grains are dark brown to brownish black. Some of the smaller grains contain a quartz nucleus and are identical with the superficial oolites of the sand fraction. The brown pellets also are found in the 0·06 to 2 mm fraction but have not been distinguished as such in thin section. Most brown pellets are internally structureless and consist of microcrystalline carbonate. X-ray diffraction with Cu-Kα radiation shows that the pellets consist of very pure calcite, and an absence of significant X-ray fluorescence suggests that there is not much iron present, notwithstanding the colour. These pellets were erroneously designated as a laterite residual by van Andel, Curray, & Veevers (1961).

These pellets or concretions are found only in shallow water (Fig. 9.5), but, unlike the terrigenous grains, are not restricted to the nearshore shelf. They are most abundant along the Australian coast between 10 and 40 to 50 fathoms; they also

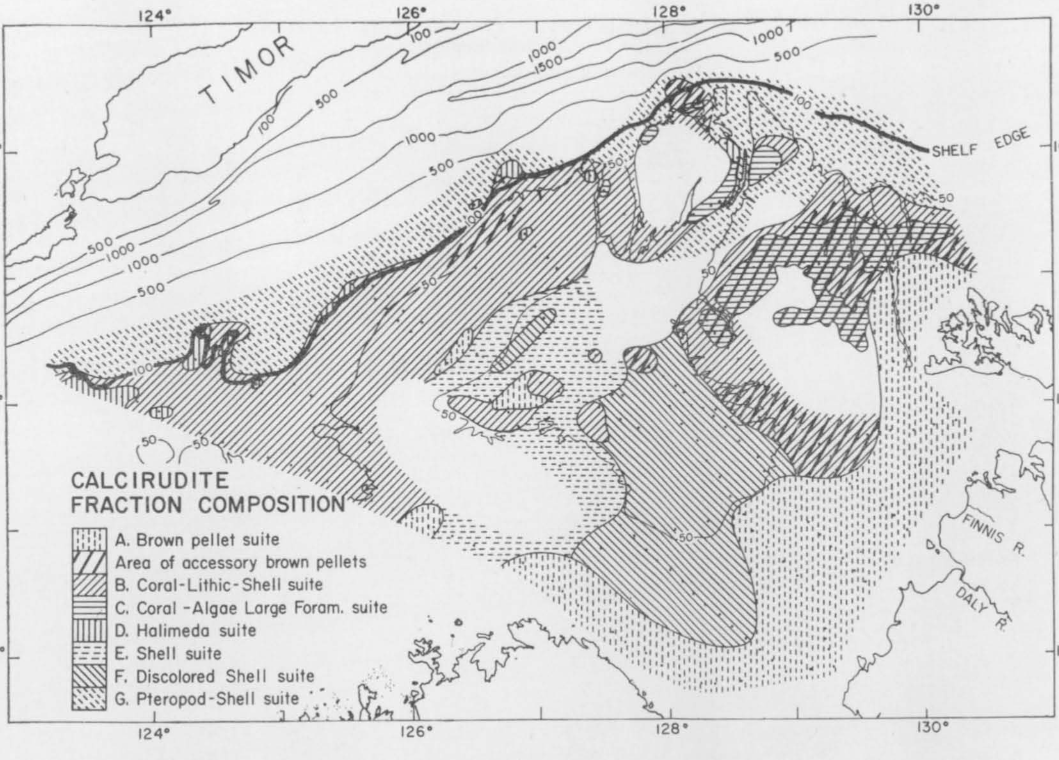

Fig. 9.5—Distribution of compositional assemblages in the calcirudite fraction (coarser than 2.0 mm) of the surface sediments of the Timor Sea. Dots are data points.

occur on nearly all middle shelf areas with depths of less than 40 fathoms. No pellets are present on the shelf-edge banks, but they may be buried there under a blanket of *Halimeda*.

The occurrence of brown concretions in areas where no terrigenous quartz is found, and where the terrigenous supply was unlikely even during the late Pleistocene regression (Wisconsin), suggest that the concretions have formed *in situ*. The restriction to depths of less than 50 fathoms indicates that they may have been produced during subaerial exposure of the shelf in Wisconsin time.

In appearance and composition, the concretions are similar to nodules occurring in calcareous kunkar soils of southern and south-western Australia and in caliche soils of North America. No kunkar soils occur in north-western Australia, which is in the laterite zone. Although this may be due to a lack of calcareous substrate, kunkar or caliche soils usually are considered the product of a specific climate, unrelated to the chemical composition of the terrain (Langford-Smith & Dury, 1965; Jackson, 1957; Jessup, 1960a, b). The widespread occurrence of kunkar soil concretions on the Sahul Shelf thus would indicate a late Pleistocene climate different from the present one (Chapter 11).

The Brown Pellet Suite contains a variety of other components, including an abundance of fresh and worn molluscan debris, many Bryozoa, and, in the nearshore areas, fragments of calcite-cemented quartzose calcarenite ('beach rock') and stained quartz. The brown concretions are a minor constituent in other assemblages on the offshore banks.

The *Coral/Lithic/Shell Suite* is dominated by fresh molluscan, coral, and bryozoan debris, with an abundance of worn grey lithic material, mainly probably altered coral fragments. In addition, echinoids, and also pteropods toward the shelf edge, are common. This reef-like assemblage is widespread on the middle and outer Van Diemen and Londonderry Rises and over the entire Sahul Rise. It is absent or unimportant on all banks of less than 20 fathoms in depth and landward of the 20-fathom contour, suggesting that there is little active reef growth at present, even in the shallower, most suitable locations. This is in accordance with the fact that, although worn and old dead coral was fairly abundant in many dredge hauls, even dominant in a few, live coral was extremely rare.

The *Algae/large Foraminifera Suite* is characterized by an abundance of algal (probably *Lithothamnium*) biscuits, ranging in size from a few millimetres to many centimetres, and of large Foraminifera, in variable proportions. Usually there is also an abundance of fresh molluscan and bryozoan debris; there are some echinoid remains, but little or no coral and *Halimeda.* Many of the Foraminifera, although fragile, are fresh and very large. Specimens up to 2 cm in diameter are common. The entire suite indicates a live, *in situ* assemblage. It is restricted to banks with depths of less than 20 fathoms on the Van Diemen Rise, along the Malita Shelf Valley and along the eastern shelf edge.

The *Halimeda Suite* largely, sometimes exclusively, consists of *Halimeda*, a small fraction of which is green and alive. Large Foraminifera are a common accessory; algal biscuits, Bryozoa, and other components are of minor importance. The assemblage is restricted to the tops of shelf-edge banks from Echo Shoal westward, and to small banks on the outer Londonderry Rise.

A *Shell Assemblage*, consisting of fresh molluscan debris with some echinoid remains, is found in fairly small quantities in the northern part of the Bonaparte Depression, on the middle Londonderry Rise, and in the form of a *shell-pteropod* assemblage in very small amounts on the outer shelf and upper slope. A *Discoloured Shell Assemblage*, identical with the Shell Assemblage except for a grey to black discolouration of the molluscan fragments, occupies the southern part of the Bonaparte Depression and the smooth slope leading to the south-western part of the Joseph Bonaparte Gulf. This assemblage occurs as coarse material sparsely disseminated in a clay matrix and has no clear relation to water depth. Burial of a shelly mud by rapid, more recent sedimentation, and discolouration of the shell debris in the resulting anaerobic subsurface environment, probably accounts for the difference between this and the other shell assemblages.

Relation between composition and texture

Comparison of the textural maps of Figures 7.2 and 7.3 and the compositional maps (Figs 9.2, 9.3, 9.5) shows at least partial correlations between grainsize and coarse fraction composition. A rapid increase of the Small Foraminifera end member over the outer shelf coincides with a decrease in grainsize; the Coral-Bryozoa and Algae-Large Foraminifera end members have a preference for coarse-grained deposits, whereas the Mollusca end member is dominant in fine-grained deposits. These relationships indicate that composition may be partly a function of size or, inversely, size a function of composition, or that both texture and composition are functions of the same environmental parameters. However, the parallelism between textural and compositional gradients is neither perfect nor universal. For example, the Small Foraminifera end member is distributed over most of the shelf quite independently of size.

Table 9.2 shows that correlations, most of which are negative (decreasing with increasing phi, that is, decreasing size), exist between the phi-median of the sand fraction (0·06–2·00 mm) and the percentages of several main constituents of this fraction. At the one-percent level, all correlations are significant, except for the one for terrigenous quartz. The only example of an increase with decreasing size is the group of the Small Foraminifera. The correlation coefficients are all small, and in no case is more than half of the variance accounted for by the regression on size.

Mollusca increase with increasing grainsize except in some fine-grained sediments.

Most Sahul Shelf sediments have polymodal size distributions. Well defined modes occur at a fairly large number of sizes. Since many sediment constituents have preferred size ranges, some of these modes may be a function of composition. Daetwyler (pers. comm.), in a study of calcareous sediments of the Gulf of Batabano, Cuba, has found that the Foraminifera have a sharply defined mode at 0·25 to 0·50 phi, Mollusca a broader mode at 0·75 to 2·25 phi. Other constituents, such as corals and *Halimeda*, occupy broad size ranges. In the Gulf of Batabano, textural modes can often be directly correlated with composition.

TABLE 9.2

CORRELATION BETWEEN GRAINSIZE, EXPRESSED AS THE MEDIAN IN PHI (= — $\log_2$ of diameter in mm) OF THE SAND FRACTION (between 2·0 and 0·06 mm) AND COMPOSITION, IN PERCENT, OF THE SAND FRACTION

Phi values decrease with increasing size; hence negative correlation with size in phi is a positive correlation with size in millimetres.

Component	r	N	P	Regression Function
Coral	—·53	250	<0·01	$\% = 9 - 3 \times Md\phi$
Large Foraminifera	—·34	250	<0·01	$\% = 12 - 3 \times Md\phi$
Small Foraminifera	·61	250	<0·01	$\% = -5 + 19 \times Md\phi$
Mollusca	—·46	250	<0·01	$\% = 27 - 6 \times Md\phi$
Bryozoa	—·54	250	<0·01	$\% = 13 - 4 \times Md\phi$
Terrigenous	·03	250	>0·05	$\% = 9 + 1 \times Md\phi$

r is correlation coefficient; **N** is number of samples; **P** is probability that correlation is due to chance.

Estimates of the composition of individual size fractions from the graded thin sections and the collation of composition and size modes of the Sahul Shelf sediments show that here the individual textural modes are usually of mixed composition, and that the polymodal size distributions are not mainly a function of composition. Most components have rather broad, overlapping size ranges, although small Foraminifera are dominant in the 2 to 4 phi (0·25–0·06 mm) range, and Mollusca, large Foraminifera, and coralline Algae are concentrated, but not necessarily dominant, in the coarsest size range. The Timor Trough deposits are exceptions (see Chapter 10).

From this, it can be concluded that although partial correlations exist between texture and composition, the distribution patterns of composition are not simply a function of size, and that, inversely, texture is not controlled by composition.

Relation between composition and environment

It has been shown above that only partial correlations exist between texture and composition and that, to a large extent, both appear to be broadly related to the regional topography.

The geographical relationships of the various assemblages support these conclusions. The Small Foraminifera suite regularly increases seaward with the increasing oceanic character of the environment, the Algae/large Foraminifera and the *Halimeda* suites occupy the shallowest bank tops, the Coral/Bryozoa suite is restricted to bank margins and slightly deeper shoals, and Mollusca characterize the deepest, muddy bottoms.

It may be noted here that the intricate small-scale topography of the area appears to have little effect on either texture or composition; the regional distribution patterns of both are generally simple, and anomalous samples are few.

Thus we may conclude that, with the exception of the Terrigenous end member and the Brown Pellet Suite, which appear to be controlled mainly by late Quaternary sea level changes (Chapter 11), the various compositional assemblages to a large extent represent ecological conditions rather than the effects of transportation, sorting, and reworking. In general, the maps of Figures 9.2, 9.3, and 9.5 are biofacies maps.

This does not necessarily imply that the assemblages reflect simple ecological units or even are related to present ecological conditions. There is abundant evidence in the live specimens and very fresh skeletal material that the Algae/large Foraminifera and *Halimeda* suites are actively growing on the shallow banks. The Small Foraminifera suite also reflects present-day conditions at least in part, although relict elements are probably included in this group. Live Bryozoa or fresh bryozoan skeletal material are also widespread, and part of the mollusca suites is probably of present-day origin. In other areas, as mentioned above, the Mollusca assemblages appear to belong to slightly earlier conditions not now prevailing.

The Coral/Bryozoa suite is found in water of intermediate depth, from 20 to 50 fathoms, below the optimal zone of coral growth, and is conspicuously absent from most very shoal areas. Fairbridge (1950) reports active coral reefs from the coastal zone and from several places along the Londonderry Rise, but live coral is unknown elsewhere in the area of investigation. Hence it seems probable that the main stage of growth of this widespread suite is not recent and perhaps belongs to a period of lowered sea level. Why live coral is not present in the numerous favourable locations on shallow banks in the area is entirely unclear.

Summary of facies distribution

The data presented in preceding pages have been combined in the compositional facies map of Figure 9.6. The map clearly shows the broad control of regional topography and distance from shore on most of the facies units. Partial exceptions are the terrigenous facies of transgressive origin and the Mollusca facies, which, at least in part, seeks low-lying mud bottom. Although some of these facies are certainly the product of present ecological conditions, others reflect environments not now existing, or are the sum of past and present changing conditions. Since the sediment thickness studied (the upper 10 cm) includes in this region of low sedimentation rates a significant part of the postglacial history, the facies map to a large extent represents the pattern of a basal transgressive sequence. We shall discuss the environmental implications and the transgressive history of the facies more extensively in later chapters.

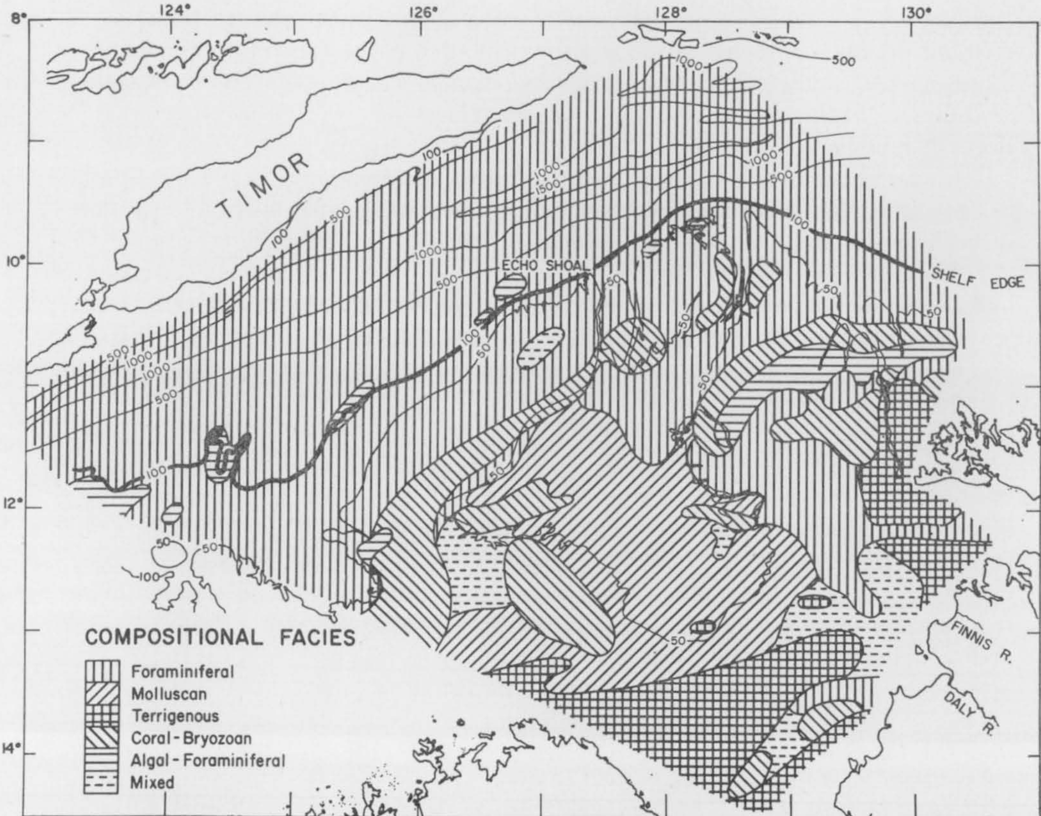

Fig. 9.6—Compositional facies (biofacies) map of the surface sediments of the Timor Sea. Based on combination of Figs 9.2, 9.3, and 9.5.

10. Sediments of the Timor Trough

The sediments of the Timor Trough are predominantly fine grained and, in comparison with those of the Sahul Shelf, they are regionally uniform. However, some important sediment properties show distinct regional gradients, and anomalously coarse samples are fairly common.

The dominant textural type is silty clay (Fig. 7.2); clays and sands are rare. The sand content of the sediments is asymmetrically distributed with respect to the trough axis (Fig. 10.1D; Table 10.1), decreasing rapidly from 70 to 90 percent near the Sahul Shelf edge to less than 10 percent in depths below 300 to 500 fathoms. There is no equivalent sandy zone along the northern margin; the shelf there is very narrow or nonexistent, and sands do not extend beyond its edge. Several deep-water stations have unusually high sand content.

The sand fraction consists entirely of biogenous material, except for a few samples from the Timor Shelf, and is dominated by planktonic organisms (80–95 percent), mainly Foraminifera and Radiolaria. Over the entire trough area between the 200 fathom contours, planktonic forms in the Foraminifera assemblage exceed 90 percent (Pl. 1, Figs 9.4, 10.1E). Benthonic Foraminifera are important only in samples from depths of less than 200 fathoms and in two deep-water samples (Fig. 10.1G; V–249, V–318). The distribution of Radiolaria is more restricted (Figs 10.1F, 10.2). Over the entire Sahul Shelf and on the upper slope on both sides of the trough, Radiolaria occur only occasionally and in very small percentages. Below 500 fathoms the percentage (expressed in terms of the sum of Radiolaria and Foraminifera) increases rapidly, and below 1000 fathoms, 50 to 70 percent of the entire coarse fraction consists of Radiolaria. A good linear correlation exists between Radiolaria percentage and depth ($r = 0 \cdot 87$ for 67 samples), and the distribution pattern conforms closely to the topography of the trough. Since the Radiolaria live in the upper few hundred metres of the water column, the causes for this distribution are not obvious. The species are all of Quaternary age (W. R. Riedel, pers. comm.). There is no reason that they should not thrive in an area much larger than that occupied by Radiolaria-bearing sediments. Preferential sorting of Radiolaria, or a lower dilution factor because of reduced sedimentation in deep water, would affect the planktonic Foraminifera in the same way and not change the ratios. Solution of carbonate would remove not only the Foraminifera but also, primarily, the abundant fine carbonate (Fig. 8.1).

Compared with the Sahul Shelf deposits, the trough sediments are deficient in carbonate. The carbonate content decreases in a northerly and north-easterly direction (Figs 7.7, 8.1) from more than 80 percent of the entire sediment along the edge of the Sahul Shelf to 15 to 20 percent near the northern margin. Nearly all carbonate resides in the fine fraction, since the entirely calcareous coarse fraction is quantitatively unimportant. The data suggest that either most of the fine carbonate is derived from the Sahul Shelf and has been transported transversely into the trough, or the main supply of terrigenous silt and clay is from the north and north-east, diluting a locally supplied carbonate sediment.

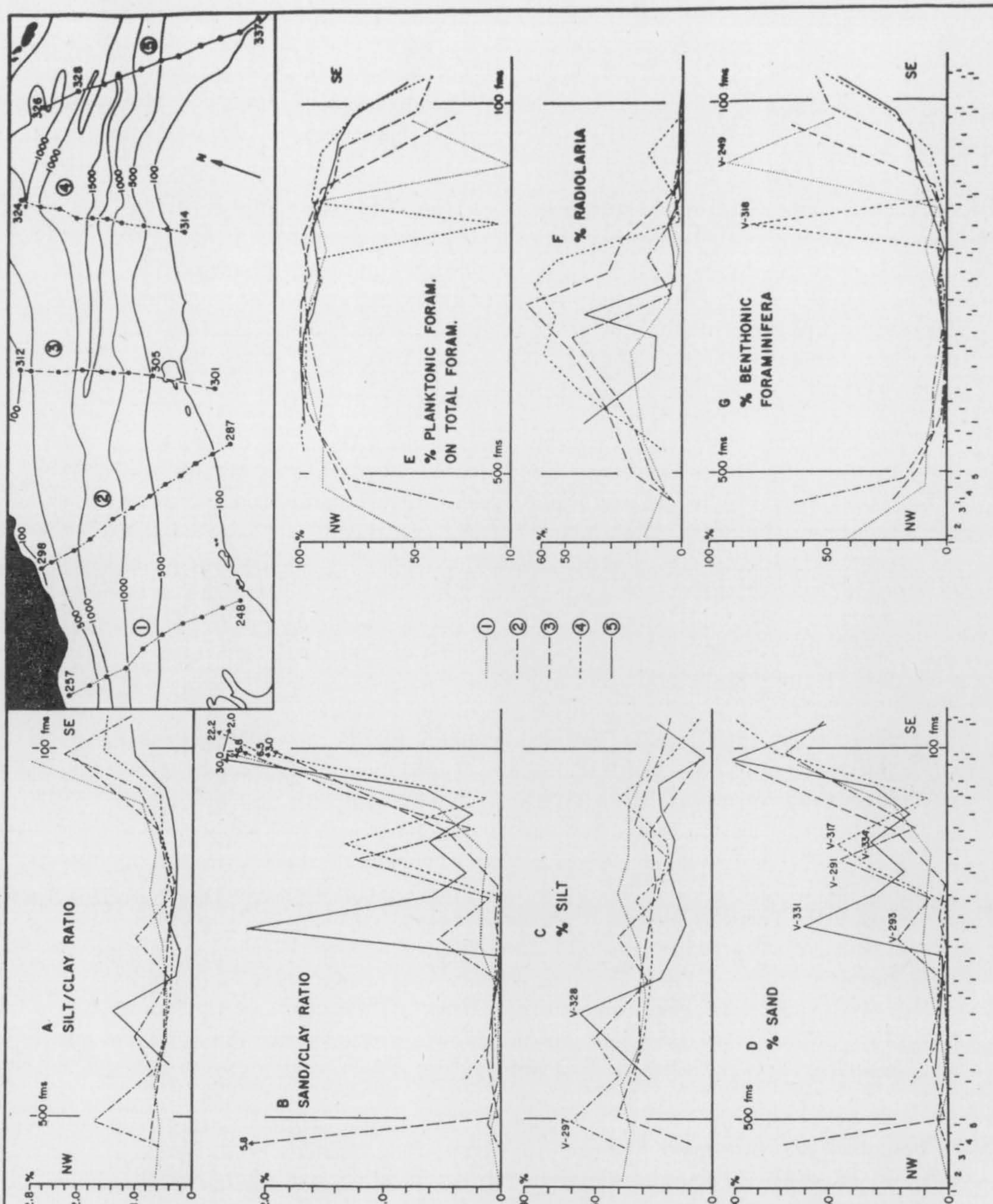

Fig. 10.1—Variation of texture and sand fraction composition of surface sediments along traverses of the Timor Trough. Horizontal scale expanded to make distance between 200 fathom contours equal in all traverses. Position of 100- and 500-fathom contours indicated. Numbered rows of dashes along bottom of each column of graphs are sample positions keyed to curves (key in centre) and to sample location map (insert). Textural components in percent by weight of the whole sample; sand fraction components in percent by number of the sum of Radiolaria and Foraminifera.

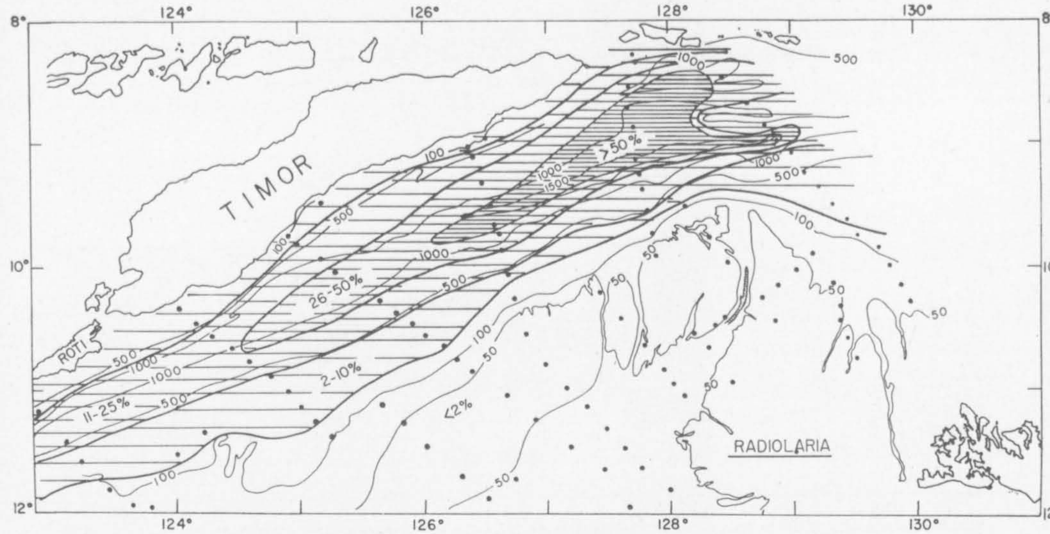

Fig. 10.2—Distribution of Radiolaria in the surface sediments of the Timor Trough and outer Sahul Shelf. In percent of the sum of Foraminifera and Radiolaria in the fraction 2.0-0.062 mm. Dots are sample locations. One degree latitude equals 60 nautical miles.

The organic carbon content (Appendix C) of the trough sediments varies from 0.6 to 1.9 percent. For the Sahul Shelf, the range is somewhat lower (0.01 to 1.2 percent organic carbon). As usual, nearly all organic carbon resides in the finest fractions, and the correlation between organic carbon content and clay content for all Timor Sea sediments is significant at the one-percent level (Fig. 10.3). However, less than half of the large variance can be accounted for by regression on grainsize. The rest may be controlled by variations in the rate of deposition of diluting particles, by variations of biological productivity, or by the degree of preservation after burial.

The regional distribution of organic carbon is shown on Figure 10.4. In order to minimize the effects of grainsize variation, the carbon content is expressed in percent by weight of the silt and clay fraction. Within this fraction, the correlation between size and carbon content is not significant at the 5-percent level. The highest concentrations occur within the Timor Trough in a broad, distinct zone on the southern slope between 200 and 600 fathoms. In addition, relatively high values are found on the central Sahul and northern Van Diemen Rises and in a few shoal areas around the Bonaparte Depression. Very low values occur near the Australian coast and on the outer Londonderry Rise. A carbon-rich sample (V-325) in Strait Sermata is unusual because of its content of large coarse plant-material content (including palm leaf fibres).

Little is known about the biological productivity of the Timor Sea. Usually, in tropical waters it is not high (Ryther, 1963), but upwelling of nutrient-rich water from below the thermocline can, in certain areas, increase the biological productivity significantly. Upwelling is widespread in low and middle latitudes along the west coasts of the continents, where eastern boundary currents and offshore wind stress produce favourable conditions (Wooster & Reid, 1963). No eastern

TABLE 10.1. SEDIMENT PROPERTIES IN TRANSVERSE SECTIONS OF THE TIMOR TROUGH; ARRANGED FROM NORTH TO SOUTH AND WEST TO EAST

Sample No.		Depth fms	Percent[1] Sand	Silt	Clay	Sand / Clay	Silt / Clay	Planktonic Forams[2]	Benthonic Forams[2]	Foram Ratio[3]	Radio-laria[2]	Fine[4] Carbonate	Organic Carbon[4]
Section 1													
V–257	....	230	....	39	61	0	0·64	43	41	51	16	16	1·00
V–256	....	390	5	35	60	0·08	0·58	83	9	90	8	12	0·99
V–255	....	980	....	39	61	0	0·64	75	8	90	17	14	0·87
V–254	....	1030	2	31	67	0·03	0·46					26	0·78
V–253	....	707	7	29	64	0·11	0·45	78	....	100	22	37	1·10
V–252	....	446	10	32	58	0·17	0·55	91	2	97	7	40	1·44
V–251	....	306	8	40	52	0·15	0·77	89	9	89	2	54	1·54
V–250	....	275	7	36	57	0·12	0·63	88	5	95	7	53	1·59
V–249	....	238	22	36	42	0·52	0·86	7	93	7	....	62	1·40
V–248	....	140	64	27	9	7·11	3·00	52	48	52	....	69	1·67
Section 2													
V–298	....	92	....	37	63	0	0·59	33	64	33	3	27	0·69
V–297	....	460	4	60	36	0·11	1·67	70	18	79	12	22	0·92
V–296	....	858	1	40	59	0·02	0·68	74	6	92	20	37	0·91
V–295	....	1383	....	50	50	0	1·00	65	6	91	29	24	1·30
V–294	....	1160	1	28	71	0·01	0·39	50	2	96	48	50	0·82
V–293	....	830	21	40	39	0·53	1·03	94	1	99	5	40	1·08
V–292	....	563	7	24	69	0·10	0·35	81	4	98	15	55	1·46
V–291	....	353	45	19	36	1·25	0·53	94	3	94	3	58	1·49
V–290	....	259	13	33	54	0·24	0·61	85	11	86	4	45	1·52
V–289	....	182	41	29	30	1·37	0·97	83	16	83	1	62	1·43
V–288	....	150	68	22	10	6·80	2·20	50	50	50	....	64	1·10
V–287	....	52	52	18	21	2·48	0·86	44	56	44	....	51	1·16
Section 3													
V–312	....	87	69	9	12	5·75	0·75	73	22	77	5	19	0·76
V–311	....	480	1	40	59	0·02	0·68	66	13	83	21	12	1·09
V–310	....	800	7	31	62	0·11	0·50	66	2	97	32	46	0·96
V–309	....	1085	3	31	66	0·05	0·47	51	....	100	49	43	0·98
V–308	....	1486	....	29	71	0	0·41	32	....	100	67	56	0·94
V–307	....	1337	3	26	71	0·04	0·37	66	2	97	32	22	0·82
V–306	....	918	1	24	75	0·01	0·32	74	....	100	26	30	1·01
V–305	....	490	22	27	51	0·43	0·53	91	6	91	3	49	1·43
V–302	....	51	90	6	3	30·0	2·00	34	66	34	....	54	0·86

Section 4											
V–325	634						90	1	99	9	15	1·42
V–324	812	15	34	51	0·29	0·67	84	....	100	16	16	1·43
V–323	992	3	29	68	0·04	0·43	55	1	98	44	15	1·57
V–322	1035	4	27	69	0·06	0·39	40	1	98	59	19	0·85
V–321	1130	3	26	71	0·04	0·37	44	1	98	55	23	0·88
V–320	1182	2	26	72	0·03	0·36	34	3	92	63	40	0·92
V–319	1750	0	33	67	0	0·49	43	3	93	54	46	0·97
V–318	1230	32	18	50	0·64	0·36	16	83	16	1	59	0·99
V–317	926	46	19	35	1·31	0·54	96	1	96	3	59	0·87
V–316	554	8	30	62	0·13	0·48	78	7	92	15	7	1·33
V–315	151	72	17	11	6·55	1·55	75	25	75	....	9	1·02
V–314	54	89	6	4	22·25	1·50	47	52	47	1	11	0·94
Section 5											
V–326	1098	5	27	68	0·07	0·40	57	1	98	42	33	0·85
V–328	975	3	56	41	0·07	1·37	88	....	100	12	40	0·72
V–329	1188	2	22	76	0·03	0·29	87	1	99	12	34	0·56
V–330	1476	2	17	81	0·02	0·21	55	3	95	42	36	0·80
V–331	820	61	11	28	2·18	0·39	92	4	93	4	26	0·89
V–332	442	31	15	54	0·57	0·28	95	1	96	4	40	1·18
V–333	294	18	18	64	0·28	0·28	89	5	95	6	41	1·42
V–334	229	32	16	52	0·62	0·31	90	9	90	1	30	1·90
V–335	196	16	22	62	0·25	0·36	85	13	85	2	37	1·64
V–336	172	30	23	47	0·64	0·49	84	15	84	1	42	1·68
V–337	132	91	3	3	30·30	1·00	77	22	77	1	....	....
V–338	86	51	24	22	2·32	1·09	53	47	53	....	43	1·50

[1] Percent gravel not listed.
[2] In percent of sum of Foraminifera and Radiolaria.
[3] Percent planktonic in total Foraminifera.
[4] In percent by weight of the fraction finer than 0·062 mm.

boundary current exists along the west coast of Australia for reasons that are not well understood (Wooster & Reid, 1963), but along the edge of the north-western shelf, water movement, wind stress and steep topography favour the occurrence of upwelling during the south-east monsoon. A moderate increase in phosphate content of the surface water (Rochford, 1962) on the shelf and continental slope and a fairly large biomass (Tranter, 1962) suggest that upwelling indeed takes place, although it has not actually been observed, and the phosphate and plankton concentrations are lower than those of areas of large-scale upwelling (Wooster & Reid, 1963). Wyrtki (1962) has discounted upwelling for the Sahul Shelf and attributed the increase in phosphate to tidal scour of shelf sediments. This explanation appears improbable, and Rochford (1962), on the basis of detailed hydrographic data including the ratio of organic phosphorus and inorganic phosphate, assumes widespread upwelling for the Sahul Shelf during the south-east monsoon.

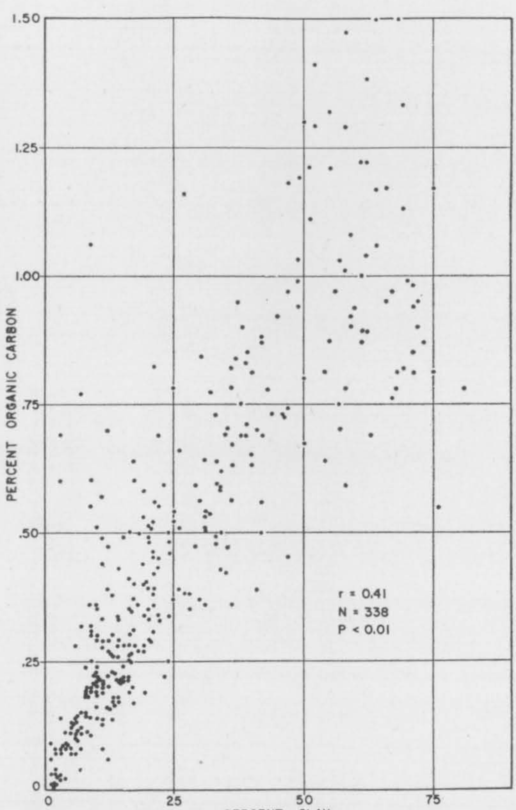

Fig. 10.3—Relation between organic carbon content (in percent of the whole sample) and clay content (fraction finer than 0.004 mm) of the surface sediments of the Timor Sea. *P* is probability that correlation is due to chance, *N* is number of samples, *r* is product moment correlation coefficient.

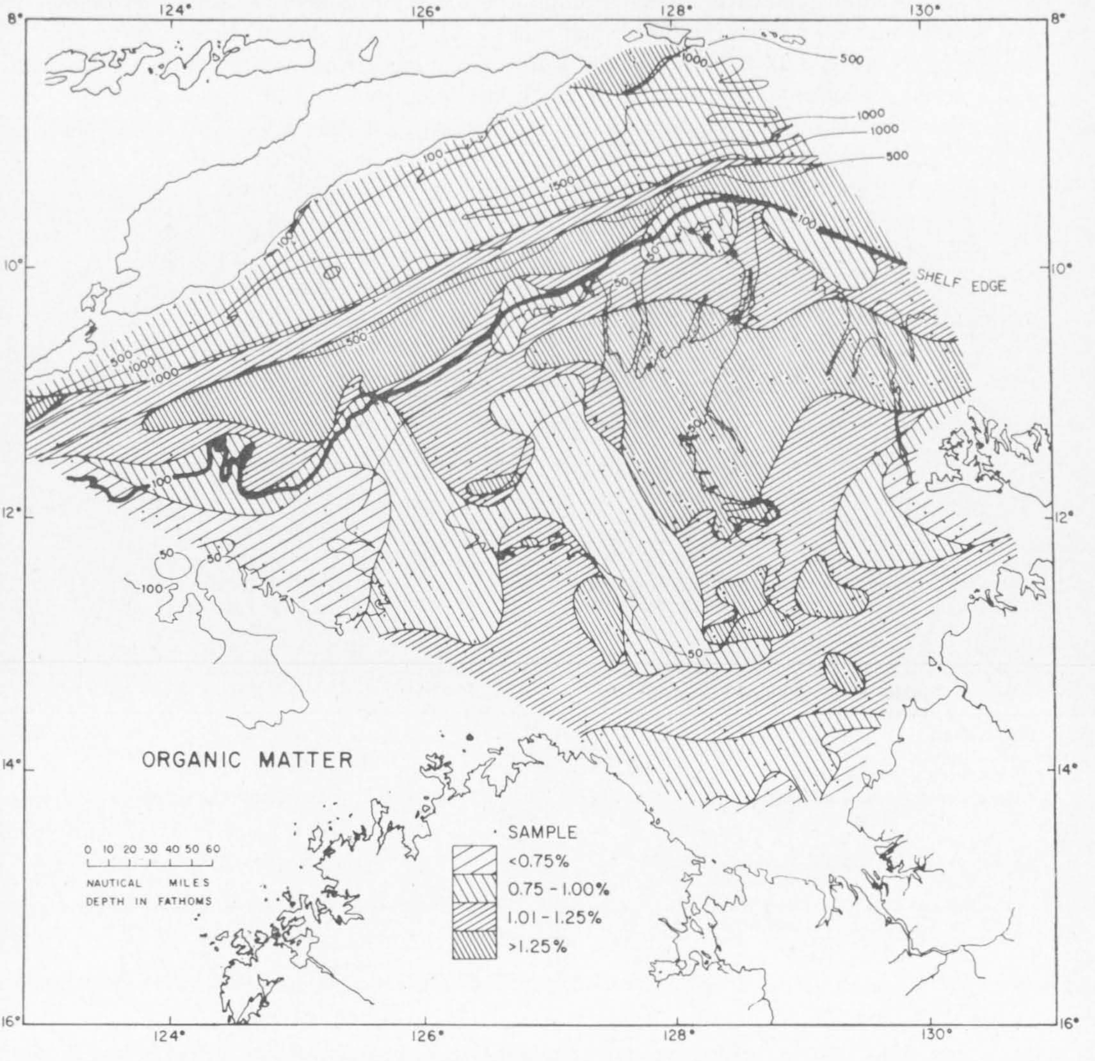

Fig. 10.4—Regional distribution of organic carbon in silt-clay fraction of surface sediments of the Timor Sea. Expressed in percent of the fraction finer than 0.062 mm to minimize grainsize effects.

Hence, the relatively high organic carbon content of the Timor Trough and outer shelf sediments may be attributed to increased biological productivity caused by upwelling. The carbon content, however, is low compared to areas of high productivity such as the Peru-Chile trench, the California Borderland, and the Gulf of California (Table 10.2), notwithstanding the low inorganic sedimentation rates of the Timor Sea. The concentrations of phosphorite nodules that frequently accompany upwelling in bank areas (Emery, 1960; d'Anglejan, 1964; Goldberg, 1963) have not as yet been found along the Sahul Shelf. Further search with more appropriate tools is indicated.

The zone of high carbon content along the southern slope of the Timor Trough coincides with an oxygen minimum that exists in the water column between 500 and 2000 metres (Fig. 3.3). In the Gulf of California, a similar oxygen minimum causes a marked reduction of the activity of benthonic organisms and produces a zone of excellent preservation of organic matter and depositional structures (Calvert, 1964; van Andel, 1964). By analogy, the high content of organic matter of the southern slope of the Timor Trough also may be the result of the presence of an oxygen minimum zone. The absence of a similar zone on the northern slope could then be explained by dilution because of a higher sedimentation rate ; approximately a 50 percent increase with respect to the Timor slope would be sufficient. The existing hydrographic data indicate also that no upwelling occurs here.

TABLE 10.2
ORGANIC CARBON CONTENT OF MARINE SEDIMENTS FROM VARIOUS AREAS

	Average	Range	Number of Samples
S.W. Florida (Scholl, 1963)		0·4–18·4	
St Josephs Bay, Florida (Stewart & Gorsline, 1962)	1·34	0·2–5·0	82
Warnbro Sound, W. Australia (Carrigy, 1956)	17·9	2·3–44·0	28
Gulf of Paria (van Andel & Postma, 1954)	0·7	0·1–1·4	39
Qatar region, Persian Gulf (Houbolt, 1957)	0·5	0·2–1·2	15
Orinoco-Guayana Shelf (Nota, 1958)		0·1–0·8	28
Paria-Trinidad Shelf (Koldewijn, 1958)		0·1–1·7	32
Gulf of Mexico (Trask, 1953)			
Shelf	0·4		
Slope	1·0		750
Sigsbee Deep	0·6		
Peru-Chile Trench (Trask, 1961)			
Upper Slope	2·4		31
Lower slope	0·6		51
California Borderland (Emery, 1960)			
Slope	1·6		30
Basins	3·9		80
Gulf of California (van Andel, 1964)			
Eastern Slope	3·6		29
Basin	2·5		30
Western Slope	4·2		15
Sahul Shelf	0·4	0·01–1·2	270
Timor Trough	0·9	0·6–1·9	61

There is no direct information concerning sedimentation rates on the Sahul Shelf, but it may be assumed that the rates are highest in the low-lying areas of fine-grained sediments and lowest on banks and rises. The high carbon content of some bank and rise sediments thus may be the result of a reduced sedimentation rate.

The occurrence and distribution of organic matter in modern calcareous sediments has received little attention. Calcareous sediments rich in organic material have been reported from coastal lagoons (Carrigy, 1956) and mangrove swamps (Scholl, 1963). Compared to these, the Timor Sea sediments are low in organic matter, but they fall well within the range of most normal marine sediments of the continental margins (Table 10.2).

Although in general the sediments of the Timor Trough are texturally uniform, close inspection reveals trends and patterns of variation (Fig. 10.1; Table 10.1). The silt content gradually and rather regularly increases from south to north (Fig. 10.1C). Comparison of graphs B, C, and D of Figure 10.1 shows that the coarse deep-water samples are the result of adding sand fraction, but that the silt content and silt/clay ratio do not vary much from average. The silt/clay ratio is fairly uniform over the entire trough (Fig. 10.1A) and shows only a small decrease from the sides to the centre; a sudden large increase occurs at the Sahul Shelf edge as a result of a decrease in the clay content.

The cumulative grainsize distribution curves of most Timor Trough sediments can be grouped into two categories (Fig. 10.5) : (1) well sorted sands with a median of 2.0 to 3.0 phi (0.250-0.125 mm) and a sorting coefficient (standard deviation) of 1.4 to 2.5 (Type I); and (2) silty clay curves, which are concave upward and in which most of the material is finer than 7.0 to 8.0 phi (Type II: mean 6.7-7.8 phi, 0.009-0.005 mm; standard deviation 0.9-1.5). The fractions between 4.0 and 7.0 phi (0.062-0.008 mm) are under-represented. Transitional size distributions are not common. Sections 4 and 5 (Fig. 10.5) show good examples of transitional series from Type I to Type II, with increasing water depth and distance from the Sahul Shelf edge. Type I samples predominate in shallow water on the outer Sahul Shelf and upper slope, while Type II samples are restricted to the deep central portions of the trough and to the northern slope (Fig. 10.6A). A few Type I and transitional samples are scattered in deep water. Fundamentally different cumulative size distributions, characterized by a large amount of silt, occur in three samples near the Sahul Banks (V-33, V-238, V-259; Fig. 10.5). The Timor Trough size distributions thus can be understood as mixtures in varying proportions of a well-sorted sand component and a slightly silty clay. The former is similar to the sediments of the Sahul Shelf edge; the latter represents a rest suspension differentiated by long-distance transport (Doeglas, 1946, 1950; van Andel & Postma, 1954). Within the area of Type II distributions, the textural uniformity is striking (Fig. 10.5).

The computed size frequency distributions of Figure 10.5 confirm this interpretation, but they also show that the coarse component is more complex than is apparent at first sight. Two size modes at 1.75 to 2.00 phi (0.297-0.250 mm) and 2.75 phi (0.149 mm) are present in most coarse-grained samples. Both modes are predominantly composed of Foraminifera. In addition, samples from the outer shelf and uppermost slope possess several coarser modes. A well defined mode at — 1.5 phi (2.828 mm) in several samples is composed largely of *Halimeda* and large Foraminifera fragments. A mode at + 1.0 phi (0.500 mm), composed of Small Foraminifera, is associated with the finer sand modes in many shelf edge samples. A coarse mode (— 3.5 phi, 11.3 mm) of molluscan and coral debris is very rare. Many samples of the southern slope of the trough contain one or more small modes in the silt range; not all of these are shown in the size-frequency graphs of Figure 10.5, which gives curves only for samples containing more than 5 percent sand. The composition of these silt modes is not known, but they are calcareous, since they disappear after treatment with dilute hydrochloric acid, leaving a simple distribution with a large mode below 8.0 phi (0.004 mm). Modes near 4.0 phi (0.062 mm) are fairly common, but these modes are largely artificial at the boundary between

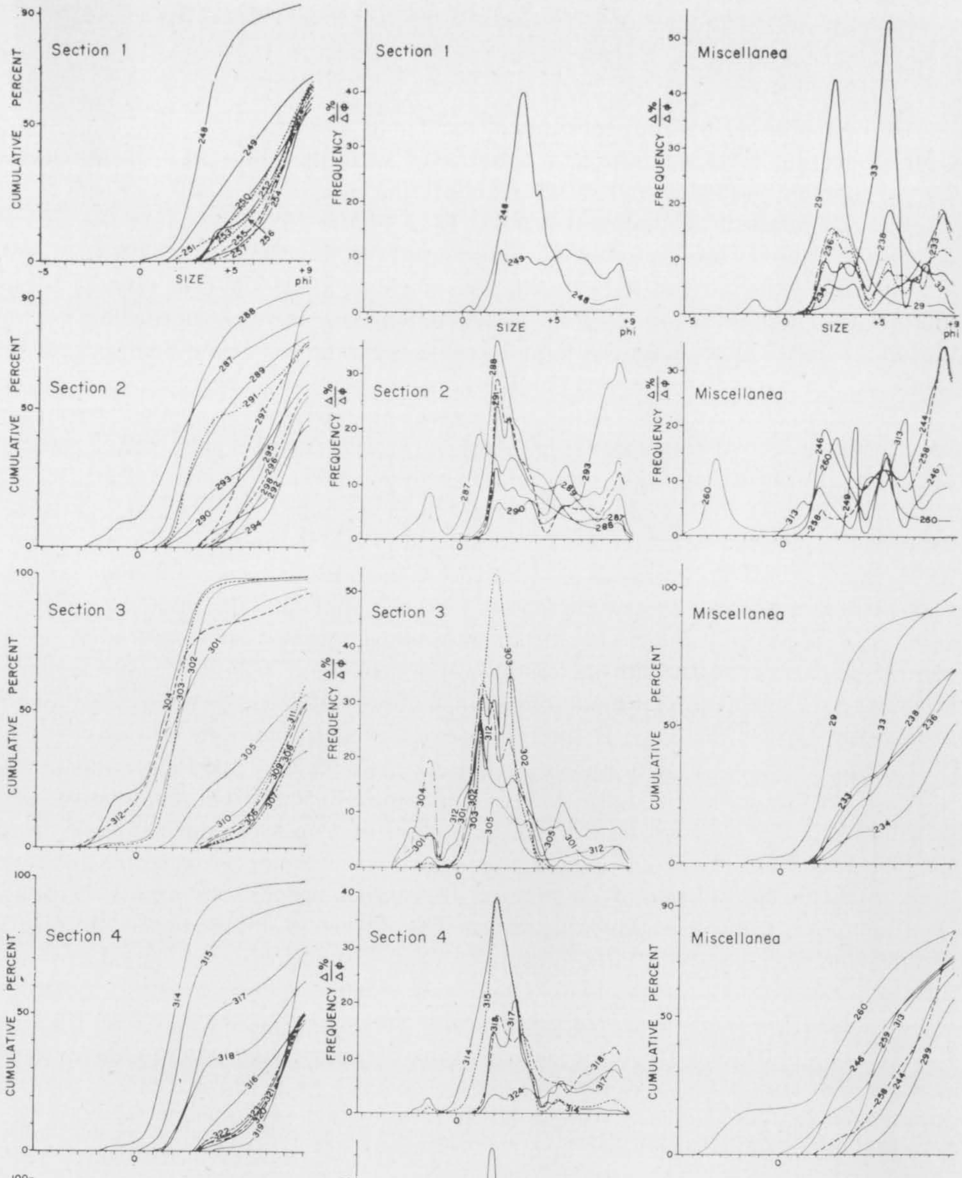

Fig. 10.5—Grainsize distributions of surface sediments of the Timor Trough and edge of the Sahul Shelf. Left column: cumulative size distributions arranged by traverses (locations on Fig. 10.1 and Plate 5); centre column: size frequency distributions by traverses ; right column: miscellaneous samples. Bottom right: zone diagram showing envelopes for curve of types I and II.

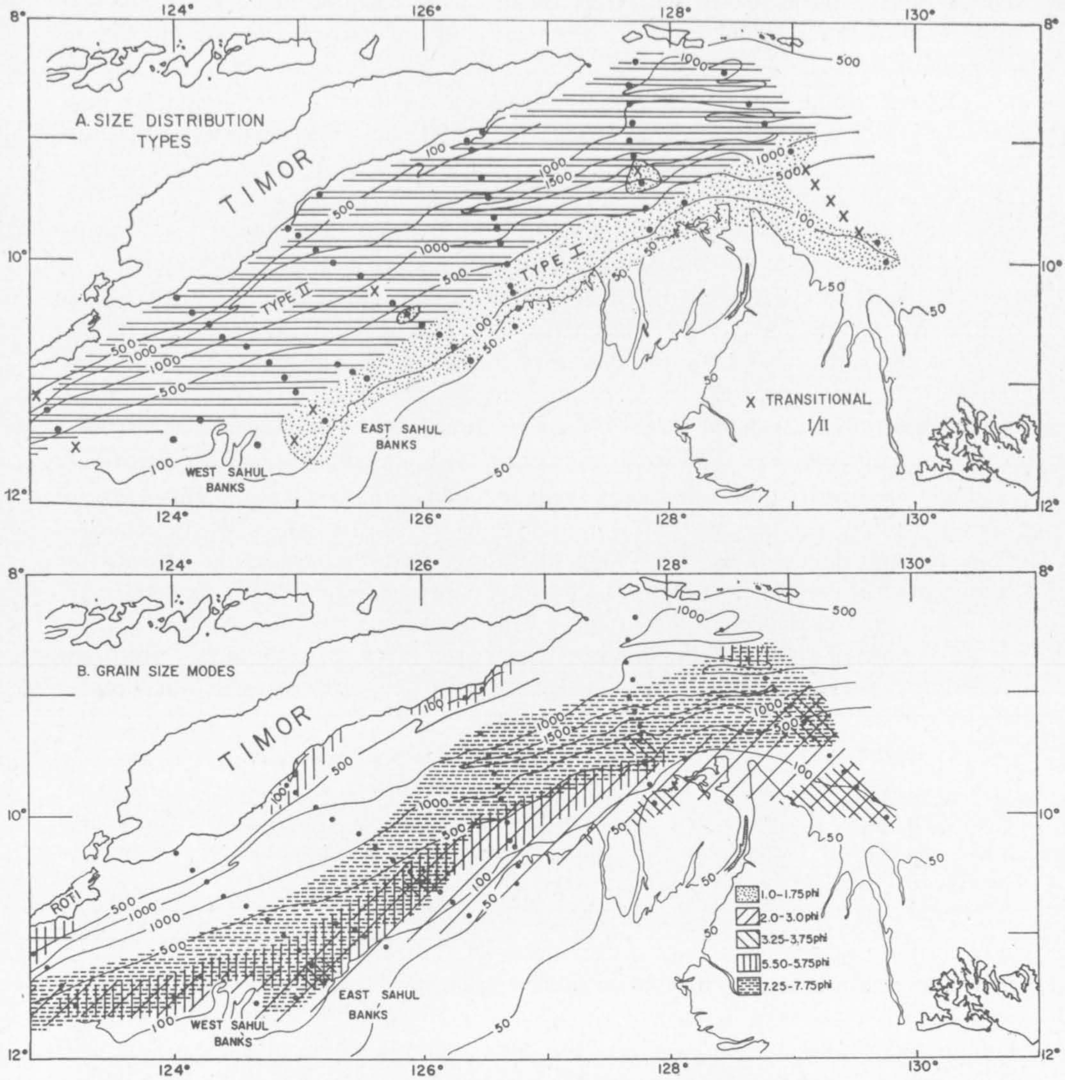

Fig. 10.6—Regional distribution of cumulative size distribution curve types (A) and modes of the frequency distributions (B) in surface sediments of the Timor Trough and edge of the Sahul Shelf. Legend for curve types and individual size distributions in Fig. 10.5. Dots are sample locations. One degree latitude equals 60 nautical miles.

sedimentation balance and pipette analysis. Since the size distributions are open-ended on the fine side, the frequency curve terminates at the last measuring point at 9.0 phi (0.002 mm) and cannot be interpreted below 8.0 phi.

The regional distribution of modes (Fig. 10.6B) shows a zonation roughly parallel to the Sahul Shelf edge. Seaward, the coarser modes progressively disappear; beyond approximately 25 nautical miles from the shelf edge only a 7.25 to 7.75 phi (0.0066-0.0046 mm) mode is present, and beyond 40 to 60 nautical miles no modes coarser than 8.0 phi (0.004 mm) are present. Even near the northern shelf edge, modes above 4 phi (0.062 mm) are very rare and are restricted to the immediate vicinity of land.

This distribution of modes strongly suggests a northward dispersal and progressive sorting of calcareous material coarser than 8.00 phi. This material apparently is derived exclusively from the Sahul Shelf. The distance from the shelf edge, rather than the water depth, apparently controls the sorting; the boundaries are very nearly parallel to the shelf edge and cross several depth contours. A similar distribution of fine modes in deep water exists in the Gulf of California (van Andel, 1964).

Normally, progressive sorting reaching into the fine silt and coarse clay is not considered possible, and a mechanism for this process is not evident. Given the great depth and considerable turbulence of the waters of the Timor Trough, even very low current velocities should permit particles finer than 5.00 phi (0.032 mm) to be uniformly distributed across the entire trough before settling to the bottom.

The noncalcareous portion of the Timor Trough sediments appears to have a simple size distribution with a large single mode finer than 8.00 phi. This fraction does not show regional textural variation, and its source cannot be determined from textural data. It has been suggested above that, because of the absence of a high organic carbon zone along the northern slope, sedimentation rates here may be higher than elsewhere in the trough. This would point to the northern islands as an important source of fine-grained terrigenous material. We have postulated earlier that the sedimentation rate in the northern half of the trough was significantly higher than on the southern flank.

Thus, the sediments of the Timor Trough can be broadly divided into two longitudinal zones. The southern zone, extending some 60 nautical miles seaward from the Sahul Shelf, is composed of polymodal sandy and silty clays, largely calcareous and progressively sorted seaward. The northern zone consists of a predominantly terrigenous and texturally uniform silty clay.

The presence of samples with anomalous texture in deep water has been mentioned above. Most of these samples occur in the southern zone of the trough. They are characterized by an anomalously large coarse fraction of planktonic organisms, as compared with adjacent samples. Moreover, while most Timor Trough cores are homogeneous in structure (Fig. 10.7), several cores show more complex structures. Thin layers of coarse material, which vary in thickness from 2 to 250 mm, occur in several samples. Some cores are mottled with sand as a result of partial destruction of sand layers by burrowing organisms. A few sections of sand-silt-clay or sandy clay probably are the final stage of postdepositional mixing. These sediment types are mainly restricted to the southern slopes of the trough (Fig. 10.7).

A few long cores have been obtained in the Timor Trough on other expeditions of Scripps Institution of Oceanography. Two of these cores contain sand layers. LSDA-149 has a 3-cm layer of silty sand on top of a 132-cm section of silty clay, with a sharp boundary. Core MSN-24, between 94 and 331 cm below the surface, consists of silty clay mottled with coarse sand pods. The upper portion, separated by a sharp contact, consists of two beds of sand, each grading from coarse sand at the bottom to silty clay at the top.

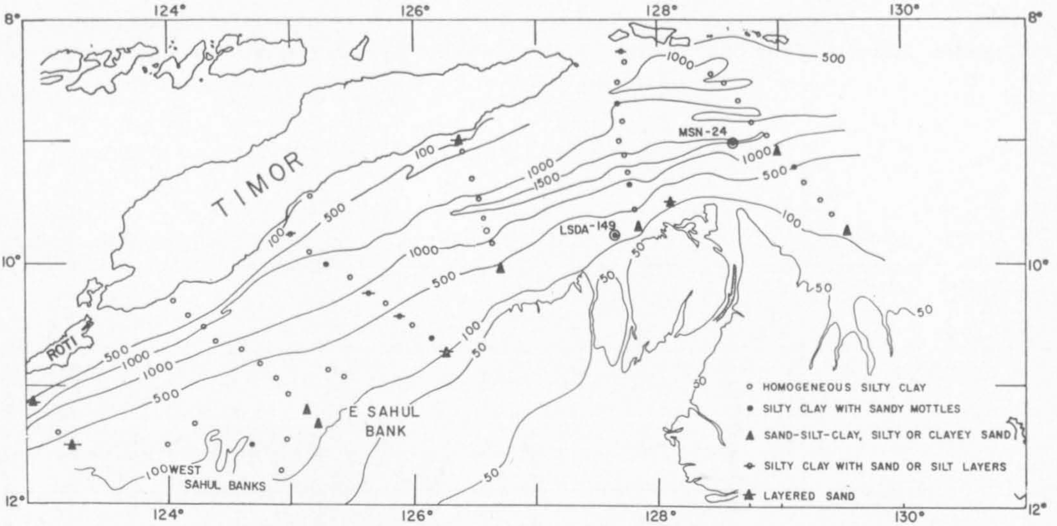

Fig. 10.7—Distribution of sedimentary structures in cores of the Timor Trough. Unnumbered locations are gravity cores varying in length from 50 to 70 cm; numbered locations are long piston cores. One degree latitude equals 60 nautical miles.

The deep-water sands are similar in texture to the sands of the shelf edge (Fig. 10.8). In both groups, the dominant mode is at 2.00 phi (0.250 mm). A subsidiary mode at 3.50 to 3.75 phi (0.088-0.074 mm), present as a shoulder in most shelf sands, is well developed in the deep-water sands, which also contain larger amounts of silt and clay. The latter may result partly from contamination during sampling or from mixing by burrowers after deposition. Thus, the textural differences between shelf-edge and deep-water sands are slight, although a small shift toward finer modes is evident.

The similarities in composition between shelf-edge and deep-water sands also are considerable (Table 10.3). The sediments of the shelf edge contain appreciable amounts of skeletal material that is not derived from Foraminifera, but Foraminifera are dominant. A few samples show displacement of components normally associated with shallow banks to depth of 100 to 200 fathoms. An examination of the species composition of the Foraminifera by F. B. Phleger indicates that there is no evidence for large-scale displacement of shallow-water Foraminifera into deep-water sands. All nonforaminiferal components are concentrated in size modes coarser than 1·0 phi (0·500 mm). The shelf-edge sediments differ from the deeper-water sands mainly in having a higher proportion of benthonic Foraminifera. Only two deep-water samples, V–249 and V–318, have significant numbers of benthonic Foraminifera. If, by some process, the deep-water sands are derived from shelf-edge deposits, most textural and compositional differences can be easily explained by progressive sorting. The difference in foraminiferal ratios, however, probably cannot be so explained; this suggests that the source of the deep-water sands must be farther down the slope, where the amount of planktonic Foraminifera normally exceeds 90 percent below 200 to 300 fathoms.

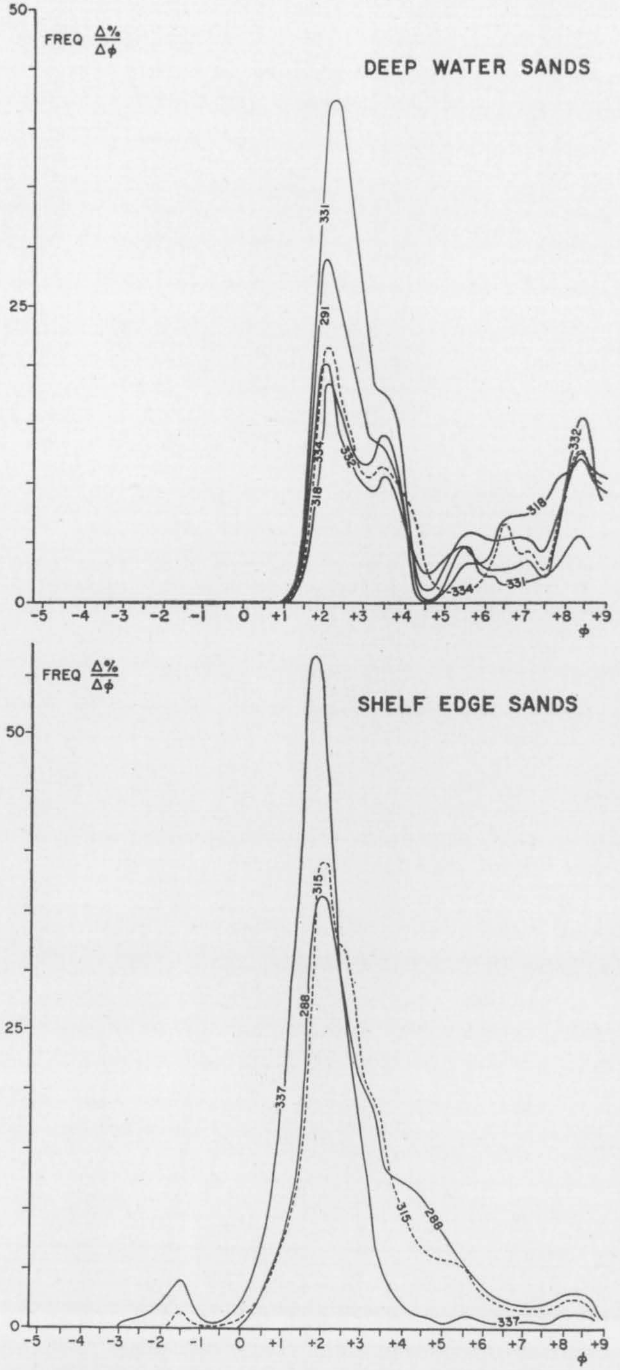

Fig. 10.8—Grainsize distributions (size frequency curves) of deepwater sands of the Timor Trough compared wtih sediments from the edge of the Sahul Shelf.

TABLE 10.3

COMPARISON OF SHELF EDGE, UPPER SLOPE AND DEEP-WATER SANDS

Station	Depth in Fathoms	% Coarser than 0·06 mm	Foraminifera	Bank Components	Foram Ratio[2]	Remarks[3]
			In percent of sand fraction[1]			
Shelf Edge and Upper Slope						
V–29	113	77	43	17	55	
V–337	132	94	58	10	77	
V–248	140	64	49	13	52	
V–33	143	11	78	3	70	
V–34	148	66	66	6	27	
V–288	150	68	62	2	50	
V–315	151	72	71	4	75	
V–260	160	48	61	9	....	
V–336	172	30	87	0	84	
V–289	182	41	90	2	83	*Globigerina* sand; benthonic Foraminifera typical for upper slope
V–335	196	16	85	....	....	
V–238	218	19	86	1	27	
Deepwater						
V–334	229	32	94	0	90	
V–249	238	22	....	....	7	*Globigerina* sand; benthonic Foraminifera normal for depth
V–291	353	45	97	0	94	*Globigerina* sand; some shelf forms (*Bigenerina* cf. *irregularis*, *Reussella* sp., *Pseudoclavulina*(?)), other benthonics normal for depth
V–233	390	28	94	0	93	Normal for depth
V–332	442	31	98	0	96	
V–297	460	4	....	....	79	
V–236	488	26	....	....	93	
V–305	490	22	....	....	91	Normal for depth
V–325	634	....	83	0	99	*Globigerina* sand; benthonic Foraminifera normal for depth
V–331	820	31	98	0	96	*Globigerina* sand; almost no benthonic Foraminifera (*Cibicides wuellerstorfi*, *Eponides* cf. *tumidulus*)
V–293	830	21	....	....	98	
V–317	926	46	98	0	96	*Globigerina* sand; rare, normal benthonic Foraminifera
V–318	1230	32	....	....	16	
V–295	1383	....	....	....	91	

[1] Coralline Algae + *Halimeda* + Coral + Large Foraminifera + Lithoclasts.

[2] $\dfrac{\text{planktonic Foraminifera}}{\text{planktonic + benthonic For.}} \times 100$

[3] Examinations of species composition by F. B. Phleger.

Deep-water sands are often ascribed to the activity of turbidity currents. The graded sands with sharp lower boundaries described above support such an interpretation. However, there is no evidence that the deep-water sands of the Timor Trough have a shallow origin. The absence of benthonic Foraminifera indicates that they cannot be easily derived from the sandy shelf deposits. On the basis of the petrographic data presented here, an alternative to the turbidite hypothesis explains the sands as the products of local current winnowing, which concentrates the planktonic organisms and prevent clay deposition. Whatever the cause, the sands are not widespread and form only a small fraction of the modern sediments of the trough.

11. Late Quaternary History and Modern Depositional Facies of the Timor Sea

In this chapter we will summarize the findings of previous sections as they relate to the distribution and origin of sedimentary facies in the Timor Sea. We will also compare these facies with the calcareous and terrigenous sediments of other shelves and continental margins.

In Chapter 5, we discussed the tectonic history of the Timor Sea region up to the time that the shelf subsided to approximately its present elevation. Subsequently, the shelf has shared with all other continental shelves a varied history of eustatic transgressions and regressions. The last of these, the post-Würm transgression, has exercised a profound influence on the sediments of shelf areas everywhere and, to a lesser extent, on deeper-water sediments. Before we can properly analyse the factors controlling the facies characteristics and distribution of the recent sediments, the late Quaternary history of the region must be examined in some detail. Such a discussion will be limited by a lack of knowledge of the late Quaternary in the adjacent land areas and of the climatic history of the Indo-Australian region, and by the shortage of absolute dates for various events.

Late Quaternary history of the Sahul Shelf

At the maximum of the last glaciation (Wisconsin II), sea level probably was some 60 to 70 fathoms below its present position (Shepard, 1963, pp. 265–267). Along the edge of the Sahul Shelf, this low stand of sea level is marked by a break in slope generally accompanied by a low cliff with its base between 60 and 70 fathoms. A radiocarbon date (V–229, Table 11.1) confirms the presence of a shallow nearshore environment at 72 fathoms some 17,000 years ago. This date is in agreement with other dates for the last maximum lowering of sea level (Curray, 1961; Shepard, 1963).

During this period the land area of north-western Australia was considerably enlarged, and the shelf-edge banks formed a string of small islands along a shoreline located very near the Timor Trough (Fig. 11.1). The Bonaparte Depression was an almost entirely enclosed embayment with a depth of about 10 to 15 fathoms. It was connected to the Timor Sea by the Malita Shelf Valley, a narrow strait over 100 nautical miles long and 3 miles wide at its narrowest point. Thus the entrance of sea water into this lagoon, into which nearly all runoff from the adjacent land drained, must have been severely restricted.

Usually the climate in the warm-temperate regions is considered to have been pluvial characterized by increased rainfall during glacial maxima. However, Mayr (1944) has pointed out that local geographic and climatic conditions in certain areas have led to a reduced rainfall as compared with that of the present time. In the region of northern Australia, the drop in sea level closed the Torres Strait between Australia and New Guinea, thus blocking the warm current now entering the Banda Sea from the east. It also greatly increased the land area and thus reduced the moisture contributed to the north-west monsoon. Moreover, the northerly and north-easterly current now flowing seasonally along the north-west coast of Australia might have penetrated farther northward, stayed longer, and been colder as a result of the compression of climatic belts on both sides of the Equator. These combined factors would have rendered the glacial climate of the Timor Sea region more arid instead of wetter than it is today.

These deductions are supported by the present study. Evidence for colder water in the Timor Trough during the late Pleistocene is contained in two cores from the Timor Trough (Fig. 11.2; T. C. Moore, pers. comm.). Core LSDA–152, on the north flank of the trough, contains in its upper portion (0–184 cm) a fauna dominated by species of planktonic Foraminifera (*Globorotalia cultrata* d'Orbigny, *G. tumida* Brady, *Globigerinoides quadrilobata sacculifer* Brady, *Pulleniatina obliquiloculata* Parker and Jones), which Phleger, Parker, & Peirson (1953), Bradshaw (1959), Parker (1962), and Beliaeva (1963) consider typical of tropical waters of the Atlantic, Indian, and Pacific Oceans. Below 184 cm, the frequency of tropical species decreases. Other species (*Globorotalia truncatulinoides* d'Orbigny, *G. crassaformis* Galloway and Wistler) appear that are temperate in origin, while the temperate species *Globoquadrina dutertrei* d'Orbigny increases in importance. The date of this change is somewhat less than 13,000 years B.P. (Before Present; Table 11.1). A change at this time from colder- to warmer-water faunas has been reported from many places in the world (Ericson, Ewing, and Wollin, 1964; Phleger, 1960). On the basis of the microfauna, the lower part of this core correlates well with core LSDA–149 on the opposite, southern side of the trough (Fig. 11.2), which contains a temperate fauna throughout. The upper, recent portion of core LSDA–149 may have been removed by slumping or erosion; a coarse concentrate of foraminiferal sand occurs from 0 to 3 cm. On the basis of this correlation, it appears that the sedimentation rate during the late Pleistocene on the south flank of the trough was almost twice that of the north flank. In the previous chapter, it was suggested that the present-day sedimentation rate is higher on the north flank. The high rate of Pleistocene sedimentation in core LSDA–149 may be due to the fact that at that time the shoreline and the main exit of Bonaparte Lagoon were very close to the core location. The post-Pleistocene sedimentation rate for LSDA–152 is 17 cm per 1000 years, which is low but well within the range of other continental slopes (van Andel, 1964). The high extrapolated surface age of this core is a common phenomenon in marine sediments; for reasons not yet fully understood, the age of the surface sediments of most deep-water cores ranges from 500 to 2000 years (Emery & Bray, 1962; van Andel, 1964).

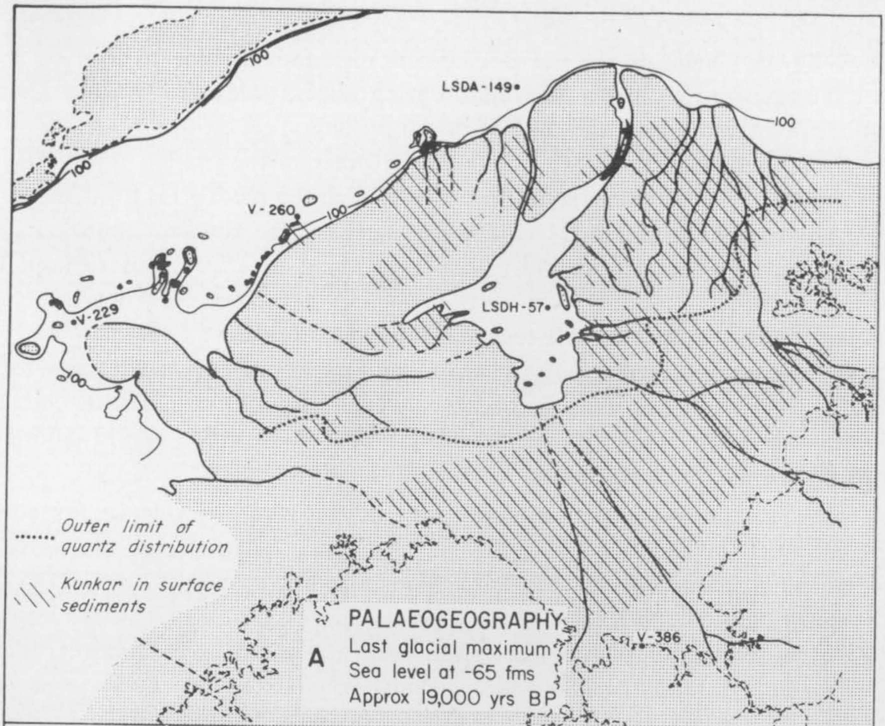

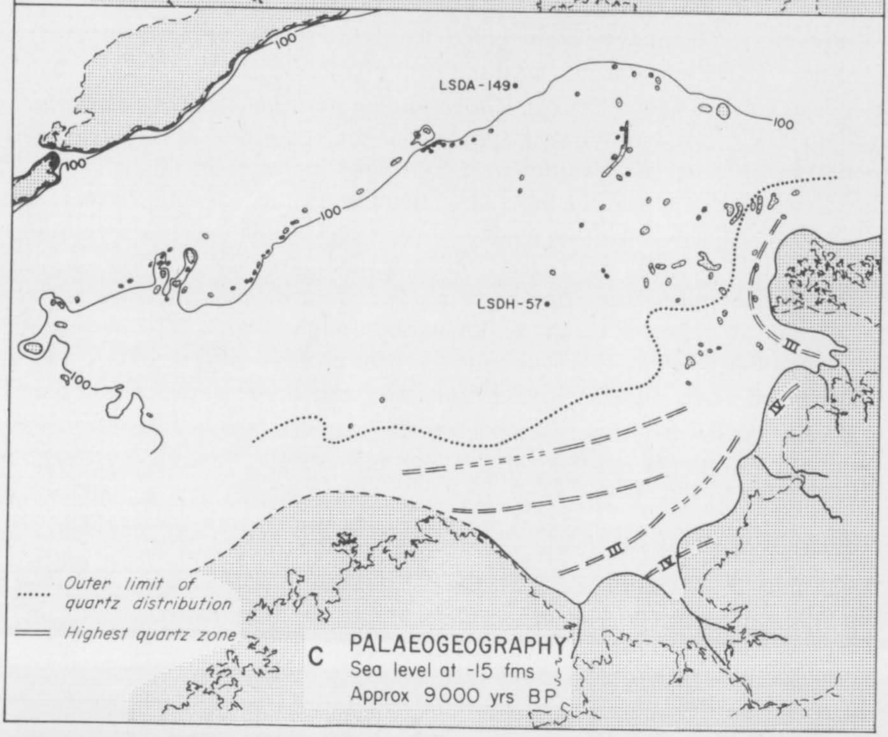

Fig. 11.1—Palaeogeography of the Timor Sea during the last glacial maximum (A) and two stages of the postglacial sea level rise (B, C). Dates for sea level positions after Curray (1960). Locations of critical long cores are shown. Distribution of kunkar (brown calcareous nodules) falls entirely within land area exposed at lowest sea level. Zones of maxi-

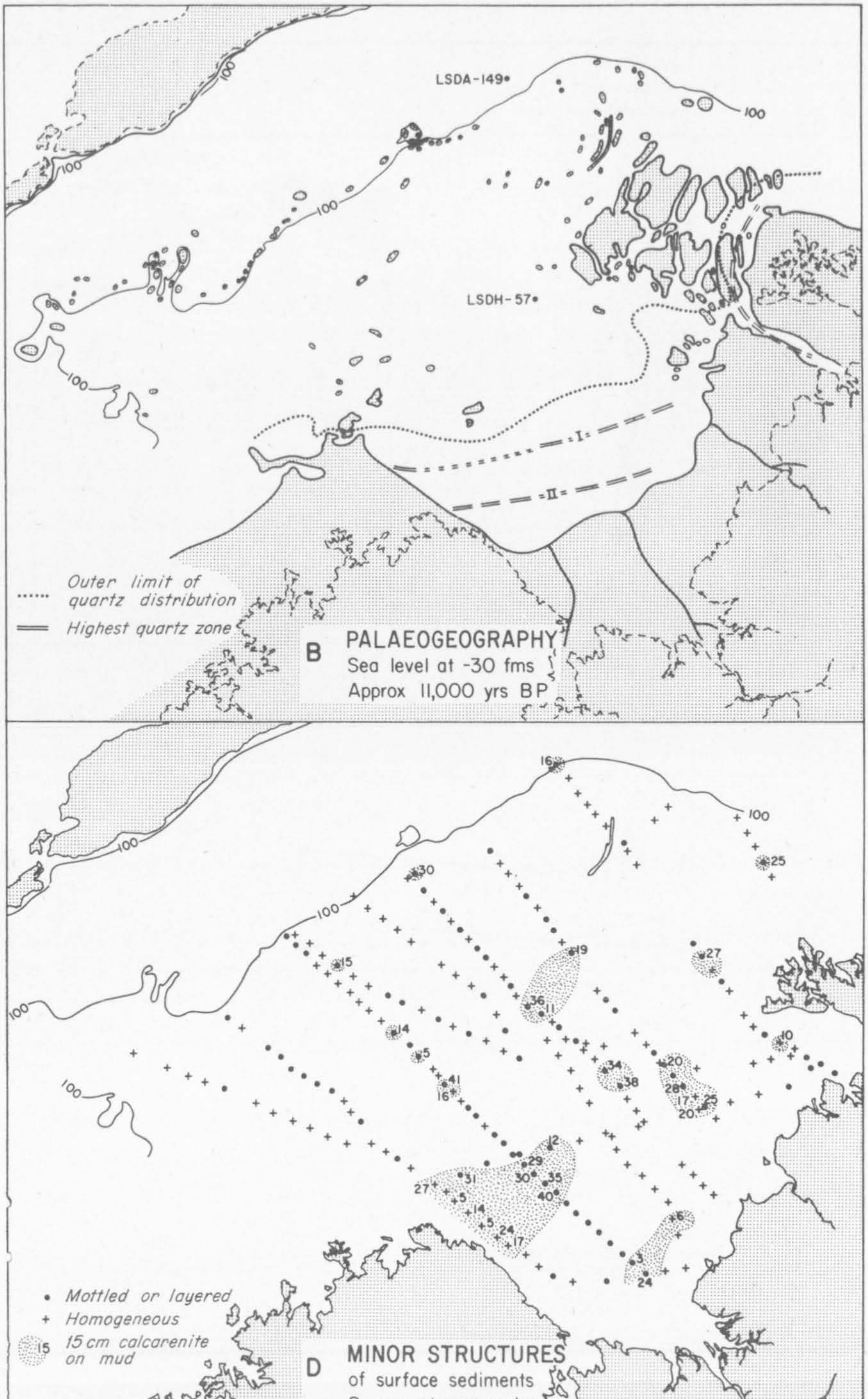

mum quartz concentration (numbered in order of decreasing depth, after Fig. 8.3) parallel former shorelines. Lower right: map (D) shows distribution of sedimentary structures and of coarse calcarenite sheets on the Sahul Shelf. Scale approximately 1 : 8,000,000.

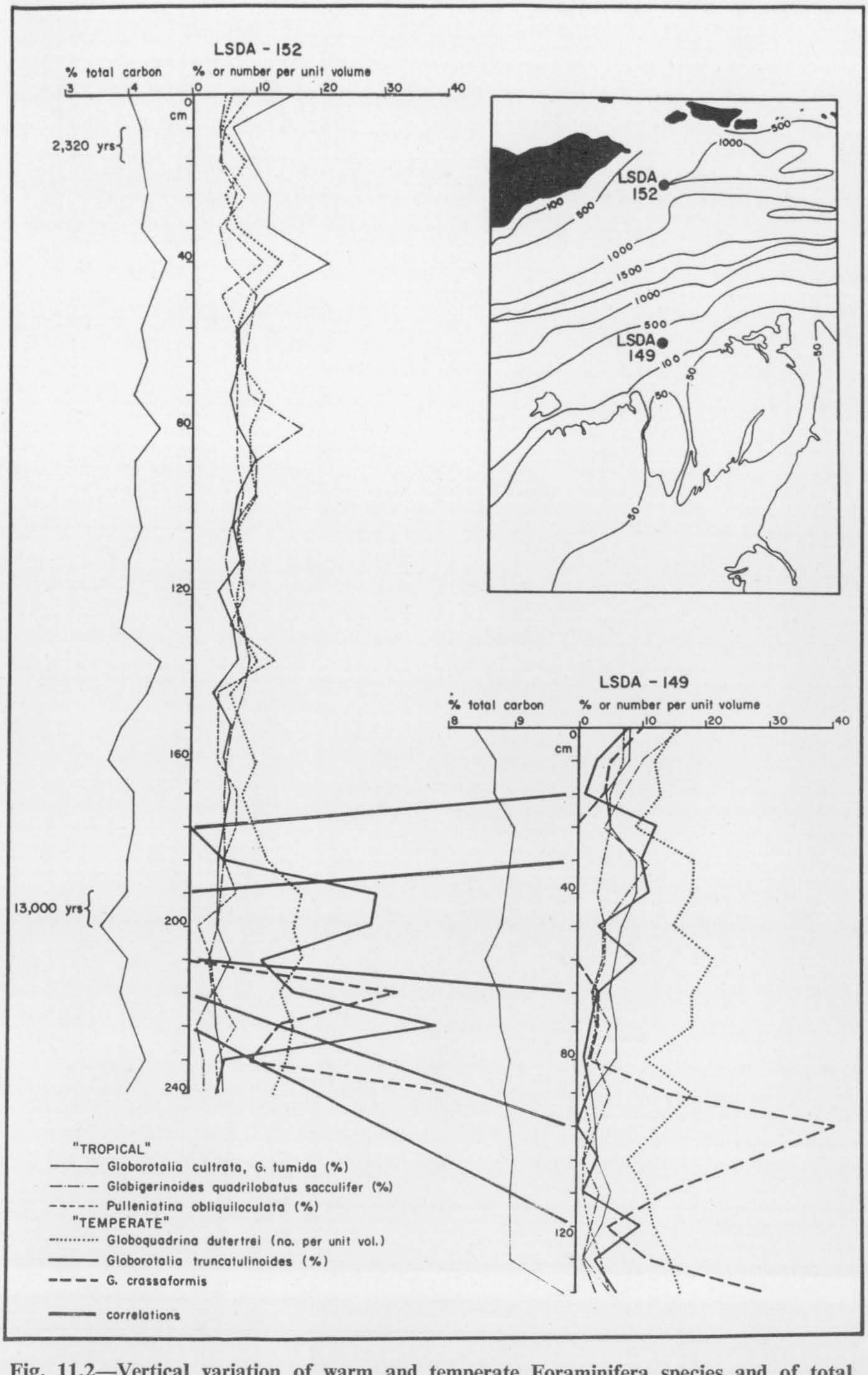

Fig. 11.2—Vertical variation of warm and temperate Foraminifera species and of total carbon (including organic and carbonate carbon) in two cores from the Timor Trough. Data provided by T. C. Moore.

TABLE 11.1

RADIOCARBON AGES OF TIMOR SEA SEDIMENTS. DETERMINATIONS BY RADIOCARBON LABORATORY, SCRIPPS INSTITUTION OF OCEANOGRAPHY. LOCATIONS, SEE FIGS 11.1, 11.2

Sample Number	Water Depth (fms)	Core interval analysed (cm)	Location		Sampler	Material Dated	Age B.P. (years)	Comments
			E. Long.	S. Lat.				
V–229	72	surface	123°50·4′	11°57·5′	dredge	*Chlamys senatorius* shells	16,910 ± 500	Living range littoral
V–260	160	surface	125°33·6′	11°00′	dredge	*Lima persquamifer* shells	23,800 ± 900	Living range shallow; since some bank debris occurs in sample (Appendix D), probably displaced
LSDH–57 (V–384)	72	9–14	127°57′	11°44′	piston core	Total carbon	3650 ± 200	Calcarenite
		84–88				Total carbon	15,500 ± 1000	Calcarenite
		97–104				Total carbon	17,400 ± 1000	Silty calcareous clay
		201–208				Total carbon	18,900 ± 1500	Silty calcareous clay
LSDA–152 (V–382)	720	9–15	127°29′	8°44′	piston core	Total carbon	2320 ± 120	Silty calcareous clay
		192–199				Total carbon	13,000 ± 600	Silty calcareous clay

A piston core 294 cm long in the Bonaparte Depression (LSDH–57, Fig. 10.1) shows the following lithological sequence (T. C. Moore, pers. comm.): 0 to 29 cm, slightly mottled olive-green silty calcarenite with abundant shell fragments; 29 to 94 cm, mottled greenish grey muddy calcarenite with abundant shell fragments gradually increasing downward in number and size from 50 to 94 cm; 94 to 294 cm, dark bluish green silty clay mottled with patches of muddy calcarenite. The surface section is similar in lithology to the adjacent surface samples and belongs in the zone of coarse sediment surrounding the group of banks at 12° S. latitude, 128° 40′ E. longitude. Sands with thicknesses ranging from 5 to 41 cm cover muds in many places on the Sahul Shelf (Fig. 11.1D) and may occur more frequently than the generally short cores reveal.

The lower 100 cm of the core contain a foraminiferal fauna consisting exclusively of benthonic species that indicate a moderately restricted marine environment. There is no evidence of either fresh and brackish or hypersaline conditions. The carbonate content of approximately 10 percent is significantly lower than that prevailing in the modern sediments of the Bonaparte Depression (25 to 50 percent) and indicates a much higher supply of terrigenous sediment than there is at present. Radiocarbon dating (Table 11.1) shows that deposition of the lagoonal phase ended about 17,000 years ago, when, according to Curray (1960), sea level had risen to approximately 50 fathoms, and, accordingly, much of the outer shelf was under water. During the last few thousand years of the lagoonal phase, the sedimentation rate was approximately 70 cm per 1000 years, a figure quite normal for this environment (Shepard & Moore, 1960; Rusnak, 1960). In the upper portion of the core the sedimentation rate drops to less than 10 cm per 1000 years, which may represent a fair estimate of the approximate rate of sedimentation for much of the Sahul Shelf.

At 192 cm, still in the upper lagoonal sequence, the first signs of a decrease of the restriction of the environment appear in the form of rare planktonic Foraminifera. Upward, the ratio of planktonic to benthonic Foraminifera and the number of Foraminifera per unit volume of sediment gradually increase. The planktonic forms constitute 4 percent of the total number of Foraminifera at 94 cm and 10 to 20 percent at the surface (compare Fig. 9.4). Coccoliths occur in abundance above 94 cm. These changes reflect the progressively more marine character of the environment as sea level started to rise about 18,000 years ago and rapidly flooded the land barriers. About 15,000 years ago, sea level stood at approximately 50 fathoms (Curray, 1961), providing an essentially open connection between the Bonaparte Depression and the sea.

From these observations we can infer that during the last glacial maximum, the Bonaparte Depression was indeed an almost enclosed embayment. All major rivers of the region drained into this lagoon (Fig. 11.1A). Today these rivers have a combined mean annual runoff of approximately 6×10^{10} cubic metres of water (Table 3.1). Since the volume of the lagoon during the maximum lowering of sea level was only about $10^{11} m^3$, the fact that there is no evidence for a fresh or brackish environment strongly suggests that rainfall and runoff were considerably less than today.

In Chapter 9, we discussed the occurrence of brown calcareous nodules in the sediments of the shallower parts of the Sahul Shelf (Fig. 9.5). These nodules are very similar to the *kunkar* that is so widespread in surface sediments of southern

Australia. The kunkar is formed in the B-horizon of certain types of soils (for example, the mallisols of Northcote (1956)), and there can be little doubt that the nodules of the Sahul Shelf also are the product of pedogenic processes operating on calcareous marine sediments of the pre-Würm interglacial. Jessup (1960a, b) ascribes the formation of the kunkar to a relatively humid climate because leaching is required, but he does not estimate the amount or the seasonal distribution of the precipitation. Whether the kunkar of southern Australia is being actively formed at present is open to debate, but if so, it is associated with precipitation of 5 to 12 inches per year, significantly lower than in north-western Australia (15 to 60 inches per year). When submerged below the level of permanent ground water, the kunkar tends to disappear rapidly, soth at a low permanent ground water table and only moderate and seasonal rainfall seem to be indicated.

To our knowledge, no kunkar has been found on land in north-western Australia. The formation of these concretions is dependent upon a calcareous substrate. In southern Australia such a substrate was provided by windblown calcareous dust that was transported inland from the exposed continental shelf. In the Timor Sea region, the shelf sediments are not rich in fine calcareous material, and during the last glacial maximum the winds were not favourable for large-scale wind transport toward the continent.

The kunkar of the Timor Sea sediments does not occur in soil profiles, but has been concentrated into lag deposits. In southern Australia such lag deposits have been ascribed to wind erosion (Jessup, 1960a, b). The abundance of fresh skeletal material mixed with the Timor Sea kunkar indicates that marine winnowing and reworking have produced these deposits, and it is not necessary to postulate a period of deflation.

Many sediment cores of the Sahul Shelf show complex depositional structures (Fig. 11.1D). Alternating layers of fine and coarse sediment are widespread, and evidence of postdepositional destruction of layered sequences by burrowing organisms is common, resulting in mottled sediments (Moore & Scruton, 1957). This process of secondary homogenization ultimately leads to homogeneous deposits of muddy sands and sandy muds; hence many of the homogeneous cores of the Sahul Shelf also may have been layered originally. By means of X-radiographs, relict fragments of layers and mottles can be detected in superficially homogeneous sediments (Calvert & Veevers, 1962), and many Sahul Shelf cores show such relicts.

Normally, the sediments of continental shelves show few lithological changes in the upper few feet, except for mottling or layering on a small scale. The Sahul Shelf sediments, on the other hand, give ample evidence of relatively large-scale changes in depositional environment. In several areas, 5 to 40 cm of coarse calcarenite overlie fine muds. These lithologic changes indicate that major changes in environment took place in the time interval represented by a few feet of deposition. Dating of core LSDH–57 has shown that one such change took place approximately 16,000 years ago and probably was related to increased erosion and supply of coarse material as the littoral zone crossed the site of the core during the postglacial transgression. The other sands may well have the same origin. If this is correct, the base of the coarse layer should decrease gradually in age in a landward direction. The restricted thickness of these layers and the abundance of mottled or secondarily homogenized cores indicate that sedimentation rates over most of the Sahul Shelf are very slow, with the possible exception of the fine-grained portions of the Bonaparte Depression (see Chapter 9).

The late Quaternary history of the Timor Sea, as derived from the preceding discussion and from data on the distribution and provenance of terrigenous material (Chapter 8), is summarized in Figure 11.1. In order to facilitate a comparison, the palaeogeography has been shown for the same sea level stands that were used by Curray (1960) in his palaeogeographic maps of the continental shelf of the Gulf of Mexico. The approximate ages for each map are derived from existing curves for the late Quaternary rise in sea level (Curray, 1960, 1961).

During the last glacial maximum the entire Sahul Shelf was subaerially exposed, with the exception of the shallow Bonaparte lagoon. A current somewhat colder than the present Timor Current traversed the Timor Trough from the south during at least part of the year; the climate of the region probably was considerably drier than today, with highly seasonal precipitation of 15 inches or less. Under these conditions, seasonal herbaceous vegetation with open forest along the stream courses is probable, in accordance with Mayr's (1944) expectations. The landscape was attractive and suitable for the migration of early man. The blanket of calcareous marine sediments left by the preceding marine transgression was transformed into soils of the mallisol type. The drainage system was mainly restricted to the shelf area itself, while the precursors of the present rivers flowed directly into the Bonaparte lagoon. This configuration restricted the distribution of terrigenous sediment to the inner shelf, the Bonaparte Depression, and an area along the large channel just west of Bathurst Island.

Approximately 18,000 years ago, sea level began to rise rapidly, and between 15,000 and 13,000 years B.P., the shoreline was already located landward of the Bonaparte Depression. A shallow but open marine environment prevailed on the outer and middle shelf, which was studded with numerous large and small islands. The situation of 11,000 years ago, when sea level had risen to — 30 fathoms, is shown in Figure 11.1B. The Van Diemen Rise was broken up into numerous closely spaced islands, separated by narrow deep channels and very similar to Bathurst and Melville or the Aru Islands of today. The Joseph Bonaparte Gulf began to take shape, and offshore from its coastline two zones of high quartz concentration (I, II) were well developed, probably by active deposition of terrigenous material in a littoral zone. These two zones occur at 22 to 28 and 35 to 38 fathoms (Fig. 8.3). They may have been formed during temporary still stands or even during slight reversals of the general transgression. Such reversals have been postulated by Curray for the Gulf of Mexico (1960) and have been demonstrated on the Guayana coast by van Andel & Sachs (1964).

Continued rapid rise of sea level brought the shoreline to approximately — 15 fathoms some 9000 years ago (Fig. 11.1C), in a position very close to the present one. Just offshore from this coastline another high quartz zone (III) borders the Bonaparte Gulf and the area of Bathurst and Melville Islands, which possibly marks another temporary still-stand or reversal. Such an event at approximately this time and level was postulated by Curray (1960) and confirmed by van Andel & Sachs (1964). Very soon thereafter, the rate of sea level rise slowed down considerably.

Another quartz zone (IV) just outside the present shore may well be related to conditions during the last few thousand years. Mineralogical studies (Fig. 8.4) show that little longshore drift took place in these littoral sand zones.

During the early rapid part of the transgression, the shoreline receded very rapidly, at times as much as 3 nautical miles per year across the centre of the shelf. The offshore islands that formed during the first part of the rise rapidly decreased in size and completely disappeared when sea level reached 12 to 15 fathoms below its present position. At this point the shelf edge banks also were finally submerged. Since most of these islands early became rapidly isolated, it is entirely possible that a considerable Pleistocene fauna was trapped on them, the remains of which could be recovered by dredging. A similar case concerns the Dogger Bank in the North Sea, which was isolated in the early part of the postglacial transgression and finally flooded, and has yielded large quantities of vertebrate remains to fishermen's nets.

The data available from this study of the Timor Sea cast no light on the controversial question of postglacial sea level stands higher than the present one, which have been postulated for nearby parts of the west coast of Australia (Fairbridge, 1954, 1961; Shepard, 1964). Shell material from a raised beach deposit on top of a bench of *Thalassina* mudstone (station V–386) in the Bonaparte Gulf gave a modern age and apparently was adventitious.

During the gradual rise of sea level, the subaerial soils were winnowed to form kunkar lag concentrates, which were subsequently mixed with skeletal material; blankets of calcarenite were deposited over preceding muds, probably during the passage of a littoral zone over the area. After the first submergence, sedimentation rates apparently have been very slow. Consequently, a large part of the shelf sediments exposed at the surface reflect the effects of the transgression, the more so as they occur in shallower depths, where post-transgressional conditions have prevailed for a shorter time. The regular seaward increase of the ratio of planktonic to benthonic Foraminifera (Fig. 9.4) probably is in large part a function of the postglacial transgression and the resulting seaward increase in the duration of the marine environment.

Sedimentary facies

The present investigation has been designed with emphasis on the broad regional aspects of the Timor Sea, and particular attention has been given to the possible application of this study to the interpretation of ancient sediments. Consequently, there is little or no discussion of detailed local features and of processes of sedimentation, but rather there is an examination of broad lithological and petrographical aspects of the sediments as related to regional factors that control sediment genesis. In earlier studies with similar objectives, these regional controls have been grouped, following P. D. Krynine, under the name *geologic setting*. Most regional studies of modern sediments of this type have stressed settings with moderate to high rates of terrigenous sediment supply and a wide variation in the degree of marine reworking and dispersal. Some of these sediments were located in essentially stable regions with a dominantly depositional morphology (for example, the Gulf of Mexico: Shepard et al., 1960; the Orinoco region: van Andel & Postma, 1954; Koldewijn, 1958; Nota, 1958); others were located in tectonically complex and unstable basins with partially restricted circulation (Gulf of California: van Andel, 1964; Calvert, 1964; California Borderland: Emery, 1960). The effects of sea level changes under conditions of a moderate to high rate of sediment supply have been explored by Curray (1964).

The present study deals with a region of very low supply of terrigenous sediment and intricate topography. The Sahul Shelf also has been tectonically stable, at least during the Quaternary. The sediments are predominantly calcareous; the environments range from neritic to bathyal. For reasons discussed in the Introduction, the nearshore deposits, a prominent part of all studies quoted above, are outside the scope of this report.

Modern calcareous sediments form the subject of a voluminous literature, comprising both detailed local studies and broad regional investigations. Many of these studies deal with the sediments of isolated midocean platforms (Bahamas, Bermuda), of landlocked basins (Persian Gulf, Caspian Sea), or of continental shelves with very limited hinterland (Florida and Yucatan shelves, Gulf of Batabano in Cuba). A majority of the studies concern themselves with sediments of atolls and coral reefs. The very large Sahul Shelf, with its extensive low tropical hinterland with sluggish seasonal rivers, represents a special case of calcareous sedimentation. It has been considered a reasonable modern counterpart of the epicontinental seas that were widespread in Palaeozoic and Mesozoic times.

Although numerous stations have been occupied, the sample spacing is wide compared to the scale of the minor relief on the shelf. Therefore, the effects of these relief changes and of the associated environmental parameters will be expressed only as an essentially random variation superimposed on existing regional trends. In previous chapters, it has been shown that the extent of this random variation is surprisingly small, and that a very large part of the total variance can be accounted for by meaningful regional gradients. In the horizontal plane, the sampling density is reasonably close to that which can be obtained in studies of ancient formations, and the use of the present set of data for purposes of comparison appears justified as far as scale is concerned.

Ten facies types, mainly based on coarse fraction composition (see Fig. 9.6) and texture (Figs 7.2, 7.10), can be distinguished in the area of study (Fig. 11.3). One of these, the *nearshore facies group*, falls almost entirely outside the area of study; only a few samples in the Joseph Bonaparte Gulf are included in it. This facies consists of extensive coastal plain, estuarine, mud flat, beach, littoral, and reef environments; from casual inspection in the field and from aerial photographs, the facies appears well worth further study.

The *Basal Transgressive Facies*, comprising the Terrigenous and Middle Shelf groups, predominantly consists of coarse quartzose calcarenites and calcareous quartz sands containing abundant brown calcareous nodules, glauconite, and relict shallow-water skeletal material, mixed with modern faunal elements, mainly Foraminifera. The occurrence of this facies is restricted to a broad zone between theAustralian coast and approximately the inner 40-fathom contour. The sediments included in this facies show considerable small-scale variation of texture and composition and have a striking zonation of alternating belts of high and low quartz content, attributed to littoral development during still-stands or temporary reversals of the postglacial

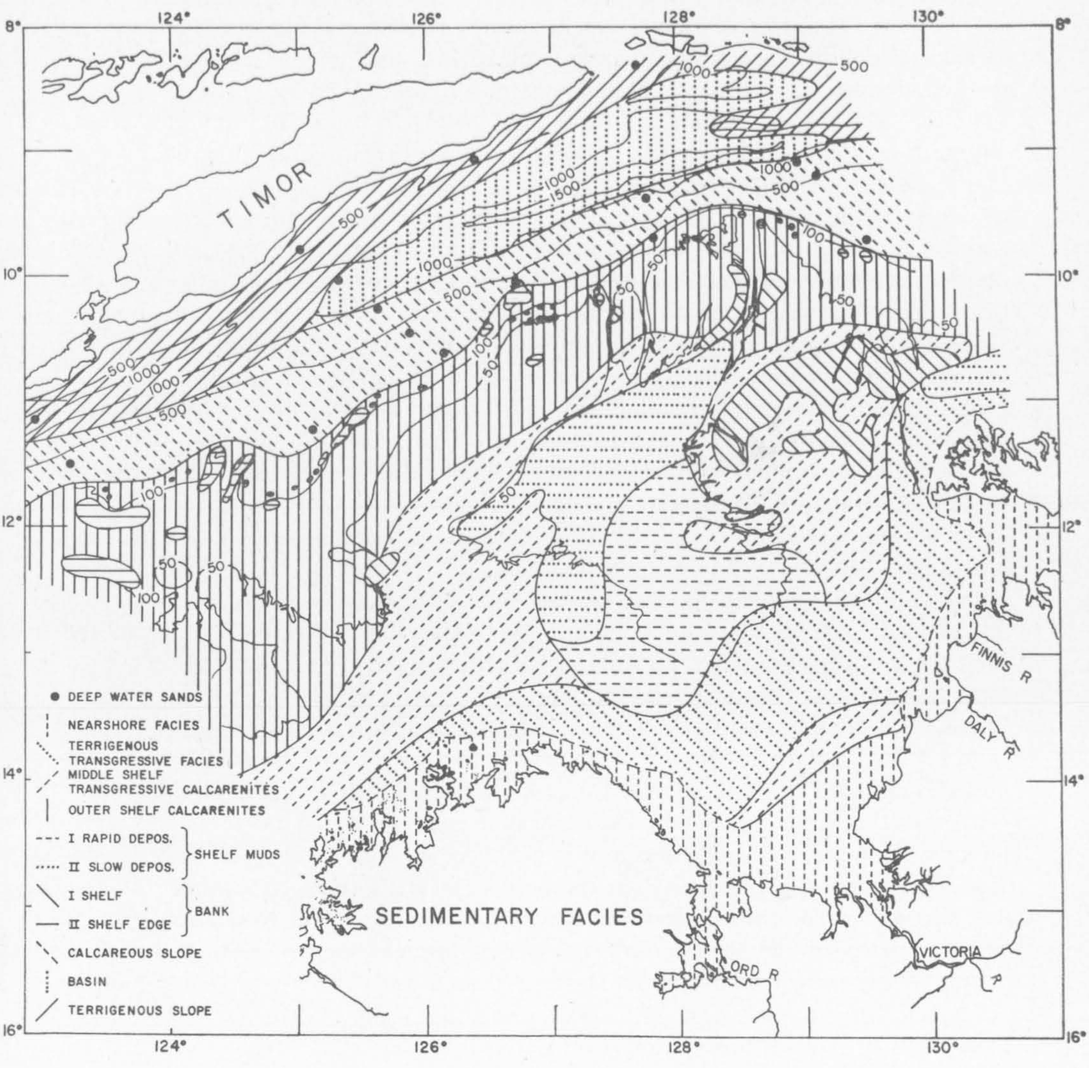

Fig. 11.3—Sedimentary facies of the surface sediments of the Timor Sea. One degree of latitude equals 60 nautical miles.

transgression. The sediments were deposited during the last part of this transgression; present deposition appears to be slow, and active burrowing by organisms is mixing relict and modern deposits, resulting in widespread mottled structures. Enhanced by the slow rate of deposition, extensive glauconitization is taking place. The seaward boundary of this facies is transitional and has been arbitrarily determined as the outer limit of coarse terrigenous material. The distribution of this terrigenous sand appears to be conditioned by the late Pleistocene drainage pattern of the shelf exposed at that time. Modern coarse terrigenous sediment is not being deposited beyond the 10-fathom contour.

The *Middle Shelf Calcarenites* are genetically similar, but are entirely composed of skeletal debris. Texturally, they are calcarenites and muddy calcarenites; fine-grained samples are very rare. Abundant corals, Bryozoa, and Mollusca occur where the facies crosses the Londonderry Rise. The coral and bryozoan fraction is especially prominent in a wide zone surrounding banks on the rises and along the margins of the Bonaparte Depression (see Fig. 9.5). Much of this material probably was eroded from the edges of the banks during the postglacial rise of sea level. Modern and live corals are rare over the entire shelf. This, combined with the considerations detailed in the previous section, indicates that in large part this facies also is a relict from the transgression. The general abundance of brown calcareous nodules supports this assumption. In addition to these components, the sediments also contain Foraminifera tests which increase seaward in abundance, as does the ratio of planktonic to benthonic Foraminifera. This foraminiferal portion of the sediments probably represents the material now being added. The mixture of recent and relict components, the abundance of glauconitized material (Fig. 7.8), and the prevalence of mottled structures all suggest very slow sedimentation rates.

The *Outer Shelf Foraminiferal Facies* consists of muddy calcarenites which are dominantly foraminiferal in composition and probably recent. Glauconitization is minor, and relict components are scarce. This facies contains larger amounts of fine-grained material than the Middle Shelf Calcarenites; toward the edge of the shelf the grainsize decreases, and the Foraminifera content and the ratio of planktonic to benthonic Foraminifera increase.

The distribution of the *Shelf Mud Facies* is largely a function of topography, since silt and clay are restricted to deep or sheltered portions of the shelf. The main area of shelf mud is the Bonaparte Depression, from which a tongue extends southward into the western part of the Joseph Bonaparte Gulf. A much smaller area, possibly the western end of a larger mud zone, occurs north-west of Bathurst Island. The distribution of the muds reflects the position of the sources of suspended matter and the pattern of the transporting currents. The restriction to deeper or more sheltered parts of the shelf indicates that deposition is largely controlled by the degree of exposure to waves. In depths shallower than 40 fathoms, little mud is permanently deposited. The shelf muds are highly calcareous, significantly more so than the silty clays of the Timor Trough, and they generally contain a higher proportion of silt- and sand-sized material. The coarse fraction is characteristic and consists largely of molluscan debris. Two subgroups can be distinguished on the basis of the colour of the molluscan material. The discolouration of the shells of the southern subgroup is probably due to the creation of an anaerobic subsurface environment in rapidly deposited muds.

Bank Facies are found on shallow (less than 20 fathoms) flat-top banks. The sediments are calcirudites or highly calciruditic and are mainly composed of large Foraminifera and coralline Algae. On most, but not all, shelf edge banks, the dominant component is *Halimeda*, while the banks on the shelf have other coralline Algae, mainly *Lithothamnium* biscuits, and numerous large Foraminifera. The difference may be due to position with respect to the margin of the shelf; *Halimeda*-rich sediments are reported near deep-water margins from other parts of the world. However, the shelf banks also are generally deeper (15–20 fathoms) than the shelf edge banks (12 fathoms), and a few samples on deeper shelf edge banks do not have a *Halimeda* assemblage, suggesting that water depth may be a factor. The bank facies are partly alive and no doubt actively developing; they are the most distinctive and best defined lithologic units of the region. There is no significant coral growth on the banks, which appear to be blanketed entirely by Algae-Foraminifera calcirudite. Wave winnowing at these shallow depths probably accounts for the deficiency of sand-sized and finer material. Small amounts of brown calcareous nodules are widespread, showing that relict deposits must be present at shallow depths below the sediment-water interface.

Three facies with gradational relationships can be distinguished in the Timor Trough. Calcilutites with 25 to 50 percent fine carbonate cover the southern slope. This *calcareous slope facies* is both finer and less calcareous than the shelf mud facies. The opposite northern slope is formed of predominantly terrigenous silty clays with little carbonate and much less silt than the calcareous slope facies. In both types of sediment, the coarse fraction consists exclusively of planktonic Foraminifera, and there is no evidence of major displacement of coarse shelf or shelf edge material into the trough. The deep-water sands, which are fairly common, also consist entirely of planktonic Foraminifera, the source of which cannot have been much shallower than 200 to 300 fathoms. A *Basin Facies* in the eastern and central deepest portions of the trough is characterized by a coarse fraction consisting entirely of Radiolaria. The occurrence of this facies is sharply limited by the 1000-fathom contour. It is quite similar in composition and texture to the hemipelagic clays of the open ocean, but in the Timor Trough the peculiar shift in proportion between the Radiolaria and planktonic Foraminifera below the 1000-fathom level cannot be explained.

The distribution of the sand- and silt-size modes, which are entirely calcareous, and of fine carbonate, indicate that the principal source of the calcareous components is the Sahul Shelf, and that this fraction is transported transversely into the trough, although little reaches the opposite slope. The provenance of the terrigenous fraction is not so evident, but circumstantial evidence suggests that an appreciable portion comes from the islands along the northern margin of the trough and perhaps from the east. Some terrigenous matter also may bypass the Sahul Shelf and be deposited in the trough. Sedimentation rates in the trough apparently are high enough that several inches to a few feet of Recent sediments have formed in most areas. As a whole, the trough facies are controlled by water depth and the type of fine-grained material supplied.

It is evident that the most important single factor affecting the lithology and distribution of sediments on the Sahul Shelf is the postglacial transgression. This is true to a certain extent of most continental shelves, but on the Sahul Shelf this influence is particularly important and widespread. The sediments of approximately three-fifths of the total shelf area are partially or dominantly relict in nature, and only the nearshore, shelf mud, and bank facies are truly recent. The reason for the dominating influence of this postglacial transgression is the very low rate of sedimentation on most of the shelf, largely caused by the very small supply of terrigenous material. Although direct information is limited, recent deposits outside the Bonaparte Depression are generally likely to be less than a few feet thick. With such a low rate of deposition, vertical mixing by burrowing organisms assumes major importance in determining the characteristics of the sediments. Thus, a low rate of sediment supply not only produces a dominantly calcareous sediment, but also it has significantly retarded the time at which an equilibrium between modern environments and sediments will be attained. If sea level remains in its present position for a long time, the transgressive facies probably will ultimately be covered with a slowly thickening blanket of foraminiferal calcarenites surrounding the relatively small areas of shelf muds in the Bonaparte Depression and the Algae-Foraminifera calcirudites of the banks.

Little or no coarse terrigenous material is transported beyond the littoral zone at present. However, appreciable amounts of fine suspended terrigenous material, supplied mainly by the Ord and Victoria Rivers, are distributed over the shelf by marine currents. Some of this material is probably carried over the outer rise into the Timor Trough, but much of it comes to rest in the Bonaparte Depression or in the sheltered zone between Bathurst Island and the banks of the Van Diemen Rise. Wave turbulence is instrumental in keeping the bank tops free of most finer-grained sediment.

The small amount of information that is available suggests that the waters of the shelf are quite homogeneous and well mixed over the entire area, and that they possess little horizontal change in salinity and little seaward decrease in bottom-water temperature. This explains why there is not much evidence of ecological variation in the sediments and why, apart from the variability induced by sediment supply and regional topography, the sediments are surprisingly uniform. The molluscan facies of the Bonaparte Depression probably owes its existence to the fine-grained bottom sediments, as contrasted with the recent foraminiferal facies of the rises and the bank assemblages.

Comparison with other shelf sediments

The study of modern calcareous sediments has emphasized relatively small-scale features such as atolls, reefs, lagoons, and bays, or it has been oriented toward

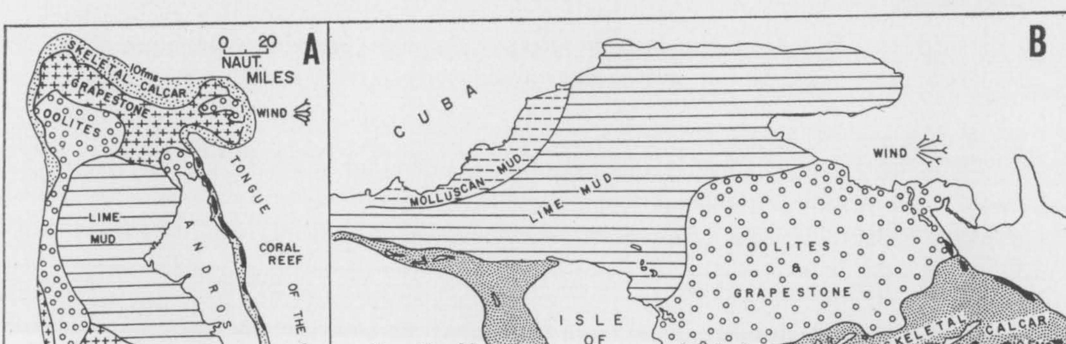

Fig. 11.4—Sedimentary facies of the Great Bahama Bank (A: modified after Newell et al., 1959; Purdy, 1963) and of the Gulf of Batabano, Cuba (B: compiled from Daetwyler & Kidwell, 1959). North is up.

an ecological or geochemical approach. Regional investigations that allow a direct comparison with the results of the present study are few. Moreover, a disproportionate amount of the total effort has been directed toward the study of the Bahamas. As a result, the Bahaman facies are frequently regarded as the normal type of modern marine carbonate deposition.

The sediments of the Bahamas are being deposited on the tops of large very slowly subsiding midocean platforms that are isolated from the influence of continents or large islands. The banks, of which Great Bahama Bank (Fig. 11.4A) is a good and well-studied example (Illing, 1954; Imbrie & Purdy, 1962; Kornicker & Purdy, 1957; Newell, Imbrie, Purdy, & Thurber, 1959; Newell, Purdy, & Imbrie, 1960; Newell & Rigby, 1957; Purdy, 1961, 1963; Seibold, 1962; Thorp, 1934, 1955), rise steeply from a depth of more than 2000 fathoms to the bank rim at approximately 10 fathoms. The upper slope is precipitous. The bank tops are flat or slightly bowl-shaped, mostly at depths of 3 to 4 fathoms. Along the eastern windward margin, wave turbulence provides a supply of cool, nutrient-rich water, and coral reefs are widespread. Elsewhere, the banks are fringed by skeletal calcarenites characteristically consisting of *Halimeda* and other calcareous Algae, coral debris, and Foraminifera. The broad shallow bank rims are covered with extensive oolites and grapestone calcarenites. These sediments are formed where the cool carbon dioxide-rich ocean water warms up while rising over the bank and precipitates carbonate in the turbulent bottom water. The central depression and the sheltered areas behind islands and reefs are blanketed with fine aragonite mud precipitated by a still some-

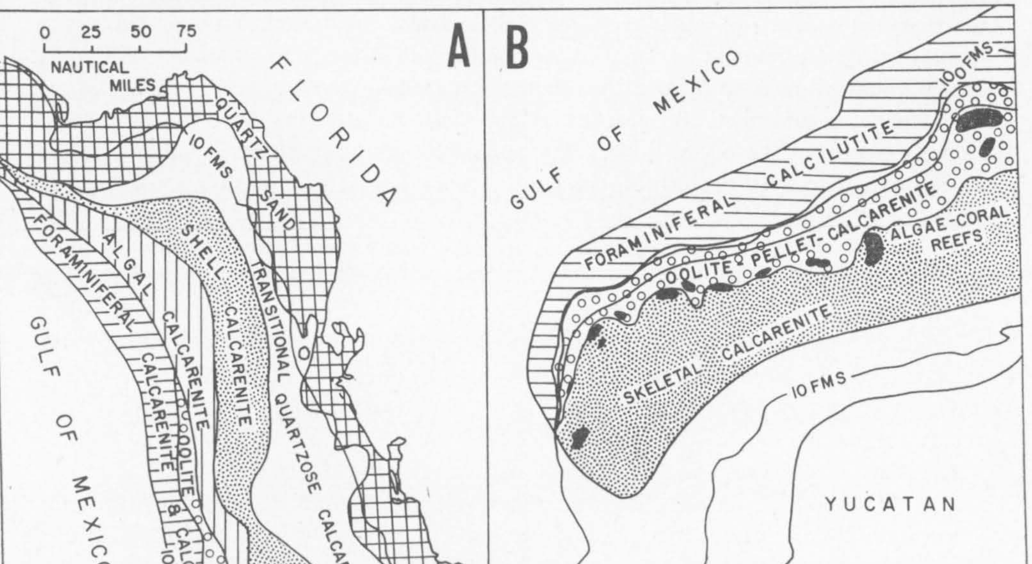

Fig. 11.5—Sedimentary facies of the Western Florida Shelf (A: compiled from Gould & Stewart, 1955) and of the Yucatan Shelf (B: modified after Williams, 1963). North is up. Scale of A and B identical.

what controversial mechanism (Cloud, 1962; Lowenstam & Epstein, 1957; Purdy, 1963). The bank sediments overlie a late Pleistocene erosion surface cut in indurated limestones, which outcrop locally. The recent sediments themselves show no evidence of relicts of the postglacial transgression and are in near-perfect equilibrium with present environmental conditions. Absence of terrigenous sediment supply, the shallow depth of the bank, position with respect to prevailing winds and distance from the bank rims, and the degree of shelter from wave exposure are the essential factors governing sediment type and distribution.

This facies group is not restricted to the Bahamas, but is also found on the Bermuda platform and in a slightly different setting in the Gulf of Batabano, Cuba (Daetwyler & Kidwell, 1959). This area is bordered by the Cuban mainland and one large island (Fig. 11.4B), but very low runoff restricts the supply of terrigenous sediment and fresh water to the immediate vicinity of the shoreline and the inner embayments. The platform is again very shallow, varying in depth from 4 to 7 fathoms, and beyond the 10-fathom contour it drops steeply to the floor of the Caribbean Sea at more than 1000 fathoms. Coral reefs border the south-eastern windward edge of the platform; elsewhere, a fringe of skeletal calcarenite consisting of calcareous Algae, mainly *Halimeda*, coral debris, and Foraminifera forms a narrow border zone. Ocean water enters over the south-eastern edge, and in warming up in the turbulent zone of the outer part of the platform it forms a broad deposit of oolites and other non-skeletal carbonates. Fine lime muds cover the inner, sheltered portions of the Gulf; in the nearshore areas the muds are rich in shell debris. The recent sediments overlie a Pleistocene erosion surface with a thin but fairly continuous blanket, and there is no evidence of relict transgressive deposits. Although asymmetrical as a result of the geographical setting, the environmental pattern with which the sediments are in equilibrium is similar to that of the Bahamas.

The facies described above occur in very shallow water; below 10 fathoms, steep slopes descend to the ocean floor. The sediments of the middle and outer shelves, in depths of from 10 to 100 fathoms, must be examined in other areas. Gould & Stewart (1955) have described the deposits of the western Florida shelf (Fig. 11.5A). This shelf slopes gently to a depth of 35 fathoms, where the gradient increases. The usual shelf break at or below 60 fathoms is absent. Ridges and low banks are common between 30 and 50 fathoms; they are covered by a coarse sediment consisting of algal (*Lithothamnium*) biscuits and algal-foraminiferal calcarenites. Gould & Stewart consider these sediments to be erosional products of outcropping Pleistocene reefs, but in the light of studies in other areas, they may well be actively developing, at least on the bank tops. Seaward of the algal calcarenites is a narrow belt of oolites, which is attributable to a late Pleistocene still stand in the rise of sea level at approximately 30 fathoms. Part of the algal sediments may be related to this still stand. Foraminiferal calcarenites that grade downslope into foraminiferal calcilutites occur beyond the oolite facies. These sediments are probably recent. Inshore from the algal zone, the shelf is covered with skeletal calcarenites, mainly consisting of molluscan debris, which grade landward into quartzose calcarenites. These deposits show much evidence of reworking and can be considered a basal transgressive sequence, grading into modern littoral quartz sands inside the 10-fathom contour. Waves and tidal currents actively rework and distribute the quartz sands. All shelf sediments are thin and patchy and overlie a Pleistocene erosion surface. With the exception of the outer-shelf foraminiferal facies and the nearshore quartz sands, the pattern is dominated by the postglacial transgression. Modern counterparts of the offshore oolitic facies have not been reported from the littoral zone of the west coast of Florida, although small amounts of scattered oolites occur (Thorp, 1955). However, most published research is concerned with bay sediments and is not representative (Goodell & Gorsline, 1961; Stewart & Gorsline, 1962; Scholl, 1963). The apparent absence of a modern littoral oolitic facies may be a result of the great width and gentle slope of the shelf, which prevent the sudden change in water temperature and the high degree of turbulence that produce the ooids in the Bahamian environment. A shoreline at minus 30–50 fathoms would be located in a more favorable position for the formation of the oolitic facies.

A similar distribution of shelf facies occurs on the Yucatan shelf (Williams, 1963; Harding, 1964). A broad belt of relict oolitic and pelletal calcarenites that covers a terrace on the outer shelf between 30 and 35 fathoms extends seaward to the 50-fathom contour (Fig. 11.5B). The oolites surround shallow banks with associated coral debris and algal-foraminiferal calcirudites. The origin of this zone is attributed to a prolonged still stand during the postglacial rise of sea level, although some of the algal-foraminiferal deposits may be recent. Seaward, the oolite-pellet facies becomes more silty and the proportion of planktonic Foraminifera increases until the sediments on the outer shelf and upper slope become foraminiferal calcilutites. This foraminiferal facies is recent. Landward, the oolite facies gives way to skeletal calcarenites that originated mainly during the latter part of the postglacial transgression. The unconsolidated sediments of the Yucatan platform are thin and again overlie an erosion-cut platform. There is no information regarding the presence or absence of a nearshore modern oolite facies.

Calcareous sediments are formed in an entirely different setting in the Persian Gulf (Emery, 1956; Houbolt, 1957). The Persian Gulf is an almost enclosed basin, communicating with the Gulf of Oman and the Arabian Sea through a narrow strait. This strait, which is located at the deepest point of the Persian Gulf, has a depth of 50 fathoms; from there the Gulf shoals to 20 fathoms in the north-west. The Gulf forms the transition between a young mountainous orogene on the north-eastern side and the Arabian craton on the south-west. The Gulf is assumed to be miogeosynclinal in nature. The only major drainage is from the Tigris and Euphrates Rivers through the Shatt-el-Arab delta; most of the sediment is trapped in the delta and only a small submarine fan exists in front of it. In the summer, evaporation in the Gulf is high, and hypersaline conditions prevail along the Arabian coast. Ocean water, which enters the Gulf from the south-east, circulates counterclockwise and departs as a saline subsurface current through the same strait. Dominant winds are from the east and north-east, and the long fetch in the southern Gulf produces considerable wave turbulence in the shallow south-western part. The sediment distribution is simple (Fig. 11.6B). Fine, dominantly terrigenous silty clays border the mountainous north-eastern margin in the deepest part of the trough, grading into calcilutites toward the south and south-east. Above 20 fathoms, the bottom along the Arabian coast is covered with skeletal calcarenites, mainly consisting of shell debris. Above 10 fathoms, the calcarenites are well rounded by wave action and active sedimentation

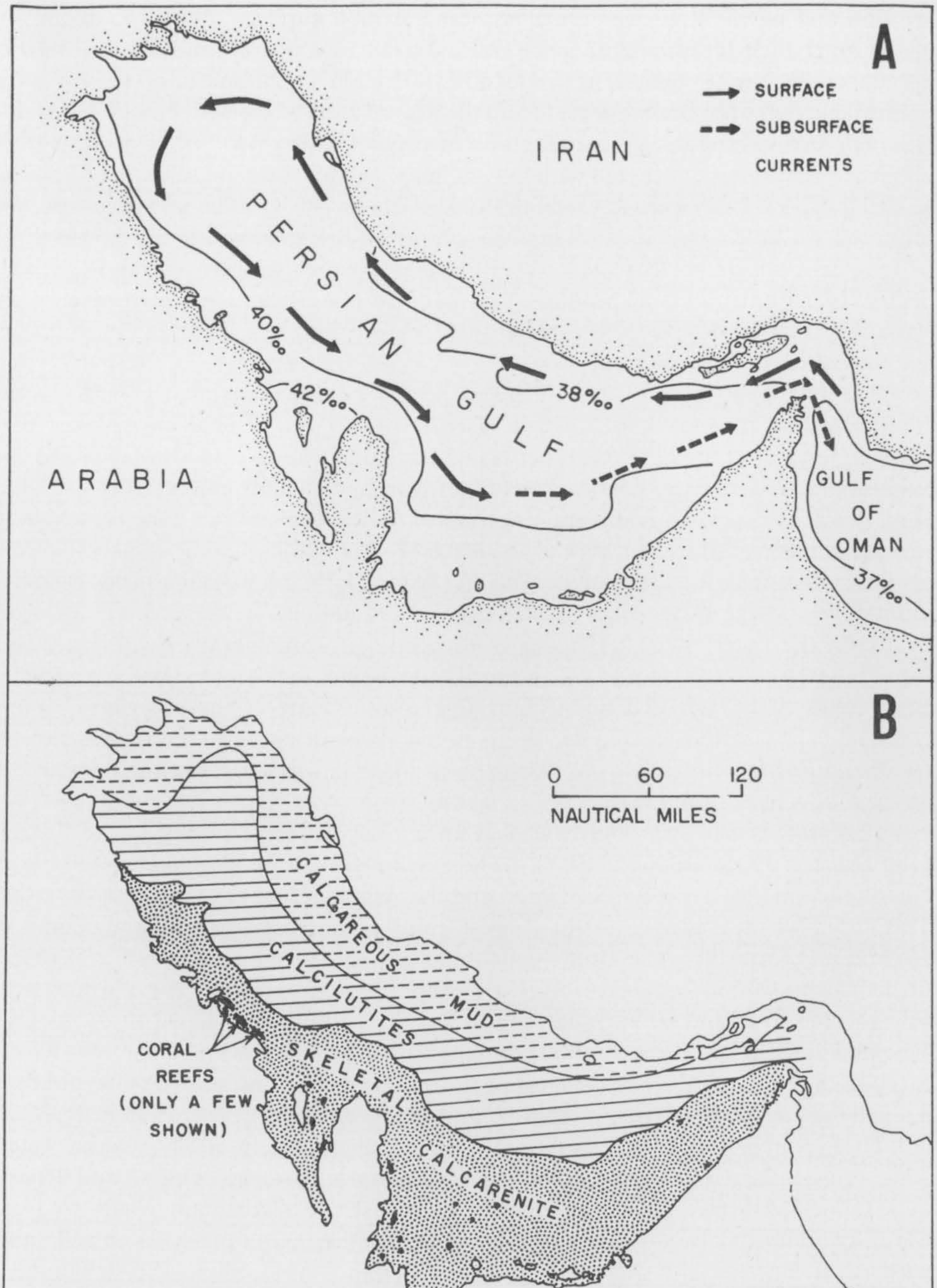

Fig. 11.6—Circulation pattern and salinity (A) and sedimentary facies (B) in the Persian Gulf (modified after Emery, 1956; Houbolt, 1957).

is taking place. The calcilutites and silty clays also are forming at present, but in the intermediate zone much of the sediment may be a relict from a lower sea level stand. In this zone, shallow banks are covered with large Foraminifera calcarenites. Formation of oolites, fine precipitated aragonite, and evaporites occurs widely in the littoral zone and in lagoons and embayments (Sugden, 1963a, b; Bramkamp & Powers, 1955; Wells & Illing, 1964; Kinsman, 1964; Evans, Kinsman & Shearman, 1964). Coral reefs fringe many islands and parts of the mainland.

Thus, the Persian Gulf contains many elements of the facies and environments previously discussed, with the exception of the relict Pleistocene littoral zones so prominent on the Florida and Yucatan shelves. These Persian Gulf formations, if they originally existed, are now buried under the calcilutites and silty clays of the central Gulf. Although the mechanism providing the turbulent zone with warm saline water needed to form the oolites is different from that of the open-ocean platforms, the result is the same. The principles governing facies types and facies distributions are similar to those of the other cases discussed above.

The calcareous shelves reviewed here have in common the fact that active deposition at present is restricted to a nearshore zone extending to approximately the 10-fathom contour, and to the outer shelf and continental slope. Between these two active zones, the shelf is covered with relict sediments deposited during the postglacial transgression. The relict sediments are undergoing some modification by waves and burrowing organisms at present, but little new sediment is being added. Both the littoral sediments formed during temporary still-stands of the rising sea and the blankets deposited during rapid landward movement of the shoreline are included in this zone of relict sediments. The two types can be distinguished on the basis of their sediments.

In shallow water, depositional facies depend on oceanographic conditions. If cool ocean water can reach this zone and be rapidly warmed, turbulent water will precipitate oolites and grapestone sediments, and aragonite muds may form in sheltered areas. Different mechanisms for achieving these conditions are illustrated by the Bahamas and the Gulf of Batabano, and by the Persian Gulf. In the first two cases, the facies pattern is a simple function of the distance to the seaward platform edge and of the degree of wave exposure. The oolite zone is formed near the deep-water edge rather than in the littoral zone. In the Persian Gulf, the wind-driven circulation and high evaporation rate combine to supply water to the downwind side of the basin, and oolites and aragonite muds are associated mainly with lagoonal development. Where no mechanism exists to ensure favourable conditions for carbonate precipitation, for instance behind the shelter of a wide, gently sloping shelf, the shallow-water deposits are skeletal in origin and sedimentation rates are comparatively slow. Quartzose calcarenites and calcarenitic quartz sands and their fine-grained equivalents of clays and clayey calcilutites are deposited depending on variations in supply of terrigenous material.

A second zone of active sedimentation occurs on the outer shelf and continental slope, where foraminiferal calcarenites are formed; with increasing water depth and diminishing wave turbulence at the bottom, they gradually pass into foraminiferal calcilutites. The sedimentation rate in this zone is apparently fairly high, and present conditions have prevailed long enough to bury all basal transgressive deposits. A foraminiferal-algal facies is developed on outer shelf banks.

All calcareous sediments discussed here occur in tropical oceans, and for some, particularly the non-skeletal phases, warm water appears to be required. However, it is clear that the dominance of calcareous material to a large extent is due to a very low past and present supply of terrigenous sediment, and that a high rate of supply of calcareous material need not be assumed. Calcareous sediments also accumulate on some high-latitude shelves; it is not evident that accumulation rates are higher in the tropical zone. Abyssal sediments in the tropical oceans are more calcareous and accumulate at a higher rate than those of higher latitudes, but this is due to the high production rates in the equatorial current systems. The effects of these current systems do not necessarily extend on to the adjacent continental shelves.

It may be noted here that not only must the present rate of supply of terrigenous sediment be low in order to allow the formation of dominantly calcareous sediments, but also the same condition must have prevailed during the late Quaternary regressions and transgressions. Shelf sediments in the tropics, where the supply of terrigenous sediments is moderate to high, as on the Guayana, Trinidad, and Paria shelves (Nota, 1958; Koldewijn, 1958), are covered with carbonates only in areas of topographic isolation. On some temperate shelves that now are largely free of terrigenous supply, such as the Gulf of Mexico or the Atlantic shelf of the United States, enough terrigenous sediment was supplied during the postglacial transgression to produce terrigenous transgressive facies.

The Sahul Shelf sediments are quite comparable to the deposits of the areas discussed earlier in this section. The outer shelf foraminiferal facies, the relict transgressive facies, and the algal-foraminiferal bank facies are all present in the same form and apparently have formed under essentially the same conditions as their counterparts on the Florida and Yucatan shelves and in the Persian Gulf. Facies representing still stands in the postglacial transgression are present, although they do not contain oolitic sediments. The formation of oolitic nearshore facies on the Sahul Shelf was probably rendered impossible by the morphology of this region, which places the depth zone above 35 fathoms, far away from the shelf edge and oceanic waters. Oolitic facies may well have formed below 50 fathoms during the maximum lowering of sea level, but these deposits, if they ever existed, are now buried under the outer shelf foraminiferal sediments.

In principle, there are many striking resemblances between the sediments of both terrigenous and calcareous continental shelves. Relict littoral deposits, related to temporary still-stands of sea level, and basal transgressive deposits formed during rapid rises are widespread on the shelves of the Gulf of Mexico (Curray, 1960), Gulf of California (van Andel, 1964), South America (Nota, 1958; Koldewijn, 1958), and on the Atlantic shelf of the United States (Merrill, Emery, & Rubin, 1965). Outer shelf and slope silty clays are the counterpart of the outer shelf foraminiferal calcarenites and calcilutites. Shelf edge banks with algal-foraminiferal facies occur not only on carbonate shelves, but also along the edge of the Gulf of Mexico (Curray, 1960; Ludwick & Walton, 1957) and along the Guayana shelf (Nota, 1958). Shelf silty clays are distributed by marine current patterns and are deposited in deep or sheltered portions of the shelf, just as the shelf calcilutites are distributed over the Sahul Shelf. Differences in mechanisms and facies patterns become obvious only in the nearshore zone. The deltas of the terrigenous supply regions have no counterpart in the calcareous basins, whereas the mechanism producing the non-skeletal carbonates, and the biostromal and biohermal structures, are peculiar to shelves of low terrigenous supply. But to a large extent, the same factors have controlled the types and distribution of sediment facies both on calcareous and terrigenous shelves: (1) location and rate of sediment supply, (2) current patterns, (3) wave action, which may prevent deposition of fine-grained material, and reworks and redistributes coarse material in shallow water, and (4) above all, the processes associated with the postglacial sea level rise.

ACKNOWLEDGEMENTS

This investigation has been supported by the U.S. Office of Naval Research under contract Nonr 2216(01) with the Scripps Institution of Oceanography, and by the National Science Foundation under Grants NSF–G14103 and GP–350. Participation of the junior author was made possible by the Bureau of Mineral Resources of the Commonwealth of Australia, and by a postdoctoral Harkness Fellowship of the Commonwealth Fund of New York.

The authors are indebted to many people for support, advice, and encouragement of many kinds. Only a few can be mentioned here; to the others we acknowledge our debt collectively.

The work at sea was accomplished successfully through the co-operation of the officers, crews, and scientific staff of *M.V. Malita* under Captain B. Cummings of Cairns, Australia, and of *R.V. Stranger* under Captain F. Miller of Scripps Institution of Oceanography. The laboratory work was organized and largely executed by Mrs Mary Franklin, who deserves special credit for this difficult task. She was assisted by P. J. Crampton, who also did part of the microscopic work, Miss Joyce Resnick, Miss Katherine Tinker, Tom Oberhuber, and Carter Newton. R. L. Rowland sorted some of the molluscan material, T. G. Moore examined piston cores and analysed the planktonic Foraminifera, and D. F. McGeary worked on the distribution of kunkar. Mrs Ann Pidd and John Wild, Jr, provided help in computer data processing. J. R. Moriarty did the cartography and most of the illustrations. R. A. DeHaven devised a method for cutting thin sections of the coarse carbonate fraction and devoted much time to the difficult task of their preparation. Miss Janet Witte assisted in data processing and in compiling the bibliography, and did most of the editorial work.

The ideas presented in this Bulletin have formed the subject of many discussions with our colleagues at Scripps, in particular G. Ross Heath, T. G. Moore, S. E. Calvert, C. C. von der Borch, E. L. Winterer, H. W. Menard, and J. R. Curray. J. Hays and A. R. Lloyd of the Bureau of Mineral Resources and M. D. Helfer of the University of California, Los Angeles, kindly allowed us to use information contained in unpublished manuscripts. B. V. Hamon, C.S.I.R.O., Division of Fisheries and Oceanography, Cronulla, read the chapter dealing with oceanography. P. R. Dunn and J. Hays, Bureau of Mineral Resources, Canberra, provided valuable discussion of the geology of north-western Australia.

We are grateful to the Hydrographic Office, Royal Australian Navy, for providing much of the bathymetric information; to the staff of the Water Resources Branch, Northern Territory Administration, and the West Australian Department of Public Works, for samples and flow data on rivers; and to the Bureau of Mineral Resources for their generosity in the publication of this Bulletin. Without the aid of Mrs Franklin, Miss Witte and Mr Moriarty, this publication would not have been possible.

REFERENCES

Beliaeva, N. V., 1963—The distribution of planktonic Foraminifera on the bottom of the Indian Ocean, *in* PROBLEMS OF PALEONTOLOGY. *Akad. Nauk USSR, Spec. Rep.*

Boutakoff, N., 1963—Geology of the offshore areas of north-western Australia. *J. Aust. Petrol. Explor. Ass.*, 1, 10–18.

Bradshaw, J. C., 1959—Ecology of living planktonic Foraminifera in the north and equatorial Pacific. *Contr. Cushman Fdn foram. Res.*, 10 (2), 25–64.

Bramkamp, R. A., and Powers, R. W., 1955—Two Persian Gulf lagoons (abstract). *J. sediment. Petrol.*, 25, 134–140.

Burst, J. F., 1958—Mineral heterogeneity in ' glauconite pellets.' *Amer. Miner.*, 43, 481–497.

Calvert, S. E., 1964—Diatomaceous sediments of the Gulf of California. *Ph.D. Dissertation, Univ. Calif., San Diego.*

Calvert, S. E., and Veevers. J. J., 1962—Minor structures of unconsolidated marine sediments revealed by X-radiography. *Sedimentology*, 1 (4), 287–295.

Carrigy, M. A., 1956—Organic sedimentation in Warnbro Sound, Western Australia. *J. sediment. Petrol.*, 26 (3), 228–239.

Carrigy, M. A., and Fairbridge, R. W., 1954—Recent sedimentation, physiography and structure of the continental shelves of Western Australia. *J. Roy. Soc. W. Aust.*, 38, 65–95.

Carroll, D., 1947—Heavy residues of soils from the lower Ord River Valley, Western Australia. *J. sediment. Petrol.*, 17 (1), 8–17.

Chayes, F., 1956—PETROGRAPHIC MODAL ANALYSIS. *N.Y., Wiley.*

Chayes, F., 1960—On correlation between variables of constant sum. *J. geophys. Res.*, 65 (12), 4185–4193.

Chayes, F., 1962—Numerical correlation and petrographic variation. *J. Geol.*, 70 (4), 440–452.

Christian, C. S., and Stewart, G. A., 1953—General report on survey of Katherine-Darwin region, 1946. *Sci. ind. Res. Org., Melb., Land Res. Ser.*, 1.

Cloud, P. B., Jr., 1962—Environment of calcium carbonate deposition west of Andros Island, Bahamas. *Prof. Pap., U. S. geol. Survey*, 350.

Cole, W. S., 1954—Larger Foraminifera and smaller diagnostic Foraminifera from Bikini drill holes. *Prof. Pap. U. S. geol. Surv.*, 260–0, 469–608.

Curray, J. R., 1960—Sediments and history of Holocene transgression, continental shelf, northwestern Gulf of Mexico, *in* RECENT SEDIMENTS, NORTHWESTERN GULF OF MEXICO, ed. F. P. Shephard. *Spec. Pub. Amer. Assoc. Petrol. Geol.*

Curray, J. R., 1961—Late Quaternary sea level: a discussion. *Bull. geol. Soc. Amer.*, 72, 1707–1712.

Curray, J. R., 1964—Transgressions and regressions, *in* STUDIES IN MARINE GEOLOGY, ed. R. L. Miller, *N.Y., McMillan*, 175–203.

Cushman, J. A., Todd, R., and Post, R. J., 1954—Recent Foraminifera of the Marshall Islands. *Prof. Pap. U. S. geol. Surv.*, 260–H, 319–384.

Daetwyler, C. C., and Kidwell, A. L., 1959—The Gulf of Batabano, a modern carbonate basin. *Proc. 5th World Petrol. Cong., N.Y.*, 1, 1–21.

d'Anglejan, B., 1964—The marine phosphorite deposit of Baja California: present environment and recent history. *Ph.D. Dissertation, Univ. Calif., San Diego.*

Doeglas, D. J., 1946—Interpretation of the results of mechanical analysis. *J. sediment. Petrol.*, 16(1), 19–40.

Doeglas, D. J., 1950—De interpretatie van korrel-grootte analysen. *Verh. Ned. geol. mijnbouwk. Gen.*, 15, 247–328.

Dunham, R. J., 1962—Classification of carbonate rocks according to depositional texture, *in* CLASSIFICATION OF CARBONATE ROCKS, ed. W. E. Ham. *Mem. Amer. Ass. Petrol. Geol.*, 108–121.

Dunn, P. R., 1962—Alligator River, N.T.—1:250,000 Geological Series. *Bur. Min. Resour. Aust. explan. Notes* D/53–1.

Ehlmann, A. J., Hulings, N. C., and Glover, E. D., 1963—Stages of glauconite formation in modern foraminiferal sediments. *J. sediment. Petrol.*, 33, 87–96.

Emery, K. O., 1956—Sediments and water of Persian Gulf. *Bull. Amer. Ass. Petrol. Geol.*, 40(10), 2354–2383.

Emery, K. O., 1960—THE SEA OFF SOUTHERN CALIFORNIA. *N.Y., Wiley.*

Emery, K. O., and Bray, E. E., 1962—Radiocarbon dating of California basin sediments. *Bull. Amer. Ass. Petrol. Geol.*, 46(10), 1839–1856.

Ericson, D. B., Ewing, M., and Wollin, G., 1964—The Pleistocene Epoch in deep-sea sediments. *Science*, 146, 723–732.

Evans, G., Kinsman, D. J. J., and Shearman, D. J., 1964—A reconnaissance survey of the environment of recent carbonate sedimentation along the Trucial Coast, Persian Gulf; *in* DEVELOPMENTS IN SEDIMENTOLOGY. *Amsterdam, Elsevier*, 1, 129–135.

Fairbridge, R. W., 1950—Recent and Pleistocene coral reefs of Australia. *J. Geol.*, 58(4), 330–401.

Fairbridge, R. W., 1951—The Aroe Islands and the continental shelf north of Australia. *Scope, J. Sci. Un. Univ. W. Aust.*, 1(6), 24–29.

Fairbridge, R. W., 1953—The Sahul Shelf, northern Australia; its structure and geological relationships. *J. Roy. Soc. W. Aust.*, 37, 1–33.

FAIRBRIDGE, R. W., 1954—Quaternary eustatic data for Western Australia and adjacent states. *Proc. Pan Indian Ocean Sci. Cong.*, sec. F, 64–84.
FAIRBRIDGE, R. W., 1958—Dating the latest movements of the Quaternary sea level. *Trans. N. Y. Acad. Sci.*, Ser. II, 20(6), 471–482.
FAIRBRIDGE, R. W., 1961—Eustatic changes in sea level; *in* PHYSICS AND CHEMISTRY OF THE EARTH. *London, Pergamon*, 4, 99–185.
FOLK, R. L., 1959—Practical petrographic classification of limestones. *Bull. Amer. Ass. Petrol. Geol.*, 43(1), 1–38.
GINSBURG, R. N., 1956—Environmental relationships of grain size and constituent particles in some south Florida carbonate sediments. *Bull. Amer. Ass. Petrol. Geol.*, 40(10), 2384–2427.
GINSBURG, R. N., 1957—Early diagenesis and lithification of shallow water carbonate sediments in southern Florida, *in* REGIONAL ASPECTS OF CARBONATE DEPOSITION: A SYMPOSIUM. *Spec. Publ. Soc. econ. Paleont. Miner*, 5, 80–100.
GOLDBERG, E. D., 1963—Mineralogy and chemistry of marine sedimentation, Shepherd, F. P., *in* SUBMARINE GEOLOGY. *N.Y., Harper & Rowe*, 436–466.
GOLDBERG, E. D., and GRIFFIN, J. J., 1964—Sedimentation rates and mineralogy in the South Atlantic. *J. geophys. Res.*, 69, 4293–4309.
GOODELL, H. G., and GORSLINE, D. S., 1961—A sedimentologic study of Tampa Bay, Florida. *Int. geol. Cong., 21st Sess., Norden, Rep.*, 23, 75–88.
GOULD, H. R., and STEWART, R. H., 1955—Continental terrace sediments in the northeastern Gulf of Mexico, *in* FINDING ANCIENT SHORELINES. *Spec. Publ. Soc. econ. Paleont. Miner.*, 3, 2–20.
GRABAU, A. W., 1904—On the classification of sedimentary rocks. *Amer. Geol.*, 33, 228–247.
GRABAU, A. W., 1913—PRINCIPLES OF STRATIGRAPHY. *N.Y., Seiler.*
HAM, W. E., ed., 1962—CLASSIFICATION OF CARBONATE ROCKS, A SYMPOSIUM. *Amer. Ass. Petrol. Geol., Mem.* 1.
HAM, W. E., and PRAY, L. C., 1962—Modern concepts and classifications of carbonate rocks, *in Ibid.*, 1, 2–19.
HARDING, J. L., 1964—Petrology and petrography of the Campeche lithic suite, Yucatan Shelf, Mexico. *Texas A & M Coll., Dep. Oceanogr., Rep.*, 64–11T.
HARMAN, H. H., 1960—MODERN FACTOR ANALYSIS. *Chicago, Univ. Press.*
HARTMAN, R. R., 1964—Interpretation report of reconnaissance airborne magnetometer profiles over the northwest continental shelf of Australia for Woodside Oil Co., N.L. *Aeroservice Ltd, Sydney* (unpubl. Rep.).
HAYS, J., 1966—Land surfaces and laterites in the north of the Northern Territory; *in* LAND FORM STUDIES IN AUSTRALIA, ed. J. A. Mabbutt and J. N. Jennings. *Canberra, Aust. Nat. Univ. Press.*
HEATH, G. R.—Glauconite in recent sediments 2: Sahul Shelf, northwestern Australia (in press).
HELFER, M. D., CAPUTO, M., and HARRISON, J. C., 1962—Gravity measurements in the Pacific and Indian Oceans, Monsoon Expedition, 1960, 1961. *Interim Rep., Inst. Geophys. planet. Phys., Univ. Calif., Los Angeles.*
HEMPEL, C. G., 1952—Fundamentals of concept formation in empirical science, *in* INTERNATIONAL ENCYCLOPAEDIA OF UNIFIED SCIENCES, ed. O. Neurath et al. *Chicago, Univ. Press*, 2(7), 1–93.
HOUBOLT, J. J. H. C., 1957—SURFACE SEDIMENTS OF THE PERSIAN GULF NEAR THE QATAR PENINSULA. *The Hague, Mouton.*
HOWER, J., 1961—Some factors concerning the nature and origin of glauconite. *Amer. Miner.*, 46, 313–334.
ILLING, L. V., 1954—Bahama calcareous sands. *Bull. Amer. Ass. Petrol. Geol.*, 38(1), 1–95.
IMBRIE, J., 1963—Factor and vector analysis programs for analyzing geological data. *Office Naval Res. tech. Rep. 6, Geogr. Br.*
IMBRIE, J., 1964—Factor analytic model in paleoecology, *in* APPROACHES TO PALEOECOLOGY, ed. J. Imbrie and N. D. Newell. *N.Y., Wiley*, 407–422.
IMBRIE, J., and PURDY, E. G., 1962—Classification of modern Bahamian carbonate sediments, *in* CLASSIFICATION OF CARBONATE ROCKS, ed. W. E. Ham. *Amer. Ass. Petrol. Geol. Mem.* 1, 253–272.
IMBRIE, J., and VAN ANDEL, Tj. H., 1964—Vector analysis of heavy mineral data. *Bull. geol. Soc. Amer.*, 75(12), 1131–1156.
JACKSON, E. A., 1957—Soil features in arid regions with particular reference to Australia. *J. Aust. agr. Sci.*, 23, 196–208.
JESSUP, R. W., 1960a—An introduction to the soils of the south-eastern portion of the Australian arid zone. *J. Soil Sci.*, 11(1), 92–105.
JESSUP, R. W., 1960b—Identification and significance of buried soils of Quaternary age in the south-eastern portion of the Australian arid zone. *J. Soil Sci.*, 11(2), 197–205.
JOHNSON, J. H., 1951—An introduction to the study of organic limestones. *Colo. Sch. Mines Quart.*, 46(2).
JOHNSON, J. H., 1952—Studies of organic limestones and limestone-building organisms. *Ibid.*, 47(2).
JOHNSON, J. H., 1954—Fossil calcareous algae from Bikini atoll. *Prof. Pap. U.S. geol. Surv.*, 260–M, 537–546.
JOHNSON, J. H., 1961—Limestone-building algae and algal limestones. *Colo. Sch. Mines.*
JOUBIN, L., 1912—Bancs et récifs de coraux (Madrepores). *Ann. Inst. Océanogr.*, 4(2).

KING, L. C., 1949—The cyclic land-surfaces of Australia. *Proc. Roy. Soc. Vic.*, 62, 79–95.
KINSMAN, D. J. J., 1964—The recent carbonate sediments near Halat el Bahrani, Trucial Coast, Persian Gulf, *in* DEVELOPMENTS IN SEDIMENTOLOGY. *Amsterdam, Elsevier*, 1, 185–192.
KOLDEWIJN, B. W., 1958—SEDIMENTS OF THE PARIA-TRINIDAD SHELF. *The Hague, Mouton.*
KORNICKER, L. S., and PURDY, E. G., 1957—A Bahamian faecal-pellet sediment. *J. sediment. Petrol.*, 27(2), 126–128.
KRUMBEIN, W. C., 1962—Open and closed number systems in stratigraphic mapping. *Bull. Amer. Ass. Petrol. Geol.*, 46(12), 2229–2245.
KRUMBEIN, W. C., and PETTIJOHN, F. J., 1938—MANUAL OF SEDIMENTARY PETROGRAPHY. *N.Y., Appleton-Century-Crofts.*
KRUMBEIN, W. C., and SLOSS, L. L., 1963—STRATIGRAPHY AND SEDIMENTATION. *San Francisco, Freeman.*
KUENEN, Ph. H., 1935—Geological interpretation of the bathymetric results, *in* THE SNELLIUS-EXPEDITION. *Reports*, 5(1).
KUENEN, Ph. H., and NEEB, G. A., 1943—Bottom samples, *in* THE SNELLIUS-EXPEDITION. *Reports*, 5(3).
LANGFORD-SMITH, T., and DURY, G. H., 1965—Distribution, character and attitude of the duricrust in the northwest of New South Wales and the adjacent areas of Queensland. *Amer. J. Sci.*, 263, 170–190.
LEMOINE, M., 1959—Un exemple de tectonique chaotique. *Rév. Géogr. phys. Géol. dynam.*, 2(4), 205–230.
LLOYD, A. R., 1967—Possible Miocene marine transgression in northern Australia. *Bur. Min. Resour. Aust. Bull.* 80 (in press).
LOWENSTAM, H. A., and EPSTEIN, S., 1957—On the origin of sedimentary aragonite needles of the Great Bahama Bank. *J. Geol.*, 65(4), 364–375.
LUDWICK, J. C., and WALTON, W. R., 1957—Shelf-edge, calcareous prominences in northeastern Gulf of Mexico. *Bull. Amer. Ass. Petrol. Geol.*, 41(9), 2054–2101.
MAYR, E., 1944—Timor and the colonization of Australia by birds. *Emu*, 44, 113–130.
MERRILL, A. S., EMERY, K. O., and RUBIN, M., 1965—Ancient oyster shells on the Atlantic continental shelf. *Science*, 147(3656), 398–400.
MOLENGRAAFF, G. A. F., 1922—Chapter 6, Geology, *in* DE ZEEËN VAN NEDERLANDSCH OOST INDIË. *Kon. Ned. Aardrijksk. Gen.*, 272–355.
MOORE, D. G., and SCRUTON, P. C., 1957—Minor internal structures of some recent unconsolidated sediments. *Bull. Amer. Ass. Petrol. Geol.*, 41(12), 2723–2751.
NEWELL, N. D., IMBRIE, J., PURDY, E. G., and THURBER, D. L., 1959—Organism communities and bottom facies, Great Bahama Bank. *Bull. Amer. Mus. nat. Hist.*, 117(4), 181–228.
NEWELL, N. D., PURDY, E. G., and IMBRIE, J. I., 1960—Bahamian oolitic sand. *J. Geol.*, 68(5), 481–497.
NEWELL, N. D., and RIGBY, J. N., 1957—Geological studies on the Great Bahama Bank, *in* REGIONAL ASPECTS OF CARBONATE DEPOSITION. *Spec. Publ. Soc. econ. Paleont. Miner.*, 5, 15–79.
NORTHCOTE, K. H., 1956—The solonized brown (mallee) soil group of southeastern Australia. *Int. Soil Sci. Cong.*, VI, *Rep.* F, 9–19.
NOTA, D. J. G., 1958—Sediments of the western Guiana Shelf. *Meded. Landbouwhogeschool Wageningen*, 58(2).
PARKER, F. L., 1962—Planktonic foraminiferal species in Pacific sediments. *Micropaleontology*, 8(2), 219–259.
PATERSON, S. J.—Geomorphology of the Ord-Victoria region. *Sci. ind. Res. Org. Melb., Land Res. Ser.* (in press).
PETTIJOHN, F. J., 1957—SEDIMENTARY ROCKS. *N.Y., Harper.*
PHLEGER, F. B., 1960—ECOLOGY AND DISTRIBUTION OF RECENT FORAMINIFERA. *Baltimore, Johns Hopkins Press.*
PHLEGER, F. B., PARKER, F. L., and PEIRSON, J. F., 1953—North-Atlantic Foraminifera. *Swedish Deep-Sea Exped. Reps.*, V, 7(1), 3–122.
PINSAK, A. P., 1958—A regional chemical and mineralogical study of surficial sediments in the Gulf of Mexico. *Ph.D. Dissertation, Indiana Univ.*
POTTER, P. E., and PRYOR, W. A., 1961—Dispersal centers of Paleozoic and later clastics of the upper Mississippi Valley and adjacent areas. *Bull. geol. Soc. Amer.*, 72(8), 1195–1250.
PRATT, W. L., 1963—Glauconite from the sea floor off Southern California, *in* ESSAYS IN MARINE GEOLOGY IN HONOR OF K. O. EMERY. *Los Angeles, Univ. S. Calif. Press.*, 97–119.
PURDY, E. G., 1961—Bahamian oolite shoals, *in* GEOMETRY OF SANDSTONE BODIES. *Spec. Publ. Amer. Ass. Petrol. Geol.*, 53–62.
PURDY, E. G., 1963—Recent calcium carbonate facies of the Great Bahama Banks. *J. Geol.*, 71(3), 334–355; (4), 472–497.
ROCHFORD, D. J., 1962—Hydrology of the Indian Ocean II. The surface waters of the southeast Indian Ocean and the Arafura Sea in spring and summer. *Aust. J. mar. freshw. Res.*, 13(3), 226–251.
ROCHFORD, D. J., 1963—Mixing trajectories of intermediate depth waters of the southeast Indian Ocean as determined by a salinity frequency method. *Ibid.*, 14(1), 1–23.

ROCHFORD, D. J., 1964a—Salinity maxima of the upper 1000 metres of the northern Indian Ocean. *Ibid.*, 15(1), 1–24.
ROCHFORD, D. J., 1964b—Hydrology of the Indian Ocean II. Water masses of the upper 500 metres of the southeast Indian Ocean. *Ibid.*, 15(1), 25–55.
RODGERS, J., 1950—The nomenclature and classification of sedimentary rocks. *Amer. J. Sci.*, 248, 297–311.
RODGERS, J., 1957—The distribution of marine carbonate sediments: a review, *in* REGIONAL ASPECTS OF CARBONATE SEDIMENTATION. *Spec. Publ. Soc. econ. Paleont. Miner.*, 5, 2–13.
ROYAL DUTCH METEOROLOGICAL INSTITUTE, 1949—Sea areas around Australia; oceanographic and meteorological data. *Publ.* 124.
RUSNAK, G. A., 1960—Sediments of Laguna Madre, Texas, *in* RECENT SEDIMENTS, NORTHWEST GULF OF MEXICO, ed. F. P. Shepard *et al. Spec. Publ., Amer. Ass. Petrol. Geol.*, 153–196.
RUSSELL, R. J., 1963—Recent recession of tropical cliffy coasts. *Science*, 139, 9–15.
RYTHER, J. H., 1963—Geographic variations in productivity, *in* THE SEA. *N.Y., Interscience*, 3, ch. 17, 347–380.
SCHOLL, D. W., 1963—Sedimentation in modern coastal swamps, southwestern Florida. *Bull. Amer. Ass. Petrol. Geol.*, 47(8), 1581–1603.
SEIBOLD, E., 1962—Untersuchungen zur Kalkfällung und Kalklösung am Westrand der Great Bahama Bank. *Sedimentology*, 1(1), 50–74.
SHEPARD, F. P., 1954—Nomenclature based on sand-silt-clay ratios. *J. sediment. Petrol.*, 24(3), 151–158.
SHEPARD, F. P., 1956—Marginal sediments of Mississippi delta. *Bull. Amer. Ass. Petrol. Geol.*, 40(11), 2537–2623.
SHEPARD, F. P., 1961—Sea level rise during the past 20,000 years. *Ann. Geomorph.*, 3, 30–35.
SHEPARD, F. P., 1963—SUBMARINE GEOLOGY. *N.Y., Harper & Rowe*, 2nd Ed.
SHEPARD, F. P., 1964—Sea level changes in the past 6,000 years: possible archeological significance. *Science*, 143(3606), 574–576.
SHEPARD, F. P., and Moore, D. G., 1955—Central Texas coast sedimentation: characteristics of sedimentary environment, recent history and diagenesis. *Bull. Amer. Ass. Petrol. Geol.*, 39(8), 1463–1593.
SHEPARD, F. P., and MOORE, D. G., 1960—Bays of central Texas coast, *in* RECENT SEDIMENTS, NORTHWEST GULF OF MEXICO, ed. Shepard, *et al. Spec. Publ., Amer. Ass. Petrol. Geol.*, 117–152.
SHEPARD, F. P., PHLEGER, F. B., and VAN ANDEL, Tj. H., 1960—RECENT SEDIMENTS, NORTHWEST GULF OF MEXICO. *Spec. Publ. Amer. Ass. Petrol. Geol.*
SILVA, H. L. E., 1956—Timor e a cultura do cafe. *Minist. Ultramar. Ser. Agronomia Tropical, Mem.* 1.
SOKAL, R. R., and MICHENER, C. D., 1958—A statistical method for evaluating systematic relationships. *Univ. Kansas Sci. Bull.*, 38(22), pt 2, 1409–1438.
STEWART, R. A., and Gorsline, D. S., 1962—Recent sedimentary history of St Joseph Bay, Florida. *Sedimentology*, 1(4), 256–286.
STEWART, G. A., TWIDALE, C. R., and BRADLEY, J., 1960—Geomorphology of the north Kimberley area, W.A., *in* THE LANDS AND PASTORAL RESOURCES OF THE NORTH KIMBERLEY AREA, ed. N. A. Speck. *Sci. ind. Res. Org., Melb., Land Res. Ser.*, 4.
SUGDEN, W., 1963a—Some aspects of sedimentation in the Persian Gulf. *J. sediment. Petrol.*, 33(2), 355–364.
SUGDEN, W., 1963b—The hydrology of the Persian Gulf and its significance in respect to evaporite deposition. *Amer. J. Sci.*, 261, 741–755.
TEICHERT, C., 1958—Australia and Gondwanaland. *Geol. Rdsch.*, 47(2), 562–590.
TEICHERT, C., and FAIRBRIDGE, R. W., 1948—Some coral reefs of the Sahul Shelf. *Geogr. Rev.*, 38(2), 222–249.
THORP, E. M., 1934—Preliminary remarks on the calcareous shallow marine deposits of Florida and the Bahamas. *J. sediment. Petrol.*, 4(3), 111–112.
THORP, E. M., 1955—Florida and Bahama marine calcareous deposits, *in* RECENT MARINE SEDIMENTS, ed. P. D. Trask. *Spec. Publ. Soc. econ. Paleont. Miner.*, 4,283–297.
TRANTER, D. J., 1962—Zooplankton distribution in Australasian waters. *Aust. J. mar. freshw. Res.*, 13(2), 106–142.
TRASK, P. D., 1953—Chemical studies of sediments of the western Gulf of Mexico, Part 2, *in* THE SEDIMENTS OF THE WESTERN GULF OF MEXICO. *Pap. phys. Oceanogr. Meteor., Mass. Inst. Tech. and Woods Hole Oceanogr. Inst.*, 12(4), 49–120.
TRASK, P. D., 1961—Sedimentation in a modern geosyncline off the arid coast of Peru and northern Chile. *Int. geol. Cong. 21st Sess., Norden*, 23, 103–118.
TRAVES, D. M., 1955—The geology of the Ord-Victoria Region, northern Australia. *Bur. Min. Resour. Aust. Bull.*, 27.
VAN ANDEL, Tj. H., 1960—Sources and dispersion of Holocene sediments, northern Gulf of Mexico, *in* RECENT SEDIMENTS, NORTHWEST GULF OF MEXICO, ed. F. P. Shepard *et al. Spec. Publ. Amer. Ass. Petrol. Geol.*, 34–55.
VAN ANDEL, Tj. H., 1964—Recent marine sediments of the Gulf of California, *in* MARINE GEOLOGY OF THE GULF OF CALIFORNIA, ed. Tj. H. van Andel and G. G. Shore, Jr. *Amer. Ass. Petrol Geol. Mem.* 3, 216–310.

VAN ANDEL, Tj. H., CURRAY, J. R., and VEEVERS, J. J., 1961—Recent carbonate sediments of the Sahul Shelf—Northwestern Australia. *Proc. 1st Nat. Coastal Shallow Water Res. Conf.*, 564–567.

VAN ANDEL, Tj. H., and POSTMA, H., 1954—Recent sediments of the Gulf of Paria. *Verh. Kon. Ned. Acad. Wetensch.*, 20(5).

VAN ANDEL, Tj. H., and SACHS, P. L., 1964—Sedimentation in the Gulf of Paria during the Holocene transgression; a subsurface acoustic reflection study. *J. marine Res.*, 22(1), 30–50.

VAN ANDEL, Tj. H., and SHOR, G. G., Jr, eds, 1964—MARINE GEOLOGY OF THE GULF OF CALIFORNIA. *Amer. Ass. Petrol. Geol. Mem.* 3.

VAN ANDEL, Tj. H., and VEEVERS, J. J., 1965—Submarine morphology of the Sahul Shelf, northwestern Australia. *Bull. geol. Soc. Amer.*, 76(6), 695–700.

VAN BEMMELEN, R. W., 1949—THE GEOLOGY OF INDONESIA. *The Hague, Govt Printing Office.*

VAN DER PLAS, L., and TOBI, A. C., 1965—A chart for judging the reliability of point counting results. *Amer. J. Sci.*, 263, 87–90.

VENING MEINESZ, F. A., UMBGROVE, J. H. F., and KUENEN, Ph. H., 1934—Gravity expeditions at sea, 1923–1932. *Pub. Neth. geod. Comm.*, 2. *Delft, Waltman.*

VERSTAPPEN, H. Th., 1959—Geomorphology and crustal movements of the Aru Islands in relation to the Pleistocene drainage of the Sahul Shelf. *Amer. J. Sci.*, 257, 491–502.

VISSER, W. A., and HERMES, J. J., 1962—Geological results of the exploration for oil in Netherlands New Guinea. *Verh. Kon. Ned. geol. mijnbouwk. Gen., geol. Ser.*, 20.

VON DER BORCH, C. C., 1965—Distribution of detrital minerals in Recent carbonate sediments from the Sahul Shelf, northern Australia. *J. geol. Soc. Aust.*, 12(2), 333–340.

WELLS, J. W., 1954a—Fossil corals from Bikini drill holes. *Prof. Pap. U.S. geol. Surv.* 260–P, 609 615.

WELLS, J. W., 1954b—Recent corals of the Marshall Islands. *Ibid.*, 260–I, 385–486.

WELLS, A. J., and ILLING, L. V., 1964—Present-day precipitation of calcium carbonate in the Persian Gulf, *in* DEVELOPMENTS IN SEDIMENTOLOGY. *Amsterdam, Elsevier.*, 429–435.

WILLIAMS, J. D., 1963—The petrology and petrography of sediments from the Sigsbee Blanket, Yucatan shelf, Mexico. *Texas A and M College, Dep. Oceanogr., Rep.* 63–12T.

WOOSTER, W. S., and REID, J. L., 1963—Eastern boundary currents, *in* THE SEA, ed. M. W. Hill, 2,253–280. *N.Y., Interscience.*

WRIGHT, R. L., 1963—Deep weathering and erosion surfaces in the Daly River Basin, Northern Territory. *J. geol. Soc. Aust.*, 10(1), 151–163.

WYRTKI, K., 1961—Physical oceanography of southeast Asian waters. *Naga Report* 2, *Scripps Instn Oceanogr., La Jolla, Calif.*

WYRTKI, K., 1962—The upwelling in the region between Java and Australia during the southeast monsoon. *Aust. J. mar. freshw. Res.*, 13(3), 217–225.

YEROSHCHEV-SHAK, V. A., 1961—Kaolinite in the sediments of the Atlantic Ocean. *Dokl. Akad. Nauk USSR*, 137(3), 695–697.

APPENDIX A.

STATION LOCATIONS AND SAMPLE DESCRIPTIONS, Timor Sea Study. Stations V–2 to V–163 were occupied in November–December, 1960, V–165 to V–377 in March, 1961

NOTES:

Depth: uncorrected echo-sounder readings; * no soundings, depth estimated from bathymetry.

Positions: indicated in degrees and minutes (to one-tenth of a minute).

Minor Relief: description of relief in immediate vicinity of station as shown on echo-sounding records.

sl.: slightly; mod.: moderately; irr.: irregular; irr., smooth, and wavy refer to local relief on scale of a few fathoms.

Sample Type: G: gravity core; D: dredge; S: snapper or grab sample; P: piston core.

Depth in Core: not corrected for core shortening; surf.: unknown thickness of surface sediment.

Colour: field comparison of wet core with Rock Color Chart, Geological Society of America. When not available: colour of wet core after opening in laboratory is shown in parentheses.

5Y 3/2	olive-grey	5GY 3/2	greyish olive-green	10Y 6/2	light greenish yellow
5Y 4/4	moderate olive-brown	5GY 4/2	dusky yellow-green	10GY 5/2	greyish yellow-green
5Y 5/2	light olive-grey	5GY 5/2	dusky yellow-green	5YR 5/2	pale brown
5Y 5/4	light olive-brown	5GY 6/1	greenish grey	5YR 6/2	very light brown
5Y 5/6	light olive-brown	5GY 6/2	greenish grey	10YR 4/2	dark yellowish brown
5Y 6/2	olive-grey	5GY 7/2	greyish yellow-green	10YR 5/2	yellowish brown
5Y 6/4	dusky yellow	10Y 4/2	greyish olive	10YR 6/2	pale yellowish brown
5Y 7/2	yellowish grey	10Y 5/2	pale greyish olive	10YR 6/6	dark yellowish orange
5Y 7/6	moderate yellow	10Y 5/4	light olive		

Structure and Lithology: structure from core descriptions; not available for dredge and grab samples.

Terminology after Moore and Scruton (1958).

homog.: homogeneous; irr.: irregularly; reg.: regularly; dist.: distinctly; indist.: indistinctly.

Textural terminology after Shepard (1954) when based on mechanical analysis (*italics*); otherwise based on approximate macroscopic description.

sl.: slightly; sh.: shelly; sd.: sandy; st.: silty; cl.: clayey.

For data on composition see Appendices C, D, E.

For dredge hauls lithology of undisturbed pipe dredge sample given as above, of washed main dredge sample capitalized.

Station Number (V–)	S. Lat.	E. Long.	Water Depth (fms)	Minor Bottom Relief	Sample Type	Depth in Core (cm)	Colour	Structure and Lithology
2	12–20·3	130–41·0	11	smooth, level	G	0–23	(5GY 5/2)	homog. *sl. sh. sand*
						23–47		irr. lay. *sl. sh. sand*
3	12–16·0	130–33·7	15	smooth, level	G	0–42	(5GY 5/2)	irr. lay. *sl. sh. clayey sand*
4	12–12·0	130–25·6	26	bottom small channel	G	0–28	(5GY 5/2)	irr. lay. *sh. clayey sand*
5	12–7·9	130–18·0	22	sl. wavy, level	G	0–19	(5GY 5/2)	homog. *s. shell*
6	12–4·0	130–10·2	29	sl. wavy, level	G	0–10		homog. *sh. clayey sand*
						10–15		homog. stiff clay
7	11–59·8	130–2·0	34	mod. irr., rise	G	0–9	(5GY 5/2)	homog. *sh. clayey sand*
						9–21	(5GY 7/2)	homog. *sh. clayey sand*; rare sand mottles
8	11–55·2	129–55·3	42	mod. irr.; level	G	0–28		homog. *cl. sand*; one sand mottle
9	11–49·0	129–50·2	32	mod. irr., on bank top	G	0–12	(5GY 5/2)	homog. *sh. sand*
						12–15		skeletal debris
10	11–43·0	129–46·5	26	smooth, level	G	0–4		homog. *sh. sand*
11	11–35·8	129–43·0	25	smooth, gentle slope	G	0–9	(5GY 5/2)	homog. *sh. sand*
12	11–30·0	129–38·0	29	mod. irr., level	G	0–36	(5GY 5/2)	irr. layered *sh. cl. sand*
13	11–24·6	129–33·0	41	irr. bank slope	G	0–8		*sh. sand*
14	11–17·4	129–28·0	31	smooth, level	G	0–32		homog. *sh. sand*
15	11–10·3	129–23·6	35	sl. wavy, between banks	G	0–10		homog. *sh. sand-silt-clay*
						10–27		indist. mottled, *sh. sand-silt-clay*
						27–50		dist. mottled *s. mud*
16	11–4·0	129–18·7	37	level, near bank	G	0–65		homog. sand-silt-clay; two thin sand layers
17	10–55·9	129–12·8	17	flat bank top	D	surf.		skeletal debris
18	10–48·6	129–7·7	18	flat bank top	G			no sample
19	10–41·0	129–2·5	33	small channel near bank	G	0–32	(5GY 5/2)	homog. *sh. st. sand*
20	10–34·2	128–56·5	23	flat bank top	G	surf.		skeletal debris
21	10–28·1	128–51·4	34	smooth low rise	G	0–21	(5GY 5/2)	homog. *sh. st. sand*
22	10–21·0	128–46·0	40	smooth, level	G	0–17	(5GY 5/2)	irr. layered *sh. st. sand*
23	10–14·5	128–41·0	31	sl. irr., level near canyon edge	GS	surf.		skeletal debris
24	10–6·0	128–35·0	65	wavy, level	G	0–27		homog. *sl. sh. sd. silt*
25	9–59·0	128–29·0	40	smooth, level	G	0–23	(5GY 5/2)	homog. *sh. st. sand*
26	9–52·3	128–25·0	47	wavy, level	G	0–45	(5Y 6/4)	homog. *sd. silt*
27	9–46·0	128–20·0	48	smooth, level	G	0–37	(5Y 5/2)	homog. *sl. sh. sd. silt*
28	9–38·5	128–16·0	50	smooth, level	G	0–47	(5Y 5/2)	homog. *sl. sh. st. sand*
29	9–31·5	128–10·5	113	smooth, gentle slope beyond shelf edge	G	0–10	(5Y 5/6)	homog. *sl. sh. sand*

APPENDIX A—*continued*

Station Number (V–)	S. Lat.	E. Long.	Water Depth (fms)	Minor Bottom Relief	Sample Type	Depth in Core (cm)	Colour	Structure and Lithology
						10–16	(5Y 5/6)	irr. layered *sl. sh. sand*
						16–50	(5Y 5/6)	mud with sand mottles
30	11–18·4	124–28·7	136	flat bank top				no sample
31	11–20·4	124–30·8	132	smooth, gentle slope				no sample
32	11–27·5	124–38·4	18	flat bank top	S	surf.		skeletal debris
33	11–31·0	124–41·3	143	irr. gentle slope	G	0–18	(5GY 5/2)	irr. layered *silt*
34	11–44·0	124–56·0	148	smooth gentle slope	G	0–7	(5GY 7/2)	homog. *st. sand*
35	11–47·0	125–0·5	170	smooth gentle slope				no sample
36	11–51·0	125–6·5	59	smooth gentle slope	G	0–54	(5GY 5/2)	irr. layered *sl. sh. sd. silt*
37	11–56·8	125–14·5	57	smooth, level	G	0–30	(5GY 5/2)	homog. *sl. sh. st. sand*
38	12–2·2	125–22·0	52	smooth, level	G	0–60		muddy sand
39	12–7·0	125–28·5	48	sl. irr., minor rise	G	0–42	(5GY 5/2)	irr. layered *sh. st. sand*
40	12–12·2	125–34·5	48	sl. irr., minor rise	G	0–49	(5GY 5/2)	reg. layered *sl. sh. st. sand*
41	12–18·0	125–40·8	40	smooth, level	G	0–32	(5GY 5/2)	irr. layered *sl. sh. st. sand*
42	12–22·0	125–48·5	42	sl. irr., level	G	0–28		irr. layered *sh. st. sand*
43	12–26·0	125–55·9	40	smooth, level	G	0–26		irr. layered *sh. cl. sand*
44	12–30·5	126–4·5	43	wavy, level, near edge of gully	G	0–41	(5GY 5/2)	indist. mottled *sh. cl. sand*
45	12–36·0	126–10·2	46	smooth, level	G	0–22		homog. *sh. cl. sand*
46	12–41·9	126–13·4	38	smooth, level	G	0–20		homog. *sh. sand*
47	12–46·5	126–18·9	35	smooth, between banks	G	0–41		indist. mottled *sh. cl. sand*
48	12–59·0	126–24·8	40	smooth, level	G	0–14		homog. *sh. cl. sand*
49	13–3·2	126–33·2	40*		G	0–16		homog. *sh. cl. sand*
						16–20		skeletal debris
50	13–7·7	126–39·5	41	smooth, level	G	0–13		irr. layered *sh. cl. sand*
						13–19		skeletal debris
51	13–11·4	126–46·0	43	smooth, level	G	0–31		homog. *sh. cl. sand*
52	13–16·5	126–52·6	45	sl. irr., level	S	surf.		sandy shell
53	13–21·0	127–0·0	47	shallow, smooth depression	G	0–27		homog. *sh. cl. sand*
						27–55		dist. mottled (sand) mud
54	13–15·5	127–14·4	50*		G	0–31		indist. mottled *sh. cl. sand*
						31–38		homog. stiff white clay
55	13–9·5	127–29·6	40*		G	0–11		irr. layered *sh. cl. sand*
						11–23		mud with white clay mottles
56	13–4·9	127–46·0	36	smooth, level	G	0–67		homog. *st. clay*
57	13–1·3	128–3·1	52	smooth, level	G	0–12		irr. layered *sh. cl. sand*
						12–47		irr. layered mud, sand layers
58	12–57·7	128–19·8	51	smooth, level	G	0–27		homog. *sl. sh. cl. sand*

59	12–54·1	128–36·6	48	smooth, level	G	0–24		homog. *sh. cl. sand*
60	12–50·0	128–52·8	45	smooth, level	G	0–23		homog. *sh. sand*
61	12–45·4	129–9·6	38	smooth, level	G	0–22		indist. mottled *sl. sh. sand*
62	12–41·0	129–25·8	34	smooth, level	G	0–20	(5Y 5/2)	homog. *sh. sand*
						20–27	(5Y 6/4)	homog: firm mud
63	12–36·8	129–42·4	27	smooth, level	G	0–7	(5Y 5/2)	homog. *sh. sand*
64	12–32·1	129–58·6	19	sl. wavy, level	G	0–15	(5Y 5/2)	homog. *sh. sand*
65	12–28·0	130–15·3	12	smooth, level	G	0–23		irr. layered *sl. sh. sand*
66	12–18·1	130–28·5	15	smooth, level	G	0–35		irr. layered *sh. sand*
67	13–2·1	129–52·4	14	smooth, level				no sample
68	12–56·0	129–46·0	19	smooth, level	G	0–1		*sh. sand*
69	12–51·5	129–41·0	24	smooth, level	G	0–10		*sh. sand*
70	12–45·0	129–35·0	27	smooth, level	G	0–26	(5GY 5/2)	homog. *sh. sand*
71	12–39·0	129–28·3	29	smooth, level	G	0–25		irr. layered *sl. sh. sand*
						25–26		sand layer
						27–31		homog. mud
72	12–34·0	129–23·3	33	smooth, level	G	0–28		homog. *sl. sh. cl. sand*
						28–35		homog. sandy mud
73	12–28·0	129–17·0	33	sl. irr., level	G	0–17		homog. *sh. cl. sand*
						17–28		reg. layered mud and muddy sand
						28–58		irr. layered mud and shell
74	12–22·0	129–12·0	39	wavy	G	0–51		irr. layered *sl. sh. cl. sand*
75	12–16·6	129–6·3	41	smooth, level	G	0–10		*sl. sh. sand-silt-clay*
						10–20		*sh. sand*
						20–28		*sl. sh. sand-silt-clay*
76	12–10·6	129–1·0	41	smooth, level	G	0–41	(5GY 5/2)	indist. mottled *sl. sh. cl. sand*
77	12–5·5	128–56·5	42	smooth, level	G	0–41		homog. *sl. sh. cl. sand*
78	11–59·0	128–50·0	41	smooth, level	G	0–21	(5GY 5/2)	homog. *sh. cl. sand*
79	11–53·8	128–45·5	38	smooth, low slope	G	0–23		irr. layered *sl. sh. cl. sand*
80	11–47·0	128–39·5	38	smooth, level	G	0–55		dist. mottled, irr. layered *sl. sh. cl. sand*
81	11–41·3	128–34·5	38	smooth, level	G	0–60		homog. *sl. sh. sand-silt-clay*
82	11–35·8	128–29·5	30*		G	surf.		*sl. sh. cl. sand*
83	11–28·5	128–24·0	20*		S	surf.		*sd. shell*
84	11–22·8	128–20·0	30*		G	0–1		*sd. shell*
85	11–15·5	128–15·8	40*		G	0–19		irr. layered *sand*
						19–57		irr. layered and mottled sandy mud
86	11–10·0	128–10·0	50*		G	0–64		homog. *sd. clay*, 2 sand layers
87	11–3·5	128–6·0	60*		G	0–65		homog. *st. clay*, 2 thin layers and few sand mottles
88	10–57·0	128–1·7	70*		G	0–66	(5GY 5/2)	homog. *cl. silt*
89	10–51·0	127–56·6	60*		G	0–19	(5GY 5/2)	homog. *sh. cl. sand*
90	10–44·0	127–52·1	50*		G	0–38	(5GY 5/2)	dist. mottled *sh. sand-silt-clay*
91	10–38·1	127–47·1	40*		G	0–33		homog. *sh. st. sand*
92	10–31·8	127–41·6	40*		G	0–24		homog. *sh. st. sand*

APPENDIX A—*continued*

Station Number (V–)	S. Lat.	E. Long.	Water Depth (fms)	Minor Bottom Relief	Sample Type	Depth in Core (cm)	Colour	Structure and Lithology
93	10–26·1	127–37·0	40*		G	0–17	(5GY 5/2)	homog. *sh. st. sand*
94	10–19·9	127–31·4	40*		G	0–52	(5Y 5/6)	irr. layered *sh. st. sand*
95	10–13·1	127–26·0	50*		G	surf.		*sd. shell*
96	10–33·8	126–48·5	54	sl. irr., level	G	0–10	(5Y 5/4)	homog. *sl. sh. st. sand*
						10–20	(5Y 5/2)	irr. layered muddy sand
						20–39	(5Y 5/2)	dist. mottled sandy mud
97	10–41·0	126–54·6	45	wavy, very gentle slope	G	0–52	(5Y 5/2)	irr. layered *sl. sh. sd. silt*
98	10–46·5	126–59·8	72	rough, edge of canyon	G	0–31		homog. *sh. st. sand*
99	10–51·7	127–4·8	47	shallow cuts/terraces	G	0–48		indist. mottled *sl. sh. sand-silt-clay*
100	10–57·0	127–9·6	48	slope of minor rise near banks	G	0–45		homog. *sh. cl. sand*
101	11–2·1	127–14·2	43	smooth, level, near banks	G	0–57		irr. layered *sh. cl. sand*
102	11–7·1	127–19·3	52	smooth, level, near banks	G	0–62		homog. *sl. sh. st. clay*
103	11–12·4	127–24·0	56	smooth, level, near banks	G	0–62		mottled and irr. layered *st. clay*
104	11–11·7	127–29·0	62	smooth, level, near banks	G	0–60		dist. mottled *sh. cl. sand*
105	11–23·0	127–33·7	64	smooth, level, near banks	G	0–65		homog. *st. clay*
106	11–28·3	127–38·5	65	smooth, level, near ridge	G	0–65		homog. *sl. sh. st. clay*
107	11–33·0	127–42·7	70	smooth, level, near ridge	G	0–65		indist. mottled *st. clay*
108	11–38·5	127–46·0	58	flat bank top	G	0–13	(5Y 5/2)	homog. *sh. sd. clay*
109	11–45·0	127–52·0	72	bank of gully, terraced	G	0–36		dist. mottled *sh. cl. sand*
						36–49		dist. mottled sandy mud
110	11–48·0	127–59·3	73	smooth, gentle slope	G	0–54		dist. mottled *sh. sd. clay*
111	11–52·9	128–4·5	63	smooth, gentle slope	G	0–11		homog. *sh. sd. clay*
						11–37		homog. sandy mud
112	11–56·5	128–9·5	58	smooth, gentle slope	G	0–37		dist. mottled *sh. cl. sand*
113	12–4·0	128–18·7	48	smooth, gentle slope	G	0–43		dist. mottled *sh. cl. sand*
114	12–7·9	128–23·4	55	smooth, level	G	0–40		homog. *sh. sand-silt-clay*
115	12–12·5	128–28·0	37	flat bank top	G	0–45		homog. *sh. sand-silt-clay*
116	12–19·5	128–34·5	54	smooth, level	G	0–34		dist. mottled *sh. sd. clay*
						34–38		homog. shelly mud
117	12–27·0	128–42·6	52	smooth, level	G	0–38	(10Y 4/2)	irr. layered *sl. cl. sand*
						38–56	(5Y 5/2)	dist. mottled mud
118	12–34·4	128–45·5	50	smooth, level	G	0–29	(5GY 5/2)	homog. *sh. cl. sand*
119	12–40·8	128–50·4	47	smooth, level	G	0–14	(5GY 5/2)	homog. *sh. cl. sand*
120	12–46·9	128–55·6	46	smooth, level	G	0–31	(5Y 5/2)	homog. *sh. sand*
121	12–52·5	129–1·2	44	smooth, level	G	0–11		*sd. shell*
122	12–58·3	129–7·0	39	smooth, level	G	0–5		*sd. shell*
123	13–4·2	129–12·0	36	smooth, level	G	surf.		*sd. shell*

124	13–9·9	129–17·2	35	sl. wavy	G	0–14	(5Y 5/2)	homog. *sl. sh. sand*
125	13–15·2	129–22·5	32	sl. wavy	G	0–28	(5GY 5/2)	homog. *sh. sand*
126	13–21·0	129–27·8	28	smooth, level	G	0–10		homog. *sh. sand-silt-clay*
127	13–26·7	129–33·0	22	smooth, level	G	0–20	(5Y 5/2)	homog. *sh. sand*
128	14–7·8	128–55·8	17	smooth, level	G	0–24		dist. mottled *sh. st. sand*
						24–39		irr. layered shelly sandy mud
129	14–3·4	128–49·0	17	smooth, level	G	0–3	(5Y 6/4)	homog. *sh. st. sand*
						3–12	(5Y 5/2)	dist. mottled shelly sandy mud
130	13–58·1	128–43·0	22	smooth, level	G	0–56	(5Y 5/6)	irr. layered *sh. st. sand*
131	13–52·9	128–36·9	27	smooth, level	G	0–54	(5Y 5/2)	irr. layered *st. sand*
132	13–47·4	128–30·6	31	smooth, level	G	0–57		dist. mottled *sl. sh. st. sand*
133	13–42·0	128–24·3	34	smooth, level	G	0–55	(5Y 5/2)	dist. mottled *sl. sh. st. sand* few sand layers
134	13–36·5	128–18·0	37	smooth, level	G	0–33	(5Y 5/2)	irr. layered *sl. sh. st. sand*
						33–37	(5Y 5/6)	irr. layered shelly muddy sand
						37–41	(5GY 5/2)	firm, irr. layered shelly muddy sand
135	13–31·0	128–12·2	37	smooth, level	G	0–55	(5Y 5/2)	irr. layered *sl. sh. cl. sand*
136	13–25·7	128–6·8	39	smooth, level	G	0–40	(5Y 5/2)	irr. layered *sl. sh. sand-silt-clay*
						40–53	(5Y 5/6)	dist. mottled muddy sand
137	13–20·5	128–0·9	41	smooth, level	G	0–35		irr. layered and mottled *sh. st. sand*
						35–38		homog. hard sandy mud
138	13–15·2	127–55·1	42	flat bank top	G	0–30		irr. layered or mottled *sh. sand-silt-clay*
						30–35		hard sandy mud, homog.
139	13–10·0	127–49·5	45	smooth, level	G	0–29	(5Y 5/2)	irr. layered or mottled *sh. sand-silt-clay*
						29–33	(5Y 6/4)	hard sandy mud, homog.
140	13–4·9	127–44·0	46	smooth, level	G	0–50		indist. mottled (sh. sand) *sh. sd. clay*
141	12–59·7	127–38·5	42	broad, smooth, rise	G	0–63	(5Y 6/4)	dist. mottled (sh. muddy sand) *sl. sh. sand-silt-clay*
142	12–54·5	127–33·0	35	very irr., level	G	0–57		irr. layered (shelly sand) *sl. sh. sand-silt-clay*
143	12–49·3	127–27·4	33	smooth, level	G	0–66		homog. *st. clay*, shell layers
144	12–44·0	127–23·0	30*		G	0–65		homog. *st. clay*, shell layers
145	12–39·9	127–19·0	40*		G	0–67		homog. *st. clay*
146	12–36·0	127–14·2	40*		G	0–10	(5Y 5/2)	homog. *sh. sd. clay*
147	12–31·1	127–10·3	40*		G	0–16	(5GY 5/2)	homog. *sh. sand-silt-clay*
						16–48	(5GY 5/2)	homog. shelly mud
148	12–27·2	127–6·0	40*		G	0–41	(5GY 5/2)	homog. *sl. sh. cl. sand*
						41–66	(5GY 3/2)	irr. layered shelly sandy mud
149	12–22·0	127–2·0	35	sl. irr., level	G	0–62	(5GY 5/2)	homog. *sh. sand-silt-clay*
150	12–19·0	126–59·0	43	irr., at edge gully	G	0–9		homog. *st. clay*
151	12–13·0	126–51·4	56	sl. wavy, level	G	0–5	(5GY 5/2)	homog. *sl. sh. cl. sand*
						5–55	(5GY 3/2)	irr. layered shelly sandy mud
152	12–5·7	126–46·5	54	sl. wavy, bottom steep slope	G	0–58	(5GY 5/2)	indist. mottled *sl. sh. cl. sand*
153	11–59·6	126–37·2	53	smooth, level	G	0–14	(5GY 5/2)	indist. mottled *sand-silt-clay*
						14–62	(5GY 5/2)	homog. shelly mud
154	11–52·5	126–31·0	54	smooth, level	G	0–61	(5GY 5/2)	homog. *sl. sh. cl. sand*

APPENDIX A—*continued*

Station Number (V–)	S. Lat.	E. Long.	Water Depth (fms)	Minor Bottom Relief	Sample Type	Depth in Core (cm)	Colour	Structure and Lithology
155	11–47·0	126–23·6	50	smooth, level	G	0–48	(5GY 5/2)	homog. *sl. sh. cl. sand*
156	11–41·8	126–18·3	50*		G	0–9	(5GY 5/2)	homog. *sh. sand*
157	11–36·8	126–12·5	40*		G	0–49	(5GY 5/2)	homog. *sl. sh. st. sand*
158	11–32·0	126–7·1	40*		G	0–9	(5GY 5/2)	homog. shelly muddy sand
159	11–26·5	126–1·4	50*		G	0–55	(5GY 5/2)	homog. *sh. sand-silt-clay*
160	11–21·5	125–55·5	50*		G	0–65	(5Y 5/2)	homog. *cl. silt*
161	11–16·0	125–49·7	50*		G	0–59	(5GY 5/2)	indist. mottled *sl. sh. sd. silt*
162	11–11·1	125–44·1	60*		G	0–32	(5GY 5/2)	irr. layered *sl. sh. sand*
163	11–6·0	125–38·8	80*		G	0–13	(5GY 5/2)	homog. *sh. sand*
164	15–4·1	128–4·2			S	surf.		Ord River silt
165	12–11·5	130–16·6	18	smooth, level	G	surf.	10Y 4/2	*cl. sd. shell*
166	12–13·0	130–6·0	20	smooth, level	G	0–21	10Y 5/2	homog. *sh. sand*
167	12–14·6	129–55·4	23	smooth, level	G	0–21	5Y 5/2	homog. *sh. sand*
168	12–16·0	129–44·9	26	smooth, level	G	0–29	5Y 5/2	homog. *sh. sand*
169	12–17·0	129–34·5	17	smooth, level	G	0–5	5Y 5/2	*sh. sand*
170	12–18·7	129–24·0	37	smooth, level	G	0–39	5Y 5/2	homog. *sl. sh. sand*
171	12–16·8	129–13·7	17	flat bank top	D	surf.		MISCELL. LIVE MATERIAL
172	12–14·5	129–3·5	43	wavy, level	G	0–52	(5Y 5/2)	homog. *sl. sh. sand*
173	12–12·5	128–52·9	43	wavy, level	G	0–16	(5GY 5/2)	homog. *sh. sand*
174	12–8·0	128–43·6	50	level, below bank	G	0–64	10Y 4/2	homog. *sh. st. sand*
175	12–6·0	128–33·6	37	flat bank top	G	0–48		homog. *sh. cl. sand*
176	12–4·3	128–23·5	47	smooth, level	G	0–49		homog. *sh. cl. sand*
177	12–2·1	128–13·0	59	smooth, level	G	0–24		homog. *sh. cl. sand*
178	12–2·5	128–3·0	62	wavy, level, near bank	G	0–57	10Y 4/2	homog. *sh. cl. sand*
179	12–10·9	128–8·4	59	smooth, level	G	0–44	10Y 4/2	homog. *sh. cl. sand*
180	12–19·6	128–14·0	57	smooth, level	G	0–44	5GY 5/2	homog. *sh. sd. clay*
181	12–28·4	128–19·3	54	smooth, level	G	0–63	5GY 5/2	homog. *sh. cl. sand*
182	12–37·1	128–24·6	53	smooth, level	G	0–58	5GY 5/2	homog. *sh. cl. sand*
183	12–45·8	128–30·1	53	smooth, level	G	0–36	5GY 5/2	homog. *sh. cl. sand*
184	12–54·1	128–35·5	48	smooth, level	G	0–30	10GY 5/2	homog. *sh. sand*
185	13–2·5	128–40·7	38	smooth, level	G	0–18	5GY 5/2	homog. *sh. sand*
186	13–10·0	128–47·7	43	smooth, level	G	0–23	5GY 5/2	homog. *sh. sand*
187	13–16·7	128–54·1	40	irr., dissected slope	G	0–13	5GY 5/2	homog. *sh. sand*
188	13–23·5	129–1·0	34	smooth, level	G	0–26	5Y 5/2	homog. *sh. sand*
189	13–30·7	129–8·1	28	smooth, level	G	0–38	5Y 5/2	homog. *sh. st. sand*
190	13–40·0	129–10·5	17	smooth, level	G	0–25	5Y 5/2	homog. *sh. sand*
191	13–49·2	129–13·4	15	small, smooth rise	G	0–6	5YR 5/2	homog. *sh. sand*

						6–12	5Y 5/2	homog. shelly mud
192	13–53·9	129–14·0	13	small triang. ridge	D	surf.		*sd. st. cl. shell*; ROCKS; SKELETAL DEBRIS
193	13–59·0	129–15·6	15	wavy, sl. irr., level	D	surf.		coarse sand; ROCKS; SKELETAL DEBRIS
194	14–6·3	129–17·6	12	smooth, level	S	surf.		*sh. sand*
195	14–8·0	129–6·6	15	smooth, level	G	0–6	5YR 6/4	homog. *sh. sand*
						6–11	10YR 6/6	homog. muddy sand
						11–18	10YR 6/6	homog. sandy mud
196	14–9·5	128–55·3	15	smooth, level, near gully system	G	0–22		homog. *sh. cl. sand*
197	14–10·9	128–44·8	15	smooth, level	S	surf.		*sh. st. sand*
198	14–12·6	128–34·6	18	smooth, level	G	0–37		homog. *sh. st. sand*
199	14–13·6	128–22·1	20	smooth, level	S	surf.		*sl. sh. sand*
200	14–15·5	128–13·5	18	on smooth rise	G	0–21	10Y 4/2	homog. *sl. sh. cl. sand*
201	14–10·6	128–5·4	23	smooth, level	G	0–56	5Y 5/2	homog. *sl. sh. cl. sand*
202	14–5·1	127–56·7	28	smooth, level	G	0–48	5Y 5/2	homog. *sl. sh. cl. sand*
203	13–59·5	127–49·3	33	sl. irr., level	G	0–41	5Y 5/2	homog. *sh. cl. sand*
204	13–54·0	127–40·8	33	smooth, level	G	0–17	5Y 5/2	homog. *sh. cl. sand*
						17–27	5Y 5/2	homog. sandy mud
						27–30	5Y 7/2	homog. shelly mud
205	13–49·6	127–34·3	41	smooth, level near small rise	G	0–24	10YR 4/2	homog. *sh. cl. sand*
						24–43	5GY 5/2	homog. shelly mud
206	13–43·6	127–25·6	43	on minor rise	G	0–5	10YR 4/2	homog. *sh. sand*
						5–45	5GY 4/2	homog. sandy mud
207	13–36·5	127–18·3	47	wavy, level	G	0–14	5Y 5/2	homog. *shell*
						14–59	5GY 5/2	homog. shelly mud
208	13–29·3	127–10·9	50	wavy, irr. between gullies	G	0–5	10YR 5/2	homog. *sh. sand-silt-clay*
						5–65	5GY 6/1	homog. mud
209	13–24·5	127–6·1	44	smooth, level, near steep valley	D	0–45		homog. *sh. sand*
210	13–18·0	126–51·2	45	very irr.	S	surf.	5Y 4/2	rocks; skeletal debris; *sh. sand*
211	13–8·0	126–29·6	41	wavy, level	G	0–5	10Y 5/2	*sl. sh. cl. sand*
212	13–3·9	126–20·0	39	irr., level	G	0–5	5Y 5/2	*sh. cl. sand*
213	12–59·8	126–11·6	45	irr., level	G	0–45	5Y 5/2	homog. *sh. cl. sand*
214	12–55·4	126–1·4	35	smooth, level	G	0–35	(5GY 5/2)	homog. *sh. sand*
215	12–51·0	125–51·7	42	smooth, level	G	0–22	(5GY 5/2)	homog. *sh. sand*
216	12–46·7	125–42·1	49	smooth, level, near rise	G	0–36	(5GY 5/2)	homog. *sl. sh. sand*
217	12–42·0	125–32·8	49	wavy, base of bank	G	0–37	(5Y 5/2)	homog. *sl. sh. cl. sand*
218	12–37·6	125–21·2	52	wavy, level	G	0–48	(5GY 5/2)	homog. *sh. sand*
219	12–33·0	125–14·3	47	flat bank top	D	surf.		*sl. sh. st. sand*; SKELETAL DEBRIS
220	12–30·0	125–4·3	50	smooth, level	G	0–47	5GY 5/2	homog. *sh. st. sand*
221	12–25·7	124–53·5	51	smooth, level	G	0–39	5GY 5/2	homog. *sh. st. sand*
222	12–22·0	124–44·0	56	smooth, level	G	0–41	5GY 5/2	homog. *sl. sh. st. sand*
223	12–18·0	124–33·3	51	smooth, level	G	0–39	5GY 5/2	homog. *sl. sh. st. sand*
224	12–14·0	124–23·0	52	smooth, level	G	0–10	5GY 5/2	*st. sand*

APPENDIX A—*continued*

Station Number (V–)	S. Lat.	E. Long.	Water Depth (fms)	Minor Bottom Relief	Sample Type	Depth in Core (cm)	Colour	Structure and Lithology
225	12–9·7	124–14·5	52	smooth, level	G	0–10	5GY 5/2	homog. *sh. st. sand*
226	12–3·9	124–3·1	56	smooth, low slope	D	surf.	5Y 7/2	*sh. sand*
227	11–59·2	123–53·3	51	smooth, level on broad rise	S	surf.	5Y 6/2	*sand*
228	11–55·5	123–47·1	80	shelf edge terrace	D	surf.	5GY 5/2	*sh. sand*
229	11–56·0	123–47·0	72	flat bank top	D	surf.		SKELETAL DEBRIS
230	11–54·0	123–39·5	97	smooth, level	D	surf.	10YR 6/2	*sl. sh. sand*; SKELETAL DEBRIS
231	11–48·2	123–27·0	21	flat bank top	D	surf.		*sd. shell*; SKELETAL DEBRIS
232	11–39·9	123–20·0	105	rough pinnacles	D	surf.		ROCKS; SKELETAL DEBRIS
233	11–32·6	123–14·5	390	smooth, moderate slope	G	0–46	(5GY 5/2)	irr. layered (muddy sand) sand-silt-clay
234	11–24·8	123–7·5	594	smooth, moderate slope	G	0–56	(5Y 5/2)	homog. *st. clay*
235	11–16·5	123–1·0	980	steep, rough slope	G			no sample
236	11–9·0	122–54·1	488	steep, rough slope	G	0–34	(5GY 5/2)	homog. *sand-silt-clay*; shell layer
237	11–4·0	122–54·0	90	steep, rough slope	D	surf.		sand
238	11–30·0	124–0·5	218	smooth, gentle slope	G	0–33	5GY 6/2	homog. *cl. silt*
239	11–39·6	124–21·0	13	flat bank top	D	surf.		SKELETAL DEBRIS
240	11–45·7	124–53·4	63	smooth, level	S	surf.	5Y 6/2	*sand*
241	11–49·7	124–48·5	70	on smooth, level terrace	D	surf.		sand; SKELETAL DEBRIS
242	11–49·0	124–47·5	81	smooth, level, below slope to 241	D	surf.		SKELETAL DEBRIS
243	11–38·8	124–36·8	12	flat bank top	D	surf.		LIVE CORAL AND ALGAE
244	11–20·2	124–13·2	321	smooth, moderate slope	G	0–52	(5Y 5/2)	homog. *st. clay*
245	11–29·9	124–39·9	105	smooth, on broad, low rise	D	surf.		ROCK; SKELETAL DEBRIS
246	11–30·0	124–59·2	233	smooth, gentle slope	G	0–39	5GY 7/2	homog. *sand-silt-clay*
247	11–30·0	125–20·5	56	on surface of shelf edge terrace	D	surf.		SKELETAL DEBRIS
248	11–22·3	125–14·0	140	smooth, gentle slope below flat top bank	G	0–13	5GY 6/2	homog. *st. sand*
249	11–14·3	125–7·3	238	smooth, gentle slope	G	0–62	5GY 5/2	homog. sand-silt-clay
250	11–6·7	125–0·5	275	smooth, gentle slope	G	0–57	5GY 5/2	homog. *st. clay*
251	10–59·2	124–53·6	306	smooth, gentle slope	G	0–54	5Y 5/2	homog. *st. clay*
252	10–51·5	124–46·2	446	smooth, moderate slope	G	0–2	10YR 5/2	homog. oxidized mud
						2–45	5Y 5/2	homog. *st. clay*
253	10–44·5	124–35·2	707	smooth, moderate slope	G	0–2	10YR 5/2	homog. oxidized mud
						2–47	5Y 5/2	homog. *st. clay*
254	10–40·2	124–24·4	1030	smooth, moderate slope	G	0–2	10YR 5/2	homog. oxidized mud
						2–57	5Y 5/2	homog. *st. clay*
255	10–32·6	124–17·3	980	steep, rough slope with pin-pinnacles	G	0–2	10YR 5/2	homog. oxidized mud

						2–63	5Y 5/2	homog. *st. clay*
256	10–26·5	124–9·6	390	rough, level	G	0–2	5YR 4/4	homog. oxidized mud
						2–50	5Y 5/2	homog. st. clay
257	10–19·0	124–2·5	230	steep slope below large peak	G	0–2	5YR 4/4	homog. oxidized mud
						2–57	5Y 5/2	homog. *st. clay*
258	10–53·5	125–19·5	296	smooth, gentle slope	G	0–58	10Y 5/2	homog. *st. clay*, oxidized top
259	10–57·4	125–28·0	204	smooth, gentle slope	G	0–62	10Y 5/2	homog. *cl. silt*
260	11–0·0	125–33·6	160	slope at foot of shelf edge bank	D	surf.		*sh. sand-silt-clay*
261	11–5·0	125–42·7	63	sl. rough, level, inside shelf edge	G	0–22	5Y 6/4	homog. *sl. sh. sand*
262	11–10·3	125–50·4	53	sl. irr., level	G	0–40	5Y 5/2	homog. *sh. st. sand*
263	11–16·0	125–58·5	49	smooth, level	G	0–61	5Y 5/2	homog. *sl. sh. sand-silt-clay*
264	11–21·7	126–6·6	48	smooth, level, in small depression	G	0–15	5Y 5/2	homog. *sl. sh. sand-silt-clay*
						15–16	5Y 5/2	sand layer
						16–71	5Y 5/2	indist. layered mud
265	11–27·6	126–14·8	43	sl. irr., level	G	0–48	5Y 5/2	homog. sl. sh. sand-silt-clay
266	11–33·5	126–23·2	31	sl. wavy, level	G	0–44	5Y 5/2	homog. *sl. sh. cl. sand*
267	11–37·5	126–31·8	52	flat bottom of channel between banks	G	0–60	5Y 5/2	homog. *sd. clay*
268	11–38·7	126–34·1	50	wavy, level	D	surf.	5Y 5/2	*st. clay*; SKELETAL DEBRIS
269	11–42·6	126–42·9	53	smooth, level	G	0–62	5Y 5/2	irr. layered (shelly layers) *sl. sh. sd. clay*
270	11–47·1	126–52·8	56	smooth, gentle slope below bank	G	0–12	5Y 5/2	homog. *sd. cl. shell*
271	11–52·0	127–1·4	65	smooth, level	G	0–32	5GY 5/2	homog. *st. clay*
						32–41	5GY 5/2	reg. layered (small shell layers) mud
						41–70	5GY 5/2	homog. mud
272	11–55·4	127–10·5	55	smooth, level	G	0–48	5GY 5/2	homog. *sh. cl. sand*
273	11–59·4	127–19·1	58	smooth, level	G	0–49	5GY 5/2	irr. layered (shell layers) *sh. sd. clay*
274	12–3·8	127–28·6	62	smooth, level	G	0–56	5GY 5/2	homog. *sh. sd. clay*
275	12–8·3	127–38·0	64	smooth, level	G	0–38	5GY 5/2	homog. *sh. cl. sand*
276	12–12·5	127–47·3	64	smooth, level	G	0–44	5GY 5/2	irr. layered and mottled *sh. sd. clay*
277	11–58·0	127–39·3	65	smooth, level	G	0–61	5Y 5/2	indist. mottled *sl. sh. sand-silt-clay*
278	11–49·6	127–34·2	66	smooth, level	G	0–48	5Y 5/2	homog. *s.l sh. sd. clay*
					D	surf.		SKELETAL DEBRIS
279	11–39·7	127–27·9	66	smooth, level	G	0–68	5Y 5/2	irr. layered *sh. st. clay*
280	11–33·4	127–20·0	62	wavy, level	G	0–69	5Y 5/2	homog. *st. clay*
281	11–27·4	127–11·6	58	smooth, level near small bank	G	0–70	5Y 5/2	homog. *st. clay*
282	11–21·1	127–3·7	57	smooth, level	G	0–56	5Y 5/2	homog. *sl. sh. sd. clay*
283	11–14·9	126–54·9	39	flat bank top	D	surf.	5Y 5/2	*sh. cl. sand*; SKELETAL DEBRIS
284	11–8·8	126–47·3	68	rough depression between banks	G	0–52	5Y 5/2	homog. *sl. sh. sd. clay*
285	11–2·7	126–39·5	50	smooth, level between small banks	G	0–31	5Y 5/2	homog. *sl. sh. cl. sand*
286	10–56·4	126–31·4	44	sl. wavy, level	G	0–47	10Y 5/2	homog. sandy mud

APPENDIX A—*continued*

Station Number (V–)	S. Lat.	E. Long.	Water Depth (fms)	Minor Bottom Relief	Sample Type	Depth in Core (cm)	Colour	Structure and Lithology
287	10–50·3	126–23·0	52	sl. wavy, level	G	0–41	5Y 5/2	homog. sh. sand-silt-clay
288	10–44·5	126–15·8	150	wavy moderate slope below bank	G	0–23	5Y 5/2	homog. *st. sand*
289	10–38·7	126–8·4	182	smooth, gentle slope	G	0–6	10Y 5/2	homog. *sand-silt-clay*
						6–18	5Y 5/2	irr. layered and mottled sand and mud
						18–30	5Y 5/2	homog. mud
290	10–33·0	126–0·9	259	smooth, gentle slope	G	0–39	5Y 5/2	homog. *st. clay*, oxidized surface
291	10–27·5	125–53·4	353	smooth, gentle slope	G	0–7	5Y 5/2	homog. *sand*, oxidized surface
						7–21	5Y 3/2	dist. mottled (sand) mud; sand layer
292	10–22·0	125–46·1	563	smooth, moderate slope	G	0–57	5GY 5/2	homog. *st. clay*; oxidized surface
293	10–16·0	125–38·5	830	smooth, steep slope	G	0–23	5GY 5/2	homog. *st. clay*; oxidized surface
						21–63	(5Y 5/2)	homog. mud; silt layer
294	10–8·4	125–30·5	1166	smooth, steep slope	G	0–67	10Y 4/2	homog. *st. clay*
295	10–1·6	125–17·6	1383	smooth, level trough floor	G	0–28	5Y 5/2	homog. *cl. silt*
						28–35		mottled (mud) fine sand
296	9–56·5	125–10·0	858	steep, rough slope	G	0–62	5Y 5/2	homog. *st. clay*; oxidized surface
297	9–48·5	125–0·8	460	wavy step in steep slope	G	0–43	5Y 5/2	reg. layered (sand) *cl. silt*; oxidized surface
298	9–44·4	124–56·6	92	steep, dissected slope	G	0–68	5Y 5/2	homog. *st. clay*; oxidized surface
299	9–28·7	125–10·7	144	steep, smooth slope	G	0–63	5Y 4/2	homog. *st. clay*
300	10–25·5	126–33·7	17	flat bank top	D	surf.		SKELETAL DEBRIS
301	10–34·0	126–46·1	43	wavy, level	G	0–53	(10Y 6/2)	homog. *sh. st. sand*
302	10–24·0	126–47·2	51	sl. irr., gentle slope	D	surf.		*sl. sh. sand*; SKELETAL DEBRIS
303	10–15·5	126–45·3	85	smooth, level near bank	G	surf.	5Y 5/4	*sand*
304	10–13·0	126–43·0	37	rough bank top	D	surf.		*sh. sand*
305	10–3·1	126–42·0	490	wavy, moderate slope	G	0–59	5GY 5/2	homog. *sand-silt-clay*
306	9–52·5	126–39·2	918	wavy, moderate slope	G	0–58	5GY 5/2	homog. *st. clay*; oxidized surface
307	9–45·4	126–36·6	1337	wavy, moderate slope	G	0–69	5GY 5/2	homog. *st. clay*; oxidized surface
308	9–41·3	126–35·2	1486	smooth, level trough floor	G	0–2	10YR 5/2	homog. oxidized mud
						2–65	10Y 5/2	homog. *st. clay*
309	9–31·4	126–32·5	1085	wavy, steep slope	G	0–2	5YR 5/2	homog. oxidized mud
						2–67	10Y 5/2	homog. *st. clay*
310	9–20·4	126–28·3	800	wavy, steep slope	G	0–2	5YR 5/2	homog. oxidized mud
						2–61	5Y 5/2	homog. *st. clay*
311	9–7·5	126–24·5	480	wavy, steep slope	G	0–2	10YR 5/2	homog. oxidized mud
						2–68	5GY 5/2	homog. *st. clay*
312	9–2·5	126–23·3	87	wavy, steep slope	G	0–25	5Y 5/2	reg. layered *sh. sand*

313	8–58·5	126–30·0	48	rough, level	D	surf.		MUD AND SHELL; *cl. silt*
314	9–54·7	127–53·1	54	rough, gentle slope	D	surf.		*sl. sh. sand*
315	9–45·9	127–51·5	151	smooth, gentle slope	G	0–46	10Y 5/4	homog. *st. sand*
316	9–34·3	127–49·4	554	wavy, steep slope	G	0–62	5GY 5/2	homog. *st. clay*; oxidized surface
317	9–23·5	127–46·5	926	smooth, level near large peak	G	0–66	5Y 5/2	indist. mottled *cl. sand*; oxidized surface
318	9–16·2	127–45·7	1230	smooth, steep slope	G	0–2	10YR 4/2	homog. oxidized mud
						2–65	5Y 5/2	homog. *sd. clay*
319	9–9·0	127–44·0	1750	smooth, level trough floor	G	0–2	10YR 5/2	homog. oxidized mud
						2–67	5Y 5/7	homog. *st. clay*
320	9–2·5	127–40·8	1182	wavy, moderate slope	G	0–2	10YR 5/2	homog. oxidized mud
						2–68	5GY 5/2	homog. *st. clay*
321	8–53·0	127–42·8	1130	smooth, hilly, moderate slope	G	0–61	5Y 5/2	homog. *st. clay*, black speckles
322	8–43·1	127–40·3	1035	smooth, hilly	G	0–66	5Y 5/2	homog. *st. clay*, oxidized surface
323	8–33·7	127–40·8	992	smooth, moderate slope	G	0–67	5Y 5/2	homog. *st. clay*, oxidized surface
324	8–22·7	127–44·0	812	irr., steep slope	G	0–60	5Y 5/2	homog. *st. clay*, oxidized surface
325	8–17·3	127–42·5	634	irr. steep slope	G	0–45	5Y 5/2	indist. mottled *st. clay*; irr. layer of *shell*; oxidized surface
326	8–29·0	128–27·0	1098	smooth, gentle slope	G	0–2	10YR 5/2	homog. oxidized mud
						2–28	5Y 5/2	homog. *st. clay*
327	8–34·4	128–33·9	1000	wavy, level	G	0–2	10YR 5/2	homog. oxidized mud
						2–74	5Y 5/2	homog. mud
328	8–42·5	128–40·5	975	smooth, hilly slope	G	0–2	10YR 4/2	homog. oxidized mud
						2–67	5Y 5/2	indist. mottled *cl. silt*
329	8–51·0	128–47·1	1188	smooth, hilly slope	G	0–2	10YR 4/2	homog. oxidized mud
						2–69	10Y 5/2	homog. *clay*
330	8–59·0	128–54·0	1476	steep, smooth slope near trough floor	G	0–2	10YR 4/2	homog. oxidized mud
						2–63	5GY 5/2	homog. *clay*
331	9–7·0	129–0·0	820	moderate, smooth, dissected slope	G	0–21	5GY 5/2	homog. *cl. sand*; oxidized surface
						21–53	5GY 5/2	dist. mottled *cl. sand*
332	9–15·4	129–7·6	442	moderate, smooth dissected slope	G	0–2	10YR 4/2	homog. oxidized mud
						2–41	5GY 5/2	indist. mottled *sd. clay*
333	9–22·7	129–12·7	294	smooth, gentle slope	G	0–2	10YR 4/2	homog. oxidized mud
						2–62	5GY 5/2	homog. *st. clay*
334	9–30·6	129–20·1	229	smooth, gentle slope	G	0–2	10YR 4/2	homog. oxidized mud
						2–59	5GY 5/2	homog. *sd. clay*
335	9–38·5	129–26·5	196	smooth, gentle slope	G	0–57	5GY 5/2	homog. *st. clay*
336	9–47·0	129–33·3	172	smooth, gentle slope	G	0–57	10Y 5/4	dist. mottled *sand-silt-clay*
337	9–51·9	129–42·6	132	smooth, level	D	surf.		*sl. sh. sand*; SKELETAL DEBRIS
338	10–1·0	129–47·7	86	smooth, level	G	0–6	5GY 5/2	homog. *sl. sh. sand-silt-clay*
						6–53		dist. mottled sandy mud
339	10–9·6	129–52·6	71	smooth, level	G	0–16	(5GY 5/2)	homog. *sh. sand*
340	10–17·3	129–57·2	62	smooth, level	G	0–31		homog. *sl. sh. sand*

Station Number (V–)	S. Lat.	E. Long.	Water Depth (fms)	Minor Bottom Relief	Sample Type	Depth in Core (cm)	Colour	Structure and Lithology
341	10–26·0	130–2·0	49	smooth, level	G	0–25	5Y 5/2	homog. *sh. cl. sand*
						25–48	10Y 5/2	dist. mottled shelly sand and mud
342	10–34·1	130–7·0	37	smooth, level	G	0–48	5Y 5/2	homog. *sh. cl. sand*
343	10–42·0	130–12·5	13	flat bank top	D	surf.		*sd. shell*; SKELETAL DEBRIS
344	10–49·6	130–15·7	40	smooth, level	D	surf.	5GY 5/2	*sl. sh. sand-silt-clay*; SKELETAL DEBRIS
345	10–58·0	130–20·3	31	smooth, level	G	0–73	5GY 5/2	homog. *sl. sh. clay*
346	10–58·0	130–10·8	30	sl. rough, level	G	0–14	5GY 5/2	homog. *sh. sd. clay*
347	10–58·0	130–6·4	32	sl. rough, level	D	surf.	10Y 5/2	*sh. cl. sand*; SKELETAL DEBRIS
348	10–57·9	129–56·6	40	sl. rough, level	G	0–40	10GY 5/2	homog. *sh. cl. sand*
349	10–57·5	129–47·2	45	level, gullies	D	surf.	5GY 5/2	*sh. sand*
350	10–57·3	129–36·9	17	flat bank top	D	surf.		*sh. sand*; ROCK
351	10–56·6	129–26·6	41	wavy, level between banks	D	surf.		*sl. sh. sand*; SKELETAL DEBRIS
352	10–56·0	129–16·5	15	flat bank top	D	surf.		*sh. sand*; LIVE MATERIAL
353	10–56·0	129–6·0	18	flat bank top	D	surf.		*sh. sand*
354	10–55·4	128–57·0	22	flat bank top	D	surf.		*sh. sand*
355	10–55·4	128–50·0	61	moderate slope of flat top bank	D	surf.		*sd. shell*; SKELETAL DEBRIS
356	10–58·5	128–42·0	18	flat bank top	D	surf.		SKELETAL DEBRIS
357	10–57·0	128–31·3	35	wavy, level	D	surf.		*sh. sand*
358	10–49·1	128–25·7	50	level, near bank	D	surf.		SKELETAL DEBRIS
359	10–39·0	128–18·8	84	sl. wavy, gentle slope	G	0–14	(5Y 5/2)	homog. *sl. sh. cl. sand*
						14–63	(5Y 5/2)	homog. mud
360	10–32·4	128–13·1	57	wavy, level	G	0–44	(5Y 5/2)	homog. *sl. sh. sand*
361	10–28·6	128–21·3	35	sl. irr. gentle slope	G	0–13	5Y 6/2	homog. *sh. sand*
362	10–25·4	128–29·0	41	wavy, level	D	surf.	10YR 6/2	*sl. sh. sand*; SKELETAL DEBRIS
363	10–22·3	128–35·1	19	wavy channel floor	G	0–58	10Y 5/2	homog. *cl. sand*
364	10–15·4	128–45·1	31	sl. irr. gentle slope	D	surf.	5Y 6/2	*sh. sand*; SKELETAL DEBRIS
365	10–9·0	128–53·5	37	irr., level	G	0–10	5Y 5/2	*sand*
366	10–3·0	129–1·6	42	smooth, level	G	0–25	5Y 5/2	homog. *sh. st. sand*
367	9–55·8	129–9·4	57	smooth, level	G	0–39	10Y 6/2	homog. *st. sand*
368	9–52·7	129–18·0	64	smooth, level	D	surf.		COARSE SHELLY SAND
369	9–58·0	129–18·0	53	smooth, level	D	surf.		LIVE GORGONIANS; probably rock bottom
370	10–8·3	129–20·1	55	smooth, level	G	surf.	5GY 5/2	*sl. sh. sand*
371	10–18·2	129–22·5	47	wavy. level	D	surf.	5GY 5/2	*sl. sh. sand*
372	10–27·8	129–24·4	51	smooth, level	D	surf.	5GY 5/2	*sl. sh. sand*

373	10–36·5	129–26·8	32	irr., level	D	surf.	*sh. sand*
374	10–44·3	129–31·2	16	flat bank top	D	surf.	*sd. shell*
375	10–53·0	129–36·5	14	flat bank top	D	surf.	*sh. sand*
376	10–59·2	129–40·8	45	wavy, level	D	surf.	*sl. sh. sand*; skeletal debris
377	11–5·6	129–42·7	39	wavy, level	D	surf.	*sh. sand*; skeletal debris, gravel
378	11–18·0	129–25·0	19	flat bank top	S	surf.	gravel
379	9–44·0	127–40·0	228		G	0–78	sandy mud and shell
380	9–28·0	127–23·0	840		P	0–138	sandy mud
					G	0–15	sandy mud and shell
381	9–14·0	127–26·0	1764		P	0–48	sandy mud
					G	0–128	mud
					P	0–334	mud
382	8–44·0	127–30·0	700		G	0–119	mud, oxidized surface
					P	0–240	sandy mud
383	12–08·0	127–14·0	53		P	surf.	mud and shell
384	11–44·0	127–57·0	74		P	0–297	mud with shell and sand layers
385	9–0·0	128–3·7	1670		P	0–331	mud and shell
386	14–50·0	128–52·0			S	surf.	shell from beach terrace

APPENDIX B

SUMMARY STATISTICS AND DESCRIPTION OF SEDIMENT TEXTURES, TIMOR SEA

Sample Number	Core Interval Analysed (cm)	Gravel Percent	Sand Percent	Silt Percent	Clay Percent	Median in Phi	Mean in Phi	Standard Deviation	Median in Phi of Sand Fraction	Classification—see App. A for Explanation
V–2	1 11	11	58	17	14	2·35	2·15	2·47	1·50	sh. st. sand
V–3	1 11	1	64	15	20	3·02	3·30	1·83	2·60	sl. sh. cl. sd.
V–4	1 11	15	59	9	17	2·45	2·00	2·37	2·10	sh. cl. sand
V–5	1 11	32	57	4	7	1·60	·67	2·44	1·30	sd. shell
V–6	1 11	29	50	9	12	2·10	1·19	3·16	1·75	sh. cl. sand
V–7	1 11	30	35	12	23	1·54	1·08	3·30	·40	sh. cl. sand
V–8	1 11	3	62	11	24	1·84	2·15	2·26	1·35	cl. sd.
V–9	1 11	20	62	7	11	1·45	1·24	2·54	1·20	sh. sand
V–10	0 4	11	78	0	11	1·55	1·12	1·26	1·40	sh. sand
V–11	1 9	12	75	4	9	1·46	1·33	1·85	1·35	sh. sand
V–12	1 11	15	60	9	16	1·79	1·47	2·51	1·35	sh. cl. sand
V–14	1 11	22	61	6	11	1·20	1·02	2·36	·90	sh. sand
V–15	1 11	8	53	20	19	2·81	2·71	2·34	1·90	sh. ssc.
V–16	1 11	0	21	36	42	6·39	4·87	1·82	3·05	ssc.
V–19	1 11	7	65	19	9	2·71	2·74	2·22	2·05	sh. st. sand
V–21	1 11	7	53	29	11	2·88	2·69	2·21	1·65	sh. st. sand
V–22	1 11	15	57	15	13	2·21	2·01	2·59	1·50	sh. st. sand
V–24	1 11	4	80	8	8	2·17	2·19	1·61	2·00	sl. sh. sand
V–25	1 11	14	50	23	13	2·47	2·33	2·71	1·35	sh. st. sand
V–26	1 11	0	33	50	17	4·67	4·27	1·68	2·70	sd. st.
V–27	1 11	2	40	44	14	4·35	3·86	1·86	2·65	sl. sh. sd. st.
V–28	1 11	2	72	16	10	3·18	3·25	1·48	2·95	sl. sh. st. sd.
V–29	1 11	2	75	14	9	2·78	2·87	1·58	2·50	sl. sh. sand
V–33	1 11	0	11	80	9	5·45	5·38	1·32	3·05	silt
V–34	1 7	0	66	24	10	3·36	3·69	1·36	3·05	st. sd.
V–36	1 11	5	34	45	16	4·46	3·81	2·14	2·70	sl. sh. sd. st.
V–37	1 11	5	53	31	11	2·98	2·96	2·25	1·85	sl. sh. st. sd.
V–39	1 11	10	48	26	16	2·63	2·67	2·65	1·30	sh. st. sand
V–40	1 11	5	60	22	13	2·95	2·95	2·09	2·35	sl. sh. st. sd.

V–41	1	11	5	70	14	11	2·04	2·21	2·15	1·55	sl. sh. st. sd.
V–42	1	11	6	65	15	14	2·40	2·48	2·13	1·90	sh. st. sand
V–43	1	11	10	63	13	14	1·33	1·64	2·37	·85	sh. cl. sand
V–44	1	11	13	52	14	21	1·79	1·82	2·66	·90	sh. cl. sand
V–45	1	11	8	67	9	16	1·79	2·00	2·46	1·35	sh. cl. sand
V–46	1	11	12	70	6	12	1·22	1·22	2·11	·95	sh. sand
V–47	1	11	15	61	8	16	1·09	1·27	2·24	·75	sh. cl. sand
V–48	1	11	15	56	10	19	1·58	1·48	2·56	1·10	sh. cl. sand
V–49	1	11	11	53	10	26	2·42	2·08	2·67	1·55	sh. cl. sand
V–50	1	11	9	49	11	31	2·32	2·12	2·75	1·25	sh. cl. sand
V–51	1	11	6	70	7	17	2·17	2·09	2·09	1·85	sh. cl. sand
V–52	0	1	62	32	0	6	1·92	·17	2·91	0	sd. shell
V–53	1	11	10	66	8	16	1·90	1·70	2·22	1·45	sh. cl. sand
V–54	1	11	10	41	18	31	3·39	2·32	2·87	·95	sh. cl. sand
V–55	1	11	11	52	13	24	1·92	1·92	2·60	1·15	sh. cl. sand
V–56	1	11	0	3	48	49	7·84	6·03	1·57	3·85	st. clay
V–57	1	11	7	59	14	20	2·56	2·36	2·37	1·65	sh. cl. sand
V–58	1	11	4	76	7	13	2·46	2·54	1·66	2·25	sl. sh. cl. sd.
V–59	1	11	20	55	11	14	1·90	1·57	2·54	1·30	sh. cl. sand
V–60	1	11	24	65	5	6	1·30	·88	2·40	1·10	sh. sand
V–61	1	11	3	83	6	8	2·18	2·24	1·49	2·05	sl. sh. sand
V–62	1	11	22	61	7	10	2·05	1·50	2·57	1·55	sh. sand
V–63	1	7	10	80	5	5	2·05	1·79	1·77	1·95	sh. sand
V–64	1	11	20	70	5	5	1·30	1·22	1·94	1·10	sh. sand
V–65	1	11	4	83	4	9	2·61	2·47	1·55	2·45	sl. sh. sand
V–66	1	11	13	66	8	13	1·61	1·48	2·22	1·25	sh. sand
V–68	1	11	10	87	0	3	1·59	1·33	1·41	1·55	sh. sand
V–69	1	10	8	78	7	7	2·29	2·12	1·74	2·15	sh. sand
V–70	1	11	16	65	9	10	2·12	1·84	2·36	1·80	sh. sand
V–71	1	11	3	81	8	8	2·30	2·37	1·70	2·10	sl. sh. sand
V–72	1	11	5	66	12	17	2·65	2·55	2·10	2·05	sl. sh. cl. sd.
V–73	1	11	13	61	11	15	2·30	2·05	2·48	1·85	sh. cl. sand
V–74	1	11	3	70	11	16	2·46	2·47	1·89	1·70	sl. sh. cl. sd.
V–75	0	10	0	61	14	24	3·03	3·23	2·19	2·25	cl. sand
V–75	10	20	15	64	7	14	2·33	1·86	2·36	1·90	sh. cl. sand
V–75	20	28	3	29	47	21	6·82	4·83	2·74	2·10	sl. sh. ssc.
V–76	1	11	3	68	11	18	2·63	2·55	2·00	2·00	sl. sh. cl. sd.
V–77	1	11	1	67	12	20	2·91	3·00	1·85	2·50	sl. sh. cl. sd.
V–78	1	11	10	49	16	25	3·13	2·72	2·63	2·25	sh. cl. sand

APPENDIX B—*continued*

Sample Number	Core Interval Analysed (cm)	Gravel Percent	Sand Percent	Silt Percent	Clay Percent	Median in Phi	Mean in Phi	Standard Deviation	Median in Phi of Sand Fraction	Classification—see App. A for Explanation
V–79	1 11	3	59	16	22	3·95	4·21	1·68	3·85	sl. sh. cl. sd.
V–80	1 11	3	46	16	35	4·32	3·14	2·51	1·90	sl. sh. cl. sd.
V–81	1 11	2	36	25	37	5·60	3·68	2·49	2·05	sl. sh. ssc.
V–82	1 11	3	55	11	31	2·96	3·31	2·56	2·30	sl. sh. cl. sd.
V–83	1 11	33	62	2	3	·31	·01	1·72	·25	sd. shell
V–84	1 11	41	59	0	0	·20	·37	1·25	0	sd. shell
V–85	1 11	0	81	5	14	4·47	2·63	1·37	2·35	sd.
V–86	1 11	0	32	19	49	7·82	4·44	1·93	3·15	sd. clay
V–87	1 11	0	7	29	64	8·54	6·86	1·78	3·85	st. clay
V–88	1 11	0	15	58	27	5·33	5·27	1·35	3·85	cl. silt
V–89	1 11	19	50	15	16	1·44	1·67	2·86	·85	sh. cl. sd.
V–90	1 11	6	43	26	25	4·14	3·09	2·74	1·29	sh. ssc.
V–91	1 11	15	54	20	11	1·49	2·42	3·18	·95	sh. st. sand
V–92	1 11	27	48	13	12	1·49	1·32	2·66	·75	sh. st. sand
V–93	1 11	6	63	22	9	2·12	2·43	2·19	1·40	sh. st. sand
V–94	1 11	7	53	28	12	3·13	2·86	2·24	2·00	sh. st. sand
V–95	1 11	40	60	0	0	3·79	1·71	2·56	3·80	sd. shell
V–96	1 11	2	70	18	10	2·57	2·73	1·85	2·10	sl. sh. st. sd.
V–97	1 11	3	38	52	7	4·54	4·21	2·55	1·90	sl. sh. sd. st.
V–98	1 11	13	54	22	11	2·16	2·78	3·13	1·30	sh. st. sand
V–99	1 11	2	46	23	29	4·27	3·50	2·23	2·45	sl. sh. ssc.
V–100	1 11	8	53	17	22	2·78	2·99	3·16	1·90	sh. cl. sand
V–101	1 11	6	55	13	26	2·41	2·39	2·46	1·40	sh. cl. sand
V–102	1 11	2	22	21	55	8·69	4·41	2·85	2·10	sl. sh. st. cl.
V–103	1 11	0	16	25	59	0	5·01	2·41	2·50	st. cl.
V–104	1 11	10	45	11	34	2·16	2·11	2·95	1·00	sh. cl. sand
V–105	1 11	0	8	23	69	0	6·27	1·90	3·85	st. cl.
V–106	1 11	0	22	22	56	8·69	5·02	2·18	2·95	sl. sh. st. cl.
V–107	1 11	0	11	25	64	0	5·74	1·66	3·85	st. clay
V–108	1 11	12	37	11	40	5·02	2·13	3·18	·85	sh. sd. clay
V–109	1 11	25	35	9	31	1·90	1·42	3·23	1·10	sh. cl. sand

V–110	1	11	8	34	12	46	6·67	2·65	3·17	1·15	sh. sd. clay
V–111	1	11	21	30	13	36	3·22	1·51	3·40	·50	sh. sd. clay
V–112	1	11	13	38	15	34	3·00	2·32	3·13	1·05	sh. cl. sand
V–113	1	11	9	52	12	27	1·84	2·41	2·98	1·05	sh. cl. sand
V–114	1	11	6	51	22	21	2·69	3·51	3·07	1·50	sh. ssc.
V–115	1	11	10	47	24	19	1·85	2·36	2·93	·65	sh. ssc.
V–116	1	11	8	37	16	39	5·40	2·80	2·86	1·50	sh. sd. clay
V–117	1	11	7	44	16	33	3·77	2·76	2·75	1·50	sh. cl. sand
V–118	1	11	14	57	10	19	1·93	1·58	2·57	1·20	sh. cl. sand
V–119	1	11	15	61	7	17	1·47	1·46	2·37	1·00	sh. cl. sand
V–120	1	11	12	70	7	11	1·91	1·66	2·15	1·50	sh. sand
V–121	1	11	41	52	5	2	·92	·12	2·78	·60	sd. shell
V–122	1	11	35	54	0	11	·95	·06	2·18	·65	sd. shell
V–123	1	11	32	57	6	5	1·58	·59	2·86	1·30	sd. shell
V–124	1	11	4	89	3	4	2·19	2·08	1·34	2·10	sl. sh. sand
V–125	1	11	14	68	8	10	1·83	1·58	2·21	1·45	sh. sand
V–126	1	10	6	39	22	33	4·42	3·32	2·63	2·05	sh. ssc.
V–127	1	11	7	73	8	12	2·15	2·07	2·01	1·75	sh. sand
V–128	1	11	21	52	14	13	1·90	1·33	2·87	1·30	sh. st. sand
V–129	1	11	15	50	20	15	1·54	1·55	2·85	·70	sh. st. sand
V–130	1	11	8	67	14	11	2·33	2·29	1·94	2·10	sh. st. sand
V–131	1	11	0	51	32	17	3·88	3·84	1·26	3·10	st. sd.
V–132	1	11	1	41	39	19	4·24	3·91	1·55	3·25	sl. sh. st. sd.
V–133	1	11	3	54	25	18	3·30	3·16	1·94	2·35	sl. sh. st. sd.
V–134	1	11	2	64	18	16	2·22	2·33	2·03	1·30	sl. sh. st. sd.
V–135	1	11	1	75	12	12	2·32	2·60	1·56	2·15	sl. sh. cl. sd.
V–136	1	11	2	51	26	21	3·18	3·19	2·01	1·80	sl. sh. ssc.
V–137	1	11	7	50	23	20	2·76	2·54	2·53	1·50	sh. st. sd.
V–138	1	11	9	40	21	30	4·19	2·76	3·01	1·05	sh. ssc.
V–139	1	11	8	33	25	34	5·02	3·84	3·38	1·15	sh. ssc.
V–140	1	11	8	39	20	33	4·53	3·03	3·16	1·25	sh. sd. cl.
V–141	1	11	1	23	32	44	6·62	4·85	2·70	1·60	sl. sh. ssc.
V–142	1	11	2	28	25	45	6·67	3·82	3·16	·75	sl. sh. ssc.
V–143	1	11	0	8	37	55	8·25	6·30	2·18	1·60	st. cl.
V–144	1	11	0	3	36	61	8·54	6·78	1·54	3·85	st. clay
V–145	1	11	0	1	34	66	8·61	7·06	1·50	3·85	st. clay
V–146	1	11	26	27	13	34	2·20	·92	3·80	0	sh. sd. clay
V–147	1	11	12	43	24	21	2·54	2·66	3·13	·80	sh. ssc.

APPENDIX B—*continued*

Sample Number	Core Interval Analysed (cm)	Gravel Percent	Sand Percent	Silt Percent	Clay Percent	Median in Phi	Mean in Phi	Standard Deviation	Median in Phi of Sand Fraction	Classification—see App. A for Explanation
V–148	1 11	1	45	19	35	4·78	3·64	2·17	2·45	sl. sh. cl. sd.
V–149	1 11	6	29	27	38	6·16	3·55	3·23	·80	sh. ssc.
V–150	1 9	0	11	31	58	0	5·85	1·62	3·85	st. clay
V–151	6 16	4	60	16	20	2·52	2·77	2·45	1·85	sl. sh. cl. sd.
V–152	1 11	4	58	19	20	2·29	2·78	2·55	1·50	sl. sh. cl. sd.
V–153	1 11	0	27	36	37	6·42	5·04	2·24	2·70	ssc.
V–154	1 11	3	56	17	24	2·57	2·89	2·48	1·65	sl. sh. cl. sd.
V–155	1 11	5	56	19	20	2·97	3·05	2·48	2·15	sl. sh. cl. sd.
V–156	1 9	25	63	9	3	·70	·83	2·32	·55	sh. sand
V–157	1 11	4	62	24	10	2·38	2·76	2·33	1·55	sl. sh. st. sd.
V–159	1 11	6	41	28	25	4·36	3·42	2·65	1·95	sh. ssc.
V–160	1 11	0	12	46	42	6·28	5·36	1·66	3·25	cl. st.
V–161	1 11	1	36	46	17	4·65	4·32	1·88	2·85	sl. sh. sd. st.
V–162	1 11	4	77	15	4	2·78	2·74	1·80	2·45	sl. sh. sand
V–163	1 11	26	56	12	6	1·56	1·28	2·62	1·15	sh. sand
V–165	1 11	53	40	0	7	1·28	·86	2·17	0	cl. sd. shell
V–166	1 11	17	74	3	6	1·90	1·38	2·10	1·80	sh. sand
V–167	1 11	18	67	7	8	1·38	1·28	2·26	1·05	sh. sand
V–168	1 11	14	71	6	9	1·37	1·29	2·00	1·15	sh. sand
V–169	0 5	28	60	7	5	1·01	·92	2·40	·65	sh. sand
V–170	1 11	2	80	10	10	2·58	2·59	1·59	2·35	sl. sh. sand
V–172	1 11	3	74	10	13	2·50	2·72	1·73	2·10	sl. sh. sand
V–173	1 11	15	67	6	12	1·68	1·50	2·25	1·30	sh. sand
V–174	1 11	10	48	27	15	2·70	2·95	2·85	1·45	sh. st. sand
V–175	1 11	11	57	11	21	1·47	1·73	2·48	1·00	sh. cl. sand
V–176	1 11	9	62	12	17	2·06	2·42	2·73	1·30	sh. cl. sand
V–177	1 11	20	53	7	20	1·63	1·68	3·17	·95	sh. cl. sand
V–177	1 4	25	75	0	0	1·32	·82	1·99	1·35	sh. sand
V–178	1 11	8	48	11	33	2·83	2·37	2·68	1·55	sh. cl. sand
V–179	1 11	23	34	12	31	2·51	1·53	3·37	·50	sh. cl. sand

V–180	1	11	22	33	12	33	2·83	1·53	3·42	·60	sh. sd. cl.
V–181	1	11	20	37	12	31	2·98	1·87	3·32	·95	sh .cl. sand
V–182	1	11	12	55	11	22	2·28	1·96	2·51	1·35	sh. cl. sand
V–183	1	11	8	68	8	16	2·06	1·91	2·09	1·50	sh. cl. sand
V–184	1	11	13	73	6	8	1·73	1·45	2·07	1·45	sh. sand
V–185	1	11	8	76	6	10	1·88	1·78	1·90	1·60	sh. sand
V–186	1	11	14	73	5	8	1·64	1·43	2·11	1·40	sh. sand
V–187	1	11	15	75	4	6	2·03	1·48	2·21	1·90	sh. sand
V–188	1	11	7	83	4	6	2·46	2·15	1·64	2·35	sh. sand
V–189	1	11	10	65	12	12	2·33	2·13	2·13	1·85	sh. st. sand
V–190	1	11	19	62	11	8	1·34	1·29	2·34	1·05	sh. sand
V–191	1	11	15	79	4	2	1·20	·99	1·64	1·15	sh. sand
V–192	1	11	36	32	17	15	2·04	·71	3·49	0	ssc. shell
V–194	1	11	16	83	0	1	1·53	·89	1·67	1·50	sh. sand
V–195	1	11	20	57	12	11	1·73	1·73	2·92	1·25	sh. st. sand
V–196	1	11	9	67	11	13	2·10	2·02	2·11	1·85	sh. cl. sand
V–197	1	11	29	50	11	10	·83	·89	2·78	·35	sh. st. sand
V–198	1	11	9	49	23	19	2·60	2·44	2·47	1·35	sh. st. sd.
V–199	1	11	2	75	10	13	2·07	2·35	1·63	1·90	sl. sh. sand
V–200	1	11	5	58	12	25	2·49	2·61	2·17	2·10	sl. sh. cl. sd.
V–201	1	11	0	68	13	19	3·18	3·33	1·57	2·80	sl. sh. cl. sd.
V–202	1	11	0	67	13	20	3·43	3·71	1·50	3·10	sl. sh. cl. sd.
V–203	1	11	14	50	12	24	2·58	2·40	3·15	1·25	sh. cl. sand
V–203	41	43	3	6	21	70	0	4·93	2·49	3·80	sl. sh. st. cl.
V–204	1	11	19	47	12	22	1·17	1·16	2·82	·50	sh. cl. sand
V–205	1	11	13	59	10	18	1·68	1·71	2·54	1·30	sh. cl. sand
V–206	1	11	13	68	6	13	1·82	1·48	2·09	1·50	sh. sand
V–207	1	11	100	0	0	0	2·07	2·09	·60	0	shell
V–208	1	11	7	21	29	43	7·35	4·87	3·60	·55	sh. ssc.
V–209	1	11	15	76	3	6	1·15	1·02	1·80	1·05	sh. sand
V–210	1	11	9	81	3	7	1·90	1·62	1·79	1·85	sh. sand
V–211	0	10	3	60	16	21	2·63	3·03	2·39	2·10	sl. sh. cl. sd.
V–212	1	5	11	45	18	26	2·88	2·42	2·84	1·40	sh. cl. sd.
V–213	1	11	22	58	6	14	1·16	·82	2·60	·75	sh. cl. sand
V–214	1	11	6	72	7	15	1·69	1·83	2·10	1·35	sh. sand
V–215	1	11	13	66	7	14	1·77	1·57	2·34	1·35	sh. sand
V–216	1	11	3	76	7	14	2·58	2·59	1·83	2·35	sl. sh. sand
V–217	1	11	3	68	13	16	2·43	2·61	2·08	1·80	sl. sh. cl. sd.
V–218	1	11	7	74	10	9	2·04	2·09	1·96	1·75	sh. sand

APPENDIX B—*continued*

Sample Number	Core Interval Analysed (cm)	Gravel Percent	Sand Percent	Silt Percent	Clay Percent	Median in Phi	Mean in Phi	Standard Deviation	Median in Phi of Sand Fraction	Classification—see App. A for Explanation
V-219	0 10	5	60	21	14	2·69	2·65	2·18	1·75	sl. sh. st. sd.
V-220	1 11	7	65	18	10	2·37	2·43	2·25	1·75	sh. st. sand
V-221	1 11	7	70	14	9	2·06	2·21	2·08	1·65	sh. st. sd.
V-222	1 11	4	64	23	9	3·09	2·93	2·00	2·30	sl. sh. st. sd.
V-223	1 11	4	68	22	6	2·55	2·67	1·98	1·95	sl. sh. st. sd.
V-224	0 10	0	52	45	3	3·91	3·77	1·48	2·90	st. sd.
V-225	1 10	11	62	24	3	2·24	2·24	2·33	1·60	sh. st. sand
V-226	1 11	9	87	0	4	1·47	1·31	1·25	1·40	sh. sand
V-227	0 0	0	100	0	0	3·38	3·32	0	3·40	sand
V-228	0 10	6	89	4	1	2·07	1·90	1·49	1·95	sh. sand
V-230	1 11	5	90	0	5	1·82	1·64	·98	1·80	sl. sh. sand
V-231	1 11	45	55	0	0	·24	·70	2·04	·25	sd. shell
V-233	1 11	0	28	25	47	7·74	5·28	2·41	2·75	ssc.
V-234	1 11	0	11	21	68	0	6·41	2·21	2·85	st. clay
V-236	1 11	0	26	25	49	7·89	5·18	2·26	3·00	ssc.
V-238	1 11	0	19	44	37	6·58	5·34	1·95	2·85	cl. st.
V-240	0 10	0	93	5	2	2·99	2·98	·85	2·90	sand
V-244	1 11	0	7	45	47	7·89	6·99	1·54	3·75	st. clay
V-246	1 11	0	33	29	38	5·91	4·86	2·29	2·65	ssc.
V-248	1 11	0	64	27	9	3·49	3·63	1·46	3·05	st. sd.
V-249	1 11	0	22	36	42	6·84	5·14	2·05	2·85	ssc.
V-250	1 11	0	7	36	57	8·52	6·30	1·65	3·85	st. clay
V-251	1 11	0	8	40	52	8·14	6·38	1·84	2·80	st. clay
V-252	1 11	0	10	32	58	8·42	6·73	1·68	3·85	st. clay
V-253	1 11	0	7	29	64	8·78	6·74	1·70	3·85	st. clay
V-254	1 11	0	2	31	67	8·62	7·40	1·27	3·85	st. clay
V-255	1 11	0	0	39	61	8·52	7·15	1·35	3·85	st. clay
V-256	1 11	0	5	35	60	8·60	6·78	1·55	3·85	st. clay
V-257	1 11	0	0	39	61	8·49	7·30	1·17	3·85	st. clay
V-258	1 11	0	8	43	49	7·92	6·64	1·92	2·80	st. clay
V-259	1 11	0	8	54	38	6·12	5·64	1·43	3·85	cl. silt

V–260	0	10	16	32	29	23	4·14	2·78	3·43	2·25	sh. ssc.
V–261	1	11	2	87	6	5	2·23	2·15	1·49	2·10	sl. sh. sand
V–262	1	11	8	52	21	19	3·21	3·15	2·85	1·80	sh. st. sd.
V–263	1	11	2	26	40	32	5·33	5·22	2·58	2·80	sl. sh. ssc.
V–264	1	11	1	31	29	39	6·30	5·07	2·80	2·40	sl. sh. ssc.
V–265	1	11	3	39	23	35	5·25	4·20	2·88	2·25	sl. sh. ssc.
V–266	1	11	17	51	11	21	1·31	1·36	2·74	·65	sl. sh. cl. sd.
V–267	1	11	0	34	20	46	7·21	4·92	2·45	2·75	sd. cl.
V–268	0	10	0	16	27	57	0	5·39	2·06	3·00	st. clay
V–269	1	11	1	32	17	50	7·98	4·44	2·76	2·50	sl. sh. sd. cl.
V–270	1	11	35	27	10	28	·63	·45	3·25	0	sd. cl. sh.
V–271	1	11	0	19	24	57	0	4·97	2·08	2·85	st. cl.
V–272	1	11	10	42	12	36	2·88	3·29	3·70	1·10	sh. cl. sand
V–273	1	11	6	25	11	58	0	3·71	3·32	2·35	sh. sd. clay
V–274	1	11	12	36	13	39	4·51	2·68	3·32	1·25	sh. sd. clay
V–275	1	11	7	47	12	34	3·29	2·52	2·73	1·50	sh. cl. sand
V–276	1	11	9	35	14	42	5·80	3·11	3·26	1·40	sh. sd. clay
V–277	1	11	1	39	24	36	6·87	3·45	2·05	2·40	sl. sh. ssc.
V–278	1	11	1	20	20	59	8·65	5·11	2·79	2·30	sl. sh. sd. cl.
V–279	1	11	6	17	19	58	0	4·13	3·23	2·15	sh. st. clay
V–280	1	11	0	6	21	73	0	6·26	1·74	3·85	st. cl.
V–281	1	11	0	6	22	72	0	6·43	1·68	3·85	st. clay
V–282	1	11	2	29	15	54	8·69	3·77	2·74	2·25	sl. sh. sd. cl.
V–283	0	10	10	54	9	27	1·94	1·90	2·62	1·20	sh. cl. sand
V–284	1	11	1	39	18	42	5·83	3·90	2·20	2·60	sl. sh. sd. cl.
V–285	1	11	3	51	16	30	3·56	3·24	2·36	2·40	sl. sh. cl. sd.
V–287	1	11	9	52	18	21	3·01	2·66	2·62	1·60	sh. ssc.
V–288	1	11	0	68	22	10	2·92	3·22	1·75	2·35	st. sd.
V–289	1	11	0	41	29	30	4·90	4·24	2·10	2·60	ssc.
V–290	1	11	0	13	33	54	8·31	5·85	2·07	2·85	st. cl.
V–291	1	11	0	45	19	36	5·41	4·31	2·35	2·55	cl. sd.
V–292	1	11	0	7	24	69	0	6·79	1·66	3·85	st. clay
V–293	1	11	0	21	40	39	7·58	6·35	2·28	2·70	st. cl.
V–294	1	11	0	1	28	71	0	7·45	1·19	3·85	st. clay
V–295	1	11	0	0	50	50	7·96	8·86	1·34	3·85	cl. silt.
V–296	1	11	0	1	40	59	8·55	6·81	1·43	3·85	st. clay
V–297	1	11	0	4	60	36	6·73	6·07	1·41	3·85	cl. silt
V–298	1	11	0	0	37	63	8·68	7·10	1·25	3·85	st. clay

APPENDIX B—*continued*

Sample Number	Core Interval Analysed (cm)	Gravel Percent	Sand Percent	Silt Percent	Clay Percent	Median in Phi	Mean in Phi	Standard Deviation	Median in Phi of Sand Fraction	Classification—see App. A for Explanation
V-299	1 11	0	0	38	62	8·62	7·22	1·18	3·85	st. clay
V-301	1 11	7	64	19	10	2·44	2·55	2·38	1·60	sh. st. sand
V-302	0 10	1	90	6	3	2·55	2·48	1·28	2·35	sl. sh. sand
V-303	0 10	0	95	2	3	2·18	2·28	1·10	2·15	sand
V-304	0 10	19	78	0	3	1·56	1·24	1·68	1·50	sh. sand
V-305	1 11	0	22	27	51	8·17	5·05	2·17	2·70	ssc.
V-306	1 11	0	3	26	71	0	6·66	1·33	0	st. clay
V-307	1 11	0	1	24	75	0	7·39	1·21	0	st. clay
V-308	1 11	0	0	29	71	0	7·37	1·18	3·85	st. clay
V-309	1 11	0	3	31	66	8·93	7·01	1·47	3·85	st. cl.
V-310	1 11	0	7	31	62	8·75	6·66	1·60	3·85	st. clay
V-311	1 11	0	1	40	59	8·52	7·04	1·28	3·85	st. clay
V-312	1 11	10	69	9	12	1·83	1·86	2·51	1·35	sh. sand
V-313	0 10	0	19	41	40	6·58	5·18	2·32	2·00	cl. st.
V-314	0 10	1	89	6	4	2·18	2·23	1·38	2·00	sl. sh. sand
V-315	1 11	0	72	17	11	2·83	3·08	1·62	2·40	st. sd.
V-316	1 11	0	8	30	62	0	6·29	1·67	3·85	st. clay
V-317	1 11	0	46	19	35	4·25	4·33	2·01	3·25	cl. sand
V-318	1 11	0	32	18	50	7·96	4·95	2·43	2·80	sd. cl.
V-319	1 11	0	0	33	67	8·45	7·83	·89	3·85	st. clay
V-320	1 11	0	2	26	72	0	7·22	1·35	3·85	st. clay
V-321	1 11	0	3	26	71	0	7·19	1·40	3·85	st. clay
V-322	1 11	0	4	27	69	0	6·99	1·53	3·85	st. clay
V-323	1 11	0	3	29	68	0	7·06	1·38	3·85	st. clay
V-324	1 11	0	15	34	51	8·04	5·92	2·10	2·95	st. clay
V-325	1 11	100	0	0	0	1·53	1·58	·32	0	shell
V-326	1 11	0	5	27	68	8·91	7·06	1·53	3·85	st. clay
V-328	1 11	0	3	56	41	7·66	7·14	1·26	3·85	cl. silt
V-329	1 11	0	2	22	76	0	7·02	1·57	3·85	clay
V-330	1 11	0	2	17	81	0	7·18	1·50	3·85	clay

V-331	1	11	0	61	11	28	3·33	3·48	1·84	2·55	cl. sand
V-332	1	11	0	31	15	54	8·33	4·79	2·50	2·65	sd. clay
V-333	1	11	0	18	18	64	0	5·19	2·41	2·55	st. clay
V-334	1	11	0	32	16	52	8·17	4·57	2·41	2·55	sd. clay
V-335	1	11	0	16	22	62	0	5·32	2·32	2·55	st. clay
V-336	1	11	0	30	23	47	7·39	4·56	2·14	2·75	ssc.
V-337	0	10	3	91	3	3	1·98	2·01	1·35	1·95	sl. sh. sand
V-338	1	11	3	51	24	22	3·72	3·42	2·08	2·50	sl. sh. ssc.
V-339	1	11	7	86	2	5	1·90	1·74	1·48	1·80	sh. sand
V-340	1	11	2	86	5	7	2·28	2·36	1·49	2·15	sl. sh. sand
V-341	1	11	10	65	6	19	2·36	1·93	2·15	1·80	sh. cl. sand
V-342	1	11	14	59	6	21	1·83	1·50	2·36	1·15	sh. cl. sand
V-343	0	10	34	64	0	2	·51	·32	1·82	·50	sd. shell
V-344	0	10	3	30	27	40	6·51	3·80	2·60	2·20	sl. sh. ssc.
V-345	1	11	3	3	19	75	0	5·73	2·79	3·75	sl. sh. clay
V-346	1	11	6	38	10	46	6·82	2·52	3·06	1·05	sh. sd. clay
V-347	0	10	8	55	8	29	2·34	2·37	2·68	1·55	sh. cl. sand
V-348	1	11	9	64	6	21	1·98	1·76	2·13	1·60	sh. cl. sand
V-349	0	10	10	70	6	14	1·83	1·72	2·03	1·50	sh. sand
V-350	0	10	15	82	0	3	1·16	·84	1·32	1·15	sh. sand
V-351	0	10	4	82	5	9	1·35	1·55	1·70	1·15	sl. sh. sand
V-352	0	10	14	84	0	2	1·05	·74	1·29	1·05	sh. sand
V-353	0	10	7	91	0	2	1·10	·95	1·04	1·10	sh. sand
V-354	0	10	11	87	0	2	1·16	1·00	1·27	1·15	sh. sand
V-355	0	10	37	52	5	6	1·07	·20	2·93	·60	sd. shell
V-357	0	10	8	78	6	8	2·24	2·14	1·84	2·10	sh. sand
V-359	1	11	2	42	17	39	5·37	3·65	2·52	2·40	sl. sh. cl. sd.
V-360	1	11	5	75	9	11	3·09	2·76	1·80	2·85	sl. sh. sand
V-361	1	11	14	78	4	4	1·26	1·15	1·75	1·20	sh. sand
V-362	0	10	1	93	5	1	2·08	2·10	1·28	2·00	sl. sh. sand
V-363	1	11	0	49	20	31	4·10	3·83	1·80	2·80	cl. sand
V-364	0	10	11	85	3	1	1·32	1·23	1·51	1·25	sh. sand
V-365	1	11	5	81	7	7	2·48	2·48	1·75	2·35	sl. sh. sand
V-366	1	11	8	66	17	9	2·58	2·39	2·06	1·90	sh. st. sand
V-367	1	11	0	63	27	10	3·72	3·80	1·06	3·35	st. sd.
V-370	0	10	2	90	4	4	2·80	2·65	1·19	2·70	sl. sh. sand
V-371	0	10	5	74	9	12	2·36	2·22	1·91	1·80	sl. sh. sand
V-372	0	10	2	85	5	8	2·72	2·68	1·32	2·60	sl. sh. sand

APPENDIX B—*continued*

Sample Number	Core Interval Analysed (cm)	Gravel Percent	Sand Percent	Silt Percent	Clay Percent	Median in Phi	Mean in Phi	Standard Deviation	Median in Phi of Sand Fraction	Classification—see App. A for Explanation
V–373	0 10	12	83	2	3	1·37	1·27	1·60	1·30	sh. sand
V–374	0 10	43	56	0	1	·16	·53	1·38	·15	sd. shell
V–375	0 10	13	86	0	1	1·03	·74	1·23	1·00	sh. sand
V–376	0 10	5	74	5	16	2·25	2·12	1·94	1·90	sl. sh. sand
V–377	0 10	23	63	4	10	1·59	·99	2·41	1·25	sh. sand

APPENDIX C

CALCIUM CARBONATE AND ORGANIC CARBON DETERMINATIONS, TIMOR SEA SEDIMENTS

(NOTE: -0 indicates no determination)

Sample Number	Core Interval Analysed (cm)	$CaCO_3$ in % of silt-clay Fraction	$CaCO_3$ in % of sand Fraction	Total $CaCO_3$	Organic Carbon in % of silt-clay Fraction	Percent clay
V-2	1 11	24	72	53	1·07	14
V-3	1 11	26	89	54	1·12	20
V-4	1 11	29	85	73	·66	17
V-5	1 11	30	66	73	·77	7
V-6	1 11	11	31	40	·31	12
V-7	1 11	24	-0	-0	·63	23
V-8	1 11	25	-0	-0	·72	24
V-9	1 11	28	63	64	·78	11
V-10	0 4	39	-0	-0	·74	11
V-11	1 11	40	43	49	·96	9
V-12	1 11	37	74	69	1·02	16
V-14	1 11	39	96	87	1·22	11
V-15	1 11	41	98	76	1·02	19
V-16	1 11	48	100	98	1·13	42
V-19	1 11	50	99	85	1·29	9
V-21	1 11	55	100	82	1·11	11
V-22	1 11	50	100	86	1·06	13
V-24	1 11	47	100	92	1·23	8
V-25	1 11	55	100	84	1·06	13
V-26	1 11	64	100	76	·90	17
V-27	1 11	71	99	83	·74	14
V-28	1 11	54	100	88	·94	10
V-29	1 11	54	99	89	·88	9
V-33	1 11	85	100	87	1·19	9
V-34	1 11	69	100	89	·84	10
V-36	1 11	67	100	88	·58	16
V-37	1 11	67	100	86	·68	11
V-39	1 11	60	100	83	·62	16
V-40	1 11	56	100	35	·74	13

APPENDIX C—*continued*

Sample Number	Core Interval Analysed (cm)	$CaCO_3$ in % of silt-clay Fraction	$CaCO_3$ in % of sand Fraction	Total $CaCO_3$	Organic Carbon in % of silt-clay Fraction	Percent clay
V–41	1 11	59	100	90	·83	11
V–42	1 11	53	99	86	·90	14
V–43	1 11	49	100	86	·79	14
V–44	1 11	40	99	64	1·04	21
V–45	1 11	35	99	74	·90	16
V–46	1 11	29	100	97	·91	12
V–47	1 11	26	100	82	1·06	16
V–48	1 11	26	96	77	·97	19
V–49	1 11	22	82	62	1·05	26
V–50	1 11	21	95	64	·87	31
V–51	1 11	22	76	64	·85	17
V–52	1 11	87	–0	–0	1·90	6
V–53	1 11	17	–0	–0	1·18	16
V–54	1 11	14	89	53	1·30	31
V–55	1 11	13	99	62	1·31	24
V–56	1 11	15	–0	–0	1·23	49
V–57	1 11	18	73	56	·87	20
V–58	1 11	21	27	29	1·32	13
V–59	1 11	25	87	74	1·37	14
V–60	1 11	30	76	77	1·32	6
V–61	1 11	24	34	35	1·30	8
V–62	1 11	36	89	82	1·34	10
V–63	1 11	40	94	89	1·20	5
V–64	1 11	44	90	87	1·08	5
V–65	1 11	17	54	51	1·21	9
V–66	1 11	18	85	73	1·10	13
V–69	1 11	40	90	84	1·19	7
V–70	1 11	43	92	84	1·16	10
V–71	1 11	36	94	85	1·20	8
V–72	1 11	44	96	81	1·06	17
V–73	1 11	39	91	79	1·08	15
V–74	1 11	39	95	80	1·30	16

V–75	0	10	34	91	68	1·20	24
V–75	1	20	36	–0	–0	1·39	14
V–75	20	28	30	88	61	1·20	21
V–76	1	11	42	95	78	1·25	18
V–77	1	11	41	88	73	1·10	20
V–78	1	11	41	91	71	1·26	25
V–79	1	11	38	99	76	1·14	22
V–80	1	11	34	98	65	1·35	35
V–81	1	11	35	99	59	1·35	37
V–82	1	11	34	99	72	1·29	31
V–83	1	11	28	100	96	1·66	3
V–85	1	11	38	96	85	1·13	14
V–86	1	11	36	99	56	1·52	49
V–87	1	11	33	100	38	1·63	64
V–88	1	11	41	100	50	1·37	27
V–89	1	11	44	100	83	1·62	16
V–90	1	11	47	100	73	1·54	25
V–91	1	11	44	54	77	1·85	11
V–92	1	11	52	100	88	1·57	12
V–93	1	11	53	100	85	1·77	9
V–94	1	11	61	100	84	1·18	12
V–96	1	11	56	100	89	1·82	10
V–97	1	11	58	100	75	1·30	7
V–98	1	11	48	100	83	1·48	11
V–99	1	11	41	100	69	1·13	29
V–100	1	11	43	100	78	·85	22
V–101	1	11	36	100	75	·99	26
V–102	1	11	34	100	50	1·15	55
V–103	1	11	32	100	43	1·10	59
V–104	1	11	30	100	68	1·12	34
V–105	1	11	27	100	33	1·23	69
V–106	1	11	27	100	43	1·25	56
V–107	1	11	24	100	32	1·32	64
V–108	1	11	24	100	61	1·24	40
V–109	1	11	20	100	68	1·34	31
V–110	1	11	22	100	55	1·26	46
V–111	1	11	20	100	61	1·29	36
V–112	1	11	21	100	51	1·26	34

APPENDIX C—*continued*

Sample Number	Core Interval Analysed (cm)	$CaCO_3$ in % of silt-clay Fraction	$CaCO_3$ in % of sand Fraction	Total $CaCO_3$	Organic Carbon in % of silt-clay Fraction	Percent clay
V–113	1 11	24	100	70	·98	27
V–114	1 11	21	98	65	1·30	21
V–115	1 11	24	100	67	1·23	19
V–116	1 11	23	100	58	1·25	39
V–117	1 11	24	98	62	1·31	33
V–118	1 11	30	98	77	1·19	19
V–119	1 11	29	93	79	1·18	17
V–120	1 11	31	86	78	1·10	11
V–121	1 11	29	–0	–0	1·17	2
V–122	1 11	26	–0	–0	1·24	11
V–123	1 11	30	73	75	1·21	5
V–124	1 11	34	47	48	1·32	4
V–125	1 11	34	79	74	1·25	10
V–126	1 11	1	76	36	1·32	33
V–127	1 11	36	92	81	1·12	12
V–128	1 11	12	69	60	·84	13
V–129	1 11	16	90	66	·62	15
V–130	1 11	15	37	35	·81	11
V–131	1 11	15	49	32	·81	17
V–132	1 11	15	58	33	1·00	19
V–133	1 11	15	56	40	1·17	18
V–134	1 11	16	40	33	1·25	16
V–135	1 11	16	27	25	1·19	12
V–136	1 11	16	50	35	1·10	21
V–137	1 11	15	85	56	1·13	20
V–138	1 11	15	92	53	1·09	30
V–139	1 11	19	95	51	·98	34
V–140	1 11	19	96	56	·91	33
V–141	1 11	21	100	41	·96	44
V–142	1 11	17	98	41	1·31	45
V–143	1 11	17	100	24	1·32	55
V–144	1 11	19	100	21	1·26	61

V–145	1	11	21	100	21	1·17	66
V–146	1	11	19	100	62	1·25	34
V–147	1	11	21	99	64	1·23	21
V–148	1	11	26	93	57	·77	35
V–149	1	11	23	99	50	1·16	38
V–150	1	9	24	100	32	1·14	58
V–151	6	16	23	96	70	1·35	20
V–152	1	11	27	97	71	1·32	20
V–153	1	11	32	96	49	·90	37
V–154	1	11	36	100	74	1·22	24
V–155	1	11	40	99	76	1·31	20
V–156	1	11	47	100	94	1·16	3
V–157	1	11	45	99	81	1·06	10
V–159	1	11	51	100	74	1·02	25
V–160	1	11	58	100	63	·99	42
V–161	1	11	56	97	71	1·04	17
V–162	1	11	66	99	99	·91	14
V–163	1	11	63	100	93	·79	6
V–165	1	11	33	100	95	·61	7
V–166	1	11	62	76	79	·84	6
V–167	1	11	46	85	82	·73	8
V–168	1	11	44	78	76	·91	9
V–169	0	5	49	92	89	·60	5
V–170	1	11	48	94	87	·99	10
V–172	1	11	49	95	85	·76	13
V–173	1	11	35	98	87	1·12	12
V–174	1	11	30	97	69	1·16	15
V–175	1	11	30	100	78	1·22	21
V–176	1	11	25	99	78	1·29	17
V–177	1	11	25	98	84	1·21	20
V–178	1	11	22	96	64	1·35	33
V–179	1	11	19	99	65	1·19	31
V–180	1	11	21	100	64	1·10	33
V–181	1	11	23	98	66	1·23	31
V–182	1	11	24	94	72	1·37	22
V–183	1	11	25	91	76	1·07	16
V–184	1	11	27	76	72	1·35	8
V–185	1	11	33	–0	–0	·88	10

APPENDIX C—*continued*

Sample Number	Core Interval Analysed (cm)	$CaCO_3$ in % of silt-clay Fraction	$CaCO_3$ in % of sand Fraction	Total $CaCO_3$	Organic Carbon in % of silt-clay Fraction	Percent clay
V–186	1 11	32	88	82	1·14	8
V–187	1 11	35	64	67	1·01	6
V–188	1 11	32	57	58	1·00	6
V–189	1 11	25	85	71	1·12	12
V–190	1 11	23	95	85	·76	8
V–191	1 11	19	94	90	·64	2
V–192	1 11	15	56	51	·71	15
V–194	1 11	4	28	38	·60	1
V–195	1 11	17	71	64	·83	11
V–196	1 11	12	44	41	·75	13
V–197	1 11	11	82	72	·75	10
V–198	1 11	7	80	51	1·05	19
V–199	1 ·11	8	57	47	·61	13
V–200	1 11	5	16	16	·99	25
V–201	1 11	5	18	14	·85	19
V–202	1 11	7	16	13	·88	20
V–203	1 11	7	67	50	·95	24
V–203	41 43	1	–0	–0	1·09	70
V–204	1 11	9	95	67	1·00	22
V–205	1 11	11	86	67	·97	18
V–206	1 11	11	43	44	·92	13
V–207	1 11	18	40	0	1·08	0
V–208	1 11	62	–0	–0	1·09	43
V–209	1 11	19	92	87	1·18	6
V–210	1 11	20	14	17	1·07	7
V–211	0 10	22	–0	–0	1·24	21
V–212	1 11	29	91	65	1·19	26
V–213	1 11	26	99	85	1·04	14
V–214	1 11	29	99	84	1·14	15
V–215	1 11	35	97	84	·84	14
V–216	1 11	35	93	81	1·17	14
V–217	1 11	48	98	84	·67	16

V–218	1	11	69	99	93	·57	9
V–219	0	10	43	99	79	·63	14
V–220	1	11	66	100	90	·66	10
V–221	1	11	80	100	95	·48	9
V–222	1	11	69	89	83	1·00	9
V–223	1	11	66	100	90	1·00	6
V–224	0	10	64	92	78	1·25	3
V–225	1	11	81	100	95	·72	3
V–226	1	11	53	100	98	·62	4
V–227	0	0	85	95	96	·74	0
V–228	0	10	75	100	99	·65	1
V–233	1	11	66	100	76	·63	47
V–234	1	11	43	100	49	·99	68
V–236	1	11	36	100	53	1·34	49
V–238	1	11	72	100	77	1·18	37
V–240	0	10	58	100	97	1·01	2
V–244	1	11	59	100	62	1·04	47
V–246	1	11	68	100	79	1·22	38
V–248	1	11	69	100	89	1·67	9
V–249	1	11	62	100	70	1·40	42
V–250	1	11	53	100	56	1·59	57
V–251	1	11	54	100	58	1·54	52
V–252	1	11	40	100	46	1·44	58
V–253	1	11	37	100	41	1·10	64
V–254	1	11	26	100	27	·78	67
V–255	1	11	14	–0	86	·87	61
V–256	1	11	12	100	16	·99	60
V–257	1	11	16	–0	16	1·00	61
V–258	1	11	56	100	60	1·02	49
V–259	1	11	73	100	70	·98	38
V–260	0	10	72	99	85	1·13	23
V–261	1	11	53	99	94	1·08	5
V–262	1	11	51	99	80	1·00	19
V–263	1	11	55	98	67	1·07	32
V–264	1	11	47	100	64	1·04	39
V–265	1	11	38	99	64	1·20	35
V–266	1	11	37	100	80	1·20	21
V–267	1	11	34	98	56	1·10	46

Sample Number	Core Interval Analysed (cm)	$CaCO_3$ in % of silt-clay Fraction	$CaCO_3$ in % of sand Fraction	Total $CaCO_3$	Organic Carbon in % of silt-clay Fraction	Percent clay
V–268	0 10	34	100	48	1·23	57
V–269	1 11	26	95	49	1·40	50
V–270	1 11	24	100	71	1·01	28
V–271	1 11	28	100	42	·86	57
V–272	1 11	26	100	64	·75	36
V–273	1 11	25	100	48	·85	58
V–274	1 11	22	98	59	·83	39
V–275	1 11	21	100	64	·94	34
V–276	1 11	19	95	53	1·01	42
V–277	1 11	24	100	54	·93	36
V–278	1 11	25	100	42	·99	59
V–279	1 11	28	100	45	·98	58
V–280	1 11	27	100	31	·93	73
V–281	1 11	30	100	34	1·01	72
V–282	1 11	30	98	51	·92	54
V–283	0 10	32	100	76	1·05	27
V–284	1 11	36	100	62	·84	42
V–285	1 11	42	99	73	·81	30
V–287	1 11	51	99	80	1·16	21
V–288	1 11	64	100	88	1·10	10
V–289	1 11	62	100	76	1·43	30
V–290	1 11	45	100	52	1·52	54
V–291	1 11	58	100	87	1·49	36
V–292	1 11	55	100	58	1·46	69
V–293	1 11	40	100	53	1·08	39
V–294	1 11	50	100	51	·82	71
V–295	1 11	24	–0	24	1·30	50
V–296	1 11	37	100	38	·91	59
V–297	1 11	22	100	24	·92	36
V–298	1 11	27	–0	27	·69	63
V–299	1 11	17	–0	17	·88	62
V–301	1 11	61	100	89	·73	10

V-302	0	10	54	100	96	·86	3
V-303	0	10	62	98	96	·58	3
V-304	0	10	59	100	99	·76	3
V-305	1	11	49	100	60	1·43	51
V-306	1	11	30	100	30	1·01	71
V-307	1	11	22	100	22	·82	75
V-308	1	11	56	–0	56	·94	71
V-309	1	11	43	100	46	·98	66
V-310	1	11	46	100	50	·96	62
V-311	1	11	12	100	13	1·09	59
V-312	1	11	19	–0	–0	·76	12
V-313	0	10	17	100	24	·80	40
V-314	0	10	11	100	91	·94	4
V-315	1	11	9	99	74	1·02	11
V-316	1	11	7	100	14	1·33	62
V-317	1	11	59	100	78	·87	35
V-318	1	11	59	100	72	·99	50
V-319	1	11	46	–0	46	·97	67
V-320	1	11	40	100	42	·92	72
V-321	1	11	23	100	26	·88	71
V-322	1	11	19	100	23	·85	69
V-323	1	11	15	100	17	1·57	68
V-324	1	11	16	100	29	1·43	51
V-325	1	11	15	97	0	1·42	0
V-326	1	11	33	100	38	·85	68
V-328	1	11	40	100	43	·72	41
V-329	1	11	34	100	36	·56	76
V-330	1	11	36	100	38	·80	81
V-331	1	11	26	100	71	·89	28
V-332	1	11	40	100	59	1·18	54
V-333	1	11	41	99	51	1·42	64
V-334	1	11	30	100	54	1·90	52
V-335	1	11	37	100	44	1·64	62
V-336	1	11	42	98	59	1·68	47
V-338	1	11	43	96	72	1·50	22
V-339	1	11	31	98	93	1·15	5
V-340	1	11	29	95	87	1·12	7
V-341	1	11	34	97	82	1·07	19

APPENDIX C—*continued*

Sample Number	Core Interval Analysed (cm)	$CaCO_3$ in % of silt-clay Fraction	$CaCO_3$ in % of sand Fraction	Total $CaCO_3$	Organic Carbon in % of silt-clay Fraction	Percent clay
V–342	1 11	32	95	79	1·14	21
V–343	0 10	24	100	98	1·39	2
V–344	0 10	15	89	40	1·21	40
V–345	1 11	15	100	94	1·25	75
V–346	1 11	18	86	49	1·32	46
V–347	0 10	20	86	63	1·27	29
V–348	1 11	23	78	65	1·57	21
V–349	0 10	29	81	68	1·38	14
V–352	0 10	5	100	98	1·61	2
V–351	0 10	37	97	87	1·46	9
V–354	0 10	31	100	99	·77	2
V–355	0 10	41	100	94	1·22	6
V–357	0 10	35	99	90	1·71	8
V–359	1 11	36	97	63	1·48	39
V–360	1 11	43	100	89	1·65	11
V–361	1 11	43	100	95	1·35	4
V–362	0 10	41	100	96	1·25	1
V–363	1 11	49	100	74	1·07	31
V–364	0 10	43	100	98	1·40	1
V–365	1 10	54	99	93	1·04	7
V–366	1 11	57	98	88	1·20	9
V–367	1 11	59	97	83	·97	10
V–370	0 10	43	96	92	·96	4
V–371	0 10	46	98	87	1·29	12
V–372	0 10	40	94	87	1·41	8
V–373	0 10	33	99	96	1·51	3
V–374	0 10	13	100	99	1·31	1
V–375	0 10	15	100	99	1·14	1
V–376	0 10	31	92	80	1·43	16
V–377	0 10	28	77	70	1·37	10

APPENDIX D

PETROGRAPHIC THIN SECTION ANALYSES, 0·062–2·000 mm FRACTION OF TIMOR SEA SEDIMENTS

Sample Number	Core Interval Analysed (cm)	Percent Sand	Coralline Algae	Halimeda	Corals	Large Foraminifera	Small Foraminifera	Mollusca	Echinoids	Bryozoa	Alcyonaria	Misc. Skeletal	Total Skeletal	Ooids	Faecal Pellets	Lithoclasts	Terrigenous	Glauconite	Misc. Non-skeletal	Total Non-skeletal	Glauconitized in percent of all others	Undetermined in percent of all others
V-2	1 11	58·0	1·3	–0	8·0	4·1	19·2	15·0	6·1	6·8	1·9	·9	63·3	–0	–0	2·9	28·1	·3	·6	31·9	·6	4·8
V-3	1 11	64·0	·3	·6	3·2	6·1	29·6	15·9	14·2	5·5	2·9	–0	78·3	–0	–0	2·0	10·4	·3	·3	13·0	4·9	8·7
V-4	1 11	59·0	–0	·6	4·3	5·2	22·9	13·0	12·5	11·0	1·4	·6	71·5	1·1	–0	3·2	15·1	–0	·3	19·7	4·6	9·8
V-5	1 11	57·0	·3	2·3	7·3	4·3	14·4	12·4	6·0	4·0	1·7	–0	52·7	1·7	–0	7·3	34·4	–0	–0	43·4	7·0	3·9
V-6	1 11	50·0	–0	–0	2·0	1·3	1·3	7·0	2·0	3·3	1·3	·3	18·5	2·7	–0	6·4	68·7	–0	–0	77·8	·7	3·7
V-9	1 11	67·0	·9	–0	2·2	3·5	2·2	23·3	7·3	10·4	–0	·9	50·7	·3	–0	10·4	37·2	–0	–0	47·9	3·5	1·4
V-11	1 9	75·0	·3	–0	5·3	5·9	3·6	10·3	3·8	6·5	1·2	–0	36·9	–0	–0	4·4	56·6	·3	·3	61·6	1·5	1·5
V-12	1 11	60·0	–0	–0	2·7	2·9	15·1	17·4	12·7	9·2	1·2	–0	61·2	–0	–0	8·0	25·4	·6	–0	34·0	9·2	4·8
V-14	1 11	61·0	–0	·9	·6	9·3	12·5	15·6	12·5	2·9	2·2	·3	56·8	–0	–0	37·4	1·9	2·2	–0	41·5	11·2	1·7
V-15	1 11	53·0	·3	·3	·3	12·2	28·4	26·1	13·1	3·4	3·1	·6	87·8	–0	–0	5·1	·3	1·7	–0	7·1	7·1	5·1
V-19	1 11	65·0	1·1	3·3	4·6	15·6	24·9	12·3	5·2	9·6	3·8	–0	80·4	–0	–0	1·9	·5	–0	–0	2·4	2·7	17·2
V-21	1 11	53·0	4·0	4·0	7·5	9·9	20·9	16·6	10·5	7·2	2·7	·8	84·1	–0	–0	1·1	–0	–0	–0	1·1	·8	14·8
V-22	1 11	57·0	·7	·3	9·4	12·9	29·4	24·7	6·6	8·7	1·0	–0	93·7	–0	–0	2·1	–0	–0	–0	2·1	2·1	4·2
V-24	1 11	80·0	4·8	3·3	8·9	13·4	12·3	16·4	5·2	4·8	6·7	1·5	77·3	–0	–0	7·1	–0	–0	–0	7·1	4·5	15·6
V-25	1 11	50·0	6·1	16·3	6·7	21·2	12·5	8·7	3·2	12·2	2·6	–0	90·4	–0	–0	1·2	–0	–0	–0	1·2	2·6	8·4
V-26	1 11	33·0	1·4	2·9	2·9	3·6	58·4	6·6	5·5	2·6	1·8	–0	86·1	–0	–0	2·6	–0	–0	–0	2·6	–0	11·3
V-27	1 11	40·0	·4	4·0	1·1	5·1	52·4	4·0	7·6	2·3	2·9	·7	80·5	–0	–0	·4	·7	–0	·4	1·5	·7	18·0
V-28	1 11	72·0	·3	1·4	·3	2·0	75·8	3·4	3·0	1·7	–0	–0	87·9	–0	–0	–0	·3	–0	–0	·3	·3	11·8
V-29	1 11	75·0	·3	5·6	1·4	8·1	42·9	7·6	9·0	2·0	4·8	·5	82·2	–0	–0	1·7	·8	–0	·3	2·8	5·3	15·0
V-33	1 11	11·0	–0	3·0	–0	–0	78·4	–0	2·2	·9	·4	–0	84·9	–0	–0	·4	–0	–0	–0	·4	–0	14·7
V-34	1 7	66·0	1·8	1·4	·7	1·4	66·3	2·8	6·6	–0	3·1	–0	84·1	–0	–0	1·0	·3	–0	–0	1·3	·7	14·6
V-36	1 11	34·0	·7	4·0	2·2	2·9	60·9	8·3	7·6	1·8	1·4	–0	89·8	–0	–0	1·4	–0	–0	–0	1·4	–0	8·8
V-37	1 11	53·0	1·8	5·3	2·5	5·7	35·7	12·4	6·0	3·2	2·8	–0	75·4	–0	–0	10·7	–0	–0	–0	10·7	·4	13·9
V-39	1 11	48·0	4·0	1·2	6·1	8·3	26·4	25·1	4·0	11·6	1·5	–0	88·2	–0	–0	8·2	–0	–0	–0	8·2	1·5	3·6
V-40	1 11	60·0	2·5	3·9	1·8	7·4	42·5	13·4	5·6	2·1	1·4	–0	80·6	–0	–0	2·1	–0	·3	–0	2·4	1·8	17·0
V-41	1 11	70·0	6·0	8·5	4·1	23·2	18·9	10·4	6·9	6·0	3·2	·3	87·8	–0	–0	6·9	·3	–0	–0	7·2	3·4	5·0
V-42	1 11	65·0	1·2	5·9	2·6	9·1	27·4	17·4	10·0	10·0	2·1	–0	85·7	–0	–0	4·7	·6	·3	–0	5·6	5·3	8·7
V-43	1 11	63·0	6·8	2·9	1·9	18·4	7·8	16·8	5·8	20·4	2·3	–0	83·1	–0	–0	12·6	·3	–0	·3	13·2	8·7	3·7
V-44	1 11	52·0	2·5	2·8	6·0	7·4	18·7	16·9	7·7	15·5	2·1	–0	79·6	–0	–0	15·8	·7	–0	·3	16·8	4·6	3·6
V-45	1 11	67·0	3·1	2·2	6·8	6·8	12·6	21·6	9·2	15·1	1·8	–0	79·2	–0	–0	15·1	·9	·3	–0	16·3	11·4	4·5
V-47	1 11	61·0	3·7	1·5	11·8	8·1	6·2	16·4	9·3	13·7	2·8	–0	74·1	–0	–0	20·5	·3	–0	–0	20·8	14·6	5·1
V-48	1 11	56·0	2·1	2·5	5·2	4·3	20·6	21·5	7·1	9·2	2·5	–0	75·0	–0	–0	13·8	3·1	·6	–0	17·5	22·1	7·5
V-49	1 11	53·0	–0	·9	4·7	6·0	15·8	24·3	8·8	7·6	·9	·6	69·6	–0	–0	6·0	14·5	3·5	–0	24·0	17·3	6·4
V-50	1 11	49·0	2·3	1·6	9·6	8·9	10·3	19·9	8·6	10·6	3·0	–0	74·8	·7	–0	15·2	5·3	–0	–0	21·2	13·9	4·0
V-51	1 11	70·0	–0	·4	2·5	2·5	13·8	25·1	7·3	7·6	·7	1·1	61·0	1·4	–0	9·4	21·4	2·9	–0	35·1	13·5	3·9
V-54	1 11	41·0	·3	·3	7·8	4·8	16·1	22·9	9·9	5·4	·6	1·2	69·3	·3	–0	16·3	10·5	·6	–0	27·7	3·0	3·3
V-55	1 11	52·0	3·5	–0	11·3	7·4	6·1	29·4	12·0	12·6	2·9	–0	85·2	–0	–0	11·0	·6	–0	·3	11·9	10·7	2·9
V-57	1 11	59·0	–0	·3	1·7	5·8	9·6	33·5	5·1	3·7	3·4	1·4	64·5	–0	–0	4·1	23·3	3·4	·3	31·1	6·5	4·4

APPENDIX D—*continued*

Sample Number	Core Interval Analysed (cm)	Percent Sand	Coralline Algae	Halimeda	Corals	Large Foraminifera	Small Foraminifera	Mollusca	Echinoids	Bryozoa	Alcyonaria	Misc. Skeletal	Total Skeletal	Ooids	Faecal Pellets	Lithoclasts	Terrigenous	Glauconite	Misc. Non-skeletal	Total Non-skeletal	Glauconitized in percent of all others	Undetermined in percent of all others
V–58	1 11	76·0	–0	–0	–0	1·0	7·8	5·9	4·9	1·0	–0	·7	21·3	–0	–0	2·3	71·9	1·3	–0	75·8	–0	2·9
V–59	1 11	55·0	1·4	·3	2·1	5·6	16·4	24·8	8·6	5·6	3·9	–0	68·7	–0	–0	8·1	10·9	2·1	–0	22·5	9·2	8·8
V–60	1 11	65·0	·3	·6	2·7	5·3	17·5	23·7	9·2	4·7	2·1	–0	66·1	–0	–0	4·7	23·1	·6	–0	28·4	8·3	5·5
V–61	1 11	83·0	–0	·9	2·1	2·4	3·6	16·2	1·2	1·8	·3	–0	28·5	·3	–0	3·6	64·6	1·2	–0	69·7	1·8	2·1
V–62	1 11	61·0	–0	2·0	6·0	5·4	19·4	27·5	5·7	6·9	2·6	–0	75·5	–0	·3	7·1	9·7	1·4	–0	18·5	7·7	6·0
V–63	1 7	80·0	–0	1·2	2·2	7·5	17·7	25·8	8·1	11·8	1·9	·6	76·8	–0	–0	10·9	6·2	–0	·3	17·4	4·6	5·8
V–64	1 11	70·0	–0	·3	3·0	15·6	13·8	17·7	8·6	9·2	2·7	–0	70·9	–0	–0	14·1	9·8	·3	–0	24·2	6·4	4·9
V–65	1 11	83·0	–0	·3	1·2	3·5	9·3	13·7	8·2	2·3	2·0	–0	40·5	–0	–0	4·4	44·3	1·2	–0	49·9	5·5	9·6
V–66	1 11	66·0	·6	·9	6·6	4·7	15·9	21·9	7·3	5·4	1·9	–0	65·2	·6	–0	14·6	14·2	·3	–0	29·7	18·7	5·1
V–69	1 10	78·0	–0	·6	1·0	9·7	30·6	14·5	10·2	6·6	3·3	–0	76·5	–0	–0	5·9	8·5	1·0	–0	15·4	4·3	8·1
V–70	1 11	65·0	–0	1·1	1·1	14·8	26·5	16·3	4·9	4·6	1·9	–0	81·2	–0	–0	11·4	7·6	·3	–0	19·3	4·9	9·5
V–71	0 0	81·0	–0	·3	3·4	13·6	23·8	16·1	7·4	10·5	1·7	–0	76·8	–0	–0	9·3	4·5	1·1	·3	15·2	5·9	8·0
V–72	1 11	66·0	–0	·7	1·9	8·4	30·8	19·6	7·5	10·0	1·5	–0	80·4	–0	–0	8·7	2·8	1·2	–0	12·7	9·0	6·9
V–73	1 11	61·0	·3	·7	3·5	2·5	21·4	29·9	11·9	2·8	1·8	–0	74·8	–0	–0	5·7	8·5	·3	–0	14·5	3·8	10·7
V–74	1 11	70·0	–0	1·5	2·1	4·8	25·3	38·6	6·7	5·9	1·5	–0	86·4	–0	–0	2·7	3·0	1·8	–0	7·5	4·9	6·1
V–75	0 10	61·0	1·8	·3	2·8	6·0	29·9	13·0	9·5	7·4	2·8	·3	73·8	–0	–0	7·3	8·1	1·0	–0	16·4	3·2	9·8
V–75	20 28	29·0	·4	–0	2·7	7·8	31·8	12·5	5·5	4·3	2·0	·4	67·4	–0	–0	7·1	9·8	2·4	–0	19·3	2·0	13·3
V–76	1 11	68·0	·7	·7	4·1	3·7	22·8	20·4	5·8	5·4	2·4	–0	66·0	–0	–0	21·1	3·1	1·4	–0	25·6	2·7	8·4
V–77	1 11	67·0	·9	3·4	1·1	3·0	23·6	19·2	10·1	3·9	1·4	·3	64·9	–0	–0	8·6	12·1	–0	–0	20·7	2·3	12·4
V–78	1 11	49·0	1·1	·9	1·4	5·3	26·2	14·4	8·7	5·3	1·7	·6	65·6	–0	–0	4·0	7·8	·9	·9	13·6	·9	20·8
V–79	1 11	59·0	·7	1·8	10·6	6·0	24·3	21·5	9·1	3·9	2·8	·7	81·4	–0	–0	2·5	·3	·7	–0	3·5	7·4	15·1
V–80	1 11	46·0	–0	1·2	7·5	5·0	31·3	17·5	8·1	4·3	2·7	·3	77·9	–0	–0	7·0	·6	·9	–0	8·5	4·5	13·6
V–81	1 11	36·0	–0	–0	2·4	8·6	30·1	23·3	9·8	9·8	2·4	–0	86·4	–0	–0	4·0	·6	–0	–0	4·6	2·8	9·0
V–82	1 11	55·0	·9	1·5	7·0	7·9	24·7	17·7	11·3	3·7	2·7	–0	77·4	–0	–0	4·3	·3	·9	–0	5·5	·6	17·1
V–83	1 11	62·0	9·5	9·5	8·3	15·3	3·1	14·1	8·0	19·1	2·8	–0	89·7	–0	–0	6·8	–0	–0	–0	6·8	–0	3·5
V–85	1 11	81·0	–0	1·7	3·4	7·1	12·9	27·1	7·8	4·1	4·1	·3	68·5	–0	–0	5·1	4·1	·3	–0	9·5	4·1	22·0
V–86	1 11	32·0	–0	–0	–0	2·0	52·3	–0	3·4	1·0	1·5	–0	60·2	–0	–0	–0	·3	·3	–0	·6	–0	39·2
V–89	1 11	50·0	7·8	3·7	4·7	10·6	10·9	17·8	7·5	20·6	3·4	–0	87·0	–0	–0	5·6	–0	–0	–0	5·6	1·6	7·4
V–90	1 11	43·0	3·4	·9	6·7	7·8	17·5	19·3	10·7	11·6	2·5	–0	80·4	–0	–0	11·6	–0	–0	–0	11·6	3·7	8·0
V–91	1 11	54·0	4·5	·6	11·5	6·4	5·4	21·5	8·3	17·3	5·4	–0	80·9	–0	–0	11·2	·6	–0	–0	11·8	3·8	7·3
V–92	1 11	48·0	1·9	·7	9·0	10·1	23·2	14·2	4·5	14·6	6·4	–0	90·6	–0	–0	7·9	–0	–0	–0	7·9	2·6	7·5
V–93	1 11	63·0	5·7	·6	8·8	7·4	31·2	11·3	9·9	8·2	1·4	–0	84·5	–0	–0	4·7	–0	–0	–0	4·7	5·0	10·8
V–94	1 11	53·0	·7	1·7	1·7	7·6	46·5	10·8	6·2	6·6	2·4	–0	84·2	–0	–0	5·5	–0	–0	–0	5·5	1·7	10·3
V–97	1 11	38·0	3·2	·8	4·0	10·5	19·3	28·3	6·9	8·1	2·4	·8	84·3	–0	–0	6·0	–0	–0	–0	6·0	6·4	9·7
V–98	1 11	55·0	2·6	4·3	10·9	17·0	17·3	8·6	10·4	8·9	2·3	·6	82·9	–0	–0	6·7	·3	–0	–0	7·0	2·6	10·1
V–99	1 11	46·0	·3	10·3	6·3	·3	44·7	12·9	8·4	3·2	1·8	–0	88·7	–0	–0	1·1	–0	–0	–0	1·1	–0	10·7
V–100	1 11	53·0	4·8	4·0	2·2	4·4	40·3	16·1	6·2	4·8	2·6	·7	86·1	–0	–0	4·8	–0	–0	–0	4·8	2·9	9·1
V–101	1 11	55·0	2·5	·9	3·2	7·6	25·1	19·0	7·6	11·4	2·8	–0	80·1	–0	–0	12·4	–0	–0	–0	12·4	2·8	7·5

V–104	1	11	45·0	7·6	3·6	8·5	3·6	4·9	40·5	4·6	4·9	1·0	–0	79·2	6·2	–0	10·5	–0	–0	–0	16·7	4·3	4·1
V–113	1	11	52·0	2·9	–0	17·5	8·8	9·2	17·5	5·5	10·8	7·7	–0	79·9	–0	–0	12·0	·4	–0	–0	12·4	8·0	7·7
V–114	1	11	51·0	·3	·9	5·3	5·6	19·3	30·3	13·3	7·8	–0	–0	82·8	–0	–0	5·9	·3	1·8	·3	8·3	9·5	8·9
V–117	1	11	44·0	–0	–0	5·2	3·3	20·7	31·1	9·6	3·3	3·7	·7	77·6	–0	–0	12·5	1·1	·7	–0	14·3	7·0	8·1
V–118	1	11	57·0	·7	–0	10·9	4·3	22·1	25·7	6·9	7·3	1·3	·3	79·5	–0	–0	15·2	2·0	·3	–0	17·5	14·5	3·0
V–119	1	11	61·0	–0	–0	2·5	2·2	20·1	34·7	9·1	9·5	2·2	–0	80·3	–0	–0	7·7	7·3	–0	–0	15·0	10·2	4·7
V–120	1	11	70·0	·3	·3	1·6	3·9	12·0	37·2	7·4	8·7	2·3	–0	73·7	–0	–0	7·1	13·9	·3	–0	21·3	9·1	5·0
V–123	0	10	57·0	–0	3·5	4·2	6·3	8·6	21·5	6·2	6·5	3·1	–0	59·9	–0	–0	10·0	27·0	·3	–0	37·3	7·9	2·8
V–124	1	11	89·0	–0	–0	·9	3·5	12·0	17·7	4·1	2·5	–0	–0	40·7	–0	–0	3·8	52·1	·6	–0	56·5	5·0	2·8
V–125	1	11	68·0	·6	·6	1·5	7·6	12·7	20·3	10·9	10·0	·6	–0	64·8	–0	–0	10·9	19·4	1·2	–0	31·5	9·1	3·7
V–126	1	10	39·0	–0	·3	2·1	10·2	17·2	19·3	4·9	7·0	2·1	–0	63·1	–0	–0	7·4	22·8	1·0	–0	31·2	18·6	5·7
V–127	1	11	73·0	·4	·4	5·0	11·2	29·6	14·4	7·9	10·8	2·5	–0	82·2	–0	–0	6·1	7·9	·4	–0	14·4	9·7	3·4
V–128	1	11	52·0	–0	–0	7·2	6·2	7·5	19·0	5·2	5·2	1·0	–0	51·3	–0	–0	12·8	30·4	·3	·3	43·8	1·6	4·9
V–129	1	11	50·0	–0	·3	16·2	3·5	6·8	18·7	6·9	12·5	1·6	·6	67·1	–0	–0	20·0	10·3	–0	–0	30·3	1·8	2·6
V–130	1	11	67·0	–0	–0	3·6	·4	8·2	10·0	2·9	2·1	2·1	·7	30·1	–0	–0	4·6	62·9	·4	–0	67·8	1·5	2·1
V–131	1	11	51·0	–0	–0	1·5	·7	20·6	5·7	9·2	1·1	1·1	–0	39·9	–0	–0	·7	49·1	1·5	–0	51·3	1·5	8·8
V–132	1	11	41·0	–0	–0	·5	2·4	24·3	2·9	8·1	1·9	–0	–0	40·1	–0	–0	10·9	39·5	2·4	1·9	56·7	7·1	5·2
V–133	1	11	54·0	–0	–0	1·0	3·4	9·8	19·2	9·4	6·1	–0	–0	48·8	–0	–0	4·0	41·7	2·5	–0	48·2	9·1	3·0
V–134	1	11	64·0	1·3	–0	1·3	3·0	9·7	6·3	6·3	6·8	–0	·4	35·1	–0	–0	2·5	57·4	2·5	·4	62·8	4·6	2·1
V–135	1	11	75·0	·4	–0	·4	3·8	6·1	7·5	2·1	2·7	–0	–0	23·0	–0	–0	2·0	70·4	2·1	1·7	76·2	1·0	·8
V–136	1	11	51·0	–0	·6	–0	3·1	12·8	17·7	4·6	1·1	2·3	–0	42·2	–0	–0	5·2	50·3	–0	–0	55·5	3·4	2·3
V–137	1	11	50·0	–0	–0	5·6	5·6	15·8	28·9	6·7	6·7	·4	–0	69·7	–0	–0	12·7	14·8	·4	–0	27·9	4·9	2·4
V–138	1	11	40·0	1·1	–0	6·8	6·2	9·6	26·9	4·2	8·5	4·2	–0	67·5	–0	–0	19·8	7·1	·6	–0	27·5	8·2	5·0
V–139	1	11	33·0	·4	1·5	3·7	12·0	16·8	26·2	6·4	10·1	1·9	–0	79·0	·7	–0	9·4	4·5	·4	–0	15·0	9·4	6·0
V–140	1	11	39·0	·6	·3	2·8	9·2	15·0	33·1	4·9	6·1	3·7	–0	75·7	·6	–0	18·1	4·3	–0	–0	23·0	8·9	1·3
V–142	1	11	28·0	3·6	1·3	10·5	3·3	7·2	22·0	16·4	17·4	1·6	–0	83·3	·6	–0	12·5	2·0	–0	–0	15·1	6·9	1·6
V–146	1	11	27·0	3·3	·3	12·8	8·9	9·5	29·3	6·2	11·2	6·6	–0	88·1	–0	–0	7·6	–0	–0	–0	7·6	19·7	4·3
V–147	1	11	43·0	·7	–0	5·1	6·1	12·3	19·9	5·1	21·0	3·6	–0	73·8	–0	–0	23·5	–0	·7	–0	24·2	9·4	2·0
V–148	1	11	45·0	·3	–0	1·4	6·0	28·4	15·8	17·5	9·1	2·1	–0	80·6	–0	1·4	3·9	6·3	·7	–0	12·3	9·5	7·1
V–149	1	11	29·0	6·3	2·4	14·6	6·3	6·3	19·1	7·2	12·8	2·4	–0	77·4	–0	–0	13·4	·6	·6	–0	14·6	6·6	8·0
V–151	6	16	60·0	·4	–0	2·2	4·1	23·4	30·8	8·2	5·9	1·5	·3	76·5	–0	–0	13·7	2·2	1·9	–0	17·8	14·5	5·4
V–152	1	11	58·0	–0	–0	7·2	5·9	20·5	20·8	8·8	7·5	2·6	–0	73·3	–0	–0	17·9	1·6	1·3	–0	20·8	9·4	5·9
V–153	1	11	27·0	–0	·7	·7	4·8	45·3	9·0	8·7	4·5	·7	–0	74·4	–0	–0	8·3	3·1	1·0	–0	12·4	5·1	13·2
V–154	1	11	56·0	2·1	2·4	4·2	8·4	8·4	26·0	7·8	15·1	2·1	–0	76·5	–0	·6	13·3	·3	–0	–0	14·2	3·3	9·3
V–155	1	11	56·0	·7	·3	4·1	4·8	36·0	16·0	7·8	5·1	1·0	–0	75·8	–0	·7	14·3	1·0	–0	–0	16·0	4·1	8·2
V–156	1	9	63·0	5·1	4·5	8·7	11·7	5·7	20·3	9·3	16·8	1·5	–0	83·6	·3	–0	12·9	–0	–0	–0	13·2	3·0	3·2
V–157	1	11	62·0	·7	2·3	9·8	5·8	22·3	17·0	12·9	5·9	4·9	–0	81·6	–0	–0	8·3	1·1	·3	–0	9·7	5·3	8·7
V–159	1	11	41·0	–0	·7	4·0	10·0	46·3	9·3	5·7	7·3	1·3	–0	84·6	–0	–0	7·4	·3	–0	–0	7·7	·7	7·7
V–161	1	11	36·0	–0	–0	–0	2·2	63·1	3·0	7·9	·4	·7	–0	77·3	–0	–0	6·3	2·6	–0	–0	11·1	–0	11·4
V–162	1	11	77·0	–0	–0	1·7	4·9	61·9	3·5	8·3	1·4	–0	–0	81·7	–0	–0	5·5	1·4	–0	–0	6·9	1·0	11·4
V–163	1	11	56·0	6·4	2·1	6·4	4·9	28·3	10·9	4·6	10·2	3·2	–0	77·0	–0	–0	14·1	·4	–0	–0	14·5	2·1	8·5
V–166	1	11	74·0	–0	·4	1·3	3·2	24·2	1·3	9·3	2·7	1·3	–0	43·7	19·9	1·7	4·2	22·9	·8	–0	49·5	·4	6·8
V–167	1	11	67·0	·8	·8	3·0	4·7	20·8	9·5	15·2	4·8	1·1	–0	60·7	–0	1·9	12·1	14·7	–0	–0	28·7	2·3	10·6
V–168	1	11	71·0	–0	–0	3·9	8·0	23·2	9·0	6·1	8·4	2·6	–0	61·2	–0	2·9	9·6	21·2	·3	–0	34·0	4·1	4·8
V–169	0	5	60·0	–0	·6	2·1	7·5	8·3	23·1	3·8	5·8	1·8	·6	52·7	–0	–0	36·6	6·8	1·5	–0	44·9	4·1	2·4
V–170	1	11	80·0	·7	·3	1·3	11·0	26·1	15·2	10·3	4·0	1·0	–0	69·9	–0	·3	9·6	5·3	1·0	·3	16·5	2·3	13·6
V–172	1	11	74·0	·9	·3	2·5	6·6	33·0	10·7	14·8	4·7	·9	–0	74·4	–0	–0	8·4	3·1	2·2	·9	14·6	1·8	11·0
V–173	1	11	67·0	·3	2·7	3·9	4·8	24·3	26·4	5·4	6·4	1·8	–0	76·0	–0	–0	11·4	·6	·9	–0	12·9	3·6	11·1
V–174	1	11	48·0	3·0	4·6	5·9	6·6	18·4	22·7	7·9	5·6	1·3	–0	76·0	–0	·3	8·9	2·0	1·3	–0	12·5	5·9	11·5
V–175	1	11	57·0	2·3	·8	14·3	4·3	13·2	16·9	7·7	22·9	2·3	–0	84·7	–0	–0	11·7	–0	–0	–0	11·7	6·9	3·6
V–176	1	11	62·0	·7	–0	3·4	4·1	19·9	41·3	13·0	4·1	3·4	–0	89·9	–0	–0	2·3	–0	1·0	–0	3·3	11·0	6·8
V–177	1	11	53·0	2·8	–0	2·8	2·5	20·0	44·1	5·3	5·3	4·3	1·0	88·1	–0	–0	5·6	·7	1·0	–0	7·3	9·1	4·6

Sample Number	Core Interva Analysed (cm)	Percent Sand	Coralline Algae	Halimeda	Corals	Large Foraminifera	Small Foraminifera	Mollusca	Echinoids	Bryozoa	Alcyonaria	Misc. Skeletal	Total Skeletal	Ooids	Faecal Pellets	Lithoclasts	Terrigenous	Glauconite	Misc. Non-skeletal	Total Non-skeletal	Glauconitized in percent of all others	Undetermined in percent of all others
V–178	1 11	48·0	·4	·4	2·9	2·9	35·4	18·7	16·5	3·2	3·2	–0	83·7	–0	·4	4·0	2·2	1·4	–0	8·0	4·3	8·3
V–179	1 11	34·0	2·4	·3	3·0	3·0	20·9	46·8	6·1	3·3	2·9	5·0	93·7	–0	–0	1·5	·9	–0	–0	2·4	3·9	3·3
V–180	1 11	33·0	–0	·6	–0	·9	38·9	25·8	5·9	11·2	1·9	–0	85·2	–0	–0	4·4	·3	–0	–0	4·7	1·9	10·1
V–181	1 11	37·0	1·8	–0	·7	3·0	28·5	30·4	8·9	5·9	2·6	–0	81·8	–0	–0	7·0	1·8	·4	–0	9·2	3·3	9·0
V–182	1 11	55·0	–0	·3	4·2	3·6	18·8	37·1	7·3	11·2	2·4	–0	84·9	–0	–0	1·5	6·4	–0	–0	7·9	7·3	7·2
V–183	1 11	68·0	–0	·3	4·6	2·8	17·6	25·4	9·6	9·9	3·1	–0	73·3	–0	–0	11·1	8·0	1·2	–0	20·3	10·2	6·4
V–184	1 11	74·0	–0	–0	1·4	2·9	12·7	36·6	6·1	6·5	2·2	·3	66·7	–0	–0	5·4	23·5	·7	–0	29·6	5·8	1·7
V–186	1 11	73·0	–0	–0	2·7	3·7	19·0	26·1	15·6	7·8	2·4	·7	78·0	–0	–0	9·1	10·2	1·3	–0	20·6	5·8	1·4
V–187	1 11	75·0	·4	–0	3·9	3·5	8·8	16·1	6·0	4·6	1·8	–0	45·1	–0	–0	14·1	35·5	·7	–0	50·3	3·5	4·6
V–188	1 11	83·0	–0	–0	2·0	5·0	13·0	13·7	6·7	5·0	1·0	–0	46·4	–0	–0	4·3	42·0	1·3	–0	47·6	3·7	6·0
V–189	1 11	65·0	–0	–0	2·0	5·0	26·7	16·3	9·0	6·7	·3	1·1	67·1	–0	–0	12·6	13·2	1·4	–0	27·2	10·4	5·7
V–190	1 11	62·0	–0	–0	6·4	6·4	17·0	15·1	10·2	16·7	1·6	–0	73·4	–0	–0	18·9	4·8	–0	·3	24·0	5·1	2·6
V–191	1 11	79·0	–0	–0	9·4	4·5	10·6	20·8	12·4	16·0	2·4	–0	76·1	–0	–0	16·0	6·0	·3	–0	22·3	–0	1·6
V–192	1 11	32·0	1·1	–0	3·3	2·2	18·6	8·9	5·6	3·0	2·6	–0	45·3	·7	–0	1·8	44·0	–0	–0	46·5	–0	8·2
V–194	1 11	85·0	·3	1·0	3·5	1·9	1·3	7·9	1·3	2·5	·3	–0	20·0	·6	–0	7·3	72·4	–0	–0	80·0	–0	–0
V–195	1 11	57·0	·3	–0	7·1	5·0	14·2	7·4	5·3	3·2	2·1	–0	44·6	2·1	·7	20·2	28·6	·3	·3	52·2	3·9	3·2
V–196	1 11	67·0	–0	–0	6·9	2·2	9·5	5·1	5·5	4·7	1·1	–0	35·0	2·9	–0	2·6	52·6	3·3	–0	61·4	1·1	3·6
V–197	1 11	50·0	–0	–0	8·7	6·1	6·4	11·4	7·4	11·8	1·3	·7	53·8	–0	–0	23·3	17·5	·7	·7	42·2	·3	4·0
V–198	1 11	49·0	·3	–0	4·7	1·9	12·5	21·6	7·5	17·9	·3	–0	66·7	–0	–0	11·6	19·4	·6	–0	31·6	1·9	1·7
V–199	1 11	75·0	–0	·3	3·7	3·4	6·1	7·4	4·0	5·1	·3	–0	30·3	9·5	–0	15·9	41·2	1·4	·3	68·3	·7	1·4
V–200	1 11	58·0	–0	–0	–0	–0	1·7	4·2	2·1	2·4	–0	–0	10·4	–0	–0	2·4	82·7	1·0	2·8	88·9	–0	·7
V–201	1 11	68·0	–0	–0	–0	·3	7·1	1·0	2·3	·6	–0	–0	11·3	–0	–0	1·9	81·7	·6	·6	84·8	–0	3·9
V–202	1 11	67·0	–0	–0	·4	–0	5·8	2·5	·8	·4	·4	–0	10·3	–0	–0	·8	79·9	4·5	·4	85·6	–0	4·1
V–203	1 11	50·0	·3	·3	3·8	3·2	7·9	27·1	9·8	4·7	·6	·6	58·3	–0	–0	6·0	31·6	1·3	–0	38·9	2·2	2·8
V–204	1 11	47·0	–0	–0	6·6	·6	3·9	28·9	9·6	12·6	2·1	–0	64·3	–0	–0	28·9	5·1	–0	–0	34·0	3·0	1·7
V–205	1 11	59·0	·3	·3	5·3	2·5	5·9	32·5	5·6	8·1	5·3	–0	65·8	–0	–0	16·8	14·0	·3	–0	31·1	4·0	3·1
V–206	1 11	68·0	–0	·6	1·5	2·8	4·6	11·8	4·3	2·5	1·5	–0	29·7	–0	–0	10·5	56·1	·6	–0	67·2	1·8	3·1
V–207	1 11	0	–0	–0	4·1	2·1	4·4	11·8	6·5	1·8	2·1	-0	32·8	–0	–0	2·7	59·2	·9	–0	62·8	2·7	4·4
V–209	1 11	76·0	·7	3·0	10·6	2·3	3·6	33·6	6·6	1·3	3·3	1·6	66·7	1·0	–0	23·4	5·9	1·7	–0	32·0	4·3	1·3
V–210	1 11	81·0	·3	–0	1·0	·7	1·0	4·9	1·7	·3	–0	·7	10·8	–0	–0	1·4	86·1	·3	·3	88·2	·7	1·0
V–212	1 5	45·0	·7	5·5	3·5	4·1	7·9	30·8	9·7	12·8	1·7	1·4	78·8	–0	–0	6·6	5·2	3·5	–0	15·3	10·0	5·9
V–213	1 11	58·0	7·1	·6	8·8	4·5	6·2	28·2	11·4	12·0	1·3	·6	80·7	–0	–0	10·7	·6	·3	–0	11·6	16·2	7·7
V–214	1 11	72·0	8·0	3·0	13·0	4·6	7·2	25·0	11·8	11·9	3·0	–0	87·5	–0	–0	7·7	·7	·3	–0	8·7	8·7	3·8
V–215	1 11	66·0	3·7	1·5	5·6	6·5	19·3	16·8	10·6	13·7	2·8	1·5	82·0	–0	–0	5·9	2·5	–0	–0	8·4	10·0	9·6
V–216	1 11	76·0	1·0	2·0	2·3	3·6	41·3	6·5	10·5	10·2	1·6	·7	79·7	–0	–0	4·3	6·2	1·0	–0	11·5	5·9	8·8
V–217	1 11	68·0	1·3	1·7	5·0	7·0	40·2	11·3	11·6	10·6	1·7	–0	–0	–0	–0	5·3	1·3	·7	–0	7·3	3·0	2·3
V–218	1 11	74·0	1·8	3·1	6·5	7·7	35·8	9·6	6·5	10·5	·9	·9	83·3	–0	–0	7·4	1·2	–0	·3	8·9	3·7	7·8
V–219	0 10	60·0	1·3	2·8	4·1	5·2	36·7	14·1	8·5	7·3	2·5	–0	82·4	–0	–0	8·8	·6	–0	·3	9·8	3·1	7·8

V–220	1	11	65·0	1·6	2·6	4·2	5·8	38·4	10·5	11·1	8·2	2·3	–0	84·7	–0	–0	5·5	·3	–0	–0	5·8	1·3	9·5
V–221	1	11	70·0	4·4	3·4	3·0	5·4	36·7	8·1	9·1	4·3	4·3	·7	79·4	–0	–0	12·5	–0	–0	–0	12·5	1·0	8·1
V–222	1	11	64·0	2·3	·6	3·4	5·3	51·5	7·7	5·7	3·6	1·7	–0	81·8	–0	·3	–0	10·8	–0	–0	11·1	3·1	7·1
V–223	1	11	68·0	1·8	3·3	2·6	12·1	43·0	8·1	6·2	3·3	1·5	1·1	83·0	–0	–0	5·9	–0	–0	·7	6·6	6·5	10·4
V–224	0	10	52·0	–0	–0	1·2	2·1	61·5	4·5	3·3	·6	2·1	–0	75·7	–0	–0	1·2	7·9	–0	–0	9·1	·9	15·2
V–225	1	10	62·0	2·4	–0	5·2	7·3	45·7	5·8	6·2	3·7	2·7	–0	79·0	–0	–0	5·1	–0	–0	–0	5·1	6·5	15·9
V–226	1	11	87·0	7·1	13·8	5·2	6·2	10·9	18·4	6·0	3·1	4·1	·4	75·3	–0	–0	20·6	·4	–0	–0	21·0	–0	3·7
V–227	0	0	100·0	2·1	·9	·6	5·9	33·1	22·2	12·3	2·8	3·6	–0	83·5	–0	·9	3·6	4·2	·6	–0	9·3	8·4	7·2
V–228	0	10	89·0	2–1	1·4	1·4	8·6	27·7	19·1	9·7	4·3	2·1	1·1	77·5	3·2	–0	5·4	–0	–0	–0	8·6	·7	13·9
V–230	1	11	90·0	1·1	1·4	1·1	1·1	54·1	14·2	7·8	–0	4·6	–0	85·4	–0	–0	8·5	·8	–0	–0	9·3	3·2	5·3
V–231	1	11	55·0	4·8	49·6	9·9	17·7	·7	4·4	1·0	6·4	1·0	–0	95·5	–0	–0	3·4	·4	–0	–0	3·8	–0	·7
V–233	1	11	28·0	–0	–0	–0	–0	93·9	·3	·3	–0	·9	–0	95·4	–0	–0	·3	·3	–0	·6	1·2	–0	3·4
V–238	1	11	19·0	–0	–0	–0	·4	86·1	·4	·4	–0	7·0	–0	92·2	–0	–0	1·2	–0	–0	–0	1·2	–0	1·6
V–240	0	10	93·0	·3	–0	–0	2·3	54·3	·3	5·0	–0	·3	–0	62·7	–0	–0	1·0	·3	–0	–0	1·3	–0	36·0
V–246	1	11	33·0	–0	–0	–0	·4	91·9	–0	·4	–0	2·6	–0	96·6	–0	–0	–0	–0	·4	–0	·4	–0	3·0
V–248	1	11	64·0	·4	4·6	·4	3·5	49·0	5·4	5·1	·7	2·7	·7	72·5	–0	–0	3·9	–0	–0	–0	3·9	·4	23·6
V–260	0	10	32·0	2·2	3·7	·9	1·2	61·1	2·5	2·2	·9	·3	·3	75·3	–0	–0	1·9	·6	–0	–0	2·5	·6	22·2
V–261	1	11	87·0	2·1	2·1	4·9	7·7	31·3	12·7	7·0	8·1	3·5	1·0	80·4	·6	–0	8·1	1·0	·3	·3	9·7	·7	9·3
V–262	1	11	52·0	1·2	–0	9·7	4·6	42·4	11·6	7·2	2·6	5·7	–0	85·0	–0	–0	4·3	·3	·3	–0	4·9	·9	10·1
V–263	1	11	26·0	·7	–0	–0	·7	71·3	3·1	·7	–0	3·8	–0	80·3	–0	–0	1·3	1·7	·3	–0	3·3	·7	16·4
V–264	1	11	31·0	2·7	3·1	4·1	1·7	49·1	8·6	5·8	11·0	1·0	–0	87·1	–0	–0	3·1	·3	–0	–0	3·4	·7	9·5
V–265	1	11	39·0	2·5	·6	4·1	1·8	44·0	6·9	8·8	12·4	4·7	–0	85·8	–0	–0	1·3	·9	–0	–0	2·2	1·6	12·0
V–266	1	11	51·0	7·0	2·6	5·6	10·8	12·9	17·3	7·0	17·9	1·5	·6	83·2	–0	–0	12·9	–0	–0	–0	12·9	5·3	3·9
V–267	1	11	34·0	1·3	–0	1·6	4·7	50·0	7·9	9·8	2·8	2·2	–0	80·3	–0	·3	2·3	1·0	1·0	–0	4·6	3·2	15·1
V–269	1	11	32·0	·9	·9	1·2	3·1	38·4	12·6	10·9	2·2	2·9	–0	73·1	–0	·3	·9	2·1	2·4	·3	6·0	3·8	20·9
V–272	1	11	42·0	5·0	4·0	24·9	4·7	6·1	22·2	2·0	5·7	3·0	2·0	79·6	–0	–0	13·5	–0	–0	–0	13·5	6·1	6·9
V–274	1	11	36·0	–0	1·3	3·8	3·4	7·7	68·9	3·8	4·3	1·3	–0	94·5	–0	·4	1·3	2·1	–0	–0	3·8	·4	1·7
V–276	1	11	35·0	1·8	–0	·7	4·6	26·8	39·7	8·2	·7	2·8	–0	85·3	–0	–0	·4	4·3	1·1	–0	5·8	2·5	8·9
V–282	1	11	29·0	1·1	1·5	1·5	4·5	34·8	26·9	7·9	1·5	3·4	–0	83·1	–0	–0	2·3	1·1	·7	·3	4·4	1·5	12·5
V–283	0	10	54·0	3·3	2·4	5·1	6·0	15·5	19·7	10·7	17·9	2·7	–0	83·3	–0	–0	10·4	·3	–0	–0	10·7	2·4	6·0
V–284	1	11	39·0	–0	·3	·3	1·5	52·5	6·3	13·2	2·4	4·5	–0	81·3	–0	–0	1·5	–0	–0	–0	1·5	·9	17·2
V–285	1	11	51·0	·9	·9	1·2	4·0	52·7	9·2	8·0	3·1	3·0	1·0	84·0	–0	–0	3·1	·6	–0	–0	3·7	1·2	12·3
V–287	1	11	52·0	·3	1·1	·3	4·8	55·8	10·3	6·7	4·3	4·4	–0	86·0	–0	–0	3·3	·6	–0	–0	3·9	1·1	8·1
V–288	1	11	68·0	–0	–0	–0	1·8	61·6	2·1	4·0	1·1	2·9	–0	73·5	–0	–0	·3	·3	–0	–0	·6	·3	25·9
V–289	1	11	41·0	–0	–0	–0	1·4	90·2	–0	·7	·3	–0	–0	92·6	–0	–0	–0	–0	·3	–0	·3	2·5	7·1
V–291	1	11	45·0	–0	–0	–0	–0	96·7	·8	–0	–0	–0	–0	97·2	–0	–0	–0	–0	–0	·3	·3	–0	2·5
V–301	1	11	64·0	4·3	1·0	3·6	9·2	41·9	14·5	8·9	2·0	·7	–0	86·1	–0	–0	5·0	–0	·3	–0	5·3	2·0	8·6
V–302	0	10	90·0	1·1	3·7	·3	7·4	48·3	6·3	5·7	12·0	·6	·6	86·0	–0	–0	2·3	–0	–0	·3	2·6	·6	11·4
V–303	0	10	95·0	2·2	10·2	5·1	6·2	23·9	9·2	4·8	9·8	3·5	·3	75·1	–0	–0	6·7	1·6	–0	–0	8·3	8·9	16·6
V–304	0	10	78·0	10·1	15·8	4·3	10·1	21·3	8·2	2·1	15·2	·6	·3	88·1	–0	–0	1·0	·3	–0	–0	1·3	4·6	10·6
V–312	1	11	69·0	–0	–0	–0	·3	13·6	·9	1·5	–0	–0	–0	16·3	–0	–0	6·4	71·0	2·4	–0	79·8	–0	3·9
V–314	0	10	89·0	1·3	2·6	3·2	13·8	25·6	15·1	5·8	6·7	1·3	–0	75·4	–0	–0	8·3	–0	–0	–0	8·3	2·9	16·3
V–315	1	11	72·0	–0	1·4	–0	1·4	70·5	5·9	6·6	·3	·7	–0	86·8	–0	–0	2·4	·9	–0	·7	3·4	3·8	9·8
V–317	1	11	46·0	–0	–0	–0	–0	98·2	–0	–0	–0	–0	–0	98·2	–0	–0	–0	–0	–0	1·8	1·8	–0	–0
V–325	1	11		–0	–0	–0	–0	83·0	–0	–0	–0	1·3	·3	84·6	–0	–0	–0	2·9	·3	·8	4·0	–0	11·4
V–331	1	11	61·0	–0	–0	–0	–0	98·2	–0	–0	–0	1·2	–0	99·4	–0	–0	·3	–0	–0	–0	·3	·7	·3
V–332	1	11	31·0	–0	–0	–0	–0	98·3	–0	·7	–0	·3	–0	99·3	–0	–0	–0	–0	–0	·7	·7	·7	–0
V–334	1	11	32·0	–0	–0	–0	–0	93·8	–0	–0	–0	1·6	–0	95·4	–0	–0	–0	–0	·8	–0	·8	–0	3·8
V–336	1	11	30·0	–0	–0	–0	·7	87·2	–0	·7	–0	–0	–0	88·6	–0	·7	–0	1·1	·7	–0	2·5	3·2	8·9
V–337	0	10	91·0	1·0	·7	1·7	2·3	57·6	11·4	8·2	–0	3·0	–0	85·9	–0	–0	5·7	–0	·3	–0	6·0	1·0	8·1
V–338	1	11	51·0	–0	–0	1·7	3·8	55·4	8·7	10·8	1·0	3·1	–0	84·5	–0	–0	2·4	1·0	3·1	–0	6·5	6·6	9·0
V–339	1	11	86·0	–0	1·2	·6	6·3	40·6	25·4	11·0	5·4	·6	–0	91·1	–0	–0	3·9	·9	1·2	–0	6·0	2·4	2·9

APPENDIX D—*continued*

Sample Number	Core Interval Analysed (cm)	Percent Sand	Coralline Algae	Halimeda	Corals	Large Foraminifera	Small Foraminifera	Mollusca	Echinoids	Bryozoa	Alcyonaria	Misc. Skeletal	Total Skeletal	Ooids	Faecal Pellets	Lithoclasts	Terrigenous	Glauconite	Misc. Non-skeletal	Total Non-skeletal	Glauconitized in percent of all others	Undetermined in percent of all others
V–340	1 11	86·0	·6	·9	1·3	4·2	35·6	12·0	6·6	4·0	2·2	6·0	73·4	–0	–0	5·7	3·2	1·9	–0	10·8	5·7	15·8
V–341	1 11	65·0	4·0	1·4	4·7	6·8	37·5	8·7	8·7	9·6	2·6	1·0	85·0	–0	–0	2·2	2·9	·4	–0	5·5	9·8	9·5
V–342	1 11	59·0	3·7	3·3	4·0	4·4	28·8	18·6	7·0	8·9	3·0	1·0	82·7	–0	–0	2·7	4·3	1·0	–0	8·0	6·6	9·3
V–343	0 10	64·0	11·2	3·7	8·6	37·4	·7	9·4	3·7	6·0	1·9	·4	83·0	–0	–0	13·5	–0	–0	–0	13·5	4·5	3·5
V–344	0 10	30·0	2·8	·9	5·8	5·7	20·7	19·7	15·4	5·1	1·8	–0	77·8	–0	–0	3·1	10·8	·3	–0	–0	–0	8·0
V–346	1 11	38·0	2·6	1·0	5·8	3·5	4·2	26·2	4·5	16·2	3·2	3·2	70·4	–0	–0	12·0	14·2	–0	–0	26·2	2·9	3·4
V–347	0 10	55·0	1·4	4·1	16·2	6·2	6·0	17·2	7·6	7·6	3·4	1·0	71·6	–0	·3	10·3	14·4	–0	–0	25·0	2·7	3·4
V–348	1 11	64·0	·4	2·2	3·7	4·7	24·6	9·9	6·9	5·9	2·9	–0	61·2	–0	–0	6·2	22·0	–0	–0	28·2	12·5	10·6
V–349	0 10	70·0	1·6	1·6	16·3	7·2	6·8	6·0	6·4	20·3	2·4	·4	68·9	–0	–0	7·6	18·0	·8	–0	26·3	8·8	4·8
V–350	0 10	82·0	3·9	2·1	4·9	44·4	4·2	12·0	3·9	4·9	1·8	–0	82·1	–0	–0	9·1	–0	–0	–0	9·1	9·8	8·8
V–351	0 10	82·0	2·2	·6	6·8	9·9	27·5	14·2	8·9	6·7	2·1	·6	79·9	–0	–0	4·9	2·5	·6	–0	8·1	–0	12·0
V–352	0 10	84·0	2·7	4·1	7·1	31·3	5·1	13·9	7·8	9·9	–0	–0	81·9	–0	–0	10·2	–0	–0	–0	10·2	·3	7·9
V–353	0 10	91·0	4·5	9·0	8·9	39·1	3·1	9·3	9·3	2·2	·7	–0	8·9	–0	–0	6·3	·3	–0	–0	6·6	–0	4·5
V–354	0 10	87·0	5·3	5·3	15·5	34·8	4·4	11·1	3·6	7·5	3·9	–0	91·4	–0	–0	5·0	–0	–0	–0	5·0	·3	3·6
V–355	0 10	52·0	3·6	2·3	9·3	24·9	11·3	12·0	8·3	5·3	6·0	–0	83·0	–0	–0	8·7	–0	–0	–0	8·7	3·3	8·3
V–357	0 10	78·0	1·2	2·1	3·6	8·4	28·7	16·0	9·4	6·3	1·5	·6	77·8	–0	–0	6·6	–0	·6	–0	7·2	2·4	15·0
V–359	1 11	42·0	·3	–0	1·7	4·1	47·6	10·7	9·0	2·9	·3	2·3	78·9	–0	–0	2·5	·3	2·9	–0	5·7	3·5	15·4
V–360	1 11	75·0	·4	–0	–0	1·6	61·9	·4	5·8	·4	·4	2·3	73·2	–0	–0	1·9	–0	–0	–0	1·9	3·5	24·9
V–361	1 11	78·0	2·0	1·0	5·1	7·5	27·1	10·6	8·2	18·5	1·4	–0	81·4	·3	–0	10·0	·3	–0	–0	10·6	5·1	8·0
V–362	0 10	93·0	3·3	4·5	7·8	6·3	24·2	19·1	5·7	8·5	4·5	·3	87·3	–0	–0	3·5	–0	·3	·3	4·1	1·8	8·6
V–363	1 11	49·0	1·3	3·8	1·0	3·2	47·5	4·5	7·7	2·6	3·5	–0	75·1	–0	–0	1·3	–0	–0	–0	1·3	1·0	23·6
V–364	0 10	85·0	3·6	4·6	7·2	16·4	13·8	10·5	6·6	18·1	2·6	–0	83·4	–0	–0	9·2	–0	–0	–0	9·2	3·3	7·4
V–365	1 10	81·0	3·6	4·3	4·5	8·0	31·9	9·4	8·9	8·9	1·1	·7	81·3	–0	–0	3·6	1·4	–0	–0	5·0	2·5	13·7
V–366	1 11	66·0	3·5	1·9	5·4	6·0	38·3	11·2	6·1	5·5	2·5	1·0	81·1	–0	·3	2·9	·6	1·0	–0	4·5	2·6	14·1
V–367	1 11	63·0	·3	–0	–0	·7	62·5	·7	5·9	–0	1·0	–0	70·9	–0	–0	–0	2·4	·7	–0	3·1	·7	26·0
V–370	0 10	90·0	·6	1·5	·9	2·6	47·6	6·2	5·7	6·2	3·5	–0	75·0	–0	–0	1·2	3·5	–0	·3	5·0	·6	20·0
V–371	0 10	74·0	2·6	·7	4·5	3·4	46·6	14·4	7·9	6·4	2·3	·7	89·5	–0	–0	1·1	1·1	1·1	–0	3·3	2·3	7·2
V–372	0 10	85·0	–0	1·0	3·3	3·3	42·2	5·7	10·4	2·3	4·0	–0	72·2	–0	–0	1·0	3·7	2·3	–0	7·0	5·0	20·8
V–373	0 10	83·0	5·5	2·9	2·6	7·0	18·9	18·6	5·8	14·6	2·0	–0	77·9	–0	–0	11·6	·6	·6	–0	12·8	5·5	9·3
V–374	0 10	56·0	6·7	3·4	10·5	20·1	1·8	15·1	7·7	8·9	2·5	–0	76·7	–0	–0	20·4	–0	–0	–0	20·4	–0	2·9
V–375	0 10	86·0	3·1	4·3	8·1	38·4	2·7	10·5	5·0	5·8	3·5	–0	81·4	–0	–0	15·5	–0	–0	–0	15·5	·4	3·1
V–376	0 10	74·0	–0	–0	2·2	2·2	25·8	18·5	11·9	9·1	1·6	–0	71·3	–0	–0	8·8	7·9	·3	–0	17·0	6·9	11·7
V–377	0 10	63·0	–0	–0	3·2	2·9	9·9	13·4	7·3	9·3	1·9	–0	47·9	–0	–0	23·0	20·8	2·5	·3	46·6	10·2	5·5

APPENDIX E

PLANKTONIC AND BENTHONIC FORAMINIFERA IN TIMOR SEA SEDIMENTS

(In percent of sum of Foraminifera, Radiolaria, and Diatoms; diatom percentages not listed)

Sample Number	Core Interval Analysed (cm)	Benthonic Foraminifera	Planktonic Foraminifera	Radiolaria	Percent Planktonic in Total Foraminifera
V-3	1 11	98	2	0	2
V-5	1 11	99	0	0	0
V-7	1 11	99	0	0	0
V-9	1 11	99	0	1	0
V-11	1 9	97	3	0	3
V-14	1 11	93	7	0	7
V-16	1 11	89	11	0	11
V-19	1 11	96	4	0	4
V-21	1 11	68	32	0	32
V-25	1 11	61	39	0	39
V-27	1 11	48	52	0	52
V-29	1 11	45	55	0	55
V-33	1 11	30	70	0	70
V-34	1 7	71	27	2	27
V-36	1 11	69	31	0	31
V-37	1 11	67	33	0	33
V-39	1 11	69	31	0	31
V-41	1 11	80	20	0	20
V-43	1 11	87	12	1	12
V-45	1 11	89	9	2	9
V-47	1 11	88	10	2	10
V-48	1 11	97	3	0	3
V-50	1 11	97	3	0	3
V-53	1 11	94	6	0	6
V-68	1 11	99	0	0	0
V-70	1 11	99	0	0	0
V-72	1 11	99	1	0	1
V-74	1 11	93	6	1	6
V-76	1 11	94	6	0	6
V-78	1 11	97	3	0	3
V-80	1 11	95	5	0	5
V-82	1 11	95	5	0	5
V-85	1 11	94	6	0	6
V-87	1 11	91	9	0	9

APPENDIX E—*continued*

Sample Number	Core Interval Analysed (cm)	Benthonic Foraminifera	Planktonic Foraminifera	Radiolaria	Percent Planktonic in Total Foraminifera
V-89	1 11	86	13	1	13
V-91	1 11	88	12	0	12
V-93	1 11	69	30	1	30
V-95	1 11	86	14	0	14
V-96	1 11	73	27	0	27
V-98	1 11	70	30	0	30
V-100	1 11	77	22	1	22
V-102	1 11	77	22	0	22
V-104	1 11	80	20	0	20
V-106	1 11	86	14	0	14
V-108	1 11	84	16	0	16
V-110	1 11	87	13	0	13
V-114	1 11	95	5	0	5
V-116	1 11	93	7	0	7
V-118	1 11	94	6	0	6
V-120	1 11	98	2	0	2
V-122	1 11	96	4	0	4
V-124	1 11	98	2	0	2
V-126	1 10	92	7	0	7
V-128	1 11	99	1	0	1
V-130	1 11	95	5	0	5
V-132	1 11	98	2	0	2
V-134	1 11	93	7	0	7
V-136	1 11	93	7	0	7
V-138	1 11	95	5	0	5
V-140	1 11	97	3	0	3
V-142	1 11	92	7	1	7
V-144	1 11	84	15	1	15
V-146	1 11	91	9	0	9
V-148	1 11	86	10	4	11
V-150	1 9	83	13	4	14
V-152	1 11	72	28	0	28
V-154	1 11	84	16	0	16
V-156	1 9	73	26	1	26
V-159	1 11	67	32	1	32
V-161	1 11	55	43	2	43
V-163	1 11	48	51	1	51

V-177	1	11	87	13	0	13
V-197	1	11	92	8	0	8
V-199	1	11	96	4	0	4
V-201	1	11	98	2	0	2
V-203	1	11	93	7	0	7
V-205	1	11	91	8	1	8
V-207	1	11	97	3	0	3
V-213	1	11	91	9	0	9
V-215	1	11	91	9	0	9
V-218	1	11	81	19	0	19
V-220	1	11	72	28	0	28
V-221	1	11	73	27	0	27
V-222	1	11	73	27	0	27
V-223	1	11	66	34	0	34
V-224	0	10	67	33	0	33
V-225	1	10	70	30	0	30
V-226	1	11	57	43	0	43
V-227	0	10	52	48	0	48
V-228	0	10	73	27	0	27
V-230	1	11	23	77	0	77
V-231	1	11	88	10	2	10
V-233	1	11	3	93	4	93
V-234	1	11	1	86	13	99
V-236	1	11	2	92	6	98
V-238	1	11	5	89	6	95
V-240	0	10	69	29	2	29
V-244	1	11	2	94	4	95
V-246	1	11	15	85	0	85
V-248	1	11	48	52	0	52
V-249	1	11	93	7	0	7
V-250	1	11	5	88	7	95
V-251	1	11	9	89	2	89
V-252	1	11	2	91	7	97
V-253	1	11	0	78	22	100
V-255	1	11	8	75	17	90
V-256	1	11	9	83	8	90
V-257	1	11	41	43	16	51
V-269	1	11	60	33	7	35
V-276	1	11	82	16	2	16
V-277	1	11	94	6	0	6
V-279	1	11	80	19	1	19
V-281	1	11	84	15	1	15
V-283	0	10	86	14	0	14
V-285	1	11	76	24	0	24
V-287	1	11	56	44	0	44

APPENDIX E—*cotinued*

Sample Number	Core Interval Analysed (cm)	Benthonic Foraminifera	Planktonic Foraminifera	Radiolaria	Percent Planktonic in Total Foraminifera
V–288	1 11	50	50	0	50
V–289	1 11	16	83	1	83
V–290	1 11	11	85	4	89
V–291	1 11	3	94	3	97
V–292	1 11	4	81	15	95
V–293	1 11	1	94	5	98
V–294	1 11	2	50	48	96
V–295	1 11	6	65	29	91
V–296	1 11	6	74	20	92
V–297	1 11	18	70	12	79
V–298	1 11	64	33	3	33
V–299	1 11	60	40	0	40
V–302	0 10	66	34	0	34
V–303	0 10	67	33	0	33
V–305	1 11	6	91	3	94
V–306	1 11	0	74	26	100
V–307	1 11	2	66	32	97
V–308	1 11	0	32	67	100
V–309	1 11	0	51	49	100
V–310	1 11	2	66	32	97
V–311	1 11	13	66	21	83
V–312	1 11	22	73	5	77
V–314	0 10	52	47	1	47
V–315	1 11	25	75	0	75
V–316	1 11	7	78	15	92
V–317	1 11	1	96	3	99
V–318	1 11	83	16	1	16
V–319	1 11	3	43	54	93
V–320	1 11	3	34	63	92
V–321	1 11	1	44	55	98
V–322	1 11	1	40	59	98
V–323	1 11	1	55	44	98
V–324	1 11	0	84	16	100
V–325	1 11	1	90	9	99
V–326	1 11	1	57	42	98
V–328	1 11	0	88	12	100
V–329	1 11	1	87	12	99

V-330	1	11	3	55	42	95
V-331	1	11	4	92	4	96
V-332	1	11	1	95	4	99
V-333	1	11	5	89	6	95
V-334	1	11	9	90	1	91
V-335	1	11	13	85	2	87
V-336	1	11	15	84	1	85
V-337	0	10	22	77	1	78
V-338	1	11	47	53	0	53
V-339	1	11	49	51	0	51
V-340	1	11	56	44	0	44
V-342	1	11	61	39	0	39
V-344	0	10	76	22	2	22
V-352	0	10	99	1	0	1
V-354	0	10	99	1	0	1
V-357	0	10	93	7	0	7
V-359	1	11	61	38	1	38
V-360	1	11	77	22	1	22
V-362	0	10	65	33	2	34
V-363	1	11	62	36	2	37
V-364	0	10	78	19	3	20
V-365	1	10	79	21	0	21
V-366	1	11	56	43	1	43
V-367	1	11	50	49	1	49
V-370	0	10	58	41	1	41
V-371	0	10	57	42	1	42
V-372	0	10	65	33	2	34
V-373	0	10	81	19	0	19
V-374	0	10	99	1	0	1

ALEX. B. DAVIES, Government Printer, Western Australia
(Printed in Australia)
1290/7/66—1300 Bks.

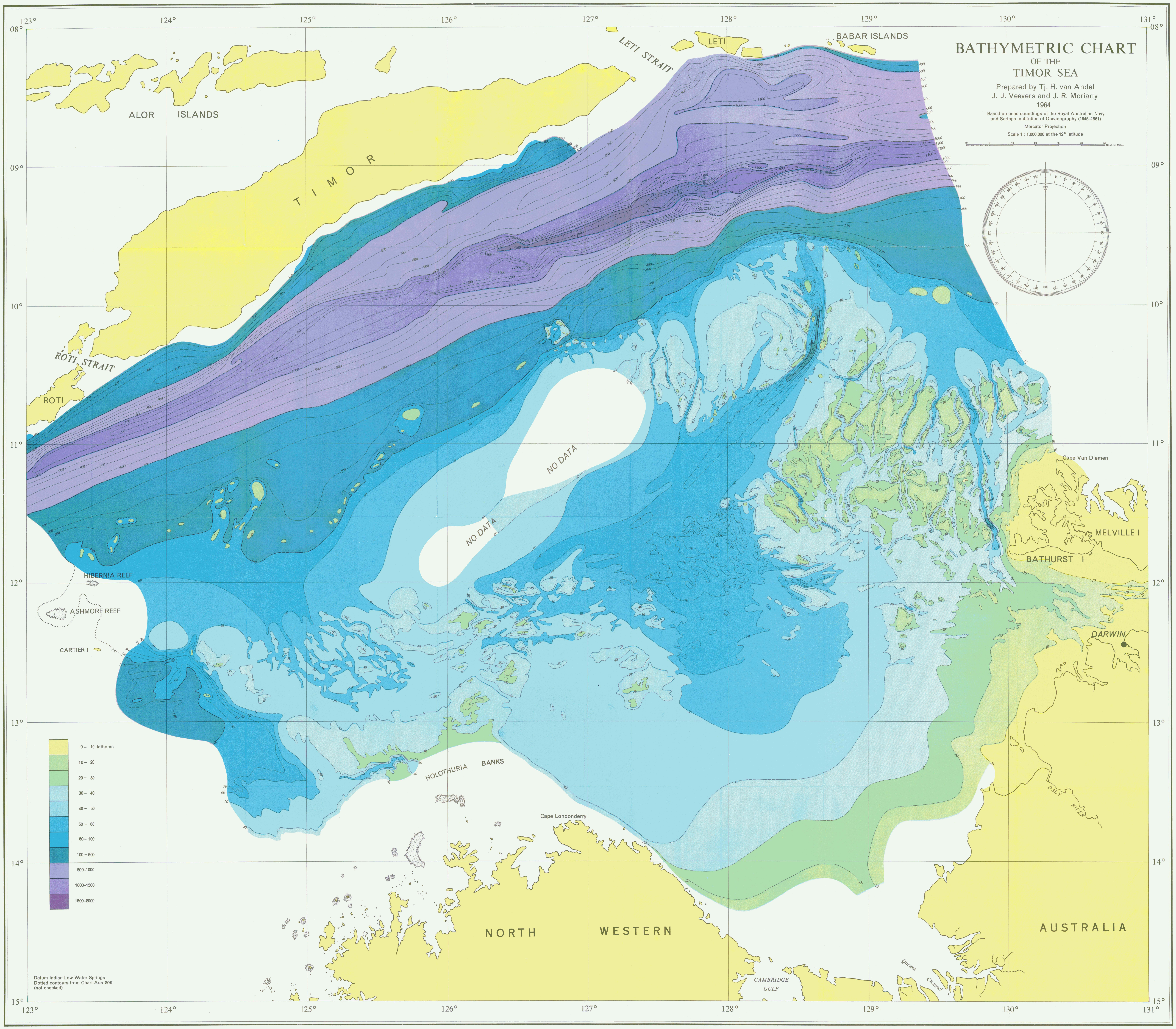
BATHYMETRIC CHART
OF THE
TIMOR SEA
Prepared by Tj. H. van Andel
J. J. Veevers and J. R. Moriarty
1964
Based on echo soundings of the Royal Australian Navy
and Scripps Institution of Oceanography (1945–1961)
Mercator Projection
Scale 1 : 1,000,000 at the 12° latitude
10 0 10 20 30 40 50 Nautical Miles
0 – 10 fathoms
10 – 20
20 – 30
30 – 40
40 – 50
50 – 60
60 – 100
100 – 500
500–1000
1000–1500
1500–2000
Datum Indian Low Water Springs
Dotted contours from Chart Aus 209
(not checked)
ALOR ISLANDS
TIMOR
LETI STRAIT
LETI
BABAR ISLANDS
ROTI STRAIT
ROTI
NO DATA
NO DATA
HIBERNIA REEF
ASHMORE REEF
CARTIER I
HOLOTHURIA BANKS
Cape Londonderry
Cape Van Diemen
MELVILLE I
BATHURST I
DARWIN
DALY RIVER
NORTH WESTERN
AUSTRALIA
CAMBRIDGE GULF
Queens Channel
123° 124° 125° 126° 127° 128° 129° 130° 131°
08° 09° 10° 11° 12° 13° 14° 15°

Bulletin 83

DETAILED BATHYMETRIC CHART OF TYPICAL SHELF EDGE BANKS, SAHUL SHELF

Bulletin 83

PLATE 3

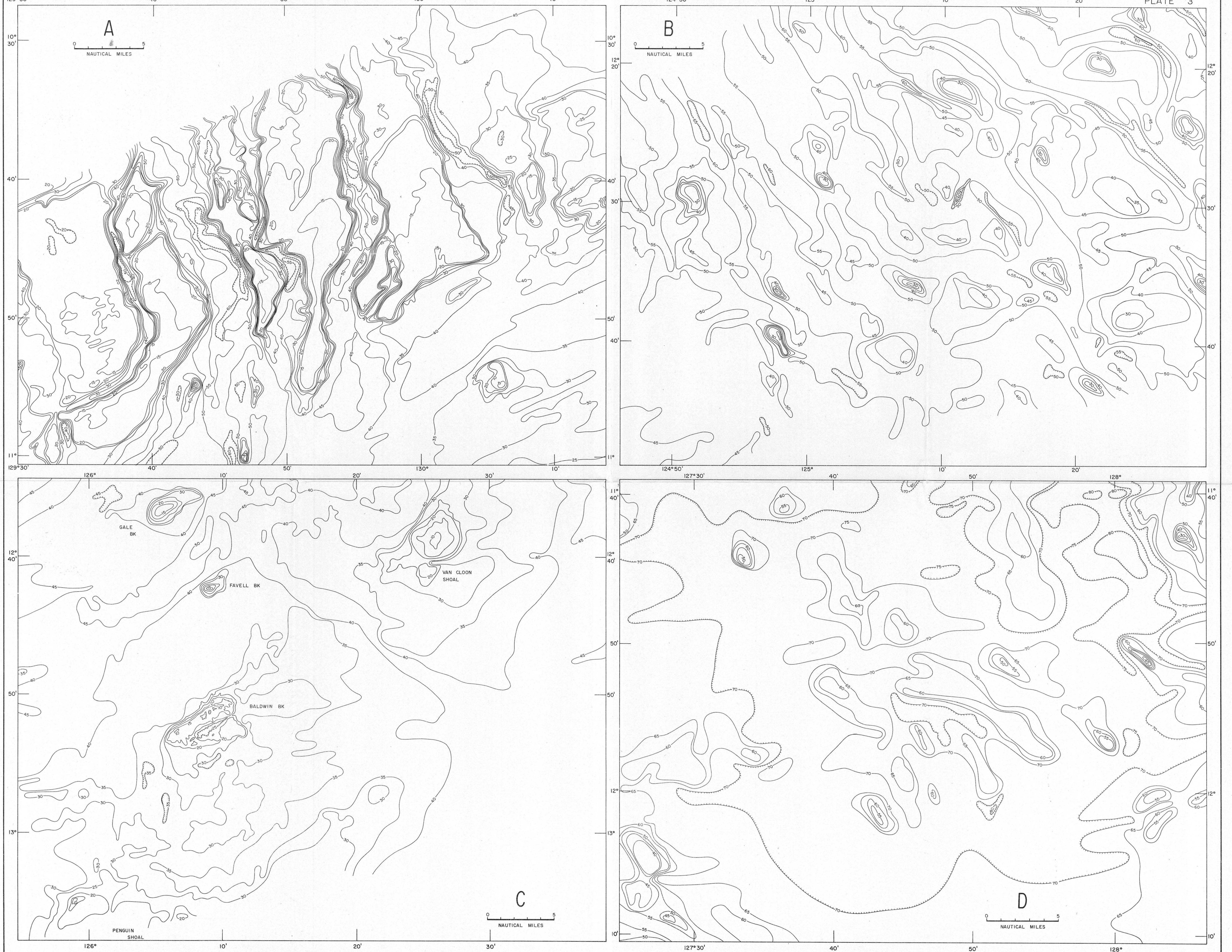

DETAILED BATHYMETRIC CHARTS OF TYPICAL AREAS OF THE SAHUL SHELF


PLATE 4
TOPOGRAPHIC CROSS-SECTIONS OF THE SAHUL SHELF
b-b', e-e' AND l-l' FROM SCRIPPS INST. OCEAN. SOUNDINGS; ALL OTHERS FROM R.A.N. SOUNDING SHEETS
II POSTULATED REGIONAL SURFACES
m CROSSING OF TWO SECTIONS
LOCATIONS ON TEXT FIGURE 3-11
VERTICAL EXAGGERATION 200x
0 2 4 6 8 10 NAUTICAL MILES
SAHUL RISE
MALITA SHELF VALLEY
VAN DIEMEN RISE
BONAPARTE DEPRESSION
SHELF EDGE
ECHO SHOAL
W. LONDONDERRY RISE
E. LONDONDERRY RISE
S. VAN DIEMEN RISE
LONDONDERRY RISE

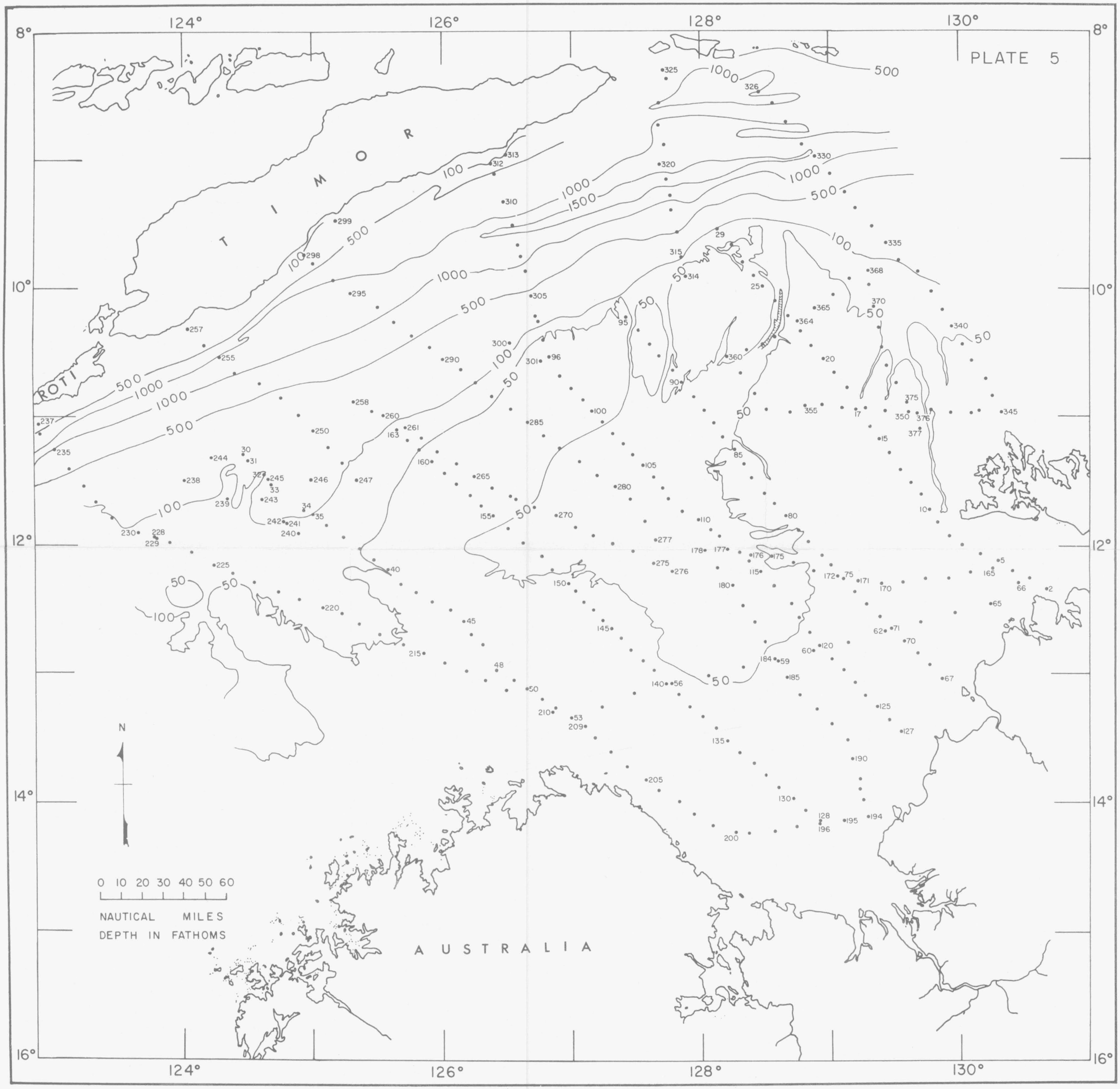

LOCATIONS OF SAMPLE STATIONS, TIMOR SEA